Universidade do Minho
Escola de Ciências da Saúde

Sara Carina Duarte da Silva

Searching for therapeutic strategies in a mouse model of Machado-Joseph disease: targeting proteostasis

Rastreio de estratégias terapêuticas num modelo de ratinho da doença de Machado-Joseph: foco na proteostase

outubro de 2015

Universidade do Minho
Escola de Ciências da Saúde

Sara Carina Duarte da Silva

Searching for therapeutic strategies in a mouse model of Machado-Joseph disease: targeting proteostasis

Rastreio de estratégias terapêuticas num modelo de ratinho da doença de Machado-Joseph: foco na proteostase

Tese de Doutoramento em Ciências da Saúde

Trabalho efectuado sob a orientação da
Professora Doutora Patrícia Espinheira de Sá Maciel

outubro de 2015

DECLARAÇÃO DE INTEGRIDADE

Declaro ter atuado com integridade na elaboração da presente tese. Confirmo que em todo o trabalho conducente à sua elaboração não recorri à prática de plágio ou a qualquer forma de falsificação de resultados.

Mais declaro que tomei conhecimento integral do Código de Conduta Ética da Universidade do Minho.

Universidade do Minho, 29 de Outubro de 2015

Nome completo: Sara Carina Duarte da Silva

Assinatura: Sara Carina Duarte da Silva

This work was supported by Fundação para a Ciência e Tecnologia (FCT) and COMPETE through a Bolsa de Doutoramento (SFRH/BD/78388/2011).

Agradecimentos/Ackonlowgments

Paixão. Perseverança. Curiosidade. Equipa. Companheirismo. Luta. Derrota. Conquista. Desânimo. Lágrimas. Risos. Sorrisos. Alento. Conforto. Amizade. Extra. Êxtase. ***Ciência.***

As palavras impressas hoje são o meu reconhecimento público a todos os que me de alguma forma contribuíram para a realização deste trabalho de tese.

Por tudo, a todos, muito obrigada!

The words today printed here are my public gratitude to those that contributed in any way to this thesis.

Thank you all for everything!

ICVS

À Patrícia, pela oportunidade de integrar a sua equipa ao longo destes 9 anos, pela orientação, apoio e acompanhamento. Por acompanhar o meu crescimento, pelos desafios. Pela energia com que luta por fazer Ciência onde, nem sempre é fácil atingir os objetivos. Pela perseverança, pela paixão. Por me fazer sentir orgulho de pertencer a esta equipa. Pela exigência e rigor. Por querer sempre mais. Obrigada.

À Professora Doutora Cecília Leão e restantes membros do Concelho Científico, em particular ao Professor Doutor Jorge Pedrosa presidente do Instituto de Investigação em Ciências da Vida e da Saúde (ICVS) e ao Professor Doutor Nuno Sousa presidente do Domínio de Investigação em Neurociências (NeRD), por me terem aceitado como aluna de doutoramento da Escola de Ciências da Saúde (ECS) e do seu Instituto de Investigação e por terem reunido todas as condições necessárias à realização deste trabalho.

A todos os funcionários do ICVS, que contribuem diariamente para o bom funcionamento do laboratório. Obrigada pelo apoio e disponibilidade.

À Fundação para a Ciência e Tecnologia (FCT) pelo financiamento.

Domínio de Neurociências

A todos os NERDs, pelo espírito crítico, pelas discussões de terça à 1 p.m., por tudo que nos une. Pelas risadas na cozinha, pelos excelentes Retiros, pela amizade. A todos, muito obrigada!

Em especial...

À Carina Cunha, por ter sido a "minha" primeira "aluna". Por ter vindo na melhor altura e por ter estado sempre à altura. Pelo jeito especial de ser, pela personalidade forte, por me fazer ver as coisas tal e qual como elas são. Por me permitir entrar na sua vida profissional e pessoal. Por simplesmente ser um exemplo para todos os alunos de doutoramento. Por ser minha amiga. Por perceber quando preciso de ajuda. Tenho tanto orgulho em ti.

À Joana Silva (aka Joaninha), pelos miminhos, pelas palavras de apoio, pelas bolachinhas. Por seres teimosa e acreditares sempre. Por colaborares nos meus projetos, por me revelares westerns, por toda a ajuda no laboratório. Por todas as palavras de encorajamento. Pelos belos jantares em tua casa. Por me teres formatado a tese! Muito obrigada por tudo!

À Bárbara Coimbra (aka Barbarita), pelo jeito único de ser. Pelas palavras (bem baixinho) de carinho. Por achares que tudo é "bem bom". Pelos teus conhecimentos preciosos de informática que tanto me ajudaram! Obrigada!

Ao John, que já devias entender o que te estou a escrever. Obrigada, thank you, σας ευχαριστώ. Because you are always there for me. Thank you for your scientific input to this thesis and for your support. Thank you for all the advices. Thank you for being just you.

À Ana João (aka Joni) por tudo que me ensinaste até hoje. Contigo aprendi o mundo maravilhoso dos Western-blots: troubleshooting, troubleshooting!! Obrigada pela amizade.

Ao Fábio (aka Fabinho) por todos os mimos! Pela boa disposição e amizade!

À Mónica Morais, pela companhia no baroke!

Ao Hugo Almeida por seres um exemplo a seguir. Pela paixão pela ciência. Por partilhares o gosto pelos *Beatles* comigo. Perseverança e Ciência *sont des mots qui vont bien ensemble.*

Macielitas (o)

A todos os alunos da Patrícia que já não estão no ICVS, muito obrigada! Em especial à Andreia Carvalho, Marina Amorim, Carmo Costa e Mónica Santos.

Mice team

Anabela (aka Belita): por sermos *a equipa*! Silva & Silva Lda. Por me teres acompanhado desde o início. Por me teres ensinado a caminhar na ciência. Por seres o meu exemplo. Pelo teu rigor. Pela tua capacidade de trabalho. Mereces o melhor! Pela nossa *roulotte* de serviços de genotipagem e churros. Pelas (*longas*) conversas no biotério. Por não seres simplesmente uma colega de trabalho, mas por seres uma das minhas amigas. Obrigada por tudo Anabela.

Sofia Esteves, ainda não comecei a escrever e já me estou a rir. E foram tantos momentos que passamos juntas. Começamos o dito PhDesc (aka PhDoc) juntas, e foi uma grande aventura! Nunca me esquecerei da época em que vivemos juntas. Pelo teu esforço (e não era preciso muito) para me fazeres rir para eu adormecer. Pelo trabalho que fizemos juntas. Pelas horas infindáveis no biotério amarelo. Por arranjarmos sempre forma de trabalhar juntas num espaço condicionado e sempre com boa disposição. Pelas palhaçadas filmadas durante o *beam walk*. Em especial, neste reta final, pelo teu apoio incondicional. Pela ajuda constante no *sítio do costume* ao fim de semana. Pelo salmo 91. És uma lutadora! Obrigada.

C.elegans team

Andreia Castro (aka De Castro), pelo teu espirito crítico e rigor científico. Pelos conselhos e ajuda. Por lutares em prol da equipa. Obrigada pela ajuda durante todos estes anos, pela honestidade. Obrigada por tudo.

Ana Jalles, pela companhia e partilha. Pelos nossos contrastes. Pelos breaks. Pelo cafezinho em tua casa. Pela paixão incondicional pela ciência. Obrigada pela amizade.

Liliana Santos (aka Li), por teres integrado na equipa e teres trazido novas energias e novas ideias. Por seres o meu braço direito nas encomendas, por teres sido a única a compreender que a burocracia das encomendas é mais difícil do que aquilo que se imagina! Obrigada por seres tão *terra-a-terra.*

Marta Costa, por estares todos os dias à minha frente. Pela tua ajuda com os qRT-PCR's. Pelo teu rigor com o desvio padrão. Pela tua capacidade de *multitasking e hard working…é sempre a bombar*! Obrigada por fazeres parte desta equipa.

Dulce Mary, pela boa disposição diária e por estar sempre tudo bem.

Stephanie, pela discrição e calma. Obrigada por integrares (muito recentemente) no mundo das ratices. A tua calma é perfeita para fazer *animal behavior*!

Neurodevelopment team

Carlos Bessa, pela tua pacificidade e capacidade de nos resolveres todos os problemas informáticos. Obrigada pela partilha de conhecimento.

Fátima Lopes, pelo teu *timing* perfeito. Pelo sentido de responsabilidade e rigor científico.

Um agradecimento (muito) especial…

Ao Gonçalo Gonçalves. Por ter tido uma importância imensurável na reta final desta tese. Por ter sido, para mim, uma motivação diária. Por ser um excelente aluno. Pelas horas (e foram muitas!) passadas a trabalhar. Por me ouvires a reclamar da vida sempre com um sorriso e com uma palavra de conforto. Por seres um *gentleman*. Por corares com elogios. *lalalalala*. Tenho a certeza que serás um excelente médico e um GRANDE homem! Do fundo do coração, obrigada. Teşekkürler!

Aos meus amigos

Andreia Carvalho, por toda a amizade ao longo destes anos. Por estares sempre presente em todos os momentos da minha vida. Por todas as horas passadas a trabalhar e a discutir ciência. Pelo companheirismo. Pelas lágrimas e pelas gargalhadas. Por não me deixares desistir nunca. Por me teres convencido a entrar nesta aventura chamada PhD. Por acompanhares todos os meus sonhos e todos os meus pesadelos. Por me saberes de cor. Simplesmente, obrigada.

Loirinha, por seres como uma irmã. Por muito que não entendas aquilo que realmente faço, sempre entendes-te a minha paixão pela ciência. Por estares SEMPRE comigo. És simplesmente a minha mana do coração. Obrigada ao Zé por compreender e se interessar comigo por ciência. Obrigada pelo orgulho que sentem por mim.

Joana, Gonçalo, Tiago e Cláudia, por serem amigos de sempre e para sempre! Por todos os bons (e maus) momentos passados juntos. Obrigada por tudo!!!

À minha família

Avô Cristiano, avô Carino, avó Maria, Sr. Joaquim, embora longe, estão sempre comigo no meu coração. Por tudo que me ensinaram. A vós devo grande parte da pessoa que sou hoje. Obrigada.

D.Mena, por ser como uma verdadeira mãe. Por me tratar por "minha filha". Pela comidinha boa ao domingo. Obrigada.

Carla, Jorge, Bela, Vitor, Lando e Céu, obrigada por me mimarem tanto! Obrigada por fazerem parte da minha vida.

Zé Lando, Catarina, Francisca e Matilde, os "meus" meninos! Por ser a tia "emprestada". Por me fazerem sorrir mesmo quando a vontade é chorar. Pela azáfama que criam nos dias de festa. Por tornarem a minha vida colorida e cheia de esperança!

Um agradecimento especial à família da Isabel (D.Conceição, Branca, Beto, Rui, Mónica e restantes familiares), por me receberem tão bem e me fazerem sentir em casa. Obrigada!

Avó Mimi, pelos ensinamentos ao longo de toda a minha vida. Por me ensinar o lado "real" da vida. Por ser um exemplo de mulher, de mãe, de avó. Por me teres ensinado que acima de tudo, estamos sempre nós. Por te preocupares diariamente com a minha comida. Por seres a avó babada que és (mesmo que queiras fazer parecer o contrário). Por me deixares escrever grande parte desta tese na tua cama ao teu lado. O teu quarto é milagroso! Por tudo que representas para mim, o meu exemplo, obrigada.

Nhi, a minha madrinha. Sempre presente em todos os momentos da minha vida quer a nível pessoal, quer académico. TODOS. Obrigada por seres tão amiga. Obrigada por fazeres parte da minha vida. Obrigada por tudo que fazes por mim (incluindo comprares donuts para eu comer!).

Ao meu irmão Sérgio e à minha cunhada Isabel, por tornarem a minha vida melhor. Por estarem presentes constantemente. Sérgio, obrigada pelo orgulho que sentes pela tua mana. Isabel, obrigada por seres como uma irmã para mim, obrigada por representares tanto para mim e para a minha família, não imaginas a importância que tens no meu coração. Adoro-vos.

Zé, *meu Zé*. Decididamente o companheiro de sempre. O amigo de todas as horas. Por seres o meu suporte. Por seres aquele que mais compreende a minha paixão pela ciência, por partilhares comigo essa paixão. Por treinares comigo todas as apresentações que faço e cronometrares o "meu" tempo. Por seres aquele que me incentiva a fazer aquilo que realmente gosto. Por me fazeres companhia (e até ajudar!) quando trabalho ao fim de semana. Pelos infindáveis vídeos de "beam" que me ajudaste a ver. Por perceberes a minha linguagem. Por todo o amor e carinho. Infelizmente não tenho palavras capazes de definir o "nosso significado". Por seres o *meu Zé*.

Mãe e Pai, por serem verdadeiramente os meus melhores amigos. Por mim sois capazes de tudo, acredito que até coisas que eu acharia inimagináveis em pessoas tão serenas como vós. Espelho-me em vós e tenho tanto orgulho! Orgulho-me da educação que me deste, de todos os ensinamentos, de todos os "não". Orgulho-me por serem um exemplo a seguir, como pessoas individuais e como casal. O berço onde nasci e cresci foi verdadeiramente um berço de ouro! Toda a envolvência familiar me permitiu crescer num ambiente saudável, de paz e amor e, assim tornar-me uma mulher capaz de lidar com os obstáculos da vida com serenidade. Obrigada mamã por seres a minha melhor amiga, e às vezes te "esqueceres" que és

minha mãe para seres simplesmente a “amiga”. Obrigada por tanto carinho! Obrigada por cuidares de mim. Papá, o meu amigo de sempre e para sempre. Por estares SEMPRE lá. Por ser a tua “menina”. Por seres aquele que mais orgulho sente em mim, independentemente do meu sucesso. Por sempre me aconselhares a seguir os sonhos. Por nos deixares fazer escolhas livremente. Aos meus pais devo todo o trabalho desta tese. Aos meus pais devo o meu sucesso. *Aos meus pais.*

“Choose a job you love, and you will never have to work a day in your life”

Confúcio

"**Searching for therapeutic strategies in a mouse model of Machado-Joseph disease: targeting proteostasis"**

Abstract

Machado-Joseph Disease (MJD) belongs to the group of nine Polyglutamine (PolyQ) diseases, which are characterized by the appearance of misfolded protein species, protein aggregates, neuronal dysfunction and ultimately cell death, of which is triggered by the presence of an expanded CAG repeat in the respective disease-causing genes. Along with the pathogenic motif, all these disease-associated proteins are widely expressed but the diseases only affect specific subsets of neurons. So far there is no effective treatment available for these disorders. Because the pathogenic mechanism(s) underlying MJD are poorly understood, which might be hampering the progression of effective therapeutical targets, this work focused on the search for new therapies based on hypotheses that additionally allow the study of molecular mechanism of disease. For this, we used the CMVMJD135 mouse model, which recapitulates the human disease both at the phenotypic and neuropathologic levels. We tested the efficacy of several compounds acting on different aspects of cellular function: (i) **molecular chaperone load**, (Hsp90 inhibitor - 17-dimethyl aminoethylamino-17-demethoxygeldanamycin hydrochloride - 17-DMAG); (ii) **autophagy** (lithium chloride and a combination of lithium chloride – LiCl - and temsirolimus - CCI-779); (iii) **Endoplasmic reticulum (ER) stress response**, (taroursodeoxycholic acid - TUDCA), also known to have multiple actions in the cells, and (iv) the **energy status** in the cell (creatine).

Chronic treatment of CMVMJD mice with 17-DMAG resulted in a delay in progression of the motor coordination deficits and a reduction in neuropathology. While we observed limited induction of heat-shock proteins with treatment, we found evidence that 17-DMAG could be acting through autophagy, as levels of LC3-II and beclin-1 were induced in the brain of treated animals. This resulted in decreased levels of the mutant ataxin-3 (ATXN3) and reduced intranuclear aggregation of this protein. To further test autophagy induction as potential therapeutic approach for MJD, we tested LiCl alone and a combination of LiCl with CCI-779 (m-TOR independent and dependent inducers, respectively). In spite of activating autophagy, as suggested by the increased levels of Beclin-1, Atg7, and LC3- II, and a reduction in the p62 protein levels, lithium had no overall beneficial effects in MJD model concerning motor performance. Furthermore, the

combined therapy using LiCl and CCI-779 proved to be deleterious to both WT and transgenic animals, failing to rescue their neurological symptoms in the first and exerting in neurotoxic effects in the latter.

TUDCA is an orally bioavailable and BBB permeable bile acid with known neuroprotective action, through its anti-amyloidogenic and chemical chaperone activities and its ability to modulate apoptotic pathways. In addition, TUDCA is FDA-approved for chronic use in humans to treat liver disorders, but has also been shown to be beneficial in several models of different neurodegenerative diseases. In the CMVMJD135 model, TUDCA delayed the onset of disease and improved the motor phenotype, including balance, motor coordination and gait parameters, and ameliorated neurological reflexes, exploratory movement deficits and muscular strength problems. Although TUDCA treatment did not reduce the ATXN3 aggregate load in the brain, it normalized the RNA levels of TNF-α, Il1β and Il10 in the brainstem and reduced the astrogliosis in the *substantia nigra* and brainstem. These results demonstrated the therapeutic efficacy of TUDCA supplementation for MJD, most likely mediated by its anti-inflammatory properties, making this compound an attractive for the treatment of neurodegenerative diseases, including MJD.

Lastly, we tested the efficacy of creatine, another naturally-occurring compound known to balance energy status in the cell. Creatine-supplemented diet led to an overall improvement in the motor phenotype of CMVMJD135 mice, namely improved motor coordination, limb strength and gait quality, and amelioration of some neurological parameters such as tremors and abnormal reflexes. Remarkably, chronic creatine treatment delayed the onset of several symptoms and, in some cases, completely abolished their appearance, supporting creatine supplementation as a useful strategy to slow the progression of MJD.

In summary in this work we validated a new MJD mouse model for use in preclinical trials as a powerful tool to study simultaneously pathogenic mechanisms associated with the disease and to develop novel therapeutic strategies. Furthermore, we found that Hsp90 inhibitors, TUDCA and creatine are relevant therapeutic candidates for MJD, some of which could be advanced to clinical trials in MJD patients.

"**Rastreio de estratégias terapêuticas num modelo de ratinho da doença de Machado-Joseph: foco na proteostase"**

Sumário

A doença de Machado Joseph (DMJ) pertence ao grupo de nove doenças de poliglutaminas em que o gene causador da doença possui uma expansão anómala do codão CAG. A presença desta expansão conduz ao aparecimento de espécies proteicas com conformação incorreta, agregados proteicos, disfunção neuronal e consequentemente, morte celular. Para além da expansão, todos os genes associados a este grupo de doenças possuem expressão ubíqua apesar de só afetarem subconjuntos específicos de neurónios. Atualmente, não existe tratamento eficaz para a DMJ. Uma das razões pelas quais há um atraso no desenvolvimento de alvos terapêuticos está relacionada com o conhecimento incompleto do(s) mecanismo(s) de patogénese associados à DMJ. Assim sendo, o objetivo deste estudo centrou-se na procura de novas terapias, usando uma abordagem baseada em hipóteses, que pode também permitir o estudo dos mecanismo(s) moleculares da doença.

Para tal, foi usado o modelo de ratinho CMVMJD135 que recapitula a doença humana a vários níveis, nomeadamente fenotípico e neuropatológico. Testámos a eficácia de diversos compostos com alvos terapêuticos relacionados com diferentes funções celulares: (i) níveis de **chaperonas moleculares** (inibidor da Hsp90 – 17-dimetil aminoetillamino 17- demetoxigeldanamicina - 17-DMAG); (ii) **autofagia** (cloreto de lítio e combinação de cloreto de lítio –LiCl e temsirolimus - CCI-779); (iii) resposta ao **stress do retículo endoplasmático** (ácido tauroursodesoxicólico – TUDCA), com múltiplas acções celulares, e (iv) **estado energético celular** (creatina).

O tratamento crónico com 17-DMAG no ratinho CMVMJD135 resultou num atraso da progressão da descoordenação motora e redução da neuropatologia. Apesar de ter sido observada uma indução limitada das chaperonas moleculares, este tratamento poderá ter atuado a nível da autofagia na medida em que houve indução dos níveis de LC3-II e beclina-1 no cérebro de animais tratados. Esta indução resultou na diminuição dos níveis de ataxina-3 (ATXN3) e uma redução da agregação intranuclear desta proteína. Para testar mais aprofundadamente a indução da autofagia como potencial terapia para a DMJ, foi testado LiCl isoladamente e em combinação com CCI-779 (atuando de forma independente e dependente da sinalização mTOR, respectivamente). Apesar da ativação da autofagia, sugerida pelos níveis

aumentados de beclina-1, Atg7, LC3-II e redução dos níveis proteicos de p62, o tratamento do modelo DMJ com lítio foi de uma forma geral ineficaz ao nível do desempenho motor. Além disso, a terapia combinada de LiCl e CCI-779 revelou-se prejudicial em ambos os ratinhos WT e transgénicos, falhando na recuperação de sintomas neurológicos e sendo neurotóxico.

O TUDCA é um ácido biliar com administração oral e permeável à BBB com funções neuroprotectoras conhecidas, através da sua capacidade anti-amiloidogénica, actividade de chaperona química e de modulação de vias apoptóticas. Adicionalmente, o TUDCA é um composto aprovado pela FDA para administração crónica no tratamento de doenças hepáticas, sendo também benéfico em diversos modelos de doenças neurodegenerativas. No modelo CMVMJD135, o tratamento com TUDCA atrasou o início da doença e melhorou o fenótipo motor incluindo equilíbrio, coordenação motora, e parâmetros da marcha, reduziu os reflexos neurológicos anómalos, melhorou os défices no movimento exploratório e força muscular. Apesar de o tratamento com este composto não ter reduzido os níveis de agregação da proteína ATXN3, foi eficaz na redução dos níveis de expressão de TNF-α, Il1β e Il10, tendo também reduzido a astrogliose no tronco cerebral e substantia nigra. Estes resultados demonstram a eficácia terapêutica da suplementação com TUDCA na DMJ, muito provavelmente através das suas capacidades anti-inflamatórias, o que torna este composto atrativo no tratamento de doenças neurodegenerativas, incluindo a DMJ.

Por fim foi testada a creatina, outro composto natural reconhecido pela eficácia em restabelecer o equilíbrio energético na célula. A dieta suplementada com creatina conduziu a uma melhoria geral no fenótipo motor do ratinho CMVMJD135; nomeadamente, melhorou a coordenação motora, força nos membros e qualidade da marcha. Também teve impacto positivo em parâmetros neurológicos como os tremores e reflexos anormais. Surpreendentemente, o tratamento crónico com creatina atrasou o início do aparecimento de diversos sintomas e até aboliu a presença de alguns, o que reinforça a suplementação com creatina como uma estratégica eficaz no atraso na progressão de DMJ.

Em conclusão, este estudo validou o novo modelo DMJ de ratinho para ensaios pré-clínicos como uma ferramenta valiosa para estudar simultaneamente mecanismos patogénicos associado à doença e para desenvolver novas estratégias terapêuticas. Além disso foi demonstrado que inibidores da Hsp90, TUDCA e creatina são candidatos terapêuticos relevantes para a DMJ, alguns dos quais com possibilidade de avançarem para ensaios clínicos em doentes.

Contents

Abbreviations

17-AAG:17-N-Allylamino-17- demethoxygeldanamycin

17-DMAG:17-dimethylaminoethylamino-17-Demethoxygeldanamycin

3-NP: 3-nitroproprionic acid

7N: facial nuclei

A2AR: adenosine A2A receptor

AD: Alzheimer's disease

ALS: Amyotrophic lateral sclerosis

AMPA: -Amino-3-hydroxy-5-methyl-4-

AONs: antisense oligonucleotide-mediated

AR: androgen receptor

Atg: autophagy-related genes

AVV 1: adeno-associated virus serotype 1

BA: bile acid

BAI: Beck anxiety inventory

BBB: blood brain barrier

BD: bipolar disorder

BDI: Beck depression inventory

BDNF: brain-derived neurotrophic factor

C. elegans: *Caenorhabditis elegans*

CBP: CREB-binding protein

CCFS: composite cerebellar functional score

CCI-779: Cell Cycle inhibitor-779

CGI: clinical global impression

CHIP: C-terminus of Hsp70-interacting protein

CNS: Central nervous system

CoQ10: coenzyme Q10

Cr: Creatine

CSF: cerebrospinal fluid

DARPP-32: dopamine and cAMP-regulated phosphoprotein)

DCN: deep cerebellar nuclei

DN: dentate nuclei

DRG: Dorsal root ganglia

DRPLA: Dentatorubral-pallidoluysan atrophy

DUB: Deubiquitylting enzyme/deubiquitylase

EGCG: epigallocatechin-3-gallate

EM: electron microscopy

EQ: ethoxyquin

ER: endoplasmic reticulum

FAP: Familial Amyloidotic Polyneuropathy

FDG-PET: F-18 fluorodeoxyglucose positron emission tomography

FOXO: forkhead box O

FRET: fluorescence resonance energy transfer

HAT: histone acetyltransferase

HD: Huntington's disease

HDAC: histone deacetyltransferases

HPRT:hypoxanthine-guanine phosphoribosyltransferase

HSC70: heat-shock complex 70

HSF1: heat-shock factor 1

HSP: Heat shock protein

HSR: Heat shock response

Htt: huntingtin

ICARS: International Cooperative Ataxia Rating Scale

IMPase: inositol monophosphatase

kDa: Kilodalton

LiCl: lithium chloride

LRT: lateral reticular nucleus

miRNA: microRNAs

MJD: Machado-Joseph disease

mPTP: mitochondrial permeability transition pore

MRI: Magnetic resonance imaging

mRNA: Messenger RNA

MSC: mesenchymal stem cell

mTOR: mammalian target of rapamycin

NES: Nuclear export signals

NESSCA: Neurological Examination Score for the Assessment of Spinocerebellar Ataxia

NGM: nematode growth medium

NI: nuclear inclusion

NLS: Nuclear localization signal

NMDA: N-methyl-aspartic acid

NNI: neuronal nuclear inclusion

nt: nucleotide

NT3: neurotrophin-3

OLST: one leg standing test

OXIGON: indole-3-proprionic acid

PBS: Phosphate-buffered saline

PCAF: p300/CREBBP associated factor

PCr: phosphocreatine

PCR: polymerase chain reaction

PD: Parkinson's disease

PET: Positron emission tomography

PFA: paraformaldehyde

PGI: patient global impression

PN: pontine nuclei

PolyQ: Polyglutamine

PTD: protein transduction domains

QBP1: PolyQ-binding protein 1

qRT-PCR: quantitative reverse-transcriptase PCR

RNAi: RNA interference

ROCK: Rho-kinase

SAHA: Suberoylanilide hydroxamic acid

SARA scale: Scale for the Assessment and Rating of Ataxia

SB: sodium butyrate

SBMA: Spinobulbar muscular atrophy

SCA: Spinocerebellar ataxias

SCA3: Spinocerebellar ataxia type 3

SCAFI: spinocerebellar ataxia functional index

SDS: Sodium dodecyl sulphate

SF36: Short-Form 36

shRNA: short hairpin RNA

SMER: small-molecule enhancers of rapamycin

SMIR: small-molecule inhibitors of rapamycin

SN: Substantia nigra

SNP: single nucleotide polymorphism

SSRIs: serotonin reuptake inhibitors

TBP: TATA-binding protein

TGase: transglutaminase

TGI: tandem gait index

TH: tyrosine hydroxylase

TLT: total length traveled

TRE: tripterygium regelii extract

TUDCA: taurourdeoxycholic acid

UDCA: Ursodeoxycholic acid

UPS: Ubiquitin proteasome system

USP: Ubiquitin specific proteases

VCP: valosin-containing protein

Veh: vehicle

VN: vestibular nuclei

WT: Wild type

YAC: yeast artificial chromosome

Thesis planning

The present thesis is divided into 7 chapters. Chapter 1 consists of a general introduction; Chapters 2 to 6 describe hypothesis-driven pre-clinical trials performed in a mouse model of MJD generated in the lab – the CMVMJD135 transgenic line. In Chapter 7 a general discussion of the work is presented.

In **Chapter 1** a brief overview on polyglutamine diseases is provided and the potential mechanism (s) underlying these disorders are discussed. A more extensive part of the introduction focuses on reviewing the current therapeutic strategies for polyglutamine diseases. An outline of Machado-Joseph disease is presented, as well as the neuropathology behind this incurable disease. Furthermore, an emphasis is given to the existent mouse models of MJD from a phenotypic and neuropathologic perspective. The pre-clinical trials performed to date in these models are also described, and in the end of this chapter the clinical trials completed so far in MJD patients are presented.

In **chapter 2** the work "*Chronic treatment with 17-DMAG improves balance and coordination in a new mouse model of Machado-Joseph disease"*, describes the generation of a new MJD mouse model – CMVMJD135 – its extensive phenotypic and pathologic evaluation, and a pre-clinical trial which was performed in this model using 17-DMAG, a small molecule known to induce the heat-shock response in cells by interfering with the negative feedback imposed by Hsp90 upon Hsf-1. We show that 17-DMAG was effective in delaying disease onset and progression but was not able to induce the expected increase in heat-shock protein expression; rather, it induced autophagy in the brain of the CMVMJD135 mice. At the phenotypic level, this compound showed to transiently ameliorate the phenotype of these animals and markedly decreased ATXN3 aggregation.

In **chapter 3** the work entitled *"Lithium Chloride therapy fails to improve motor function in a transgenic mouse model of Machado-Joseph Disease"* is presented. In this work we treated the CMVMJD135 mice with lithium chloride, a mood stabilizer widely used in the clinics and known to induce autophagy independently of the mTOR pathway. This compound failed to rescue the phenotype of CMVMJD135 animals despite its ability to induce autophagy in the brain.

Chapter 4,*"Combined therapy with m-TOR-dependent and –independent autophagy inducers causes neurotoxicity in a mouse model of Machado-Joseph disease"* is an extension of the work included in chapter 3 and focuses on a combined therapy using two autophagy inducers acting through

different/complementary pathways. We show that this combined therapy did not improve the CMVMJD135 phenotype but rather worsened the phenotype of transgenic and wild-type animals, suggesting neurotoxicity caused by the combined therapy. This work highlights the possible dangers of manipulating autophagy in the central nervous system.

In **chapter 5, "***TUDCA reduces neuroinflammation and improves motor symptoms in a transgenic mouse model of Machado-Joseph disease"* a pre-clinical trial using a compound currently used for liver diseases is presented, but proposed by others to have neuroprotective effects. TUDCA is a safe compound known to be beneficial in several neurodegenerative diseases and to act thought different cellular mechanisms. In this work we show that chronic treatment with TUDCA was indeed able to improve the overall phenotype of the CMVMJD135 mice. We also show that TUDCA was able to reduce the neuroinflammation observed in the CMVMJD135 animals.

Chapter 6, "*Creatine-supplemented diet improves the overall phenotype and neuropathology of a transgenic mouse model of Machado-Joseph disease"* focuses on the capacity of a natural-occurring compound to modulate the symptoms and neuropathology of the CMVMJD135 mice. We also show that creatine improves the overall phenotype of CMVMJD135 mice, and to some extent also the performance of wild-type mice when compared to animals under standard diet. Of notice, creatine treatment delayed the onset of some phenotypic parameters in CMVMJD135 mice. Creatine had no impact on the levels of mutant ATXN3 in the brainstem both at mRNA and protein levels, but did reduce aggregation of ATXN3.

A general discussion of this thesis work and future perspectives are presented in **chapter 7**.

Chapter 1

General introduction

General Introduction

1.1 Summary

Polyglutamine (PolyQ) diseases are a group of neurodegenerative disorders caused by the expansion of an unstable CAG trinucleotide repeat within the coding region of several otherwise unrelated genes. This expansion encodes an abnormally long polyQ tract that which, above a threshold size, leads to misfolding and aggregation, eventually resulting in neurodegeneration.

These disorders all share key features including: (i) dominant transmission; (ii) adult onset; (iii) abnormal protein aggregation; (iv) selective neuronal susceptibility, despite the widespread expression of the disease-related proteins and (v) cellular toxicity that impacts at the organism level. These commonalities point to shared mechanism(s) underlying their pathogenesis.

To date, effective therapeutic strategies are still lacking for polyQ diseases, although some symptoms can be controlled with specific treatments. Moreover, neuroimaging studies in mutation carrying individuals suggest that nervous system dysfunction begins many years before the onset of any diagnosable symptoms. Thus, the development of therapeutic interventions becomes of great importance, not only to slow progression of manifest disease but also to delay, or ideally prevent, its onset.

Potential therapeutic targets for polyQ disorders can be divided into (i) those that are aimed at the polyQ proteins themselves, namely gene silencing, attempts to enhance mutant protein degradation or inhibition/prevention of aggregation; or (ii) those that intercept the toxic downstream effects of the polyQ protein, such as mitochondrial dysfunction and oxidative stress, transcriptional abnormalities, UPS impairment, excitotoxicity, or activation of apoptotic pathways.

The existence of relevant animal models and the recent contributions towards the identification of putative molecular mechanisms underlying polyQ diseases are impacting on the development of new drugs. Here, we provide an overview of the therapeutic strategies for polyQ disorders in cellular and animal models and their possible translation into the clinics.

1.2 Polyglutamine diseases

Expansions of repeating units of DNA, especially CAG triplet repeat expansions, are known to underlie several inherited neurodegenerative disorders (1) including Huntington disease (HD) (2), spinal and bulbar muscular atrophy (SBMA) or Kennedy's disease (3), dentatorubropallidoluysian atrophy (DRPLA) (4, 5), and the spinocerebellar ataxias (SCAs) 1, 2,3, 6, 7, and 17 and (6-12). The CAG expansion leads to an abnormally long polyQ tract within all the proteins involved in the mentioned diseases. The clinical manifestations of each disease result from brain pathology involving a specific subset of neurons that is, for the most part, particular to each disease. A common feature among all these disorders is a progressive neuronal dysfunction/death leading to neurological symptoms beginning at mid-life (13).

The dominant transmission, progressive neurodegeneration, symptoms with onset in adulthood and some shared clinical manifestations in these polyQ diseases suggest a shared mechanism for their pathogenesis. The pathogenic mechanism of these diseases is believed to arise from a genetic gain of function related to the abnormal conformation(s) acquired by the elongated polyQ tracts. Besides the polyQ tract, the proteins involved in polyQ diseases share no homology and no functional similarity, which suggests that the polyQ stretch itself confers toxic properties to these proteins through a "toxic gain of function" (14). In agreement with this hypothesis the expression of a simple polyQ tract, in the absence of any additional protein context has been shown to be neurotoxic, in cell culture, mouse, *Drosophila* and *C. elegans* models (15-19). This toxic effect of the polyQ tract was further reinforced by a study describing the effect of the insertion of a CAG tract in the mouse hypoxanthine-guanine phosphoribosyltransferase (*HPRT*) gene, encoding a metabolic enzyme, which normally does not bear such a repeat and is not known to be involved in any neurodegenerative disease. These mice developed a progressive late-onset neurological phenotype, including ataxia, seizures and premature death (20).

Interestingly, and despite the ubiquitous expression of polyQ mutated proteins, only some subsets of neurons are affected in each polyQ disorder (Table 1), indicating that there are other factors influencing the pathogenesis (21).

The CAG repeat tracts are normally highly polymorphic, but above a threshold length of around 35 to 40 glutamine units, the symptoms of the diseases are manifested (Table 1) (1, 4). Interestingly, above the pathogenic threshold the CAG tracts are also unstable across generations, and they may expand or contract, biases towards expansion or contraction depending on the gender of the transmitter: while

maternal meioses are generally more stable or tend to lead to contractions, paternal transmissions display more instability and tend to lead to expansions. This intergenerational instability leads to a phenomenon called anticipation, since the disease symptoms appear earlier and are more severe in later generations (22-24).

Table 1. Molecular and pathogenic features of polyglutamine diseases. (adapted from (21, 25))

Disease name	Mutated gene	Protein Product	Known or putative function	Normal (CAG)n	Expanded (CAG)n	Regions most affected	Clinical features
HD	*HD*	Huntingtin	Signaling, transport, transcription regulation	6–34	36–121	Striatum, cerebral cortex	Chorea, dystonia, dementia
DRLPA	*DRPLA*	Atrophin 1	Transcription regulation	7–34	49–88	Cerebellum, cerebral cortex, basal ganglia, Luys body	Myoclonus epilepsy, ataxia, chorea, dementia
SBMA	*AR*	Androgen receptor	Steroid-hormone receptor (transcription regulation)	9–36	38–62	Anterior horn and bulbar neurons, dorsal root ganglia	Weakness, bulbar symptom, fasciculations, tremors, gynecomastia
SCA1	*SCA1*	Ataxin-1	Transcription regulation	6–39	40–82	Cerebellar Purkinje cells, dentate nucleus, brainstem	Ataxia, bulbar symptom, spasticity, polyneuropathy, cognitive impairment
SCA2	*SCA2*	Ataxin-2	RNA metabolism	15–24	32–200	Cerebellar Purkinje cells, brainstem, frontotemporal lobes	Ataxia, slow saccades, ataxia, polyneuropathy, parkinsonism
SCA3/MJD	*ATXN3*	Ataxin-3	Deubiquitinating activity and transcription regulation	10–51	55–87	Deep cerebellar nuclei, brainstem, ganglia, subthalamic nuclei, red nucleus, spinal cord	Ataxia, ophtalmoplegia, diplopia neuropathy dysphagia, dystonia
SCA6	*CACNA1A*	$CACNA1_A$	P/Q-type α1A calcium channel subunit	4–20	20–29	Cerebellar Purkinje cells, dentate nucleus, inferior olive	Ataxia, dysarthria, down-beating nystagmus
SCA7	*SCA7*	Ataxin-7	Transcription regulation	4–35	37–306	Cerebellum, brainstem, macula, visual cortex	Ataxia, retinal degeneration, ophthalmoplegia
SCA17	*SCA17*	TBP	Transcription	25–42	47–63	Cerebellar Purkinje cells, inferior olive	Ataxia, dementia, psychosis, seizures, extrapyramidal signs

At a molecular level, the brains of patients with all polyQ diseases display proteinaceous aggregates in neurons, usually termed neuronal inclusions (NIs), mainly located in the nucleus (25). These inclusions are a common hallmark of these diseases, however it is still controversial if they are pathogenic or not. Several mechanisms have been implicated in polyglutamine toxicity, most of which are not mutually exclusive (21). Figure 1 summarizes these mechanisms and the therapeutic intervention strategies currently being developed for polyQ diseases. These potential therapeutic strategies can be divided into those that target the primary pathological events of the disease, including the therapies decreasing the levels of the toxic protein and inhibiting the (relevant forms of) aggregation of the mutant protein, and those intercepting the downstream effects of the expanded polyQ protein such as impairment in proteostasis, transcription abnormalities, mitochondrial dysfunction, excitotoxicity and/or apoptotic pathways (26).

Therapeutic strategies that directly target for polyQ diseases include: i) gene silencing that leads to decreasing levels of the mutant protein; ii) enhancement of mutant protein degradation by modulating cellular degradation pathways; (iii) transcription modulation by promoting histone acetylation and (iv) increasing neuroprotection by decreasing excitotoxicity, improving calcium homeostasis, balancing energy availability and/or increasing neurotrophic factors.

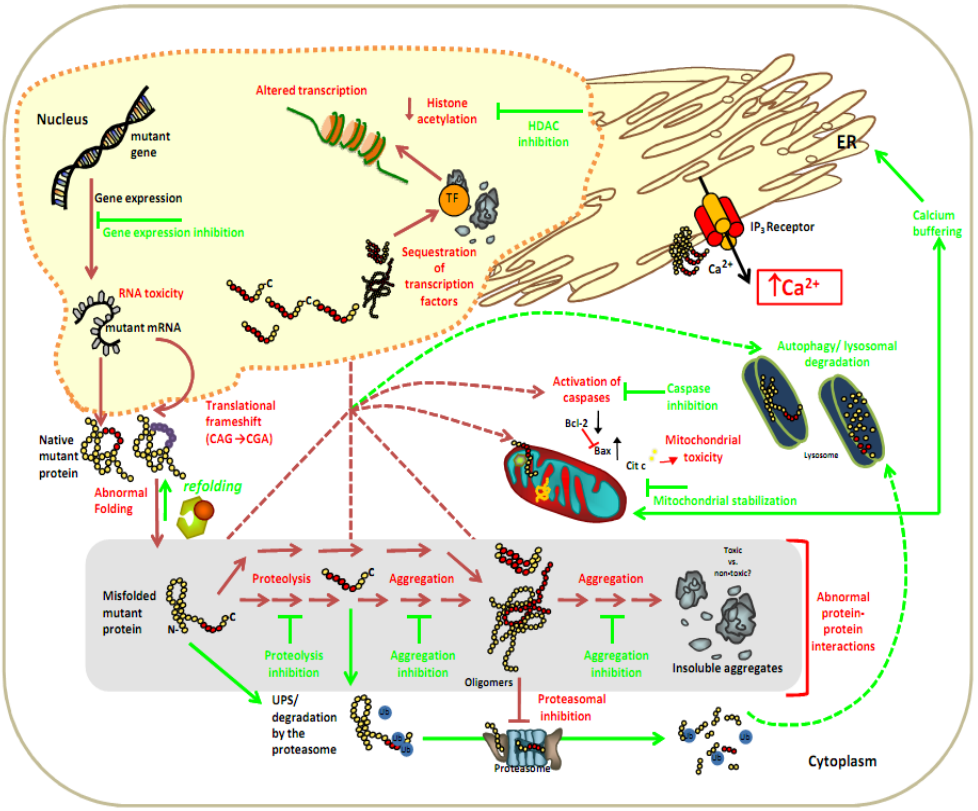

Figure 1 - Mechanisms suggested to underlie polyglutamine pathogenesis. The pathogenic process (red arrows) begins with the synthesis of a protein with an expanded polyQ tract. The expanded polyQ tract alters the native conformation of the protein making it more prone to aggregate. This can be modulated by the presence of molecular chaperones and co-chaperones. At least a fraction of the abnormally folded protein is ubiquitylated (Ub) and degraded via the proteasome and another portion is subject to lysosomal-dependent proteolysis. Cleavage of the abnormally folded mutant protein may produce polyQ-containing fragments that function as "seeds" favoring the aggregation process. The mutant proteins shift, in part, from a monomeric random coil or β-sheet into oligomeric β-sheets and eventually into insoluble aggregates. Some of these species might contribute to pathology through impairment of the ubiquitin-proteasome system, mitochondrial dysfunction and/or dysregulation of calcium homeostasis and alterations in transcription. As a simplification, mutant proteins are depicted as originating in the cytoplasm, although some of them might also be located in the nucleus or cycle between the cytoplasm and nucleus. Presence in the nucleus seems to be key for pathogenesis. To date, no effective treatment has been developed for any polyQ expansion disease. In consideration of the mechanisms mentioned above, several efforts have been made in order to reestablish cellular proteostasis (green arrows) such as mutant gene silencing and transcriptional modulation with HDAC inhibitors, blocking cleavage and aggregation, restoration of the quality control machinery and improving neuronal function and survival (neuroprotection). The results of these strategies will be detailed in the next section. Adapted from (27).

1.3 Therapeutic strategies for PolyQ diseases

1.3.1 Gene Silencing

The efficacy of terminating the downstream neurotoxic effects trough silencing of mutant polyQ-encoding genes even after overt disease manifestation was demonstrated in conditional tetracycline-regulated mouse and rat models of HD (28, 29) and SCA3 or Machado-Joseph disease (MJD) (30) and in a doxycycline-regulated mouse model of SCA1 (31). When the mutant proteins were inducibly expressed, pathological and behavioral features of the disease developed, including the neuronal inclusions and abnormal motor behavior. Upon shutting-down of the transgene expression some neuropathological features, such as aggregate formation, were reverted (28, 29, 31) and there was an amelioration of the neurological phenotype for all the models (28-31).

The RNAi pathway is a natural physiological sequence-specific gene silencing mechanism in which, through the action of small RNAs (miRNAs), the regulation of expression of key genes involved in fate determination, proliferation as well as other vital biological processes may occur (32). In mammalian cells, primary micro-RNA (pri-miRNA) is first transcribed by RNA polymerase II as hairpins with large single stranded flanking-sequences in the nucleus (33). These hairpins are then cleaved by the nuclear Drosha-

DGCR8 microprocessor complex into shorter precursor or pre-miRNAs (34, 35), which are subsequently exported into the cytoplasm by exportin-5 (36). In the cytoplasm, they are further processed by Dicer into ~22 nucleotide (nt) long miRNA with characteristic 2-nt 3 overhangs (37). After being separated into two strands, the guide strand of the miRNA is next loaded onto the RNA-induced silencing complex RISC to silence target transcripts (38, 39). The mode of target repression primarily depends upon the degree of complementarity; near perfect base-pairing is required for target transcript cleavage by Argonaute 2, one of the principal protein components of RISC, while imperfect binding induces translational repression and mRNA decay (40). To reprogram the RNAi pathway for therapeutic intervention, inhibitory RNAs can be designed to mimic primary miRNA stem-loops (artificial miRNAs), processed pre-miRNAs (short hairpin or shRNAs), or mature miRNAs with perfect complementarity to their targets (small interfering RNAs or siRNAs) (41).

The potential of RNAi therapies in polyQ diseases was first demonstrated in a cell-based model in which the inhibition of a truncated version of the human AR containing 112 GAG trough dsRNA significantly reduced polyQ-mediated cell death and caspase-3 activity as well as protein aggregation (42). Soon after this *in vitro* evidence was obtained, the viability of RNAi therapeutics was demonstrated *in vivo*, in a SCA1 mouse model using a shRNA for human ataxin-1 (43). Since this mouse model expressed mutant (82 CAG) ataxin-1 at high levels in cerebellar Purkinje cells (44), a recombinant adeno-associated virus serotype 1 (AAV1) expressing shRNA was developed and injected into the cerebella of 7-week-old transgenic mice (43). Following treatment, these mice showed improved motor coordination on the rotarod and normalization of several aspects of the cerebellar pathology, such as reduction of intracellular inclusions and preservation of the integrity of the cerebellar molecular layer (43). A similar approach was also used in a mouse model of HD. Intrastriatal injection of AVV1-exppressing shRNA targeting human huntingtin in 4-week-old HD-N171-82Q mice reduced mutant htt expression and prevented the formation of the disease-associated neuronal inclusions (45). The treatment also had a positive effect in behavior, as treated mice displayed a better motor performance, both in rotarod and in stride length measurements, 3 months after vector injection. However it had no effect on weight loss, a systemic manifestation of disease that is very relevant in patients (45). In a parallel study, AAV5 vectors were used to deliver anti-mutant Htt shRNAs to the striata of R6/1 mice, another model of HD (46). The RNAi treatment revealed to be effective in reducing the levels of mutant HTT mRNA and neuronal intranuclear inclusions. Furthermore, htt gene silencing resulted in a mild improvement of HD-associated behavior abnormalities such as clasping behavior, although it had no effect

on the rotarod performance and body weight (46). Even after the onset of symptoms, transgenic HD mice treated with AVV-shRNA demonstrated an amelioration of HD-induced neuropathology, such as decrease of neuronal aggregates and restoration of DARPP32 expression (47).

Although these studies highlight the potential of RNAi as a therapeutic tool, the translation to the clinics may not be so straightforward; one limitation may be the non-specific ablation of the expression of the normal gene copy, which may compromise cellular function and viability (26). This is important because, even though neurodegeneration in CAG-repeat diseases is thought to be the result of a toxic gain-of-function, some data suggest that a partial loss-of-function also contributes to the disease pathogenesis. A way to overcome this problem is to adopt an allele-specific approach by using RNAi sequences directed at single nucleotide polymorphisms (SNPs) in linkage disequilibrium with CAG expanded alleles (40). In MJD, there is a SNP (G987C) at the 3´end of the CAG tract of the ataxin-3 gene (*ATXN3*) that is in linkage disequilibrium with the disease-causing expansion (48, 49). Worldwide, 70% of MJD patients carry the C variant at this locus (50). Taking advantage of this SNP, Miller and collaborators (2003) were successful in developing siRNA with different vectors that silencing the mutant allele (51). Alves and collaborators (2008) assessed the efficacy and selectivity of this approach *in vivo* by injecting a lentiviral vector encoding human mutant *ATXN3* together with the corresponding shRNA into rat striatum (52). Treated rats showed a decrease in the levels of mutant ATXN3 that was accompanied by a decrease in the formation of disease-associated inclusions and neuronal dysfunction (52). The impact on behavior was not assessed in this study. In SCA7, a shRNA was designed against a SNP localized in the 3´region of ataxin-7 gene (*ATXN7*) (53) and, when expressed in a heterozygous ataxin-7 disease model, not only a significant decrease in the mutant ataxin-7 protein levels and protein aggregation was denoted but also the wild-type protein was normalized to a non-aggregated diffuse cellular distribution, suggesting that allele-specific silencing could counter some of the loss-of-function effect contributing to pathogenesis (54). In HD, several SNPs are present in ~85% of the North-American and European HD patients (55, 56), however the allele-specific siRNAs remains to be evaluated *in vivo* for efficacy and safety. Nevertheless, it was shown *in vitro* that the Δ2642 deletion in exon 58 of the HD gene, a mutation more frequently found (37%) in polyQ-expanded alleles (57), could be targeted by siRNA without affecting its wild-type counterpart (58). This silencing allowed a decrease of abnormal nuclear morphology and rescued caspase-3 activation (58).

Another strategy involves adapting endogenous miRNA-like targeting: mismatch-containing duplex siRNAs complementary to the CAG repeat allowed a highly selective inhibition of mutant HTT expression in

two HD skin cell lines (59, 60). In SCA6, two different approaches were taken. In the first method (gene knockdown and replacement), both mutant and wild-type alleles were inhibited by siRNA, and wild-type protein was restored with a mRNA modified to be resistant to the siRNA (61). The second method took advantage of the fact that in this disease, due to alternative splicing, there is an expression of two distinct and functional $Ca_v2.1$ isoforms that either lack or contain the C-terminal polyQ tract and a splice-isoform-specific(SIS)-RNAi was developed (62). This RNAi selectively suppressed *in vitro* transiently expressed and endogenous polyQ-encoding $Ca_v2.1$ splice variants (62). Nevertheless, given the level of $Ca_v2.1$ silencing, it will be important to test this system *in vivo* in order to assess the extent to which SIS-RNAi targeting of polyQ-encoding $Ca_v2.1$ mRNAs affects overall $Ca_v2.1$ levels.

The fact that allele-specific silencing is conceptually an ideal approach does not necessarily mean that the non-allele-specific approach should not be developed. As examples we have MJD and HD. In spite of the undeniable relevant role of htt in several cellular processes, it was recently shown that the simultaneous silencing of mutant human transgene and endogenous wild-type htt was tolerable and provided beneficial effects in rodent (63, 64) and in nonhuman primate models of HD (65). In the study conducted by Boudreau and collaborators (2009) the miRNA designed and injected in the striatum of HD-N171-82Q mice was able to silencing all htt alleles by 75% (63). Treated animals presented a significant improvement in behavior, although the treatment did not restore body weight. This silencing also lead to transcriptional alterations in more than 400 genes, which is in agreement with the pivotal role of htt in cells. The lentiviral vectors expressing shRNA that targets all htt transcripts developed by Drouet and colleagues (2009) were injected in an acute rat model of HD and a reduction in HD-mediated pathology was observed, namely the partial restoration of striatal gene expression and reduced inclusion formation. Importantly, no apparent evidence of toxicity was observed for up to nine months of treatment (64). In the Rhesus macaque, 45% reduction of htt in the mid- and caudal putamen did not induce motor deficits, neuronal degeneration, astrogliosis, or an immune response (65). In MJD, the non-allele-specific silencing in an acute rat model of MJD lead to a ~80% reduction of mutant ataxin-3-positive inclusions and to the preservation of DARPP-32 expression in the striatum where the mutant protein was overexpressed, although was not demonstrated whether this silencing improved behavior (66). Recently, the same authors used an allele-specific strategy for silencing mutant ataxin-3 in a transgenic mouse model of the disease. This RNAi approach showed beneficial effects in motor and gait impairments and reduced the levels of

soluble and aggregated human ataxin-3 without affecting the endogenous levels of the murine ataxin-3 (67).

The choice of therapeutic silencing effectors is also of importance. Both siRNA and shRNA cause gene silencing but they differ in mode of delivery and persistence. Whilst shRNAs can be expressed from DNA-encoded plasmids to allow incorporation into viruses for long-lasting expression, chemically synthesized siRNAs are delivered as dsRNA duplexes that are targets for nuclease digestion and clearance from the body, making their effects short-lived.

There are viral and non-viral approaches to achieve delivery of RNAi gene silencing molecules. Viral methods include Adeno-associate virus (AVV) and lentiviruses. Because of its relatively low immunogenicity and its ability to exist in a stable episomal form, and thus being less prone to causing insertional mutagenesis within the host genome, AVV has been the most widely used vector for delivery of RNAi contructs for polyQ diseases (68). The long-term silencing of polyQ transgenes trough this approach has been demonstrated in several models. Another advantage of AVV lies in the malleability of the hairpin-expressing promoter, enabling the design of tissue- and cell-specific expression in disease-susceptible tissues (69). Nevertheless, cytotoxicity and neuronal damage have also been recognized. AAV.shHD2.1 injection in mice impaired rotarod performance of wt animals at 10 weeks, although this effect was resolved at 18 weeks (45). Furthermore, both control shRNA (containing mismatches) and shRNA targeting HD caused neuronal cell death associated with increased inflammation in the striatum and resulted in short-term deficits in motor behavior in the mouse (63, 70). This toxicity was maintained even when the dosage was reduced. These toxic effects are thought to be the consequence of a potential interference of shRNA with the endogenous small RNA processing in the case of HD. To reduce shRNA toxicity, an artificial miRNA driven by RNA polymerase II promoter was designed to silence the same HD target and a reduction of the striatal toxicity was observed, while maintaining the same level of HD silencing (70). These studies underscore the need to optimize the currently available RNAi methods in order to achieve a fine adjustment of shRNA expression and to avoid RNAi-related adverse effects. The efficacy of a conditional shRNA expression using lentivirus in a rat HD model, concerning its effects on endogenous htt levels, was demonstrated *in vivo*, although specificity and reversibility were not fully evaluated (64). More recently it was shown that mesenchymal stem cells (MSCs) can also be useful to transfer shRNA molecules to neural cell lines (71). Since MSCs have demonstrated a strong safety profile (immune system modulation, homing

to injury sites, cytokine release into damaged microenvironments), this delivery approach can offer multiple advantages, although several parameters need to be further optimized and tested in *in vivo* models (71).

The use of synthetic siRNAs also offers an alternative approach for gene silencing that avoids the problem of switching off a virally delivered shRNA and circumvents the toxicity associated with specific shRNAs (41). Nevertheless, the fact that they can be easily degraded in vivo by endonucleases and filtered through the renal system, leading to a short half-life, are important disadvantages of siRNAs (72). Paradoxically, this transient effect also makes them attractive due to the resulting ability to regulate treatment; upon any indication of danger adverse effects could be halted by discontinuing treatment (69). Nonetheless, for long-term stability and bioavailability, chemical modifications to the sugars, backbone, or bases of nucleic acids appear to be a successful strategy (73-75). Intraventricular injection of siRNAs against *huntingtin* together with lipofectamine in 2-day-old R6/2 mice had long-lasting effects. Although the silencing of *htt* was almost completely diminished one week after, treated mice showed a stabilization of the body weight, reduced hind-limb clasping, improved open-field behavior and better rotarod retention at ages when symptoms would otherwise have already advanced. The lifespan of treated animals was increased by 14%. Additionally, siRNA induced down-regulation of transgenic htt expression and decreased the density and number of NII in striatal neurons (76). However, delivery of siRNA with a transfection reagent is not a practical means to treat humans because of the neuronal toxicity of most lipid-based transfection agents. In another type of siRNA application, a cholesterol-conjugated siRNA against *htt* was injected into the striatum of an acute HD model generated by intrastriatal injection of AVV vector carrying expanded human HTT fragments. Coadministration of a cholesterol-conjugated siRNA improved neuronal survival, reduced monomer levels and HTT protein aggregation and ameliorated motor deficits (77). No long-term effects or behavioral improvements were measured.

In conclusion, therapy using RNAi for polyQ diseases is promising and may provide beneficial to human patients. Still, several remaining questions or issues related to safety and efficacy of *in vivo* delivery need to be addressed to further advance this technology.

Blocking Cleavage

It has become evident that proteolysis of polyQ proteins is a biologically relevant event. The conformational change in the proteins with expanded polyQ leads to misfolding and may favor proteolytic cleavage into smaller toxic fragments. As a consequence of the cleavage, the resulting fragment could have

an enhanced toxic effect (15, 78) and/or could more easily enter the nucleus and/or more rapidly aggregate (79, 80). This “toxic fragment” hypothesis is strongly supported by evidence, showing that in most polyQ diseases (1) aggregates are mainly formed by small polyQ-containing fragments rather than the full-length polyQ proteins (81-85) and (2) truncated proteins with polyQ expansions appeared more prone than full-length proteins to form inclusions or to cause cell toxicity including cell death by apoptosis (15, 86-88). These reports highlight the importance of post-translational events that occur in polyQ diseases. Furthermore, several polyQ proteins are known to be cleaved by specific caspases, calpains and other proteases (82, 89-94).

The cleavage of mutant htt at the 568 amino acid by caspase 6 has been proposed to be essential for the HD-related behavioral phenotype and selective neuropathology in the YAC128 mouse model of HD. Moreover, caspase-6 resistant mutant htt mice showed a delay in nuclear translocation of expanded htt (95). More recently, a transgenic mouse expressing the N-terminal 586 aa of Htt, a putative cleavage fragment mediated by caspase-6, with a polyQ expansion was generated (N586-82Q). Although these mice showed a behavioral deficit as well as nuclear accumulation of htt aggregates, their phenotype was less severe than that HD mouse models expressing shorter fragments suggesting that the caspase-6 fragment is an intermediate of the cascade leading to disease progression (96). Atrophin 1 is also cleaved by caspases at aspartate 109, and cleavage site mutations reduce nuclear localization, aggregate formation and cytotoxicity (78, 97). Ataxin-7 is cleaved by caspase-7 at amino acid positions D266 and D344. The proteolytic cleavage of polyQ expanded ataxin-7 was related to the formation of inclusions in granule neurons of the cerebellum, transcriptional repression, disruption of nuclear export and subsequent accumulation of N-terminal fragments in the nucleus. Importantly, the caspase-7 cleavage products detected *in vitro* were similar in size to proteolytic cleavage fragments detected in SCA7 transgenic mice (98).

Data from transgenic mouse models and human disease tissues indicate that the pathogenic ataxin-3 is proteolyzed *in vivo*. The detection of a 36-kDa polyQ fragment in a transgenic MJD mouse that was proposed to be closely linked with neurological symptoms and the detection of a similar fragment in brain samples of MJD patients supported this notion (94, 99, 100). Caspases and calcium-dependent calpains are possible cleavage proteases whose actions were reported to increase the aggregation of polyQ expanded ataxin-3 (94, 99, 100). Consistently, Jung and collaborators demonstrated the occurrence of ataxin-3 cleavage in a fly model of MJD and by mutating six caspase sites in the protein there was a delay

in progression of neurodegeneration caused by expanded ataxin-3 protein expression (100). However, a more recent study suggested that aggregation of ataxin-3 is calpain- rather than caspase-dependent since treatment with calpain inhibitors prevented the formation of SDS-insoluble aggregates in MJD patient-specifc neural cultures; the addition of caspase inhibitors had no effect (101). Results from our lab demonstrate that in a *C. elegans* model of MJD, the expression of ataxin-3 bearing 75Qs leads to the formation of protein aggregates in the *C.elegans* nervous system within C-terminal regions, but not in the full-length protein (102). However, no obvious cleavage products were detected in several symptomatic mouse and *C. elegans* models of MJD expressing full-length ataxin-3, suggesting that these cleavage products may not be very abundant in these more "physiological" models (102, 103).

Globally, these data support a model in which proteolysis of polyQ expanded proteins may be relevant in polyQ-expanded toxicity, possibly with seeding effects. With this in mind, development of protease inhibitors that would prevent polyQ proteins into a more toxic form and alter their cellular sub localization could be beneficial. Nevertheless, we must be cautious because by inhibiting these proteases we can deregulate several essential signaling pathways (104, 105); therefore, appropriate validation of these strategies *in vivo* is required.

Blocking aggregation

Although the toxic(s) structure (s) relevant for polyQ diseases remain unknown, many efforts have been made in order to identify compounds that inhibit aggregate formation. This therapeutic approach is based on the premise that by inhibiting protein aggregation there will be a reduction of abnormal interactions and direct toxic effects of the misfolded polyQ proteins. This will in turn reduce the pathogenic stress on cells and normalize intrinsic proteostasis (106).

Small Chemical compounds

Toward developing a pharmacological therapy for the polyQ diseases, numerous screenings for small chemical compounds that inhibit polyQ aggregation have been conducted in the past years.

The first demonstration of the potential of such small compounds arose from the finding that Congo Red, a compound with affinity for proteins with □-sheet-enriched conformations, could interfere with processes of polyQ protein aggregation. The administration of this compound inhibited HD exon 1 aggregation in transiently transfected COS cells (107), modulated aggregate formation in hippocampal

slices from the R6/2 mouse (108) and prevented the assembly of mutant htt into mature fibrils (109). The effect of Congo Red was assessed *in vivo* using the R6/2 model. The treatment was conducted after the onset of symptoms and was able to ameliorate weight loss and diabetes (110). In addition to that, several neurological signs were improved, with preservation of normal gait and stride length, inhibition of the dyskinesia of hindlimbs and better motor performance on the Rotarod test. This treatment also extended life span resulting in a mean survival length of 106 days as compared with 91 days in vehicle-treated mice. Immunostaining of the basal ganglia of treated mice revealed clearance of polyglutamine aggregates, and in the hippocampus there was a moderate reduction in the number of aggregates (110). In a posterior study, however, chronic administration of Congo Red to the same model and before the onset of clinical signs, did not improve either motor or cognitive deficits. There was also no effect on neuronal inclusion load, which might be expected since this compound has a limited ability to cross the brain-blood barrier (BBB).

The same group that detected the potential of Congo red i*n vitro* also developed an automated filter retardation assay for the identification of HD exon1 aggregation inhibitors (111). This assay is based on the finding that polyQ-containing aggregates are resistant to SDS and selectively retained on a cellulose acetate filter, whereas SDS-soluble protein under the same conditions is not. Captured aggregates are detected by immunobloting analysis using specific antibodies (112). Compounds that can reduce the signal intensity of theses aggregates are considered as hit compounds. From a library of 184 000 chemicals, 300 were identified as supressors of polyQ aggregation. Among these chemicals, they found that benzothiazole derivatives, including PGL-135 and riluzole, inhibited htt aggregation *in vitro* and in cell culture (111). However, a further study demonstrated that PGJ-135 was metabolically instable and riluzole, when administered in the R6/2 mouse at the maximum tolerated concentration, could not inhibit aggregation or have a positive impact in the disease phenotype (113).

The automated filter retardation assay was further used to screen a library of natural compounds (114). From a library of ~5000 natural substances, (-)-epigallocatechin-3-gallate (EGCG), a green tea polyphenol, was identified as an inhibitor of htt aggregation *in vitro*. It reduced toxicity and aggregate load in a yeast model of HD and when administered in a Drosophila model of HD, it allowed a reduction in photoreceptor degeneration and motor impairment. This compound seemed to exert its positive effect on aggregation *in vitro* by suppressing the formation of small oligomers and stimulating the formation of larger aggregation species (114).

Nukina and colleagues took a different approach. Since expanded polyglutamine sequences are

insoluble in water, which makes it difficult to prepare polyglutamine-containing proteins in large scale, they established an assay based on large-scale preparation of myoglobin bearing an expanded polyglutamine, to search for inhibitors of protein aggregation (115, 116). Among of ~200 non-toxic chemical compounds that can be administered orally, trehalose showed the strongest inhibitory effect. Trehalose is a naturally occurring non-reducing disaccharide found in many organisms that is synthesized as a stress-responsive factor when cells are exposed to environmental stresses like heat, cold, desiccation, dehydration and oxidation (117, 118). They further demonstrated that oral administration of this compound in the R6/2 mouse model reduced weight loss, striatal atrophy and intranuclear aggregates in the cerebrum and liver (119). In addition, the trehalose treatment also improved motor dysfunction, delayed the onset and reduced the frequency of foot clasping and extended lifespan. This effect was specific since the oral administration of glucose, a potential metabolite of trehalose did not exert any beneficial effect. Furthermore, the detection of trehalose in the brain of homogenates of trehalose-supplemented mice as well as the results from western blot and Immunohistochemistry analysis suggested that the protective effect induced by this compound could be through binding to expanded polyQ and stabilization of the partially unfolded mutant protein (119). Nevertheless, the effects of trehalose may not be solely due to its action as aggregate inhibitor, as trehalose has also been shown to regulate the heat shock transcription factor HSF1 (120) and to activate macroautophagy in a mTOR-independent way to accelerate the clearance of mutant htt (121).

Chemical compounds that target polyQ aggregation have been also identified using cell model-based assays. Pollit and colleagues established a cellular polyglutamine protein aggregation assay based on fluorescence resonance energy transfer (FRET) (122). In a screen for biological active molecules that inhibit inclusion body formation of fluorescently-tagged polyQ proteins in cultured cells, the authors identified Y-27632, a known ROCK inhibitor, as a hit compound. They further demonstrated the therapeutic effect of Y-27632 in a Drosophila model of HD in which it was able to reduced htt-induced neurodegeneration (122). In a posterior study, the efficacy of oral administration of this compound in the R6/2 mouse model was evaluated (123). Y-27632 improved rotarod function in treated mice although it had no effect in the clasping behavior, lifespan, brain weight, gross atrophy, inclusion formation or neuron counts in the striatum. The authors suggested that these results were a consequence of using a sub-saturating dose of Y-27632 (123).

Through a yeast model-based high-throughput screening assay, Kazantsev and colleagues have screened 16,000 chemical compounds for their ability to suppress the cytotoxicity caused by the presence

N-terminal fragment of htt containing 103 glutamines. They identified nine compounds able to increase yeast growth and htt-103Q expression levels. After an optimization for potency, they found that one compound, C2-8, inhibited polyQ-mediated aggregation *in vitro* and brain slices from HD transgenic mice and rescued photoreceptor degeneration in a *Drosophila* model of HD (124). Posterior studies revealed that this compound was non toxic, available orally, had favorable brain pharmacokinetics and had no concerning pharmacological interactions. In addition, C2-8 reduced the decline motor performance in R6/2 mice although it had no impact on weight loss or survival and reduced striatal neuronal nuclear aggregate volume. The authors suggested that this compound can affect aggregate growth but not initiation since it had no effect on aggregate number (125).

More recently, a luciferase-based assay was developed to monitor protein aggregation and disaggregation of polyQ proteins (126). The principle of this assay is based on the fact that the activity of luciferase is lost in the presence of aggregated protein. In that way, huntingtin exon1 containing 72 glutamines was fused to the N-terminal of firefly luciferase (httQ72-Luc) and, since it only aggregates in the presence of expanded polyQ, this reporter system was co-transfected with Q80-cfp in HEK-293 cells. The screening of the Johns Hopkins Clinical Compound Library (over 1500 compounds) revealed the existence of four drugs able to increase luciferase activity by at least 50%. The authors demonstrated that leftunomide and its active metabolite, teriflunomide, inhibited protein aggregation in a dose-dependent manner through prevention of polyQ incorporation into an aggregate protein (126).

Intrabodies

Intracellular antibodies or intrabodies are small, recombinant antibody fragments that target antigens intracellularly via the Fv variable regions, that are responsible for antibody affinity and specificity, but can be selected and engineered as genes, providing a protein-based approach to neutralizing the pathogenic characteristics of toxic misfolding proteins (106).

The intrabody C4, generated from a synthetic phage library, recognizes the 17 N-terminal amino acids of Htt exon1 and was shown to inhibit htt inclusion body formation in non-neuronal cell lines (127) and to prevent mutant htt (mHtt) toxicity in organotypic brain slice cultures (128). Posterior studies demonstrated that this intrabody neutralizes the toxic effects of mhtt by selectively binding to the soluble fraction of mHtt N-terminal fragments, having only weak activity against endogenous full-length mhtt and wild-type htt, possibly due to epitope inaccessibility (129). *In vivo*, in a *Drosophila* model of HD, the

expression of C4 increased eclosion rates, extended lifespan and slowed both neurodegeneration and aggregation although the effect became less robust as the flies aged (130). A similar effect was found with AAV gene therapy delivery of C4 into the striatum of B6.HDR6/1 mice. Treatment initiation at various stages of the disease resulted in a significant reduction in the size and number of htt aggregates, however the treatment was more effective when the delivery of the intrabody was conducted prior to the appearance of mtt aggregates. Furthermore, the neuroprotective effect also weakened with age beyond 6 months; the impact on phenotype was not assessed (131).

V(L)12.3 is another intrabody that targets the N-terminal of Htt exon1 (132). After increasing its efficiency and affinity trough removal of its disulfide bond and mutations, respectively, this intrabody was able to inhibit aggregation and toxicity in a *Saccharomyces cerevisae* model and in a corticostriatal brain slice model of HD (132, 133). However, like C4, V(L)12.3 also increases the level of soluble mutant htt and promotes its nuclear localization which may increase toxicity *in vivo* (133). Indeed, although when co-expressed in a lentiviral model of HD this intrabody improved behavior and neuropathology, it had no effect on the YAC128 HD model and actually increased severity of the phenotype and mortality in the R6/2 HD model. Perhaps the presence of V(L)12.3 prior to the introduction of mHtt may be required in order for this inhibitor to have a therapeutic effect (133), which may limit its clinical application.

There are also intrabodies that target the proline rich region of mutant htt exon1 as well as the polyQ tract. MW7 recognizes the two polyP stretches of htt exon1 gene product (134). It reduced mHtt-induced aggregation and toxicity in cell culture (135) and acute brain slice models of HD (133). Since there was the potential risk of this intrabody also recognizing other cellular proteins containing a polyP domain, intrabodies that recognize the unique P-rich epitope between the polyP domains of were developed and denominated as Happ1 and Happ3 (133). Like MW7, these intrabodies showed a preferential effect on the mutant form of htt and increased turnover without altering localization. However, the Happs were more effective at lower ratios to htt than MW7. *In vivo*, the intrastriatal AVV delivery of Happ1 in several mouse HD models corrected several cognitive and motor deficits as well as neuropathology (133).

EM48 is an intrabody that has affinity for an epitope in the C-terminal of Htt exon1. It suppressed the cytoplasmic toxicity of mHtt in a cell culture model of HD with no impact on nuclear inclusions. When expressed in the striatum of R6/2 and N171-82Q HD mice model via AVV infection there was a reduction in neuropil aggregate formation and improvement of motor performance in N171-82Q mice (136). *In vitro* studies suggested that this intrabody promotes the degradation of cytoplasmic mHtt by increasing its

ubiquitination (136). Intriguingly, and in contrast with this positive effect, intrabodies that target polyQ domains exacerbated the toxicity and aggregation of mhtt, presumably by stabilizing a toxic conformation (127, 135). Currently there are two major problems that should be overcome for the development of intrabodies-based therapies of the polyQ. First, the ratio between the amount of intracellular antibody and the target mutant protein should be taken in consideration and second, the brain delivery issue.

Peptides

Peptides have potential as therapeutic molecules since they are highly specific, selective and relatively low in molecular size, and therefore expected to be easily delivered to the target organs (137). Nevertheless, this therapeutic approach faces some limitations that should be considered, such as low ability to cross the BBB, short half life and difficulties in administration routes.

Based on the knowledge that the monoclonal antibody 1C2 recognizes the altered conformation of abnormal expanded polyQ stretch (138), Nagai and collaborators hypothesized that peptides that selectively bind to pathogenic–length polyglutamine domains might inhibit interaction with other proteins thereby slowing, or preventing disease pathology (139). By combinatorial peptide library screening, the authors identified PolyQ-binding protein 1 (QBP1) as an inhibitor of the toxic β-sheet conformational transition and aggregation of the expanded polyQ *in vitro* (139, 140). Trough a transgenic approach, the ability of this compound to inhibit polyQ aggregation and to prevent neurodegeneration was further demonstrated in a *Drosophila* model expressing a truncated form of ataxin-3. Importantly, there was a rescue of polyQ-induced cell death that allowed a dramatic increase of the median lifespan (141). However, since this peptide is too large to cross the cell membrane and to reach the target polyQ protein efficiently, efforts have been made in order to enable a more efficient intracellular delivery of QBP1. The fusion of protein transduction domains (PTDs) enabled the intracellular delivery of QBP1, inhibited polyQ aggregation *in vitro* and suppressed polyQ inclusion body formation and cytotoxicity in Cos-7 cells expressing 87 glutamines (142) . In the same Drosophila model, oral administration of PTD-QBP1 suppressed polyQ-induced premature death and inclusion body formation (142). However, only when this molecule was administered in the R6/2 mouse model via intraperitoneal injection, did the weight loss phenotype improved, oral administration being ineffective (143). Although it was shown that PTD-QBP1, by virtue of the PTD, was delivered into brain cells, the efficiency of delivery still needs improvement (143).

In order to overcome the problems associated with mode of delivery, pharmacokinetics and efficiency of small molecules and peptides *in vivo*, Chen and collaborators proposed to identify a polyQ-binding small molecule with "drug-like" properties that would have the potential to inhibit the formation of aggregates (144). They generated chemically a library of 60 000 of peptoids (oligomers of N-substituted glycines) that was screened for molecules that specifically bound to an amino-terminal fragment of mHtt protein (144). This screening resulted in the identification of HQP09. This peptoid prevented the aggregation of mHtt *in vitro* and in YAC128 medium spiny neurons (MSN) cultures, stabilized glutamate-Induced Ca^{2+} signals and protected from glutamate-induced apoptosis. *In vivo*, intracerebroventricular delivery of HQP09 to the YAC128 HD model resulted in reduced accumulation of mHtt aggregates and improved motor performance. Nevertheless, this molecule needs further optimization and testing since it has a poor BBB permeability (144).

Recently, another peptide, P42, was found to have beneficial effects in a Drosophila HD model (145). To further test the beneficial effects of P42, Arribat and collaborators tested it in the R6/2 mouse model o HD, using a systemic delivery route of administration. For that, they used a combinatory approach fusing P42 to the protein transduction domain of TAT from HIV, allowing the delivery to living cell via endocytosis. Also, they used a novel water-in-oil microemulsion drug delivery vector called Aonys®, providing a transmucosal (buccal) route of administration. P42 daily administration showed to be safe and improve behavior deficits observed in the R6/2 mice as well as to reduce htt aggregates and astrogliosis (146).

Transglutaminase inhibitors

The relatively increased amount of glutamine in the mutant protein suggested that there is a similarly increased target for transglutaminase (TGase) to form bonds with glutamine and facilitate the aggregation process (147). The observation that TGase is upregulated in the brains of HD patients and of HD mice (148-151) and is recruited into neuronal intranuclear inclusions (151, 152) support this idea. In that sense cystamine, a TGase inhibitor, was tested and shown to ameliorate the behavior and neuropathological severity, reduce mHtt agreggation and extend survival in the R6/2 mouse model (151). In another study, cystamine treatment also improved the mice phenotype although it had no effect in aggregation (149). The effects of cystamine may not be solely due to its action as a transglutaminase inhibitor however, as cystamine has also been shown to inhibit caspase 3 activity and to increase the levels of glutathione (153) and BNDF (154).

1.3.2 Inducing refolding/degradation of mutant protein

Polyglutamine diseases share several common aspects regarding their pathogenic mechanism, namely concerning the involvement of the protein homeostasis mechanisms: misfolding, refolding, degradation and aggregation. The expanded polyQ tract in the causative protein results in a conformational alteration that increases the tendency of the protein to misfold and polymerize – *misfolding* (137). This constitutes a challenge to the cell that will recognize the non-native conformation(s) and attempt to restore the appropriate conformation of the protein, through the action of molecular chaperones – *refolding.* When this system fails, the proteins are sent for *degradation*; the inefficient removal of misfolded proteins leads to a steady-state of increased *aggregation* and possibly to disease.

Cells possess a highly efficient protein quality control machinery to regulate protein homeostasis and to ensure that misfolded proteins do not accumulate (155-157). It is know that these mechanisms are tightly regulated to maintain cellular homeostasis, and this is well demonstrated by the fact that around 30% of newly synthesized proteins do not pass in control checkpoints, being sent to degradation (158). In misfolding diseases there is an imbalance between the capability/activity of this quality control system and the amount of altered proteins in the cells, leading to intracellular accumulation of abnormal proteins. This is reinforced by experimental evidence that overexpression of molecular chaperones in animal or cellular models of these diseases ameliorated polyQ toxicity (159-162). Cells have three main lines of defense against misfolded/aggregated-prone proteins: (i) molecular chaperones, (ii) the ubiquitin-proteasome system (UPS) and (iii) autophagy.

Stimulating refolding and degradation pathways that preferentially target misfolded proteins or direct targeting of polyQ aggregation has been a focus of therapeutic development for several years.

(i) Molecular Chaperones

Molecular chaperones are crucial for the maintenance of native protein conformation and recent research has shown that defective chaperone action *per se* may have pathogenic consequences (163-165). Most of the chaperones belong to the family of Heat shock proteins (Hsps) with the ability to recognize misfolded species such as expanded polyQ proteins and act by correcting their abnormal folding (162, 166, 167). Several studies have shown that chaperones have a protective effect on polyQ aggregation and neurodegeneration. For example, it was shown that htt expressed in mammalian cells formed oligomers and aggregates, that were decreased in cells overexpressing HSC70, suggesting that this complex prevents

polyQ toxicity by reducing the amount of soluble oligomers/aggregates in living cells (168). Also, it was demonstrated that Hsc70 and its co-chaperone Hsp40 inhibits HttEx1Qn aggregation in a polyQ-dependent manner, as Hsc70 is a molecular interactor of huntingtin exon 1 fragment (169).

In a cellular model of SCA1, overexpression of the chaperone HDJ2/HSDJ (a human HSP40 homologue) was able to decrease ataxin-1 aggregation, whereas overexpression of Hsp70 was shown to suppress neuropathology and improve motor function in a SCA1 mouse model (170, 171). Interestingly, overexpression of Hsp70 was also able to suppress polyQ toxicity in a *Drosophila* MJD model, although without a visible effect on aggregation (160). The protective role of chaperones was also shown in other MJD *Drosophila* model, where the overexpression of two Hsp40s, DNAJ-1 and DNAJ-2, suppressed the aggregation of mutant ataxin-3 (172). MJD progression was accelerated by genetic reduction of the co-chaperone and ubiquitin ligase CHIP (C-terminus of Hsp70-interacting protein), which also lead to increased levels of ataxin-3 microaggregates in a transgenic mouse model (161). These results suggest that increasing CHIP activity could be a possible therapy for MJD and other polyQ diseases. Recently, in a *Drosophila* MJD model, was demonstrated that ataxin-3 interacts with Rad23 leading to increased levels of the co-chaperone DnaJ-1 and depends on it to exert neuroprotection (173) In a SBMA cell model, it was demonstrated that overexpression of Hsp70 and Hsp40 increased expanded repeat AR solubility and decreased the half-life of expanded repeat AR (174). Overexpression of these two chaperones could also suppress aggregate formation and apoptosis in a neuronal cell model of SBMA (162). The first *Drosophila* model was very recently generated for SCA6 where it was shown that DnaJ-1 reduced the nuclear localization of the mutant protein as well as the mutant protein aggregates (175).

HSF-1 is the major regulator of the heat-shock response (HSR) in mammalian cells (176). Hsp90-containing HSF-1 complexes are present in the unstressed cell and dissociate during stress allowing dislocation of this transcription factor to the nucleus where it exerts its effects, initiating expression of several molecular chaperones. This includes Hsp90, which will contribute to terminating this stress response in a classic negative feedback loop. Therefore, Hsp90 by itself and/or associated with multichaperone complexes, is a major repressor of HSF-1 (177). In that sense, pharmacologic inactivation of Hsp90 leads to the overexpression of several molecular chaperones activating the Heat Shock Response (HSR) via HSF-1 (177, 178). Hsp90 is an ATP-dependent molecular chaperone and Hsp90 inhibitors mimic the unusual ATP structure adopted in the chaperone's N-terminal nucleotide-binding pocket and cause potent and selective blockade of ATP binding/hydrolysis, inhibiting chaperone function (179).

Potent Hsp90 inhibitors, such as 17-AAG or 17-DMAG, have been shown to reduce aggregate load and toxicity in cell, fly, *C. elegans*, mouse brain and slice culture models of neurodegeneration dependently on HSF-1 (102, 180-185). These two compounds have also shown beneficial effects in a SBMA mouse model (184, 186). 17-AAG was the first Hsp90 inhibitor studied in clinical trials for cancer therapy; since Hsp90 is responsible for the stability of several signaling proteins, including mutated, chimeric, or overexpressed signaling proteins which enable cancer cell growth, survival or both, inhibiting Hsp90 could lead to inactivation, destabilization and eventually degradation of Hsp90 client proteins (187, 188). Despite its high potency, 17-AAG showed poor solubility and stability and demonstrated moderate toxicity in several clinical trials (189). This compound is able to increase the efficacy of other drugs, being for this reason in phase III of clinical trials (190). Since Hsp90 inhibitors showed to have a big potential, new synthetic inhibitors were designed (191, 192). Chemical compounds such as BIIB021 demonstrate to be more potent compared with 17-AAG (193); this compound is currently in phase II clinical trials for solid tumors. Other Hsp90 inhibitors identified include PU3, presenting better solubility than 17-AAG, but less potency (194) and NVP-AUY922, which entered clinical trials (phase I/II) and demonstrate early success in cancer field (195, 196). In fact, NVP-AUY922 was recently tested in HdhQ150 embryonic stem cells and showed to reduce the levels of soluble full-length mHtt (197). HSP990, another Hsp90 inhibitor, currently under clinical trials (phase I) in advanced solid tumors to test dosage, efficacy and tolerability, was shown to improve motor performance, aggregate load in a transgenic mouse model of Huntington disease (198). Recently, ethoxyquin (EQ), an antioxidant, was tested in peripheral neuropathy caused by paclitaxel, a common chemotherapeutic agent used in solid tumors (199). In this study the authors showed that EQ is able to inhibit Hsp90 activity and found that ataxin-2 is a client protein of this action. Furthermore EQ was shown to be neuroprotective in DRG cell cultures previously treated with paclitaxel (200). Based on these studies, Hsp90 seem to be a good therapeutic target for neurodegenerative disease; taking this, Ernst and colleagues suggested that Hsp90 inhibition should take in consideration the four different Hsp90 isoforms. Inhibition of the specific cytosolic isoforms (α and β) appears to be sufficient to reduce mutant huntingtin protein levels (201). Compounds that selectively inhibit Hsp90 (α and β) versus the endoplasmic reticulum (GRP94) and the mitochondrial (TRAP1) versions of this chaperone might confer a beneficial effect. This selectivity may also offer the opportunity to generate more well tolerated Hsp90 inhibitors (201)

These studies provide good evidence of the beneficial role of increasing chaperone levels in polyQ diseases.

(ii) Ubiquitin-proteasome system (UPS)

The UPS is an evolutionarily conserved pathway that controls the levels of critical proteins and is responsible for the degradation of misfolded or irreversibly damage proteins (reviewed in (202). This pathway is tightly regulated and involves two main steps: the selective polyubiquitylation of a given substrate and the indiscriminate proteolysis of the protein inside the proteasome core (203). Protein aggregates are a common feature of polyQ diseases (204, 205) and often these aggregated species are immunoreactive for ubiquitin, and for proteasome components (206-208). This co-localization led to subsequent studies regarding the involvement of UPS dysfunction in polyQ disorders. However, is still under debate whether UPS impairment is a cause or a consequence in neurodegenerative disorders. For example, a study suggested that accumulation of mutant htt in cells, transgenic mice and HD patients brains, drives the formation of aggregates as a consequence of age-related UPS dysfunction (209). Also, a decrease in synaptic UPS activity was shown in cell and mouse models of HD, suggesting the importance of the UPS in the synaptic dysfunction and selective neuropathology observed in HD (210). Supporting this, impairment of the UPS was shown in a cellular model, upon polyQ aggregation, even before inclusion formation (211). In contrast, more recent studies in different HD mouse models suggested that mutant htt does not impair the UPS (212) and globally no impairment of the UPS activity was found in the brain of the R6 (1 and 2) mouse models of HD (213). Also, in a mouse model of SBMA a well-preserved proteasome function was shown (185).

Recently several studies were performed in an attempt to further explore the UPS involvement in polyQ diseases. For example, in MJD, it is thought that the UPS may be involved in the disease pathogenesis. Support to this theory is given by the interaction of ataxin-3 with parkin – an E3 ligase - (214, 215), with the C terminus of Hsc-70-interacting protein (CHIP) (216), with valosin-containing protein (VCP) (217), as well as with proteasome components (218). It was suggested that mutant ataxin-3 has increased affinity for VCP, preventing the assembly of the VCP/Ufd1-Npl4 complex, responsible for the retrotranslocation of proteins from the endoplasmic reticulum to the cytoplasm, where ubiquitylated proteins are degraded by the proteasome (219). The ubiquitin ligase CHIP interacts with chaperones to promote the degradation of misfolded proteins (220). As mentioned before, ataxin-3 interacts with CHIP, although the functional meaning of this interaction is mostly unknown. Recently, it was shown that the ubiquitin-conjugating enzyme Ube2w is responsible for CHIP monoubiquitylation and that this ubiquitylation stabilizes the interaction of CHIP with ataxin-3 (216). The dynamic interaction between ataxin-3 and CHIP

is disturbed in the context of expanded-polyQ ataxin-3, since mutant ataxin-3 has increased affinity for CHIP compared to wild-type ataxin-3 (221); this increased affinity may result in increased CHIP degradation and consequent impairment of protein quality control mechanisms. Accordingly, an increased affinity of mutant ataxin-3 for parkin – an E3 ligase responsible for a familial form of Parkinson disease (222) was demonstrated, resulting in increased parkin degradation (215), which correlated with decreased parkin levels found in a mouse model of the disease (223).

Although the involvement of the UPS in polyQ diseases is still under debate, its modulation has been taken as therapeutic target for these pathologies. Amiloride and its derivate, benzamil, known to increase UPS activity, reduced polyQ aggregation and toxicity in HD models (224). As mentioned before, in a HD *Drosophila* model, Y-27632 - an inhibitor of the Rho-associated kinase p160ROCK lead to reduction in polyQ toxicity (122). Interestingly, this compound increased UPS activity and also increased macroautophagy; this particular effect of modulating the two main cellular degradation pathways, led to reduced levels and reduced aggregation of mutant huntingtin and ataxin-3 in cellular models (26). USP14 is a deubiquitylating enzyme (DUB) associated with the proteasome that blocks the degradation of ubiquitylated substrates. Mutations in specific ubiquitin-specific protease 14 (USP14) have previously been linked to neurodegenerative disease, and loss of USP14 leads to an ataxic neurological phenotype in mice (225). Supporting this, neuronal expression of USP14 was able to reverse the motor symptoms observed in ataxic mice (226). However, recent work described the inhibition of ubiquitin-protein conjugate degradation by USP14. In cellular models, a USP14 inhibitor, IU1, indirectly accelerated proteasomal degradation of proteins, such as tau and ataxin-3 (227). Because polyQ diseases are associated with accumulation of misfolded proteins, it has been proposed IU1 or other small molecule USP14 inhibitors may be used to increase the clearance of these toxicity-causative proteins and improve the prognosis in neurodegenerative diseases.

(iii) Autophagy

Macroautophagy, commonly referred as autophagy, is an important process for the bulk degradation of proteins and organelles and plays a major role in cellular stress conditions such as nutrient deprivation and infection (228). During nutrient starvation, increased levels of autophagy lead to the breakdown of non-vital components and the release of nutrients, ensuring that vital processes can continue (229). Autophagy it is also involved in neuronal and astrocytic cell survival and function, as demonstrated in

cerebral ischemia and/or reperfusion models, where physiological levels of autophagy, caused by mild hypoxia or ischemia, appear to be protective. In contrast, high levels of autophagy, caused by severe hypoxia or ischemia and/or reperfusion, may cause self-digestion and eventually neuronal and astrocytic cell death (230). Initiation of the process of autophagy begins with the formation of double-membrane structures called autophagosomes that fuse with lysosomes (autolysosomes) and lately degrade their contents by lysosomal hydrolytic enzymes (231, 232). Autophagy serves to recycle cytoplasmic proteins in normal conditions, and generate nutrients necessary under starvation status. Mice lacking *Atg7* (autophagy-related 7 gene) specifically in the central nervous system demonstrated behavioral deficits, such as abnormal limb-clasping and motor uncoordination, and died prematurely. *Atg7* deficiency caused massive neuronal loss in the cerebral and cerebellar cortices. Polyubiquitylated proteins accumulated in the neurons of these mice as inclusion bodies which increased in size and number with ageing (233). Another study using mice deficient for *Atg5* (autophagy-related 5 gene) specifically in neurons, showed that these animals developed motor deficits and it was possible to observe abnormal intracellular proteins that accumulated and formed aggregates and cytoplasmic inclusion bodies in neural cells. These results suggest the importance of basal autophagy for preventing the accumulation of abnormal proteins that can lead to neurodegeneration (234).

The fact that accumulation of misfolded proteins in the cell is a common mechanism in several neurodegenerative disorders (235), makes autophagy a prominent target for the treatment of such diseases; these include Alzheimer disease (AD), Parkinson's disease (PD), Amyotrophic Lateral Sclerosis (ALS), Huntington's Disease (HD), Machado-Joseph disease (MJD/SCA3) and other polyQ diseases (236-248). Autophagy is modulated by several mechanisms, being directly regulated by the mammalian target of rapamycin (mTOR), as a negative regulator (249). Lentiviral vector-mediated overexpression of beclin-1, important for autophagosome formation, was shown to be protective in neuronal culture and a lentivirus-based rat model of SCA3 (246). Drugs that potentially modulate autophagy are increasingly being used in clinical trials, and screens are being performed for the discovery of new drugs that induce autophagy. Administration of rapamycin to different animal models of neurodegenerative disorders was demonstrated to be beneficial by enhancing autophagy function (231, 238, 245, 250, 251). Autophagy can also be regulated independently of mTOR, which can be achieved through lithium, sodium valproate and carbamazepine, compounds that lower myo-inositol-1,4,5-triphosphate levels (252, 253).

Another compound that is able to induce autophagy independently on mTOR is Rilmenidine, used in clinics as an anti- hypertensive agent (254, 255). Rilmenidine was shown to induce autophagy, attenuate the symptoms of disease observed in these mice and diminish the levels of mutant htt in a transgenic mouse model of HD (256). As rilmenidine is used chronically in hypertension, it is considered a safe compound for chronic use (257), which makes it a very interesting drug for therapeutic approaches in polyQ diseases. It is important to identify new safe autophagy inducers to be used in chronic treatments. As already mentioned, it was shown that trehalose has also the ability to induce autophagy independently on mTOR pathway, and enhance the clearance of autophagy substrates such mutant htt and mutant α-synuclein (121). Recently a small molecule screen in yeast identified new molecules that are able to enhance autophagy (258, 259). The authors identified small molecules that are suppressors of the effects of rapamycin – small-molecule inhibitors of rapamycin (SMIRs) – and enhancers of these effects – small-molecule enhancers of rapamycin (SMERs). These molecules, were further tested in mammalian cells. From this screen, three SMERs (10, 18 and 28) appear to be interesting, since they could enhance the clearance of mutated α-synuclein in a cellular model. Furthermore, the combination treatment with these SMERs and rapamycin dramatically enhanced the effects of rapamycin (or the SMER) alone on mutated α-synuclein clearance (259).

1.3.3 Increasing histone acetylation

Transcriptional deregulation is a unifying feature of polyQ disorders (260-265); however, the relationship between polyQ-induced deregulation of gene expression and the ongoing degenerative processes remains unclear.

More than 20 nuclear proteins relevant to transcription are known to interact with polyglutamine disease associated-proteins (261, 266). Mutant polyQ proteins have been shown to interact abnormally with proteins involved in the transcription machinery, namely the CREB-binding protein (CBP), p300/CREBBP associated factor (PCAF), TATA-binding protein (TBP), TAFII130, and SP1 (261, 265, 267). Overexpression of some of these transcription regulators was shown to overcome polyQ toxicity, both in cellular models for MJD, SBMA, and HD (262, 267) as well as *in vivo* in a polyQ model in Drosophila (263). This suggests that expanded polyQ proteins may contribute for the depletion of key transcriptional regulators with toxic effects to the cell and reinforces the idea of an important role for transcription deregulation in polyQ pathogenesis.

Many proteins that interact with polyglutamine disease associated-proteins are distributed around the core transcription machinery, which is now also known to exert DNA methylation, histone acetylation and RNA modification simultaneously (reviewed in (268)). CBP has attracted attention because it is a representative co-activator that possesses HAT (histone acetyltransferase) activity and interacts with numerous transcription factors, and its abnormal binding to disease proteins should affect the expression of a wide range of genes. Several polyQ-protein interactors have acetyltransferase activity. Acetylation of histones relaxes the DNA structure promoting transcription, whereas hypoacetylation represses gene activity (269). The equilibrium of histone acetylation/deacetylation is controlled by histone acetyltransferases and deacetylases (HDACs). HATs can be divided in two groups: HAT A and HAT B, based on cellular localization and mechanism of action. The proteins of the HAT A family are found in the nucleus where they transfer the acetyl group from Acetyl-CoA to an ε-NH_2 group of histone N-tails after the assembly into nucleosomes, whereas the HAT B members are present in the cytoplasm and transfer the acetyl group from Acetyl-CoA to an ε-NH_2 group of free histones prior to their deposition on the DNA (270). Many transactivation factors possess HAT activity. Mammalian HDACs are a family of 18 proteins divided in four classes based on structural and functional similarities: class I (HDACs:1, 2, 3, 8), Class IIa (HDACs: 4, 5, 7, 9), class IIb (HDACs: 6, 10), class III (sirtuins 1-7) and HDAC11 as the only member of class IV (271).

Thus, the current conceptual model is that polyQ proteins may be toxic by their direct inhibition of the acetyltransferase activity of transcription regulators, leading to diminished gene expression. The reactivation of the deregulated gene transcription, in particular by targeting histone acetylation using different compounds, albeit conceptually a very unspecific approach, is a growing field of research. In fact, treatment of polyQ disease models with HDAC inhibitors has been shown to ameliorate the disease phenotype and to decrease cell degeneration, with the increase of histone acetylation and consequent transcription activation (272-277).

Sodium butyrate (SB), an HDAC inhibitor, was tested in several polyQ diseases and shown to be beneficial (273, 275, 278). Pharmacological treatment using SB to modulate transcription significantly extended survival, improved body weight and motor performance, and delayed the neuropathological damage in a transgenic mouse model of HD, with an increase in histone acetylation (273). A transgenic mouse model of SBMA was also treated with SB and the authors were able to demonstrate an improvement in neurological phenotypes, as well as increased acetylation of nuclear histones in neural tissues. The therapeutic effects observed were obtained within a narrow range of SB concentrations (2, 4, 8, 16 and 40

g/L were tested and SB was only beneficial at 4 and 8 g/L), indicating the importance of the dosage used for this type of studies (278). Biochemical analysis of a DRPLA transgenic mouse model revealed hypoacetylation of histone H3 in brain tissue, indicating a global gene repression. Treatment of this mouse with SB rescued the histone hypoacetylation as well as the motor phenotype observed in this model; the treatment also extended lifespan of this transgenic mouse model (275). In a conditional pan-neuronal *Drosophila* model of SCA7, histone acetylation was found to be globally decreased and this mechanism of pathogenesis was further explored in primary neuronal cultures, where treatment with SB improved survival time of the neurons, indicating this small molecule as a good candidate for studies in higher models (279). Chou and colleagues demonstrated a hypoacetylation of H3 and H4 and a transcriptional downregulation in the cerebellum of a SCA3 mouse model when compared to wild-type animals (280). Recently, these authors used SB as therapeutic agent in this SCA3 mouse model, and observed that pre-symptomatic daily administration of SB was able to revert histone hypoacetylation as well as the transcription donwregulation. SB treatment also delayed the ataxic symptoms, improved neurological phenotypes and increased survival of SCA3 transgenic mice (276).

Suberoylanilide hydroxamic acid (SAHA or vorinostat), is a potent HDAC inhibitor (acting preferentially on class I HDACs and HDAC6) that acts on gene expression and is an inducer of growth arrest, differentiation and/or apoptotic cell death in transformed cells, *in vitro* and *in vivo* (281-285). SAHA treatment of a transgenic mouse model of HD showed beneficial effects in the motor phenotypes observed in this model, and partial rescue of striatal neuron loss; the authors demonstrated that SAHA is able to cross the blood brain barrier, a common challenge in the field, and that it is able to increase acetylation in the brain (274). More recently, the same group demonstrated that SAHA is also a HDAC class IIa inhibitor. They showed that HDAC2 and HDAC4 were decreased after SAHA treatment in the cortex and brainstem at the protein level but not at mRNA level (286). The authors speculate that the mechanism by which SAHA reduces HDAC4 is through RANBP2-mediated proteasome degradation, as determined for cancer cell lines (286, 287).

Table 2. Summary of the most relevant side effects observed for compounds tested in non-human and human trials (drugs.com). The side effects presented in this table are the most common symptoms and might not occur in all population. Compounds currently in human clinical trials for polyQ diseases (clinicaltrials.gov). Date of search: June 2015.

Pathway	Compound	Most common side effects	Clinical trials (In polyQ)
Inducing refolding/ degradation of mutant protein	17-AAG	Nausea, vomiting, fatigue and liver enzyme disturbances, ocular disturbances	not yet
	17-DMAG	Diarrhea, fatigue, headache, arthralgia, náusea	not yet
	Amilorade	Hyperkalemia, diarrhea; headache; loss of appetite; nausea; weakness.	not yet
	Rapamycin	Acne; constipation; diarrhea; headache; joint pain; nausea; stomach pain; dyspnea; hypertension	not yet
	Lithium	Drying or thinning of the hair; hair loss; mild hand tremor; mild loss of appetite; mild thirst; mild tiredness; ataxia; temporary, mild nausea and general discomfort at the beginning of treatment	Phase II (SCA2, NCT00998634); Phase II/III (SCA3, NCT01096082); Phase I (SCA1, NCT00683943); Phase II (HD, NCT00095355)
	Carbamezapine	Dizziness; drowsiness; dry mouth; nausea; unsteadiness; vomiting.	not yet
	Valproate	Change in appetite; constipation; diarrhea; dizziness; drowsiness; hair loss; headache; indigestion; mild pain or redness at the injection site; nausea; stomach cramps or pain; trouble sleeping; vomiting; weakness; weight changes.	not yet
	Rilmenidine	Very rare side effects	not yet
	Trehalose	gastrointestinal symptoms	not yet
Promoting histone acetylation	Phenylbutyrate	Bad taste in mouth; body odor; decreased appetite; absent or irregular menstrual periods.	SCA3 (phase II, NCT01096095) and HD (phase II, NCT00212316)
	SAHA/vorinostat	Constipation; cough; diarrhea; dizziness; dry mouth; fatigue; hair loss; headache; loss of appetite; muscle aches; nausea; taste changes; vomiting; weight loss	not yet
	Mithramycin	Anorexia, nausea, vomiting, diarrhea, and stomatitis, headache, fever, weakness, lethargy, malaise, and drowsiness	not yet
	Rolipram	Low blood pressure, dry mouth, constipation, altered sleep cycle, vomiting, headache, chest pain, afternoon drowsiness, reduction in alcohol tolerance, fainting, weight gain, orthostatic hypotension, sexual dysfunction, stiff neck, nausea, palpitations, sweating, chills, flushing, pallor and fear.	not yet

Table 2 (continued). Summary of the most relevant side effects observed for compounds tested in non-human and human trials (drugs.com). The side effects presented in this table are the most common symptoms and might not occur in all population. Compounds currently in human clinical trials for polyQ diseases (clinicaltrials.gov). Date of search: June 2015.

Pathway	Compound	Most common side effects	Clinical trials (In polyQ)
Neuroprotection	Creatine	Stomach pain; nausea; diarrhea and muscle cramping	HD (phase III, NCT00712426)
	Co-enzyme Q10	Diarrhea; loss of appetite; nausea; stomach upset; trouble sleeping.	HD (phase III, NCT00920699; NCT00608881)
	Nicotinamide	Diarrhea; dizziness; headache; itching; nausea; stomach upset; temporary feeling of warmth or flushing of the skin.	not yet
	TUDCA	Constipation; diarrhea; dry skin; gas; headache; indigestion; metallic taste; muscle or joint pain; nausea; skin rash; stomach pain; swelling; tiredness.	HD (phase I, NCT00514774)
	N-acetylcysteine	Cold; clammy skin; drowsiness; fever; inflammation of the mouth or tongue; nausea; runny nose; vomiting.	not yet
	Dantrolene	Decreased grip strength; diarrhea; dizziness; drowsiness; general body discomfort; lightheadedness; muscle weakness; nausea; pain or redness at injection site; unusual tiredness; weakness.	not yet
	Riluzole	Abnormal skin sensations around the mouth; diarrhea; dizziness; drowsiness; headache; loss of appetite; muscle weakness; nausea; stomach pain; vomiting; weakness.	HD (phase III, NCT00277602)
	Remacemide	Lightheadedness, dizziness, vomiting, nausea and gastrointestinal disturbances	HD (*)

(*) A randomized, placebo-controlled trial of coenzyme Q10 and remacemide in Huntington's disease. Neurology. 2001;57:397–4.

Another histone deacetylase inhibitor, phenylbutyrate, improved survival, and attenuated gross brain atrophy and ventricular enlargement in N171-82Q HD transgenic mice (81). On the other hand, inhibition of histone H3 methylation by mithramycin lead to an increase of the lifespan and improvement in motor performance and striatal pathology of R6/2 mice (288). Another drug shown to alleviate the transcriptional dysfunction is the phosphodiesterase type IV inhibitor rolipram, proposed to act by increasing the phosphorylation and activity of CREB. R6/2 HD mice treated with rolipram showed an extension in lifespan as well as an improvement of the neuropathology and a slowed progression of neurological phenotype. Interestingly, the expression of BNDF, which is impaired in HD (289, 290), was induced in treated mice through restored function of CREB (291). In another study, it was shown that rolipram also prevented the sequestration of CBP into nuclear aggregates (292). HDACi 4b, that preferentially targets HDCA1 and HDCA3, was extensively tested in models of disease (reviewed in (293)). Early studies showed that HDCAi 4b was able to improve the body weight loss, strial volume reduction and motor impairments in the R6/2 mouse model of HD (294). Accordingly, later studies also showed that HDCAi 4b could improve the striatal volume loss and clasping behavior in two different model of HD (295). Combinatory treatment using HDCAi 4b and a related inhibitor (HDCAi 874) was shown to reduce mutant huntingtin aggregation in several brain regions (296).

In spite of the promising results obtained using HDCA inhibitors in the context of polyQ diseases, this strategy lacks specificity (297-300) and knowledge on their actual mechanism of action is lacking; furthermore, not all HDCA inhibitors have the same protective activity. These issues hamper the translation of promising findings in the laboratory context, to the clinical application. Their chronic use in humans, using the currently available molecules, might be limited by the existence of several toxic effects (Table 2). Furthermore, since the specific targets of HDACs are not known, it will be very hard to restructure these compounds to reduce their toxicity. From a pharmacokinetic perspective, most of the HDAC inhibitors in clinical phase I studies have a short half-life in plasma (2-8 hours) and the collateral effects found included fatigue, somnolence, confusion and diarrhea, thus limiting therapeutical applications (301-304). Nevertheless, it is conceivable that, if one single therapeutic agent has limited potential because of its side effects, the combination of drugs might be a useful strategy in the attempt of obtaining maximal therapeutic effects at lower dosages, thus reducing undesired symptoms (305). Additionally, and given the increasing knowledge on HATs and their function in neuronal survival, the stimulation of acetyltransferase function emerges as a new therapeutic possibility in the fight against neurodegenerative disorders (306).

1.3.4 Neuroprotection

Although progressive accumulation of specific protein aggregates is a defining feature of polyQ diseases (307), the specific mechanisms by which mutant proteins cause neuronal dysfunction and eventually cell death are not well understood. Evidence for mitochondrial deficits, oxidative stress and excitotoxicity, all of which might cause neuronal death have been found in different models of polyQ diseases. These three main mechanism may act separately or cooperatively to cause neurodegeneration (308).

Metabolic deficits of neurons can be caused by mitochondrial neurotoxins, such as carbon monoxide, 3-nitroproprionic acid (3-NP), MA, MPTP and others. Neurons are highly energy-demanding cells and the synthesis of ATP occurs mainly in the mitochondria, therefore, mitochondrial poisoning results in ATP depletion, which can be cytotoxic. Evidence supporting these facts came from the study where 3-NP was administered systemically to rats causing cytotoxicity mainly in the striatum (309). Cerebral studies using F-18 fluorodeoxyglucose positron emission tomography (FDG-PET) showed decreased cerebral metabolic rates for glucose, providing strong evidence for metabolic deficits in HD patients (310-313). Increased lactate levels were also detected in HD patients using imaging methods (314). Reduced concentrations of creatine and phosphocreatine have been observed in the basal ganglia of HD patients (315); there are also descriptions of a decrease in mitochondrial electron transport enzymes in HD postmortem tissue (316), such as cytochrome C oxydase I (317), reinforcing the idea that oxidative stress and mitochondrial dysfunction could be implicated in polyQ pathogenesis (318). Moreover, it was recently shown that mtDNA damage can be an early biomarker for HD neurodegeneration (319) since increased amounts of mtDNA deletion were observed in leucocytes of HD patients (320). Recently, a study using a transgenic mouse model of MJD also revealed a decreased mtDNA copy number in affected brain regions, that was aggravated with age, and also the accumulation of mtDNA 3867bp deletions, particularly in the initial stages of the disease (321). This is agreement with findings in MJD patients' samples and in cells expressing mutant ataxin-3, which also showed decreased mtDNA copy number and an accumulation of mtDNA deletions (322).

Several defects in the activities of the mitochondrial respiratory chain were also found in polyQ diseases. For example, defects in complex II/III were found in the striatum of HD patients (323). A proteomic approach in the striatum of R6/2 mouse model (324) and in the striatum of HD patients (325), has lead to the identification of reduced levels of aconitase due to increased oxidative damage. Aconitase is

vulnerable to free radicals and the decrease of aconitase activity is more prominent than the activity of the complex II/III when cells are exposed to stress. Furthermore, an important mediator of mitochondrial biogenesis, PGC-1α, was shown to be downregulated in HD patients and in animal models of the disease (326, 327). Abnormalities of mitochondrial permeability transition pore (mPTP) and calcium handling might be also relevant for polyQ pathogenesis. It was shown that mutant htt accumulates in mitochondrial membranes and that mitochondrial calcium is defective when normal mitochondria are incubated with a fusion protein containing a long polyQ tract (328). These results suggest that the polyQ tract, common to all polyglutamine diseases, is directly responsible by mitochondrial calcium-handling defects. It was also demonstrated that lymphocyte mitochondria from HD patients present a lower membrane potential (329) and depolarize at lower calcium loads than controls (330). Mitochondria isolated from striatum cells expressing mutant htt (331) and from muscle of R6/2 transgenic mice (332), showed induced mPTP opening and disruption of mitochondrial calcium homeostasis. PolyQ expansions cause multiple cellular alterations, leading to an early increased resistance to calcium in mitochondria, that undergo compensatory changes in calcium sensitivity (333) in an age-dependent manner. Comparing mitochondrial respiratory function from R6/2 mice with 12 weeks of age and transgenic animals with 12 months, the later shows higher respiratory control ratios and exhibits increased resistance to calcium loading; however when challenged with energy-demanding stimuli, the neurons from these old mice are more vulnerable to calcium deregulation (334). Dantrolene, a ryanodine receptor antagonist and clinically relevant Ca^{2+} signaling stabilizer, was shown to be beneficial in a transgenic mouse model of HD. After glutamate exposure in striatal cells, it was possible to observe an increase in Ca^{2+} release from intracellular stores; pre-treatment with dantrolene protected these cells from glutamate excitotoxicity. Feeding transgenic animals with dantrolene also improved motor deficits (335). This benefic effect was also possible to observe in models of other polyglutamine disorders, such as spinocerebellar ataxia type 3 and 2 (336, 337). Together, these studies indicate that mitochondrial impairment and energy dysfunction might play a role in HD and perhaps in the other polyQ disorders, and that any treatment that might serve to buffer intracellular energy stores may delay the onset and/or progression of HD pathogenesis.

Oxidative stress might also play a role in polyQ disorders, given by the increased levels of 8-hydroxydeoxyguanosine (8- OHdG), an oxidized DNA marker, in HD patients' brains (323). Similar results were found in the striatum and forebrain of the R6/2 mouse model of HD at 12 and 14 weeks of age (338). Also, markers for lipid peroxidation were found to be increased in HD brains (339) and in the R6/2

mouse model (340). There are also observations of decreased antioxidant enzymes SOD and the oxidized form of glutathione in post-mortem HD brain (341). A reduction of Zn/Cu-superoxide dismutase (Cu/Zn-SOD) was found in R6/1 HD transgenic mice at 35 weeks of age, when these animals present a severe phenotype (342). This reduction in Zn/Cu-SOD was also found in erythrocytes of HD patients (320). A study in MJD, using SK-N-SH and COS7 cells stably transfected with full-length ataxin-3 with 78 polyglutamine repeats demonstrated a significant reduction in the ratio of GSH/GSSG and total glutathione content (GSH + 2x GSSG) in mutant MJD cells compared with the wild-type cells, under normal or stressful conditions. It was also shown in the same study that both cell lines had lower activities of catalase, glutathione reductase, and superoxide dismutase (322). Interestingly, another study showed that wild-type ataxin-3 and the forkhead box O (FOXO) 4 interact, activating the transcription of the SOD2 gene. Mutant ataxin-3 demonstrated a reduced capability to activate FOXO4-mediated SOD2 expression, therefore compromising the antioxidant activity of cells (343). Conversely, some evidence suggests that oxidative stress could promote mutant huntingtin (htt) aggregation and cell death by impairing proteasomal function (344) and that this toxicity promoted by mutant htt could be suppressed by overexpression of Hsp27 in a cellular model of HD (345). This suggests that increased oxidative stress, metabolic deficits and mitochondrial abnormalities likely play a role in polyQ diseases. Therefore, therapeutic agents targeting these pathways could be beneficial for these patients. Several compounds have been tested and shown to have an impact in patients, and some of them are currently under clinical trials.

Bioenergetic supplements, such as creatine, were shown to be beneficial for HD mice (346, 347), however a one-year study of creatine intake by HD patients did not improve functional or cognitive deficits (348). Another study, a phase II clinical trial of the safety and tolerability of creatine was performed in HD patients, in which biomarkers were assessed in the serum. This creatine supplementation study demonstrated that the levels of 8OH2'dG were normalized and that the dosage used (8g/day) was tolerable and safe to patients (349). Given the efficacy of creatine in this phase II trial, a phase III clinical trial has been approved and performed in several centers ClinicalTrials.gov Identifier: NCT00712426) that was terminated in March 2015 but no results are published yet. These results strongly support the effectiveness of creatine as a neuroprotector. Two other supplements, coenzyme Q10 (CoQ10) and nicotinamide, were shown to be beneficial in the reduction of neurotoxicity of the metabolic poisons 3-NP and MA in rodents. Rats fed with CoQ10 showed less striatal lesion induced by MA and reduced lactate levels (350, 351). A NAD precursor, nicotinamide, is an electron acceptor which releases energy when it is re-oxidized during

phosporylation of ADP to ATP and showed to be neuroprotector in MA lesions in rats (350, 351). Co-treatment with nicotinamide and CoQ10, produces additional neuroprotection, since it was possible to reduce lesion volume, reduction in lactate levels and restoration of ATP levels (350, 351). A study with HD patients, however, showed no beneficial effects with 300 mg of CoQ10 (352). Since the best balance between tolerability and blood levels achieved in HD patients was found for a dosage of 2,400 mg/day (353), a phase III clinical trial in currently ongoing using this higher dosage.

Other antioxidants such as tauroursodeoxycholic Acid (TUDCA), BN82451 and N-acetylcysteine have been tested in animal models and showed several positive effects (354-356). Other potent antioxidants might be potential candidates: indole-3-proprionic acid (OXIGON) which is a β-amyloid fibril formation inhibitor and neuroprotector (357); and synthetic triterpenoids, which are able to upregulate genes involved in antioxidant and anti-inflammatory responses (358), reduce oxidative stress, improve motor problems and extend survival of a transgenic mouse model of HD (359). Also, Vitamin E, an antioxidant, also showed positive effects *in vitro* (360, 361) and *in vivo* (362, 363).

Excitotoxicity can be defined as neuronal damage resulting from the toxic effects of the excessive action of excitatory amino acids. Glutamate is the major excitatory neurotransmitter, and in the central nervous system, the neuronal excitotoxicity is commonly referred to the damage and death arising from prolonged exposure to glutamate and the associated excessive influx of ions into the cell, resulting in calcium overload. This excessive glutamate is neurotoxic, leading to the activation of enzymes that degrade proteins, membranes and nucleic acids (364). Excitotoxicity may play a central role in HD, since the striatum receives glutamatergic input from the cortex (365). When excitotoxins are injected into the striatum the resulting neuropathology pattern is similar to that observed in HD (366, 367); therefore, it is not surprising that antagonists of the glutamate receptor NMDA can prevent striatal neurodegeneration (368). Additionally, NMDA antagonists may also protect against neuronal damage caused by other toxins, such as mitochondrial 3-NP and MA. It has been shown that mutant htt enhances NMDA receptor activity and disturbs calcium signaling (369). Recently, expanded htt has been proposed to be able to enhance expression of different subunits of the NMDA receptor, NR1A and NR1B, perhaps inducing excitotoxicity (370). It is possible to establish an interplay between excitotoxicity, oxidative stress and mitochondrial function. Oxidative stress damages proteins, lipids and nucleic acids and is able to open the mPTP, that in turn, can stimulate ROS production, and consequently there is an energy failure and the release of

proapoptotic factors, such as cytochrome c into the cytoplasm (371). Ultimately, high levels of ROS and downregulation of antioxidant mechanism may lead to neuronal cell death (372).

Deprivation of neurotrophic factors may also be involved in the pathogenesis of polyQ disorders. For example, both mRNA and protein levels of BDNF are decreased in patients and animal models of HD (373-375) and the BDNF receptor TrkB is also reduced in a cellular model of HD (376). It seems reasonable to consider that increasing BDNF levels would be beneficial; indeed, BDNF, neurotrophin-3 (NT3) and NT4/5 prevent neuronal cell death in an animal model of HD (377). BDNF seems to have positive effects in in HD pathogenesis; however, previous clinical trials showed several side effects of neurotrophins as well as poor penetration into the BBB (378). For this reason, there is a major effort ongoing to find compounds that upregulate BDNF. A traditional herbal medicine, *tripterygium regelii* extract (TRE) was shown to be able to increase BDNF levels in SH-SY5Y cells after a stressful stimulus. In addition to its effects on polyQ aggregation described before, riluzole also interferes with glutamatergic neurotransmission (379), thereby reducing excitotoxicity, enhancing neurite formation in damaged motor neurons and interestingly, increasing serum concentrations of BDNF (380, 381). Riluzole was shown to have promising results both in animal models and HD patients, and a phase III clinical trial is being now completed (382, 383).

Remacemide, an NMDA glutamate receptor ion-channel blocker, seems to ameliorate the phenotype of a transgenic mouse model of HD (384). A pilot study demonstrated that remacemide is well tolerated in HD patients, as expected (385), since this compound is already used in the clinics as an anticonvulsant for the chronic treatment of epilepsy. However, a multi-center, randomized, placebo-controlled, trial of remacemide in 347 HD patients has recently been completed which showed that the 30 month treatment was ineffective at the doses used (200 mg/day and 600mg/day), and caused some secondary effects such as dizziness, nausea and vomiting (352). Very recently, the herbal formula B401 was found to be neuroprotective in a mouse model of HD. This compound is widely used in traditional Chinese medicine. This formula B401 showed to reduce the levels of mutant huntingtin aggregates in the brain as well as the levels of TNF-α. Furthermore, B401 increased the levels of BDNF and VEGF expression in the brain of the R6/2 HD mice and was able to ameliorate brain atrophy. To complete this study, the survival of the animal was prolonged and the body weight loss ameliorated as well as mice performance in the rotarod (386)

Further studies with neuroprotective molecules, ideally multi-target ones, may lead to improved effects on polyQ diseases.

1.3.5 Other treatment possibilities

There are other emergent strategies for the development of an effective therapy for polyQ diseases such as stem cell, neural cell replacement and growth factor gene therapy. Although still in early experimental stages, these approaches are promising since the stimulation of endogenous stem cells in the brain could generate new and functional neurons (387), the replacement of dead and/ or dying neurons by new cells capable to connect and function appropriately (388) and the provision of neuroprotective trophic factors (389, 390) may provide neuroprotection and possibly promote neuroregeneration, restoring neuronal homeostasis.

1.4 Machado-Joseph disease or Spinocerebellar Ataxia type 3 (MJD/SCA3): general oveview

Machado-Joseph disease (MJD), also known as Spinocerebellar Ataxia 3 (SCA3), is the most common autosomal dominant ataxia worldwide (22). The disease was first described in families from the Azores Islands, being reported some years later in other countries and in families with no Portuguese ancestrality. This late-onset disorder was first described as an autosomal dominant ataxia in William Machado family and named as Machado disease (391). In the same year, another case was reported (Thomas family) with similar clinical symptoms, and this disease was entitled "Nigro-spino-dentatal degeneration with nuclear ophthalmoplegia" (392). Later on, in 1976 a "particular type of autosomal dominant hereditary ataxia" was described in the family of Antone Joseph, which was designated as Joseph disease (393).

Two years later, after an intensive study in Azorean families and regarding the common features of the three families described above and the overlap with previously described Machado and Joseph families, a new "autosomal dominant system degeneration in Portuguese families of the Azores Islands" was introduced (394). In the 80's, this disease was named Machado-Joseph disease (MJD) and some clinical criteria for diagnosis were introduced (395). The prevalence of this disease was from the beginning thought to be the highest among people of Portuguese/Azorean descendent. For immigrants of Portuguese Azorean ancestry in New England, the prevalence was described to be around 1:4000. The highest prevalence in the world, about 1:140, occurs on the small Azorean island of Flores (396).

Later, however, researchers, based in DNA studies, have identified MJD cases in many ethnic backgrounds. Its relative frequency among the spinocerebellar ataxias is higher in Portugal (49%), China

(49%), Brazil (44%), the Netherlands (44%), Japan (43%), and Germany (42%); its relative frequency is lower in France (33%), the United States (21%), and Australia (12%); and it is rare in the United Kingdom (5%), India (3%), and Italy (1%) (50, 397-407).

MJD patients suffer from a progressive neurodegenerative disorder appearing more frequently between the ages of 20 and 50 years, in which the intellect is preserved (394). The preservation of cognitive function is a key feature of MJD in its differential diagnosis among the vast group of spinocerebellar ataxias. MJD is characterized by motor uncoordination and gait ataxia, difficulty with speech and swallowing, spasticity, altered eye movements, double vision, and frequent urination. Some patients have dystonia (sustained muscle contractions that cause twisting of the body and limbs, repetitive movements, abnormal postures, and/or rigidity), others have peripheral neuropathy and loss of muscle strength or symptoms similar to those of Parkinson's disease. Twitching of the face or tongue, or peculiar bulging eyes due to lid retraction may also be present. The severity of the disease is related to the age of onset, an earlier onset being associated with a more severe and rapidly progressive form of the disease. Symptoms can begin any time between early adolescence and old age up to 70 years of age (396). MJD is also a progressive disease, meaning that symptoms accumulate and become worse with time. Life expectancy ranges from the mid-thirties, for patients with severe forms of MJD, to a normal life expectancy for those with mild forms. For patients who die early from the disease, the cause of death is often aspiration pneumonia due to immobility and poor coordination of swallowing and breathing. The clinical spectrum of SCA3 is highly pleomorphic and led to the definition of four clinical sub-phenotypes: **type I**, characterised by the dominance of pyramidal and extrapyramidal anomalies, in addition to ataxia and other signs, with an early age-at-onset and fast progression; **type II**, with typical cerebellar ataxia, progressive external ophtalmoplegia and pyramidal signs appearing at an intermediate age; **type III**, with late onset and slow progression of peripheral signs, such as loss of proprioception and muscle atrophies; and **type IV**, the rarest, characterised by the presence of Parkinsonic signs, associated to the core clinical features (394, 395, 398).

1.4.1 MJD pathology: a heterogeneous and complex disease

The cerebellum and brainstem atrophy is well documented in MJD (408-411). Recent studies have shown that the neuropathology of this disease is not limited to cerebellum and brainstem, eventually

affecting the integrity of several functional and neurotransmitter systems resulting in severe and widespread neuropathology throughout the brain (412, 413) (Figure 2).

The neuropathology of MJD includes severe neuronal loss in the anterior horn and Clarke's column of the spinal cord and in restricted brain regions such as dentate nucleus (cerebellum), pontine nuclei and locus coeruleus (brainstem), substantia nigra (basal ganglia) and other regions such as the thalamus, as well as subthalamic, red and cranial nerve nuclei (414). It is also characterized by axonal neuropathy of peripheral motor and sensory axons (415). Also, post-mortem analysis revealed neuronal loss and gliosis in the substantia nigra, pontine and vestibular nuclei, as well as in cranial nerves, Clarke's columns and anterior horns of the spinal cord (414). An additional finding in MJD brains is the fact that the brain weight of MJD patients is lower comparatively with healthy individuals, which by itself can be an indicator of brain atrophy (408). Most of the neuropathological studies in MJD were performed using routine pathoanatomical examination (4-6 μm thick sections) that might mask subtle pathological alterations in the patient's brains. These studies restricted the neuropathology of MJD to the dentate nucleus, pallidum, substantia nigra, subthalamic, red and pontine nuclei, the anterior horn and the Clarke's column of the spinal cord. Also, in these same studies, the involvement of the Purkinje cell layer of the cerebellum and the inferior olive is still controversial (85, 402, 416-418). Rüb and collaborators developed an unconventional examination of MJD patient's brains, using 100 μm thick serial sections. The thickness of these brain sections due to their optical superposition allows the observation of more nerve cells than the conventional approaches used by neuropathologists (397, 401, 419-423). This new approach allowed the identification of new brain regions that suffers degeneration in MJD that might explain the heterogeneity of the symptoms observed in these patients. All these data is reviewed in (413). As a summary of these data, the authors found a more extensive damage affecting areas of the cerebellothalamocortical motor loop, the basal ganglia-thalamocortical motor loop, and several other systems: visual, auditory, somatosensory, vestibular, oculomotor, ingestion-related brainstem nuclei, precerebellar brainstem, cholinergic and dopaminergic midbrain, and pontine noradrenergic systems (Figure 2) (413).

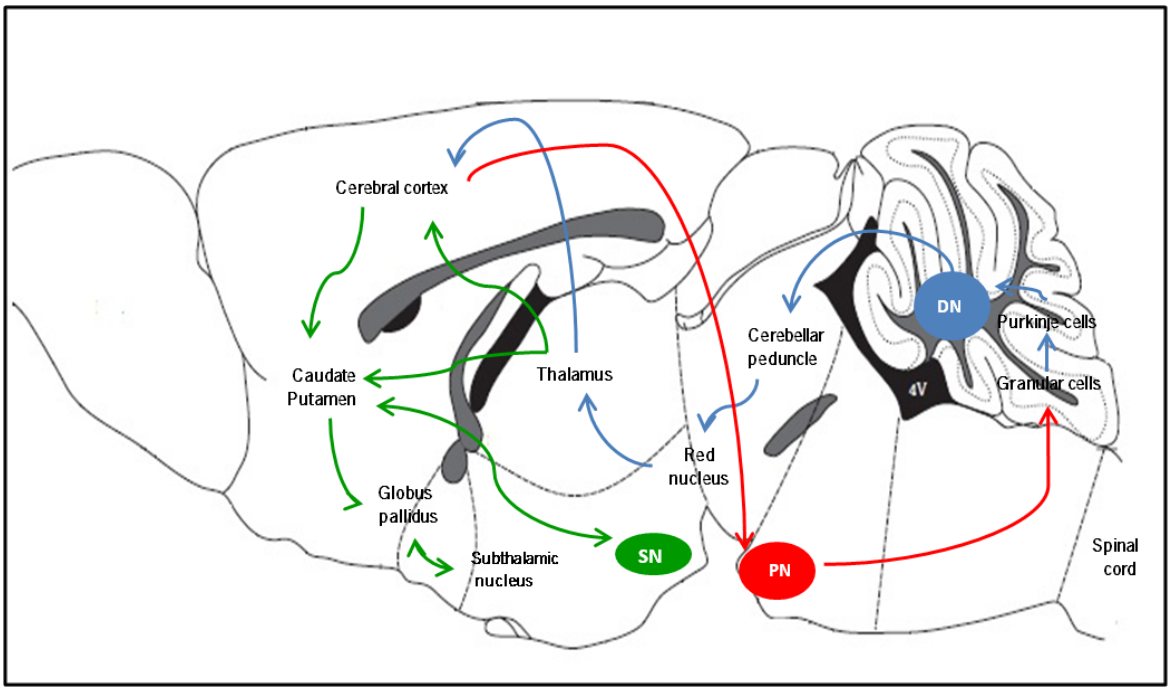

Figure 2. Neuronal circuits most affected in MJD. Illustration of cortico-pontine (PN)-cerebellar pathway (the red arrows correspond to cerebellar afferent system (corticopontine and pontocerebellar tracts)); the major basal ganglia loop (the green arrows correspond to the principal afferent and efferent fibers forming basal ganglia loops; it includes the dopaminergic projections from substantia nigra (SN) to caudate/putamen; and of the dentato(rubro)thalamocortical pathway (the blue arrows represent efferent projections of cerebellum that arise from dentate nuclei (DN) and continue their way to the motor cortex).

The ataxin-3 protein (the MJD disease protein) is expressed ubiquitously and when it presents the expanded allele it tends to aggregate forming neuronal nuclear inclusion bodies (NNIs) in the brain (85, 86). These NNIs are present in affected and non-affected brain regions, indicating that there is no direct correlation between the occurrence of these protein aggregates and disease pathology (399, 413, 424). Even so, the NIIs are ubiquitin positive and in their content it is possible to detect several proteins such as heat-shock proteins, proteasome subunits, transcriptions factors, among other proteins (86, 172, 425, 426). Axonal aggregates were also found in human patients, and, as similar to intranuclear aggregates they were immunopositive for ubiquitin and p62; with this finding one can be hypothesize that axonal inclusions might be detrimental to axonal transport mechanisms, contributing to degeneration of nerve cells in SCA3 (427). Despite the controversial topic on toxicity and/or protective role of NIIs (reviewed in (427)) they constitute an important morphological hallmark on MJD (86, 427), and are also present in the cytoplasm and in axons (399, 427, 428).

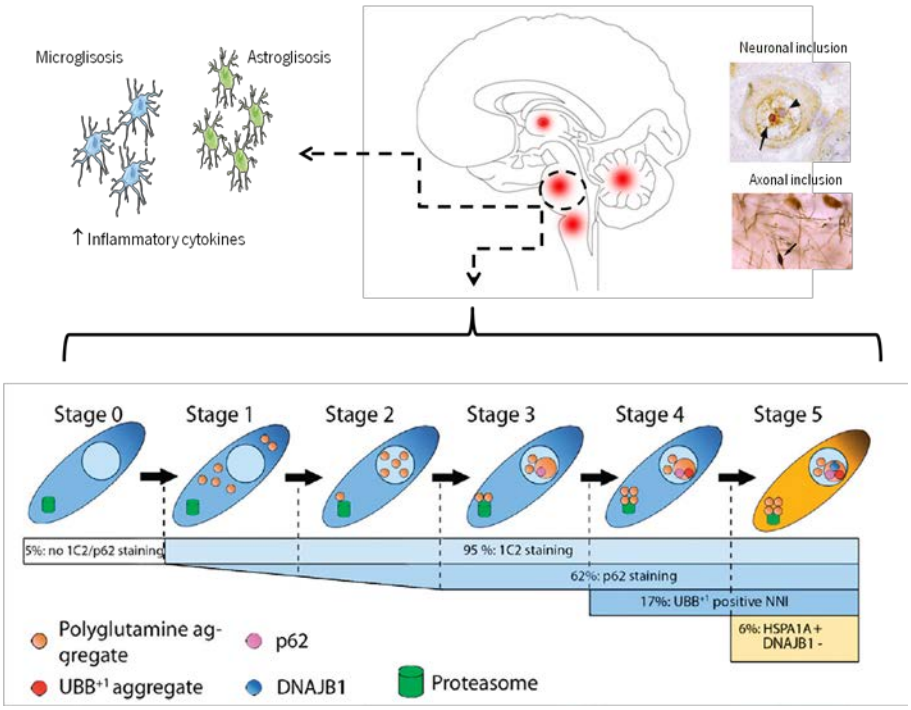

Figure 3. Neuropathology observed in MJD. Red marks indicate regions with more prominent dysfunction/degeneration in SCA3/MJD patients' brains according to neuropathological studies, including the thalamus, pons, medulla oblongata and cerebellum. On the cellular model, it is possible to find the model of progressive alterations in protein control proposed by Seidel et al. Brown dots represent aggregated ataxin-3 that occurs in Stage 1 as granular cytoplasmic staining, progressing to diffuse nuclear staining (stage 2) and finally to neuronal nuclear inclusion (NNI) (stage 3). In stage 4 it is possible to observe proteasomal dysfunction observed by the red dots that only occurs in the presence of NNI. In stage 5, corresponding to a final dysfunction phase, is found the sequestration of chaperones into the NNI. It is also possible to observe astroglisosis and microgliosis in MJD brains as well as increased inflammatory cytokines. The neuropathologic findings in this illustration are relative to the pons of MJD patients. Furthermore, neuronal nuclear and axonal inclusions are a neuropathological finding in MJD brains. Adapted from (86, 427, 429).

Positron emission tomography (PET) studies on the regional cerebral glucose metabolism revealed significantly decreased glucose utilization in the cerebellum, brainstem, striatum and whole cerebral cortex (430). Furthermore a decreased binding for dopamine transporter in these brain regions was also found in symptomatic MJD patients (431). Although it is thought that white matter pathology in MJD is less pronounced when compared to grey matter, metabolic abnormalities were found in MJD brains white matter by magnetic resonance spectroscopy, suggesting axonal dysfunction (432). Recently, both white and grey matter were studied in 12 MJD patients using voxel-based morphometry to analyze tissue loss and tract-based statistics (TBSS) on diffusion magnetic resonance imaging (MRI) to structural pathology. The

authors correlated the structural changes in the brain and the symptoms severity given by the SARA score, and found that the white matter integrity of frontal, thalamic, brainstem and left cerebellar structures is negatively correlated with ataxia scores. Also, MJD patients demonstrated loss of both grey and white matter in the cerebellum, brainstem (including the pons) and in the thalamus. These results showed that the white matter pathology is evident in MJD patients and is correlated with ataxia severity (433). The most striking feature of brain pathology in MJD is the enlargement of the fourth ventricle that is clearly observed in MRI of patients. A comparative study between MJD, SCA1 and SCA6 showed that MJD and SCA1 patients have severe atrophy in total brainstem, including midbrain, pons and medulla, total cerebellum, cerebellar hemispheres and cerebellar vermis, putamen and caudate nucleus. In this MRI study, the cerebellar cortex presented integrity in all disorders (434). There are some controversial findings regarding the progressive neuropathology and its correlation with patient's age and CAG repeat length. Onodera and collaborators observed a close correlation between brainstem and cerebellar vermis atrophy with CAG repeat size and age in MJD patients (410). Another study, demonstrated that the cerebellum and brainstem atrophy is progressive and dependent on the length of the CAG tract and the age of the patients (435). Other study failed to demonstrate a correlation with patient's age and progression of atrophy in a longitudinal study using volxel-based morphometry within one year (411). Consistent with this observation, Schulz and colleagues demonstrated a weak negative correlation with repeat length of the expanded allele and the volume of the brainstem, pons, caudate and putamen nucleus in MJD patients (434). Recently, Reetz and collaborators and the Ataxia Study group investigators undertook a longitudinal study using MRI at baseline and after a 2-year follow-up in MJD, SCA1 and SCA6 patients (436). The authors also determined the rate of volume loss and compared morphology changes and clinical features measured by different ataxia scales. The authors found the strongest volume loss change in the basal ganglia (specifically the caudate and putamen of the striatum), followed by the brainstem and found only mild atrophy in the cerebellum. The authors hypothesize that the strong atrophy of the brainstem and cerebellum at baseline could lead to a ceiling effect in the longitudinal study. Nevertheless, they proposed the involvement of the striatum in MJD. No correlation was found between neuropathology progression and CAG repeat length or disease duration (436).

1.4.2 Mouse models

Rodents are the mammals of choice used in biomedical research, and extensive research has been performed using rats, mice, guinea pigs and hamsters. Among these rodents, and especially in those studies involving disease, mice are the most used. The big challenge faced by the mouse genetics field is the determination of the phenotype of each mutant (437) and three criteria are commonly used to validate a mouse model: **(i)** *construct validity,* stating that the animal model has to carry the same biological features that cause the human disease, such as the same genetic alteration or anatomical abnormality, **(ii)** *face validity,* that comprises a conceptual correspondence to the behavioral phenotype (symptoms) and endophenotype (physiological/anatomical alterations) of the human disease, and **(iii)** *predictive validity,* where the response to treatments (preventive or curative) should be analogous between mice and humans (438). Each model generated for a specific human disorder attempts to mimic some of its particularities, however, few replicate all the symptoms. MJD is not an exception. In the last 20 years, eight mouse models were generated for this disease (Table 3).

1.4.3 MJD mouse models: phenotype overview

The first MJD mouse model was generated in 1996 at Kakizuka's lab. They were the first showing neurodegeneration and a neurological phenotype in a transgenic mouse model with an expanded CAG trinucleotide repeat within the ataxin-3 cDNA. This mouse was generated using truncated and full-length cDNAs of the ATXN3 gene (MJD1a isoform), with the L7 promoter directing expression specifically in Purkinje cells. In these constructs the cDNA encoded for Q79C, Q79, Q35C (truncated forms with or without C-terminal) or MJD79 (full-length context). The transgenic mice expressing truncated forms (Q79C, Q79) of the protein showed an ataxic phenotype (given by qualitative measures of wide-based hindlimb stance and falling down when moving), whereas the animals expressing the full-length protein (MJD79) or control individuals (Q35C) did not reveal any characteristic symptom of the disease. The onset of the symptoms in affected animals was around 4 weeks of age and the strong ataxic phenotype was more prominent in animals with a higher copy number of the transgene. This work showed that the expanded polyglutamine is responsible for neuronal loss and degeneration (15).

Some years later, another mouse model was created in an attempt to properly mimic the temporal and spatial expression of the human disease gene, using yeast artificial chromosome (YAC) constructs

carrying the full-length ATXN3 gene with expanded polyglutamine tracts, containing all the enhancers and long-range regulatory elements needed for cell-specific expression at physiological levels. Two additional genes were also part of the cloned genomic region. Homologous recombination in the yeast host was used to generate three YAC constructs with 15, 76 and 84 repeats, corresponding to the human wild-type, intermediate and early-disease-onset MJD alleles, respectively. The mice carrying expanded alleles showed abnormal gait, tremor, hypoactivity, limb clasping, an inability to correct geotaxis, reduced grip strength, abnormal toe pinch responses, progressive loss of weight and balance deficits, but no premature death was observed. These symptoms aggravated with repeat length and with the gene dosage. Regarding the onset of the disease, homozygous mice showed an earlier onset, with faster and worse disease progression (223). Recently, a more extensive characterization of the motor phenotype of this model (YACMJD84.2 mice) was performed both in hemi and homozygous mice. Hemizygous animals showed a mild phenotype only detectable at 75 weeks of age (reduced locomotor and exploratory activity) and a reduced body weight, while homozygous mice developed an early motor deficit, gait problems and decreased locomotor and exploratory activity (439).

In 2004, a third mouse model for MJD was published. This transgenic mouse expresses human mutant (Q71B and Q71C) or normal (Q20) ataxin-3 mjd1a under control of the mouse prion promoter, driving expression throughout the brain and spinal cord. Homozygous (Q71B and C) animals only displayed a phenotype that included progressive postural instability, gait and limb ataxia (footprinting analysis), loss of limb strength (Grip strength meter), motor uncoordination (Rotarod), weight loss and premature death only when the mutated protein was expressed above a critical concentration, only in their Q71C line. The heterozygous animals were indistinguishable in appearance and behavior from wild-type mice. This line also had problems in breeding, since homozygous animals were infertile (99).

In 2007, a mouse model was generated using full-length ataxin-3 constructs (isoform 1, clone MJD1-1, with a third UIM at the C-terminus) containing 15, 70, or 148 CAG repeats under control of murine prion protein promoter. A nuclear signal (NLS) was also introduced as well as a nuclear export signal (NES) to transport ataxin-3 into the cytoplasm. Transgenic mice carrying 70 CAG repeats revealed a severe and rapidly progressive phenotype assessed in the SHIRPA protocol (tremor, wide-based hindlimbs to stabilize the body in a resting position as well as markedly reduced activity and grooming, resulting in a disheveled appearance). The footprinting analysis demonstrated mild disturbances early in life and at late stages they were almost unable to walk and died prematurely. This study demonstrated, not unexpectedly, that both the

size of the expanded CAG repeat length and the level of transgene expression are of major importance for disease onset and disease progression in mice. Mice with reduced expression of ataxin-3 with 70 CAG repeats developed a milder phenotype than lines with a stronger expression. Furthermore, transgenic mice with 148 CAG repeats merely survived the first months and had major problems to produce offspring, whereas mice with stronger expression of this transgene died very early without producing any offspring. More important, nuclear localization of ataxin-3 with 148 polyglutamine repeats accelerated and intensified the phenotype of transgenic mice even further, whereas the addition of a nuclear export signal ameliorated the phenotype (440).

In 2008, another transgenic mouse model was created using cDNA of human wild-type ataxin-3-Q22 or disease-causing ataxin-3-Q79 (ataxin-3 mjd1a isoform) under the control of mouse prion protein promoter. Mice from two ataxin-3-Q79 transgenic lines displayed various symptoms of motor dysfunction with an onset age of about 5–6 months, and the severity of neurological phenotypes progressively increased in the following months as assessed in the SHIRPA protocol. The symptoms included forelimb clasping, impaired motor coordination and shorter latency to fall in the rotarod behavioural test, less activity, incorrect body posture, ataxic gait (footprinting analysis), reduced weight and reduced pelvic elevation (280). In the same year, Torashima and collaborators generated a SCA3 mouse model (polyQ mice) that was suggested by the authors to constitute a great tool in viral-vector based screening of genes for therapeutic molecules that target the cerebellum, since the mutant ataxin-3 expression is directed to Purkinje cells. This model was generated using a truncated form of human ataxin-3 with 69 glutamines (ataxin-3 [Q69]). These mice presented a severe ataxic phenotype and disarrangement of the Purkinje cells (441). In order to analyze whether symptoms caused by ataxin-3 with an expanded repeat are reversible *in vivo*, a conditional mouse model of SCA3 with the full-length human ataxin-3 cDNA (isoform atxin-3c) with 77 repeats was created using the Tet-Off system. When the expression of the expanded ataxin-3 was induced, transgenic mice developed a progressive neurological phenotype characterized by reduced anxiety and hyperactivity (given by the open-field test), impaired Rotarod performance and decreased gain of body weight. On the other hand, when ataxin-3 was turned off at an early symptomatic stage of the disease, the transgenic mice were indistinguishable from negative controls after 5 months of treatment (30). One year later, the same group published another MJD transgenic mice model expressing ataxin-3 (isoform ataxin-3c) with 148 CAG repeats under the control of the huntingtin promoter, resulting in ubiquitous expression throughout the whole brain. The model resembles many features of the disease in humans, including a late

onset of symptoms and CAG repeat instability in transmission to offspring. They observed a biphasic progression of the disease using the home cage activity and the open-field tests, with hyperactivity during the first months (not seen in human patients) and a decline of motor coordination given the rotarod test after about 1 year of age (442).

In the same year, another transgenic mouse model (in our lab), using a human cDNA (isoform 1, MJD1-1 clone) carrying the repeat tract coding for 83 polyglutamines, under control of pCMV (cytomegalovirus) promoter was generated. From two different microinjections two female founders (background FVB/N) were obtained, A and B (94 and 83 CAG repeats, respectively). This novel transgenic mouse model for MJD has revealed some important features that recapitulate the disease. Namely, hemizygous transgenic animals developed a motor phenotype (rotarod test) in agreement with the dominant feature of the disease. Behavior studies revealed a number of findings in the mice from lineage A that differed from non-transgenic and transgenic from lineage B. We found that hemi and homozygous animals of lineage A displayed an uncoordination phenotype. Moreover, mutant mice tended to show a reduced locomotor activity in the rotarod test. In lineage A, which manifests MJD-like symptoms it was possible to establish a phenotype-genotype correlation: animals with higher CAG repeat tract spent less time on the rod (103).

Table 3. Summary of the MJD mouse models characterization at the phenotypic and pathologic levels.

		Ikeda et al, 1997	**Cemal et al, 2002**	**Goti et al, 2004**	**Bichelmeier et al, 2007**	**Chou et al, 2008**	**Boy J et al, 2009**	**Boy J et al, 2010**	**Silva-Fernandes et al, 2010**
General information	**Transgene**	cDNA MJD1a fragment with 79 CAGs ; cDNA MJD1a full-length with 79 CAGs (no phenotype)	All isoforms	Isoform ataxin-3c	Isoform ataxin-3c	Isoform MJD1a HA-tag	Isoform ataxin-3c	Isoform ataxin-3c	Isoform ataxin-3c
	Promoter	L7 (Purkinje cells)	Human ataxin-3 (YAC)	Mouse prion protein	Mouse prion protein	Mouse prion protein	Hamster prion protein (conditional expression)	Rat huntingtin (partial)	CMV
	(CAG)n	79	64, 67, 72, 76 and 84	71	70	79	77	148	94
	Inclusions	No description	Yes	Yes (homozigosity)	Yes	Yes	Yes	Yes	No
	Cellular and subcellular transgene expression	Purkinje cells	Ubiquous (cytoplasmic and nuclear)	Ubiquous but stronger in brain and spinal cord	Ubiquous but directed to brain and spinal cord (NES and NLS artificial signals)	Ubiquous but directed to brain and spinal cord	Brain (stronger in the cerebellum, but only in glia cells)	Ubiquous (cytoplasmic and nuclear)	Ubiquous (cytoplasmic and nuclear)
	Neurodegeneration	Purkinje cell degeneration and atrophic cerebellum	Peripheral neuropathy with demyelination and degeneration of the DRGs; cell loss in the DCN and Purkinje cells; astrocytosis	Substantia nigra: 38% decrease in TH-positive neurons Q71-C homozygotes	Purkinje cell loss	Purkinje cells with shrunken cell body and less dendritic arborization	Purkinje cells darkly stained	Purkinje cells darkly stained	Astrogliosis in substantia nigra and vestibular nuclei; scattered dark, shrunken cells in pontine and dentate nuclei and thalamus

Table 3 (continued). Summary of the MJD mouse models characterization at the phenotypic and pathologic levels.

		Ikeda et al, 1997	**Cemal et al, 2002**		**Goti et al, 2004**	**Bichelmeier et al, 2007**	**Chou et al, 2008**	**Boy J et al, 2009**	**Boy J et al, 2010**	**Silva-Fernandes et al, 2010**
	Age at onset (weeks)	4 (ataxic phenotype)	75 (heterozygous), 6 (homozygous) (motor deficits)		8 (tremor, hunchback, ataxic limbs)	6 (tremor, reduced activity, wide-based hindlimbs to stabilize the body in a resting position)	20 (motor deficits)	8 (limb clasping)	48 (reduced balance and coordination)	16 (motor deficits)
	Genetic background	No description	C57BL/6J (mixed?)		B6C3F1/J (C57BL/6JxC3H/HeJ	C57BL/6N (mixed?)	FVB/N	C57BL/6 (mixed?)	C57BL/6N	C57BL/6J
Phenotype										
		+/-	**+/-**	**+/+**	**+/-**	**+/+**	**+/-**	**+/-**	**+/+**	**+/-**	**+/-**
Phenotype parameters	Ataxia	Yes	X	X	No phenotype	Yes	Yes	Yes	Yes	X	No
	Gait disturbance	Yes	Yes	Yes (++)	No phenotype	Yes	Yes	Yes	Yes	X	No
	Weight loss	X	Yes	Yes (++)	No phenotype	Yes	X	Yes	Yes	X	No
	Hypoactivity	No	Yes	Yes (++)	No phenotype	Yes	Yes	Yes	X	X	Yes
	Motor uncoordination	X	X	Yes	No phenotype	Yes	X	Yes	Yes	Yes	Yes
	Appearance	Small	Normal	X	Normal	Moribund (32 weeks)	Disheveled appearance (24 weeks)	X	X	X	Normal

Table 3 (continued). Summary of the MJD mouse models characterization at the phenotypic and pathologic levels.

		Ikeda et al, 1997	**Cemal et al, 2002**		**Goti et al, 2004**		**Bichelmeier et al, 2007**	**Chou et al, 2008**	**Boy J et al, 2009**	**Boy J et al, 2010**	**Silva-Fernandes et al, 2010**
Phenotype											
		+/-	**+/-**	**+/+**	**+/-**	**+/+**	**+/-**	**+/-**	**+/+**	**+/-**	**+/-**
Phenotype parameters	Limb clasping	X	Yes	Yes (++)	No	Yes	X	Yes	Yes	X	No
	Tremors	X	Yes	Yes (++)	No	Yes	Yes	X	X	X	No
	Lowered pelvis	X	Yes	Yes (++)	No	Yes	X	Yes	X	X	No
	Limb strength deficit	X	Yes	Yes	No	Yes	X	X	X	X	No
	Other	X	X	Excessive grooming	X	X	X	X	Hyperactivity and spastic head movements (homozigoty)	Hyperactivity	X

1.4.4 MJD mouse models: neupathology overview

Taking in consideration the heterogeneity and widespread neuropathology observed in MJD it has been difficult to establish a mouse model that mimics the brain pathology of MJD. In the model generated in 1996 by Ikeda and collaborators, expressing ATXN3 in Purkinje cells, the authors observed, in 8 weeks-old mice, a severe atrophy of the cerebellum (the volume was one eighth less compared to littermate controls) and a massive loss of Purkinje cells (seen on calbindin staining). Also, the molecular and granular cell layers of the cerebellum were affected (H&E staining). The presence of NIIs was not reported in this study (15). In 2002, pathological examination of the brains of YAC-transgenic mice (12 months of age) showed degeneration and mild gliosis of the dentate and pontine nerve nuclei. The authors observed that in general the brain of transgenic mice were similar to controls. It was possible to observe that pontine neurons were abnormal, being hyperchromatic and shrunken and it were also seen scattered dark cells with pyknotic nuclei and eosinophilic cytoplasm (H&E staining). Quantitatively (quantification method not described), a 30% cell loss was observed in the pons and 40% in the dentate nucleus. In the dentate nucleus the cells showed grumose alterations. A slight increase in GFAP astrocytic marker was detected in the dentate nucleus, suggesting mild gliosis that may result from the cell loss observed in this brain region. Furthermore, Caldindin D-28k immunostaining showed Purkinje cell loss, shrinkage, cell body displacement and dendritic atrophy. The Purkinje cell loss increased with gene dose, suggesting that these cells are sensitive to the transgene dosage effects. These mice also had decreased myelin thickness in the dorsal root ganglia (DRG) and evidenced of de- and remyelination in the sciatic nerves at 9 months of age. It was possible to detect NIIs in neurons, but not in glial cells, mainly in the pontine and dentate nuclei. NIIs were not detected in cerebral cortex, hippocampus and striatum (223). In 2004, a transgenic mouse model expressing human mutant (homozygous Q71) ataxin-3 under the control of the mouse prion promoter demonstrated a 38% decrease of dopaminergic neurons (tyrosine hydroxylase [TH]-positive neurons) in the substantia nigra (by the use of unbiased stereology) when compared to controls (Q20 transgenic mice) at 2-3 months of age. Also, the authors quantified by stereology the number of Nissl-stained neurons in the dentate nucleus and found no statistical differences when compared to controls, although there was a tendency for a decrease. Finally, NIIs were evaluated and quantified (by light microscopy, counting three to six fields: 60 –120 neurons per brain region or spinal cord) in several brain regions. At 3-4 months of age the larger number of NIIs was found in deep cerebellar and pontine nuclei, spinal cord and to a lesser

extent in the olfactory bulb. In regions such as the frontal cortex, hippocampus, thalamus and cerebellum cortex NIIs were undetectable. At the age of 8 months, the number of NIIs increased in the regions analyzed and were detected also in thalamus and cerebellum cortex (very few) and not in the frontal cortex and hippocampus (99). Bichelmeier and colleagues have found Purkinje cell loss by immunostaining of cerebellar sections with anti-phosphorylated neurofilament antibody, which revealed condensed or empty baskets around Purkinje cells. Furthermore, electron microscopy analysis showed a clear pathology of Purkinje cells where it was possible to detect a shrinking of these cells to an extent of 50-80%, as well as an abnormal morphology. The granule cells of the cerebellum were not altered in this mouse. Brain sections were also evaluated for the presence of NIIs and it was possible to detect NIIs posite for both ataxin-3 and ubiquitin in several brain regions such as cerebellum (NIIs were absent in Purkinje cells), cortex, hippocampus, pons and cerebellar nuclei (440). Later on, Chou et al, focused their neuropathological study in the cerebellum by staining cerebellum sections of the mouse brain (10-11 months of age) with H&E and performed immunohistochemistry for NeuN (neuronal marker) or calbindin. The authors showed a tendency (not statistically significant) towards a decrease in the number of neurons in the dentate nucleus, granular, molecular and Purkinje cells of the cerebellum. Furthermore, calbindin staining of the Purkinje cell showed degeneration features, such as shrunken cell body and less dendritic arborization, although the authors could not find mutant ataxin-3 expression in these cells. NIIs were detected in the dentate and pontine nuclei as well as in the substantia nigra (280) at 12 months of age. Torashima also showed severe disarrangement of Purkinje cells in the polyQ mice already at 21 days of age, given by calbindin staining. Nuclear inclusions were also detected in the cerebellum of these mice (441). Also focusing the neuropathological study in Purkinje cells, Boy et al in 2009, showed that these cells presented an abnormal morphology by electronic microscopy in 20 months-old mice. Purkinje cells showed a dark staining that was considered “dark cell degeneration”. Since this model is a conditional transgenic, turning off the transgene expression it was possible to observe a reversion of this Purkinje cell degeneration. NIIs were detectable in cerebral cortex (very few); no other brain regions were reported has presenting NIIs (30). In accordance with these findings, the same authors, in 2010, described another model that also presented darkly stained Purkinje cells considered as a sign for degeneration in this mouse model at 20 weeks of age (442). However, this finding might be a little controversial, taking in consideration that many neuropathologists consider “dark neurons” as the most common histologic artefacts which can also be found in normal brains (443). Regarding NIIs, it was possible to detect in the pontine and cerebellar nuclei, red nucleus and

Purkinje cells (442). Also in 2010, Silva-Fernandes and co-workers observed neuronal atrophy in the pontine and dentate nuclei as well as astrogliosis in the vestibular nuclei and substantia nigra at 49 weeks of age. However, and in spite of its neurological phenotype, no cell death (apoptosis or necrosis) and no signals of microglial activation or neuroinflammatory response were observed in the brains of this transgenic mouse. Furthermore, it was possible to observe an abnormal cellular morphology in several brain regions, including thalamus, dentate and pontine nuclei. NIIs were not detected in this model (103). Taking advantage of lentiviral vectors, Gonçalves et al used C57Bl6 mice to produce another MJD-like model. They injected mutant and normal ataxin-3 in the striatum of these animals. These mice showed striatal pathology associated to mutant ataxin-3 overexpression, given by the reduction of DARPP32 staining and NeuN positive cells as well as increased pycnotic nuclei in the cresyl violet staining and mutant ataxin-3 inclusions. Furthermore, these animals also showed decreased synaptophysin and MAP-2 staining and increased GFAP and CD11b staining, suggesting synaptotoxicity and astrogliosis, respectively (444).

1.4.5 Pre-clinical trials in MJD mice

Despite the existence of a variety of different MJD rodent models and their potentialities, only a few preclinical trials have been performed until now (see also table 4 and 5). These trials were carried out based in different approaches that will be discussed separately.

(i) RNAi approaches and exon skipping (Table 4). RNA interference (RNAi) might be considered one the most notable discoveries in biomedical research. Indeed, specifically silencing the disease-causing genes (without interfering with the healthy allele and avoid off-target effects) would be the ideal therapeutic strategy. One of the major obstacles to the translation of this approach would be the delivery of the target RNAi in the human CNS. In the case of MJD, Alves et al have generated lentiviral vectors encoding siRNAs targeting a SNP (found in 72% of the population) that specifically silenced mutant ataxin-3 gene (when associated with that SNP-allele) and not the normal gene, and injected those vectors into the striatum of the rat (shAtaxMUT rat model). The non-allele-specific silencing in an acute rat model of MJD lead to a 80% reduction of mutant ataxin-3-positive inclusions and to the preservation of dopamine and cAMP-regulated phosphoprotein (DARPP-32) expression in the striatum where the mutant protein was overexpressed, although it remains unclear whether this silencing improved behavior (52). Using the same model system, Nascimento-Ferreira et al (from the same lab), used lentiviral vectors-mediated

overexpression of beclin-1, and important protein involved the in nucleation step of autophagy. They have shown a reduction of ataxin-3 aggregates in the rat striatum that co-express mutant ataxin-3 and beclin-1, as compared to animals only expressing mutant ataxin-3, at 4 weeks post-injection, and this result was even more pronounced 8 weeks post-injection. Also, the authors have shown that beclin-1 overexpression led to a reduction in neuronal dysfunction, given by the DARPP-32 staining at 4 weeks post-injection, and again, this reduction was maintained at 8 weeks. Furthermore, beclin-1 overexpression reduced astrogliosis and microglial activation (445) . Together these results suggest autophagy activation as a promising strategy for MJD, as suggested by others (245, 446).

Nóbrega et al, also from the same lab, used the polyQ mice (441) that expresses the mutant ataxin-3 exclusively in the cerebellum. The same strategy as in (52) was used, but this different model, allowed the phenotypic evaluation after the injection of the shRNA targeting mutant ataxin-3. The authors were able to observe a reduction in ataxin-3 inclusions in the Purkinje cells of shAtx3-injected mice when compared to shGFP control animals. Furthermore, silencing ataxin-3 preserved the Purkinje cell layer as assessed with calbindin and DARPP-32 markers. The molecular and granular layers of the cerebellum were also larger in shAtx3-injected mice as compared to shGFP controls, and Golgi staining demonstrated increased arborization in the molecular layer of animals silencing mutant ataxin-3. Silencing mutant ataxin-3 improved significantly the performance of these mice in the rotarod, both at constant speeds and in the accelerating rod. The footprinting analysis also revealed improvement in animals upon silencing of ataxin-3, given the larger stride length and increased paw overlap. Finally, in the activity box, shAtx3-treated animals travelled longer distances and walked faster than control animals (447).

In order to better understand the potentiality of RNAi approaches in a model system that more closely mimics the human disorder and the effects of this approach in a chronic situation, Costa and collaborators performed a RNAi therapy in the cerebellum of the YACMJD84.2 model (223). These authors used microRNAs (miRNAs) instead of shRNAs, due to their higher safety (448). A reduction of mutant ataxin-3 was observed in the cerebellum of the animals injected with miRATXN3 as compared to controls, and no toxicity was found in the brain, which led the authors to pursue with the chronic trial. In this study, a more detailed characterization of the YACMJD84.2 model was also performed, to complement the initial characterization conducted by Cemal et al. After an extensive behavioral and pathologic evaluation, the authors decided to use the homozygous animals in the RNAi therapy trial, since they presented a more marked phenotype when compared to heterozygous animals. The long-term administration of miRATXN3

failed to improve motor deficits of the treated SCA mice and had no impact in life expectancy. The authors showed that despite the widespread distribution of the miRATXN3 into the cerebellum and its apparent safety, it failed to rescue the phenotype of the SCA3 animals, suggesting that maybe the cerebellum is not the major origin of the motor problems observed in these mice (439). Thus, and as stated by the authors of these two last studies, the efficacy of RNAi approaches to suppress *ATXN3* is highly dependent on their ability to silence *ATXN3* throughout the brain regions affected in MJD (449)**.**

Melvin M. Evers and colleagues proposed a novel strategy for MJD treatment, proposing a protein modification approach for mutant ataxin-3 toxicity without affecting its normal function. This approach includes the removing of the toxic polyglutamine tract of ataxin-3 using antisense oligonucleotide-mediated (AONs) exon skipping, while keeping global levels of ataxin-3 unchanged. In this study, the authors used an AON that removes simultaneously exon 9 and 10 (CAG repeat expansion is located at exon 10). Since removal of exon 10 alone disrupts the reading frame, exon 9 is also removed to avoid this issue. The AONs designed were tested in human fibroblasts and the authors confirmed the exon skipping by sequencing. Afterwards, they tested if these AONs resulted in a modified protein. Indeed, the authors found a 37 kDa protein, corresponding to ataxin-3 protein lacking exon 9 and 10 in human fibroblasts. Furthermore, it was shown that the removal of these exons did not have a negative impact in the ubiquitin binding capacity of ataxin-3. To test the efficacy and safety of these AONs *in vivo*, the authors proceeded to a single intra-cerebral ventricular injection of the AONs in the brain of wild-type mice. After 7 days, the skipping efficacy was measured in the cerebellum of the mice, which demonstrated a reduction in the levels of exon 9 and 10 and not of the adjacent exons, suggesting the specificity of the AONs used (450). These results might indicate that exon skipping could be a novel therapeutic strategy for MJD.

(ii) Pharmacological approaches (Table 5). Taking advantage of the model generated by Cemal et al in 2002, Chen and collaborators performed a chronic treatment to these mice using food supplemented with dantrolene. This compound is a ryanodine antagonist and clinically relevant Ca^{2+} signaling stabilizer, being a skeletal muscle relaxant commonly used to treat hyperthermia and muscle spasticity (451). Four groups of animals (WT and SCA3 treated and vehicle) were submitted to the beam-walk test and the latency and the footslipages were measured. The authors observed that SCA3-vehicle mice have impairment in the beam walk test and that dantrolene had no effect in the WT group. The SCA3-dantrolene group had an improved performance in the beams, taking less time to traverse the different

beams and that the number of foot slips was identical to WT. Interestingly, the authors also observed a crawling behavior in the SCA3-vehicle and to a less extent in the SCA3-dantrolene group. No crawling behavior was observed in WT groups. The authors also found significant improvement in the footprinting pattern of SCA3 group treated with dantrolene. To evaluate the neuroprotective effect of dantrolene, the brains of the four groups used were weighed and dantrolene-fed SCA3 mice had no improvement in this parameter. It was also shown that SCA3-vehicle animals have loss of NeuN positive cells in the pontine nuclei and of TH-positive cells in the substantia nigra; dantrolene food supplementation diminished this neuronal loss (336).

In order to verify the therapeutic efficacy of autophagy induction in MJD, Menzies and colleagues used the model generated by Bichelmeier (440) which they chronically treated with an autophagy inducer – temsirolimus (rapamycin analog). Although the authors were not able to reproduce the phenotype previously described for this model (440), at the end of a 2 months preclinical trial they report that treated-SCA3 animals performed better in the accelerating rod when compared to placebo-treated mice, and that this compound had no effect in WT animals in the rotarod. Also, temsirolimus was able to reduce the ataxin-3 aggregates in the motor cortex and the soluble cytoplasmic, but not nuclear, mutant ataxin-3 in total brain extracts. Finally, the authors performed a microarray study at basal conditions and after temsirolimus treatment. Overall, the transcriptional alterations found were very small, probably due to the absence of a clear phenotype in the SCA3 mice. Yet, it was possible to identify genes that were decreased in SCA3-placebo mice and increased after temsirolimus treatment; the opposite effect was not found (245).

Previously, Chou and collaborators suggested that a global transcriptional deregulation was occurring in the cerebellum of a SCA3 transgenic model (280). More specifically, they have shown a generalized hypoacetylation of H3 and H4. In order to modulate these alterations in the transcriptome, the same authors treated their mouse model with sodium butyrate (SB), an HDAC inhibitor. They observed that daily administration of SB was able to revert histone hypoacetylation as well as the transcription donwregulation in the cerebellum. SB treatment improved motor performance of transgenic animals in the rotarod that is less evident in later stages. The ataxic symptoms quantified through the footprint pattern were also ameliorated with SB as well as the spontaneous locomotor activity (assessed in a Perspex box), body weight loss and survival (276). More recently, and using the same model (280), the same research group developed a preclinical trial using H1152, a Rho-kinase (ROCK) inhibitor. These authors tested several ROCK inhibitors *in vitro* and showed that H1152 was the most potent in reducing ataxin-3 protein

levels, by increasing proteasome activity. The same behavior tests used in the characterization of the model were used in this study (280). Daily intraperitoneal injections of H1152 in the SCA3 mice slightly improved motor coordination (rotarod) and locomotor activity deficits. Also, H1152 administration significantly decreased mutant ataxin-3 levels in the cerebellum, cerebral cortex, pontine nuclei and spinal cord as well as the cell death (reduction in NeuN positive cell) observed in the pontine nuclei of vehicle animals (452).

Caffeine (a non-selective adenosine receptor antagonist) as well as the selective adenosine A_2A receptor ($A_{2A}R$) blockage has been shown to be neuroprotective in brain diseases, including Huntington's disease (453-455). In a study by Gonçalves et al, caffeine was administered in the drinking water for 3 months (maximum), in a dose (1g/L) corresponding to a human diary consumption of 5 cups of coffee. Chronic caffeine treatment rescued the striatal shrinkage observed in the water-drinking animals and slightly reduced the number of pycnotic cells. Also, caffeine was able to increase the loss of NeuN positive cells observed in the water-drinking animals. These data suggests that chronic caffeine treatment is neuroprotective towards ataxin-3 overexpression in the striatum. Furthermore, loss of DARPP-32 staining volume, astrogliosis and putative microgliosis were improved in the treated group. Finally, and intriguingly, caffeine-treated mice showed an increase in the number of nuclear inclusions when compared to water-drinking animals. These observations might indicate that the final stage neuronal inclusions are protective rather than toxic. Nevertheless, the neuroprotective effects of caffeine might be of limited duration since the quantity of pycnotic cells remained in a high number. (444).

Table 4. Pre-clinical trials performed in MJD mouse models using RNAi approaches.

							Outcome		
	Therapeutic molecule	**Model**	**Target**	**Treatment duration**	**Route of administration**	**Control groups**	**Phenotype**	**Pathology**	**REF**
RNAi approaches	Recombinant lentiviral vectors encoding shAtaxMUT	*Alves S et al* 2008a (rat model)	Mutant ataxin-3	-	Intracranial injection in the striatum	shGFP	ND	Striatal neuroprotection	(52)
	Lentiviral vector-mediated overexpression of belin-1	*Alves S et al* 2008a (rat model)	Autophagy	-	Intracranial injection in the striatum	ATX3-MUT and WT	ND	Clearance of ataxin-3 and ubiquitin positive aggregates, as well as oligomeric and soluble mutant ATXN3; decreased DARPP32 and NeuN depleted volume	(445)
	Lentiviral vectors enconding shRNAs for mutant ataxin-3	*Torashima et al, 2008*	Mutant ataxin-3	-	intracranial injection in the cerebellum	shGFP	rotarod and footprinting; locomotor activity	ataxin-3 inclusions in Purkinje cells; preserved Purkinje cells, molecular and granular layers of the cerebellum; increased arborization of the neurons in the molecular layer; decreased Fluorojade B staining	(447)
	anti-ATXN3 RNAi (miRATXN3)	*Cemal et al 2002*	Mutant ataxin-3	10 months (early post-symptomatic)	intracranial injection in the cerebellum	AAV2/1-miRMis-hrGFP; AAV2/1-miR-hrGFP (YACMJD84)	No improvement in the motor impairment and survival	ND	(456)

Table 4 (continued). Pre-clinical trials performed in MJD mouse models using RNAi approaches.

							Outcome		
RNAi approaches	**Therapeutic molecule**	**Model**	**Target**	**Treatment duration**	**Route of administration**	**Control groups**	**Phenotype**	**Pathology**	**REF**
	RNAi targeting human ATXN3 3'UTR	*Cemal et al 2002*	Mutant ataxin-3	2 months (post-symptomatic)	intracranial injection in the cerebellum (deep cerebellar nuclei)	rAAV-CMV-hrGFP; rAAV-miR-Mis (YACMJD84)	ND	80% clearance of nuclear mutant ataxin-3 inclusions in DCN and Purkinje neurons	(457)
Exon skipping	antisense oligonucleotides to induce an in-frame exon skip in the ataxin-3 pre-mRNA	*WT C57Bl/6J*	ataxin-3 exon 9 and 10 (CAG containing-exon)	7 days	single intra-cerebral ventricular (ICV) injection	-	ND	Exon 9 and 10 were reduced in the cerebellum, without affecting the expression of other exons	(450)

Table 5. Pre-clinical trials performed in MJD mouse models using pharmacological approaches

								Outcome		
	Model	**Therapeutic molecule**	**Target**	**Treatment duration**	**Dosage**	**Route of administration**	**Control groups**	**Phenotype improvement**	**Pathology**	**REF**
Pharmacological approaches	*Cemal et al 2002*	Dantrolene	stabilizer of intracellular Ca2+ signaling	10 months (started post-symptomatically)	5 mg/Kg	food supplementation	wild-type animals (treated and vehicle); SCA3 mice vehicle	beam walk test; gait deficits;	restored brain weight loss; restored neuronal loss in PN; SN-TH neuronal cell loss is improved	(336)
	Bichelmeier et al 2007	CCI-779	Autophagy inducer	2 months (started pos-symptomatically)	20mg/Kg	i.p injection (3x/week)	wild-type animals (treated and vehicle)- data not shown; SCA3 mice vehicle	Rotarod (no phenotype was detected in basal conditions)	reduced aggregate number in the motor cortex; reduction in soluble ataxin-3	(245)
	Chou et al 2008	Sodium butyrate	HDAC inhibitor (Class I)	9 months (started pre-symptomatically)	400 or 800 mg/Kg	i.p injection (daily)	SCA3 mice vehicle	weight loss; rotarod; ataxic symptoms; hypoactivity; survival	ameliorates mutant ataxin-3-induced degeneration of Purkinje neurons; restored hypoacetylation status in cerebellum	(276)
	Chou et al 2008	H1152	Rho-kinase (ROCK) inhibitor	3 months (started pre-symptomatically)	10 mg/Kg	i.p injection (daily)	wild-type animals (treated); SCA3 mice vehicle	rotarod; locomotor activity deficit	reduction of ataxin-3 levels in the cerebellum, cerebral cortex, pontine nuclei or spinal cord; prevention of neuronal loss in the pontine nuclei	(452)

Table 5 (continued). Pre-clinical trials performed in MJD mouse models using pharmacological approaches

								Outcome		
Pharmacological approaches	**Model**	**Therapeutic molecule**	**Target**	**Treatment duration**	**Dosage**	**Route of administration**	**Control groups**	**Phenotype improvement**	**Pathology**	**REF**
	Lentiviral-vector mediated mouse model (striatum injections)	Caffeine	non-selective adenosine receptor antagonist	3 months maximum (pre-symptomatically)	1g/L	drinking water	C57Bl6 animals vehicle (expressing mutant and wild-type ataxin-3 in the striatum)	ND	ameliorates mutant ataxin-3 induced neurodegeneration; reduction in inclusions in the basal ganglia; reactive gliosis was reduced	(444)

1.4.6 Clinical trials in MJD patients

Currently, no disease modifying treatment exists for MJD. Yet, some symptomatic treatment is available, including genetic counseling, physical therapy programs, and speech and swallows evaluation. Symptomatic treatment for clinical findings such as parkinsonism, dystonia, cramps, depression, sleep disorders, and pain is important to improve the quality of life for those with MJD. The translation from model systems to human patients is an important and urgent issue. Considering the lack of information on the key aspects of the pathogenic mechanism(s), the clinical and molecular heterogeneity of MJD patients and the scarcity of human biological tissues available for research, the development of translational approaches is very difficult. Still, some clinical trials (very few) were performed for MJD (See table 6). The presence of undesired side effects is of major importance in clinical trials and must be taken in consideration (the known side effects of the compounds tested are summarized in the table 3). Most of these clinical trials were performed using very few MJD patients (less than 10) and only short-term effects were investigated, thus the outcome of these trials might be compromised. The combination of sulphamethoxazole and trimethoprim (Bactrim, a broad-spectrum antibiotic used in ear and urinary infections) was suggested to be effective in MJD in a small double-blind clinical trial using 8 patients. The authors observed mild improvements in some parameters evaluated, such as hyperreflexia of knee jerks and rigospasticity of the legs in the patients treated with Bactrim. It was also shown that the levels of biopterins and homovanillic were reduced in the cerebrospinal fluid (CSF) of MJD patients when compared with controls with other neurodegenerative diseases. The short-term treatment with Bactrim increased the levels of total and oxidized biopterins in the CSF (458). In the same year, another double-blind' clinical trial was performed using Bactrim in 8 additional patients. In this study, three parameters were evaluated: subjective performance, neurological examination and timed tests. The treatment with Bactrim demonstrated an improvement on gait and coordination. The authors suggested that further clinical trials using Bactrim should be performed due to the promising results obtained with this small number of patients (459). Indeed, in 2001, a third double-blind clinical trial using Bactrim was performed in 22 MJD patients. In this trial, and in contrast to previous observations, chronic treatment with Bactrim had no effect in the parameters evaluated, such as ataxia ranking scale, self-assessment score, posturography and motor performance test. The visual system and mental health were also evaluated, but no effect was observed with Bactrim treatment (460).

The progression of MJD will confine the patients to a wheelchair and ultimately the patients will be bedridden. In this condition, and having in mind their cognitive preservation, the patients might suffer depressive symptoms. Furthermore, the serotoninergic system in the cerebellum seems to play a role in motor output, such as locomotion. Serotonergic system impairment in the cerebellum was demonstrated to induce cerebellar ataxia (461). The selective serotonin reuptake inhibitors (SSRIs), such as fluoxetine, are commonly used in the treatment of depression and present few side-effects (462). Taking this into account, Monte et al, performed an open-label trial in 13 molecularly confirmed MJD patients. After 6 weeks of treatment, fluoxetine had no overall effect on motor abilities measured by functional scales and had no beneficial effect on the other neuropsychological tests (463). Again, the outcome of the study may have been compromised by the small number of patients and short duration of the study.

The use of 5-HT1A agonists has been controversial for the treatment of cerebellar ataxia, but several reports have suggested the efficacy of these agonist for the treatment of MJD (464-467). Indeed, Friedmann and collaborators have shown mild effects of buspirone in one MJD patient (468). Later, Takei et al, reported the positive effects of tandospirone, another 5-HT1A agonist, in one MJD patient. This patient showed improvement in ataxia, depression, insomnia, anorexia and leg pain (469). These positive effects lead the authors to pursue a larger clinical trial using 10 MJD patients. In this trial, the patients started tandospirone treatment at an initial dose of 15 mg/kg (as the previous case study) that was further increased to 30mg/kg for 7 weeks. The patients were examined using the international cooperative ataxia ranking scale (ICARS), the total length traveled (TLT) by stabolimetry test and the self-rating depression scale (SDS). All these parameters were alleviated with tandospirone treatment. Interestingly, all the symptoms aggravated after a transient stop of tandospirone, and improved when the therapy was restarted (470). These results suggested that 5-HT1A agonists could be effective in MJD, although more studies need to be performed to confirm these assumptions.

The involvement of *N-methyl-d-aspartate* (NMDA)-mediated apoptosis in the pathogenic mechanism of formation of neuronal inclusions has been proposed (86, 471). It was recently shown that L-glutamate-induced excitation of iPSC cells of MJD patients leads to Ca^{2+}-dependent proteolysis of ATXN3 followed by the formation of insoluble aggregates. The formation of those aggregates was also dependent on Na^{+} and K^{+} channels as well as on voltage-gated Ca^{2+} channels (101). A pilot study was performed in 6 MJD patients using Lamotrigine (25mg twice a day during 9 weeks), a commonly used antiepileptic drug acting as a sodium channel-blocking agent that might be related to the reduction of NMDA-induced toxicity. In this trial,

the patients were evaluated in the one leg standing test (OLST) and tandem gait index (TGI). Both OLST and TGI were improved during Lamotrigine treatment comparing the values obtained with the normal values for Chinese population. Furthermore, and given these positive results, the authors cultured lymphoblastoid cells of one MJD patient and treated those cells with lamotigrine. Mutant, but not normal ataxin-3 was reduced with lamotrigine in concentrations within the therapeutic range in humans. The mechanism underlying the reduction in mutant ataxin-3 levels was not investigated in this work (472).

More recently, Zesiewicz and collaborators carried out a short-term clinical trial in 20 MJD patients using Varenicline (Chantix, 1mg twice a day for 9 weeks). Chantix is a medication used for smoking cessation, being a partial agonist of the $\alpha 4\beta 2$ neuronal nicotinic acetylcholine receptors. Although the major components of the cholinergic system seem to be spared in MJD, which may be reflected in the absence of dementia in MJD patients, the midbrain cholinergic pars compacta of the pedunculopontine nucleus suffers cell loss in these patients with disease progression (413), contributing to REM sleep disturbances. Chantix was shown to be beneficial in SCA patients in some case studies (473-475). In this trial, the patients were evaluated at baseline and at the end of the treatment (after 8 weeks) primarily by the Scale for the Assessment and Rating of Ataxia (SARA scale) and secondary measurements consisted of a timed 25-foot walk, a 9-hole peg test, Beck depression inventory (BDI), Beck anxiety inventory (BAI), clinical global impression (CGI), patient global impression (PGI) and the Short-Form 36 (SF36) to evaluate daily living. Chantix was able to significantly improve some subscores of the SARA scale, such as gait and rapid alternating movements. Also, the timed 25-foot walk was ameliorated by Chantix treatment, as well as the BDI score. The BDI score improved in both groups (Chantix and placebo) probably because the patients that were enrolled in the trial became hopeful regarding new treatment possibilities. A problem concerning this study was a high rate of dropout in the placebo group (4 out of 10 patients), probably reflecting the difficulty of patients to reach the academic center. Regarding adverse events, it is possible to observe that Chantix caused, to a high extent, gastrointestinal-related events when compared to placebo patients. The mechanism by which Chantix improves ataxic symptoms was not evaluated in this study or elsewhere (476).

More recently, Saute and colleagues conducted a phase II clinical trial in 62 MJD patients using Lithium Carbonate. Lithium is commonly used to treat bipolar disorder, and is also used adjunctively with mood stabilizers and antidepressants to enhance, prolong and facilitate treatment response and remission of mood disorders (477, 478). Lithium treatment was shown to have beneficial effects in several models of

different neurodegenerative diseases (479-483), by the inhibition of glycogen synthase kinase-3β (GSK-3β) and autophagy activation. Importantly, however, irreversible cerebellar toxicity, leading to ataxia, nystagmus and dysarthria has also been observed due to lithium intoxication. In this long-term clinical trial, Lithium (at therapeutic dosages of 0.5-0.8 mEq/L) was well tolerated by patients. After 48 weeks of follow-up, patients treated with Lithium did not show significant differences in disease progression, given by the results by Neurological Examination Score for the Assessment of Spinocerebellar Ataxia (NESSCA) and SARA scale. Nevertheless, the authors were able to observe that Lithium-treated MJD patients had a slower progression concerning the PATA test (word speed) and the Click test (finger-pointing coordination) as well as in the SCAFI (spinocerebellar ataxia functional index) and CCFS (composite cerebellar functional score), when compared to patients receiving placebo (484). They suggested that larger clinical trials should be performed in order to understand the value of Lithium in the treatment of MJD.

There are many concerns regarding the clinical trials performed to date in MJD: (i) the small samples of patients, which might be difficult to overcome due to the fact that this is a rare disorder and also the collaboration of patients might represent a problem; (ii) the clinical heterogeneity of the patients could be a concern, and even if the patients have an homogeneous genetic background they could respond differently to the treatment; (iii) the short-term observation of the patients, that contrasts with the slow progression of the disease (except for the Lithium Carbonate trial, which had a duration of 48 weeks); (iv) the outcomes used for ataxia measurement which might be difficult to analyze due to the multisystem involvement in this disease and (v) lastly, the design of the studies as randomized double-blinded trials with quantifiable ataxia scales and non-ataxia measurements should be used, which was not often the case. Despite the existence of several scales to measure ataxia (reviewed in (485)), other non-ataxia scores should be applied to MJD patients since these patients also present non-ataxia symptoms, such as pyramidal and extrapyramidal signs as well as peripheral findings (486).

The link to preclinical studies was also not evident in the trials performed to date, which lacked biological evidence for the therapeutic efficacy of the molecules being tested. This thesis aims to contribute to the field by providing preclinically validated candidate therapeutic molecules for MJD.

Table 6. Clinical trials performed in MJD patients.

Therapeutic molecule	Design	Treatment duration	Number of patients	Mean age (years)	Mean repeat length	Dosage	Known collateral effects	Results	REF
Trimethoprim and sulfamethoxazole (Bactrim)	doubled-blinded	4 weeks	8	NA	NA	NA	nausea, vomiting, anorexia, rash, and urticaria	**Mild effect**; mild improvements of hyperreflexia of knee jerks and of rigospasticity of the legs. Increased levels of biopterins in the CSF after Bactrim treatment.	(458)
Trimethoprim and sulfamethoxazole (Bactrim)	doubled-blinded	NA	8	NA	NA	NA	nausea, vomiting, anorexia, rash, and urticaria	**Beneficial effect on gait and coordination;** subjective performance, neurological examination and timed tests	(459)
Trimethoprim and sulfamethoxazole (Bactrim)	doubled-blinded	24 weeks	22	NA	NA	160 mg + 800 mg twice a day in the first 2 weeks; 80 mg + 400 mg twice a day for 5.5 months	nausea, vomiting, anorexia, rash, and urticaria	**No overall effect;** Ataxia ranking scale, self-assessment score, static posturography, and results of motor performance testing. Effects on the visual system. Physical and mental health were documented using the Medical Outcomes Study 36-Item Short-Form Health Survey.	(460)
Fluoxetine	Open-label	6 weeks	13	41±13	75±3	20 mg/day	nausea, diarrhea, dry mouth, headache, dizziness, sexual dysfunction	**No effect**; functional capacity, standardized neurologic and cognitive ratings. The Montgomery-Asberg depression rating scale was used to control depressive symptoms.	463)

Table 6 (continued). Clinical trials performed in MJD patients.

Therapeutic molecule	Design	Treatment duration	Number of patients	Mean age (years)	Mean repeat length	Dosage	Known collateral effects	Outcome	REF
Buspirone	Case-study	15 weeks	1	NA	NA	12,5mg/day	dizziness, drowsiness and headache, nausea, diarrhea, increase in appetitte	**Mild effect**;improved gait and balance; Clinical rating scale for ataxia was used	(468)
Tandospirone	Case-study	8 weeks	1	51	NA	30mg/day	dizziness, drowsiness, headache, dry mouth, insomnia	**Strong effect**; ataxia, depression, insomnia, anorexia, and leg pain were improved; ICARS(1) and SDS(2) scales were used.	(469)
Tandospirone	Open-labeled	7 weeks	10	50.6±12	NA	30mg/day 15 mg/day	dizziness, drowsiness, headache, dry mouth, insomnia	**Strong effect**; ataxia, depression, insomnia, anorexia, and leg pain were improved; ICARS(1) and SDS(2) scales were used.	(470)
Lamotrigine	Open-labeled	9 weeks	6	27	78±2	25 mg twice a day	Blurred vision, changes in vision, clumsiness or unsteadiness, double vision, poor coordination, skin rash	**Positive effect;** OLST(3) and TGI(4) tests were performed and improved	(472)

Table 6 (continued). Clinical trials performed in MJD patients.

Therapeutic molecule	Design	Treatment duration	Number of patients	Mean age (years)	Mean repeat length	Dosage	Known collateral effects	Outcome	REF
Varenicline (Chantix)	doubled-blinded	8 weeks	20	50.6±11	NA	1 mg twice a day	Abnormal dreams, change in taste, dry mouth, flatulence, headache, lack or loss of strength, nausea, sleeplessness, stomach pain, trouble sleeping, unusual tiredness or weakness	**Positive effect;** SARA(5) scale, a timed 25-foot walk and 9-hole peg test, measurements of mood and anxiety, and adverse events.	476)
Lithium carbonate	doubled-blinded	48 weeks	62	40±9	75±3	Weekly lithium doses were given until a target of 0.5 to 0.8 milliequivalents per liter (mEq/L)	Confusion, poor memory, or lack of awareness, fainting fast or slow heartbeat, frequent urination, increased thirst, irregular pulse, stiffness of the arms or legs, troubled breathing (especially during hard work or exercise), unusual tiredness or weakness, weight gain, intentional tremor	**No overall effect;** NESSCA (6) and SARA scale, 9-hole peg test, 8 Meter Walking Time, Click Test and PATA-rate, Composite Cerebellar Functional Score, Quality-of-Life Questionnaire, Beck Depression Inventory, Clinical Global Impression of Change	(487)

NA – not applicable

References

1. Margolis RL, Ross CA. Expansion explosion: new clues to the pathogenesis of repeat expansion neurodegenerative diseases. Trends Mol Med. 2001;7(11):479-82.
2. Harding AE. The gene for Huntington's disease. BMJ. 1993;307(6901):396-7.
3. La Spada AR, Wilson EM, Lubahn DB, Harding AE, Fischbeck KH. Androgen receptor gene mutations in X-linked spinal and bulbar muscular atrophy. Nature. 1991;352(6330):77-9.
4. Nagafuchi S, Yanagisawa H, Sato K, Shirayama T, Ohsaki E, Bundo M, et al. Dentatorubral and pallidoluysian atrophy expansion of an unstable CAG trinucleotide on chromosome 12p. Nat Genet. 1994;6(1):14-8.
5. Nagafuchi S, Yanagisawa H, Ohsaki E, Shirayama T, Tadokoro K, Inoue T, et al. Structure and expression of the gene responsible for the triplet repeat disorder, dentatorubral and pallidoluysian atrophy (DRPLA). Nat Genet. 1994;8(2):177-82.
6. Orr HT, Chung MY, Banfi S, Kwiatkowski TJ, Jr., Servadio A, Beaudet AL, et al. Expansion of an unstable trinucleotide CAG repeat in spinocerebellar ataxia type 1. Nat Genet. 1993;4(3):221-6.
7. Nechiporuk A, Lopes-Cendes I, Nechiporuk T, Starkman S, Andermann E, Rouleau GA, et al. Genetic mapping of the spinocerebellar ataxia type 2 gene on human chromosome 12. Neurology. 1996;46(6):1731-5.
8. Imbert G, Saudou F, Yvert G, Devys D, Trottier Y, Garnier JM, et al. Cloning of the gene for spinocerebellar ataxia 2 reveals a locus with high sensitivity to expanded CAG/glutamine repeats. Nat Genet. 1996;14(3):285-91.
9. Zhuchenko O, Bailey J, Bonnen P, Ashizawa T, Stockton DW, Amos C, et al. Autosomal dominant cerebellar ataxia (SCA6) associated with small polyglutamine expansions in the alpha 1A-voltage-dependent calcium channel. Nat Genet. 1997;15(1):62-9.
10. David G, Durr A, Stevanin G, Cancel G, Abbas N, Benomar A, et al. Molecular and clinical correlations in autosomal dominant cerebellar ataxia with progressive macular dystrophy (SCA7). Hum Mol Genet. 1998;7(2):165-70.
11. Holmes SE, O'Hearn EE, McInnis MG, Gorelick-Feldman DA, Kleiderlein JJ, Callahan C, et al. Expansion of a novel CAG trinucleotide repeat in the 5' region of PPP2R2B is associated with SCA12. Nat Genet. 1999;23(4):391-2.
12. Kawaguchi Y, Okamoto T, Taniwaki M, Aizawa M, Inoue M, Katayama S, et al. CAG expansions in a novel gene for Machado-Joseph disease at chromosome 14q32.1. Nat Genet. 1994;8(3):221-8.
13. Zoghbi HY, Orr HT. Glutamine repeats and neurodegeneration. Annu Rev Neurosci. 2000;23:217-47.
14. Zoghbi HY, Orr HT. Polyglutamine diseases: protein cleavage and aggregation. Curr Opin Neurobiol. 1999;9(5):566-70.
15. Ikeda H, Yamaguchi M, Sugai S, Aze Y, Narumiya S, Kakizuka A. Expanded polyglutamine in the Machado-Joseph disease protein induces cell death in vitro and in vivo. Nat Genet. 1996;13(2):196-202.
16. Marsh JL, Walker H, Theisen H, Zhu YZ, Fielder T, Purcell J, et al. Expanded polyglutamine peptides alone are intrinsically cytotoxic and cause neurodegeneration in Drosophila. Hum Mol Genet. 2000;9(1):13-25.
17. Morley JF, Brignull HR, Weyers JJ, Morimoto RI. The threshold for polyglutamine-expansion protein aggregation and cellular toxicity is dynamic and influenced by aging in Caenorhabditis elegans. Proc Natl Acad Sci U S A. 2002;99(16):10417-22.

18. Brignull HR, Moore FE, Tang SJ, Morimoto RI. Polyglutamine proteins at the pathogenic threshold display neuron-specific aggregation in a pan-neuronal Caenorhabditis elegans model. J Neurosci. 2006;26(29):7597-606.
19. Mangiarini L, Sathasivam K, Seller M, Cozens B, Harper A, Hetherington C, et al. Exon 1 of the HD gene with an expanded CAG repeat is sufficient to cause a progressive neurological phenotype in transgenic mice. Cell. 1996;87(3):493-506.
20. Tallaksen-Greene SJ, Ordway JM, Crouse AB, Jackson WS, Detloff PJ, Albin RL. Hprt(CAG)146 mice: age of onset of behavioral abnormalities, time course of neuronal intranuclear inclusion accumulation, neurotransmitter marker alterations, mitochondrial function markers, and susceptibility to 1-methyl-4-phenyl-1,2,3,6-tetrahydropyridine. J Comp Neurol. 2003;465(2):205-19.
21. Wolozin B, Behl C. Mechanisms of neurodegenerative disorders: Part 1: protein aggregates. Arch Neurol. 2000;57(6):793-6.
22. Maciel P, Gaspar C, DeStefano AL, Silveira I, Coutinho P, Radvany J, et al. Correlation between CAG repeat length and clinical features in Machado-Joseph disease. Am J Hum Genet. 1995;57(1):54-61.
23. Rubinsztein DC, Leggo J, Coles R, Almqvist E, Biancalana V, Cassiman JJ, et al. Phenotypic characterization of individuals with 30-40 CAG repeats in the Huntington disease (HD) gene reveals HD cases with 36 repeats and apparently normal elderly individuals with 36-39 repeats. Am J Hum Genet. 1996;59(1):16-22.
24. Ravina B, Romer M, Constantinescu R, Biglan K, Brocht A, Kieburtz K, et al. The relationship between CAG repeat length and clinical progression in Huntington's disease. Mov Disord. 2008;23(9):1223-7.
25. Ross CA. Intranuclear neuronal inclusions: a common pathogenic mechanism for glutamine-repeat neurodegenerative diseases? Neuron. 1997;19(6):1147-50.
26. Bauer PO, Nukina N. The pathogenic mechanisms of polyglutamine diseases and current therapeutic strategies. J Neurochem. 2009;110(6):1737-65.
27. Teixeira-Castro A. Identifcation of modulators of ataxin-3 proteotoxicity in animal models of Machado-Joseph disease [PhD]: University of Minho; 2011.
28. Yamamoto A, Lucas JJ, Hen R. Reversal of neuropathology and motor dysfunction in a conditional model of Huntington's disease. Cell. 2000;101(1):57-66.
29. Regulier E, Trottier Y, Perrin V, Aebischer P, Deglon N. Early and reversible neuropathology induced by tetracycline-regulated lentiviral overexpression of mutant huntingtin in rat striatum. Hum Mol Genet. 2003;12(21):2827-36.
30. Boy J, Schmidt T, Wolburg H, Mack A, Nuber S, Bottcher M, et al. Reversibility of symptoms in a conditional mouse model of spinocerebellar ataxia type 3. Hum Mol Genet. 2009;18(22):4282-95.
31. Zu T, Duvick LA, Kaytor MD, Berlinger MS, Zoghbi HY, Clark HB, et al. Recovery from polyglutamine-induced neurodegeneration in conditional SCA1 transgenic mice. J Neurosci. 2004;24(40):8853-61.
32. Du T, Zamore PD. microPrimer: the biogenesis and function of microRNA. Development. 2005;132(21):4645-52.
33. Lee Y, Jeon K, Lee JT, Kim S, Kim VN. MicroRNA maturation: stepwise processing and subcellular localization. EMBO J. 2002;21(17):4663-70.
34. Lee Y, Ahn C, Han J, Choi H, Kim J, Yim J, et al. The nuclear RNase III Drosha initiates microRNA processing. Nature. 2003;425(6956):415-9.
35. Gregory RI, Yan KP, Amuthan G, Chendrimada T, Doratotaj B, Cooch N, et al. The Microprocessor complex mediates the genesis of microRNAs. Nature. 2004;432(7014):235-40.
36. Yi R, Qin Y, Macara IG, Cullen BR. Exportin-5 mediates the nuclear export of pre-microRNAs and short hairpin RNAs. Genes Dev. 2003;17(24):3011-6.

37. Provost P, Dishart D, Doucet J, Frendewey D, Samuelsson B, Radmark O. Ribonuclease activity and RNA binding of recombinant human Dicer. EMBO J. 2002;21(21):5864-74.
38. Schwarz DS, Hutvagner G, Du T, Xu Z, Aronin N, Zamore PD. Asymmetry in the assembly of the RNAi enzyme complex. Cell. 2003;115(2):199-208.
39. Khvorova A, Reynolds A, Jayasena SD. Functional siRNAs and miRNAs exhibit strand bias. Cell. 2003;115(2):209-16.
40. Boudreau RL, Rodriguez-Lebron E, Davidson BL. RNAi medicine for the brain: progresses and challenges. Hum Mol Genet. 2011;20(R1):R21-7.
41. Boudreau RL, Davidson BL. RNAi therapeutics for CNS disorders. Brain Res. 2010;1338:112-21.
42. Caplen NJ, Taylor JP, Statham VS, Tanaka F, Fire A, Morgan RA. Rescue of polyglutamine-mediated cytotoxicity by double-stranded RNA-mediated RNA interference. Hum Mol Genet. 2002;11(2):175-84.
43. Xia H, Mao Q, Eliason SL, Harper SQ, Martins IH, Orr HT, et al. RNAi suppresses polyglutamine-induced neurodegeneration in a model of spinocerebellar ataxia. Nat Med. 2004;10(8):816-20.
44. Burright EN, Clark HB, Servadio A, Matilla T, Feddersen RM, Yunis WS, et al. SCA1 transgenic mice: a model for neurodegeneration caused by an expanded CAG trinucleotide repeat. Cell. 1995;82(6):937-48.
45. Harper SQ, Staber PD, He X, Eliason SL, Martins IH, Mao Q, et al. RNA interference improves motor and neuropathological abnormalities in a Huntington's disease mouse model. Proc Natl Acad Sci U S A. 2005;102(16):5820-5.
46. Rodriguez-Lebron E, Denovan-Wright EM, Nash K, Lewin AS, Mandel RJ. Intrastriatal rAAV-mediated delivery of anti-huntingtin shRNAs induces partial reversal of disease progression in R6/1 Huntington's disease transgenic mice. Molecular Therapy. 2005;12(4):618-33.
47. Machida Y, Okada T, Kurosawa M, Oyama F, Ozawa K, Nukina N. rAAV-mediated shRNA ameliorated neuropathology in Huntington disease model mouse. Biochem Biophys Res Commun. 2006;343(1):190-7.
48. Stevanin G, Cancel G, Didierjean O, Durr A, Abbas N, Cassa E, et al. Linkage disequilibrium at the Machado-Joseph disease/spinal cerebellar ataxia 3 locus: evidence for a common founder effect in French and Portuguese-Brazilian families as well as a second ancestral Portuguese-Azorean mutation. Am J Hum Genet. 1995;57(5):1247-50.
49. Lopes-Cendes I, Maciel P, Kish S, Gaspar C, Robitaille Y, Clark HB, et al. Somatic mosaicism in the central nervous system in spinocerebellar ataxia type 1 and Machado-Joseph disease. Ann Neurol. 1996;40(2):199-206.
50. Gaspar C, Lopes-Cendes I, Hayes S, Goto J, Arvidsson K, Dias A, et al. Ancestral origins of the Machado-Joseph disease mutation: a worldwide haplotype study. Am J Hum Genet. 2001;68(2):523-8.
51. Miller VM, Xia H, Marrs GL, Gouvion CM, Lee G, Davidson BL, et al. Allele-specific silencing of dominant disease genes. Proc Natl Acad Sci U S A. 2003;100(12):7195-200.
52. Alves S, Nascimento-Ferreira I, Auregan G, Hassig R, Dufour N, Brouillet E, et al. Allele-specific RNA silencing of mutant ataxin-3 mediates neuroprotection in a rat model of Machado-Joseph disease. PLoS One. 2008;3(10):e3341.
53. Greenberg J, Solomon GA, Vorster AA, Heckmann J, Bryer A. Origin of the SCA7 gene mutation in South Africa: implications for molecular diagnostics. Clin Genet. 2006;70(5):415-7.
54. Scholefield J, Greenberg LJ, Weinberg MS, Arbuthnot PB, Abdelgany A, Wood MJ. Design of RNAi hairpins for mutation-specific silencing of ataxin-7 and correction of a SCA7 phenotype. PLoS ONE. 2009;4(9):e7232.

55. Pfister EL, Kennington L, Straubhaar J, Wagh S, Liu W, DiFiglia M, et al. Five siRNAs targeting three SNPs may provide therapy for three-quarters of Huntington's disease patients. Curr Biol. 2009;19(9):774-8.
56. Lombardi MS, Jaspers L, Spronkmans C, Gellera C, Taroni F, Di Maria E, et al. A majority of Huntington's disease patients may be treatable by individualized allele-specific RNA interference. Exp Neurol. 2009;217(2):312-9.
57. Ambrose CM, Duyao MP, Barnes G, Bates GP, Lin CS, Srinidhi J, et al. Structure and expression of the Huntington's disease gene: evidence against simple inactivation due to an expanded CAG repeat. Somat Cell Mol Genet. 1994;20(1):27-38.
58. Zhang Y, Engelman J, Friedlander RM. Allele-specific silencing of mutant Huntington's disease gene. J Neurochem. 2009;108(1):82-90.
59. Hu J, Liu J, Corey DR. Allele-selective inhibition of huntingtin expression by switching to an miRNA-like RNAi mechanism. Chem Biol. 2010;17(11):1183-8.
60. Fiszer A, Mykowska A, Krzyzosiak WJ. Inhibition of mutant huntingtin expression by RNA duplex targeting expanded CAG repeats. Nucleic Acids Res. 2011;39(13):5578-85.
61. Kubodera T, Yokota T, Ishikawa K, Mizusawa H. New RNAi strategy for selective suppression of a mutant allele in polyglutamine disease. Oligonucleotides. 2005;15(4):298-302.
62. Tsou WL, Soong BW, Paulson HL, Rodriguez-Lebron E. Splice isoform-specific suppression of the CaV2.1 variant underlying spinocerebellar ataxia type 6. Neurobiol Dis. 2011;43(3):533-42.
63. Boudreau RL, McBride JL, Martins I, Shen S, Xing Y, Carter BJ, et al. Nonallele-specific silencing of mutant and wild-type huntingtin demonstrates therapeutic efficacy in Huntington's disease mice. Mol Ther. 2009;17(6):1053-63.
64. Drouet V, Perrin V, Hassig R, Dufour N, Auregan G, Alves S, et al. Sustained effects of nonallele-specific Huntingtin silencing. Ann Neurol. 2009;65(3):276-85.
65. McBride JL, Pitzer MR, Boudreau RL, Dufour B, Hobbs T, Ojeda SR, et al. Preclinical safety of RNAi-mediated HTT suppression in the rhesus macaque as a potential therapy for Huntington's disease. Mol Ther. 2011;19(12):2152-62.
66. Alves S, Nascimento-Ferreira I, Dufour N, Hassig R, Auregan G, Nobrega C, et al. Silencing ataxin-3 mitigates degeneration in a rat model of Machado-Joseph disease: no role for wild-type ataxin-3? Hum Mol Genet. 2010;19(12):2380-94.
67. Nobrega C, Nascimento-Ferreira I, Onofre I, Albuquerque D, Deglon N, de Almeida LP. RNA interference mitigates motor and neuropathological deficits in a cerebellar mouse model of Machado-Joseph disease. PLoS One. 2014;9(8):e100086.
68. Zhang Y, Friedlander RM. Using non-coding small RNAs to develop therapies for Huntington's disease. Gene Ther. 2011;18(12):1139-49.
69. Scholefield J, Wood MJ. Therapeutic gene silencing strategies for polyglutamine disorders. Trends Genet. 2010;26(1):29-38.
70. McBride JL, Boudreau RL, Harper SQ, Staber PD, Monteys AM, Martins I, et al. Artificial miRNAs mitigate shRNA-mediated toxicity in the brain: implications for the therapeutic development of RNAi. Proc Natl Acad Sci U S A. 2008;105(15):5868-73.
71. Olson SD, Kambal A, Pollock K, Mitchell GM, Stewart H, Kalomoiris S, et al. Examination of mesenchymal stem cell-mediated RNAi transfer to Huntington's disease affected neuronal cells for reduction of huntingtin. Mol Cell Neurosci. 2012;49(3):271-81.
72. Jagannath A, Wood M. RNA interference based gene therapy for neurological disease. Brief Funct Genomic Proteomic. 2007;6(1):40-9.
73. Allerson CR, Sioufi N, Jarres R, Prakash TP, Naik N, Berdeja A, et al. Fully 2'-modified oligonucleotide duplexes with improved in vitro potency and stability compared to unmodified small interfering RNA. J Med Chem. 2005;48(4):901-4.

74. Dande P, Prakash TP, Sioufi N, Gaus H, Jarres R, Berdeja A, et al. Improving RNA interference in mammalian cells by 4'-thio-modified small interfering RNA (siRNA): effect on siRNA activity and nuclease stability when used in combination with 2'-O-alkyl modifications. J Med Chem. 2006;49(5):1624-34.
75. Jackson AL, Burchard J, Leake D, Reynolds A, Schelter J, Guo J, et al. Position-specific chemical modification of siRNAs reduces "off-target" transcript silencing. RNA. 2006;12(7):1197-205.
76. Wang YL, Liu W, Wada E, Murata M, Wada K, Kanazawa I. Clinico-pathological rescue of a model mouse of Huntington's disease by siRNA. Neurosci Res. 2005;53(3):241-9.
77. DiFiglia M, Sena-Esteves M, Chase K, Sapp E, Pfister E, Sass M, et al. Therapeutic silencing of mutant huntingtin with siRNA attenuates striatal and cortical neuropathology and behavioral deficits. Proc Natl Acad Sci U S A. 2007;104(43):17204-9.
78. Ellerby LM, Andrusiak RL, Wellington CL, Hackam AS, Propp SS, Wood JD, et al. Cleavage of atrophin-1 at caspase site aspartic acid 109 modulates cytotoxicity. J Biol Chem. 1999;274(13):8730-6.
79. Igarashi S, Koide R, Shimohata T, Yamada M, Hayashi Y, Takano H, et al. Suppression of aggregate formation and apoptosis by transglutaminase inhibitors in cells expressing truncated DRPLA protein with an expanded polyglutamine stretch. Nat Genet. 1998;18(2):111-7.
80. Hackam AS, Singaraja R, Zhang T, Gan L, Hayden MR. In vitro evidence for both the nucleus and cytoplasm as subcellular sites of pathogenesis in Huntington's disease. Hum Mol Genet. 1999;8(1):25-33.
81. Gardian G, Browne SE, Choi DK, Klivenyi P, Gregorio J, Kubilus JK, et al. Neuroprotective effects of phenylbutyrate in the N171-82Q transgenic mouse model of Huntington's disease. J Biol Chem. 2005;280(1):556-63.
82. Lunkes A, Lindenberg KS, Ben-Haiem L, Weber C, Devys D, Landwehrmeyer GB, et al. Proteases acting on mutant huntingtin generate cleaved products that differentially build up cytoplasmic and nuclear inclusions. Mol Cell. 2002;10(2):259-69.
83. DiFiglia M, Sapp E, Chase KO, Davies SW, Bates GP, Vonsattel JP, et al. Aggregation of huntingtin in neuronal intranuclear inclusions and dystrophic neurites in brain. Science. 1997;277(5334):1990-3.
84. Li M, Miwa S, Kobayashi Y, Merry DE, Yamamoto M, Tanaka F, et al. Nuclear inclusions of the androgen receptor protein in spinal and bulbar muscular atrophy. Ann Neurol. 1998;44(2):249-54.
85. Schmidt T, Landwehrmeyer GB, Schmitt I, Trottier Y, Auburger G, Laccone F, et al. An isoform of ataxin-3 accumulates in the nucleus of neuronal cells in affected brain regions of SCA3 patients. Brain Pathol. 1998;8(4):669-79.
86. Paulson HL, Perez MK, Trottier Y, Trojanowski JQ, Subramony SH, Das SS, et al. Intranuclear inclusions of expanded polyglutamine protein in spinocerebellar ataxia type 3. Neuron. 1997;19(2):333-44.
87. Martindale D, Hackam A, Wieczorek A, Ellerby L, Wellington C, McCutcheon K, et al. Length of huntingtin and its polyglutamine tract influences localization and frequency of intracellular aggregates. Nat Genet. 1998;18(2):150-4.
88. Merry DE, Kobayashi Y, Bailey CK, Taye AA, Fischbeck KH. Cleavage, aggregation and toxicity of the expanded androgen receptor in spinal and bulbar muscular atrophy. Hum Mol Genet. 1998;7(4):693-701.
89. Goldberg YP, Nicholson DW, Rasper DM, Kalchman MA, Koide HB, Graham RK, et al. Cleavage of huntingtin by apopain, a proapoptotic cysteine protease, is modulated by the polyglutamine tract. Nat Genet. 1996;13(4):442-9.

90. Wellington CL, Ellerby LM, Hackam AS, Margolis RL, Trifiro MA, Singaraja R, et al. Caspase cleavage of gene products associated with triplet expansion disorders generates truncated fragments containing the polyglutamine tract. J Biol Chem. 1998;273(15):9158-67.
91. Kim YJ, Yi Y, Sapp E, Wang Y, Cuiffo B, Kegel KB, et al. Caspase 3-cleaved N-terminal fragments of wild-type and mutant huntingtin are present in normal and Huntington's disease brains, associate with membranes, and undergo calpain-dependent proteolysis. Proc Natl Acad Sci U S A. 2001;98(22):12784-9.
92. Gafni J, Ellerby LM. Calpain activation in Huntington's disease. J Neurosci. 2002;22(12):4842-9.
93. Berke SJ, Schmied FA, Brunt ER, Ellerby LM, Paulson HL. Caspase-mediated proteolysis of the polyglutamine disease protein ataxin-3. J Neurochem. 2004;89(4):908-18.
94. Haacke A, Hartl FU, Breuer P. Calpain inhibition is sufficient to suppress aggregation of polyglutamine-expanded ataxin-3. J Biol Chem. 2007;282(26):18851-6.
95. Graham RK, Slow EJ, Deng Y, Bissada N, Lu G, Pearson J, et al. Levels of mutant huntingtin influence the phenotypic severity of Huntington disease in YAC128 mouse models. Neurobiol Dis. 2006;21(2):444-55.
96. Waldron-Roby E, Ratovitski T, Wang X, Jiang M, Watkin E, Arbez N, et al. Transgenic mouse model expressing the caspase 6 fragment of mutant huntingtin. J Neurosci. 2012;32(1):183-93.
97. Poukka H, Karvonen U, Janne OA, Palvimo JJ. Covalent modification of the androgen receptor by small ubiquitin-like modifier 1 (SUMO-1). Proc Natl Acad Sci U S A. 2000;97(26):14145-50.
98. Young JE, Gouw L, Propp S, Sopher BL, Taylor J, Lin A, et al. Proteolytic cleavage of ataxin-7 by caspase-7 modulates cellular toxicity and transcriptional dysregulation. J Biol Chem. 2007;282(41):30150-60.
99. Goti D, Katzen SM, Mez J, Kurtis N, Kiluk J, Ben-Haiem L, et al. A mutant ataxin-3 putative-cleavage fragment in brains of Machado-Joseph disease patients and transgenic mice is cytotoxic above a critical concentration. J Neurosci. 2004;24(45):10266-79.
100. Jung J, Xu K, Lessing D, Bonini NM. Preventing Ataxin-3 protein cleavage mitigates degeneration in a Drosophila model of SCA3. Hum Mol Genet. 2009;18(24):4843-52.
101. Koch P, Breuer P, Peitz M, Jungverdorben J, Kesavan J, Poppe D, et al. Excitation-induced ataxin-3 aggregation in neurons from patients with Machado-Joseph disease. Nature. 2011;480(7378):543-6.
102. Teixeira-Castro A, Ailion M, Jalles A, Brignull HR, Vilaca JL, Dias N, et al. Neuron-specific proteotoxicity of mutant ataxin-3 in C. elegans: rescue by the DAF-16 and HSF-1 pathways. Hum Mol Genet. 2011;20(15):2996-3009.
103. Silva-Fernandes A, Costa Mdo C, Duarte-Silva S, Oliveira P, Botelho CM, Martins L, et al. Motor uncoordination and neuropathology in a transgenic mouse model of Machado-Joseph disease lacking intranuclear inclusions and ataxin-3 cleavage products. Neurobiol Dis. 2010;40(1):163-76.
104. Ono Y, Sorimachi H. Calpains: an elaborate proteolytic system. Biochim Biophys Acta. 2012;1824(1):224-36.
105. Hyman BT, Yuan J. Apoptotic and non-apoptotic roles of caspases in neuronal physiology and pathophysiology. Nat Rev Neurosci. 2012;13(6):395-406.
106. Butler DC, McLear JA, Messer A. Engineered antibody therapies to counteract mutant huntingtin and related toxic intracellular proteins. Prog Neurobiol. 2011.
107. Heiser V, Scherzinger E, Boeddrich A, Nordhoff E, Lurz R, Schugardt N, et al. Inhibition of huntingtin fibrillogenesis by specific antibodies and small molecules: implications for Huntington's disease therapy. Proc Natl Acad Sci U S A. 2000;97(12):6739-44.

108. Smith DL, Portier R, Woodman B, Hockly E, Mahal A, Klunk WE, et al. Inhibition of polyglutamine aggregation in R6/2 HD brain slices-complex dose-response profiles. Neurobiol Dis. 2001;8(6):1017-26.
109. Poirier MA, Li H, Macosko J, Cai S, Amzel M, Ross CA. Huntingtin spheroids and protofibrils as precursors in polyglutamine fibrilization. J Biol Chem. 2002;277(43):41032-7.
110. Sanchez I, Mahlke C, Yuan J. Pivotal role of oligomerization in expanded polyglutamine neurodegenerative disorders. Nature. 2003;421(6921):373-9.
111. Heiser V, Engemann S, Brocker W, Dunkel I, Boeddrich A, Waelter S, et al. Identification of benzothiazoles as potential polyglutamine aggregation inhibitors of Huntington's disease by using an automated filter retardation assay. Proc Natl Acad Sci U S A. 2002;99 Suppl 4:16400-6.
112. Wanker EE, Scherzinger E, Heiser V, Sittler A, Eickhoff H, Lehrach H. Membrane filter assay for detection of amyloid-like polyglutamine-containing protein aggregates. Methods Enzymol. 1999;309:375-86.
113. Hockly E, Tse J, Barker AL, Moolman DL, Beunard JL, Revington AP, et al. Evaluation of the benzothiazole aggregation inhibitors riluzole and PGL-135 as therapeutics for Huntington's disease. Neurobiol Dis. 2006;21(1):228-36.
114. Ehrnhoefer DE, Duennwald M, Markovic P, Wacker JL, Engemann S, Roark M, et al. Green tea (-)-epigallocatechin-gallate modulates early events in huntingtin misfolding and reduces toxicity in Huntington's disease models. Hum Mol Genet. 2006;15(18):2743-51.
115. Tanaka M, Morishima I, Akagi T, Hashikawa T, Nukina N. Intra- and intermolecular beta-pleated sheet formation in glutamine-repeat inserted myoglobin as a model for polyglutamine diseases. J Biol Chem. 2001;276(48):45470-5.
116. Tanaka M, Machida Y, Nishikawa Y, Akagi T, Morishima I, Hashikawa T, et al. The effects of aggregation-inducing motifs on amyloid formation of model proteins related to neurodegenerative diseases. Biochemistry. 2002;41(32):10277-86.
117. Benaroudj N, Lee DH, Goldberg AL. Trehalose accumulation during cellular stress protects cells and cellular proteins from damage by oxygen radicals. J Biol Chem. 2001;276(26):24261-7.
118. Jain NK, Roy I. Effect of trehalose on protein structure. Protein Sci. 2009;18(1):24-36.
119. Tanaka M, Machida Y, Niu S, Ikeda T, Jana NR, Doi H, et al. Trehalose alleviates polyglutamine-mediated pathology in a mouse model of Huntington disease. Nat Med. 2004;10(2):148-54.
120. Conlin LK, Nelson HC. The natural osmolyte trehalose is a positive regulator of the heat-induced activity of yeast heat shock transcription factor. Mol Cell Biol. 2007;27(4):1505-15.
121. Sarkar S, Davies JE, Huang Z, Tunnacliffe A, Rubinsztein DC. Trehalose, a novel mTOR-independent autophagy enhancer, accelerates the clearance of mutant huntingtin and alpha-synuclein. J Biol Chem. 2007;282(8):5641-52.
122. Pollitt SK, Pallos J, Shao J, Desai UA, Ma AA, Thompson LM, et al. A rapid cellular FRET assay of polyglutamine aggregation identifies a novel inhibitor. Neuron. 2003;40(4):685-94.
123. Li M, Huang Y, Ma AA, Lin E, Diamond MI. Y-27632 improves rotarod performance and reduces huntingtin levels in R6/2 mice. Neurobiol Dis. 2009;36(3):413-20.
124. Zhang X, Smith DL, Meriin AB, Engemann S, Russel DE, Roark M, et al. A potent small molecule inhibits polyglutamine aggregation in Huntington's disease neurons and suppresses neurodegeneration in vivo. Proc Natl Acad Sci U S A. 2005;102(3):892-7.
125. Chopra V, Fox JH, Lieberman G, Dorsey K, Matson W, Waldmeier P, et al. A small-molecule therapeutic lead for Huntington's disease: preclinical pharmacology and efficacy of C2-8 in the R6/2 transgenic mouse. Proc Natl Acad Sci U S A. 2007;104(42):16685-9.
126. Fuentealba RA, Marasa J, Diamond MI, Piwnica-Worms D, Weihl CC. An aggregation sensing reporter identifies leflunomide and teriflunomide as polyglutamine aggregate inhibitors. Hum Mol Genet. 2012;21(3):664-80.

127. Lecerf JM, Shirley TL, Zhu Q, Kazantsev A, Amersdorfer P, Housman DE, et al. Human single-chain Fv intrabodies counteract in situ huntingtin aggregation in cellular models of Huntington's disease. Proc Natl Acad Sci U S A. 2001;98(8):4764-9.
128. Murphy RC, Messer A. A single-chain Fv intrabody provides functional protection against the effects of mutant protein in an organotypic slice culture model of Huntington's disease. Brain Res Mol Brain Res. 2004;121(1-2):141-5.
129. Miller TW, Zhou C, Gines S, MacDonald ME, Mazarakis ND, Bates GP, et al. A human single-chain Fv intrabody preferentially targets amino-terminal Huntingtin's fragments in striatal models of Huntington's disease. Neurobiol Dis. 2005;19(1-2):47-56.
130. Wolfgang WJ, Miller TW, Webster JM, Huston JS, Thompson LM, Marsh JL, et al. Suppression of Huntington's disease pathology in Drosophila by human single-chain Fv antibodies. Proc Natl Acad Sci U S A. 2005;102(32):11563-8.
131. Snyder-Keller A, McLear JA, Hathorn T, Messer A. Early or late-stage anti-N-terminal Huntingtin intrabody gene therapy reduces pathological features in B6.HDR6/1 mice. J Neuropathol Exp Neurol. 2010;69(10):1078-85.
132. Colby DW, Chu Y, Cassady JP, Duennwald M, Zazulak H, Webster JM, et al. Potent inhibition of huntingtin aggregation and cytotoxicity by a disulfide bond-free single-domain intracellular antibody. Proc Natl Acad Sci U S A. 2004;101(51):17616-21.
133. Southwell AL, Ko J, Patterson PH. Intrabody gene therapy ameliorates motor, cognitive, and neuropathological symptoms in multiple mouse models of Huntington's disease. J Neurosci. 2009;29(43):13589-602.
134. Ko J, Ou S, Patterson PH. New anti-huntingtin monoclonal antibodies: implications for huntingtin conformation and its binding proteins. Brain Res Bull. 2001;56(3-4):319-29.
135. Khoshnan A, Ko J, Patterson PH. Effects of intracellular expression of anti-huntingtin antibodies of various specificities on mutant huntingtin aggregation and toxicity. Proc Natl Acad Sci U S A. 2002;99(2):1002-7.
136. Wang CE, Zhou H, McGuire JR, Cerullo V, Lee B, Li SH, et al. Suppression of neuropil aggregates and neurological symptoms by an intracellular antibody implicates the cytoplasmic toxicity of mutant huntingtin. J Cell Biol. 2008;181(5):803-16.
137. Nagai Y, Popiel HA. Conformational changes and aggregation of expanded polyglutamine proteins as therapeutic targets of the polyglutamine diseases: exposed beta-sheet hypothesis. Curr Pharm Des. 2008;14(30):3267-79.
138. Trottier Y, Lutz Y, Stevanin G, Imbert G, Devys D, Cancel G, et al. Polyglutamine expansion as a pathological epitope in Huntington's disease and four dominant cerebellar ataxias. Nature. 1995;378(6555):403-6.
139. Nagai Y, Tucker T, Ren H, Kenan DJ, Henderson BS, Keene JD, et al. Inhibition of polyglutamine protein aggregation and cell death by novel peptides identified by phage display screening. J Biol Chem. 2000;275(14):10437-42.
140. Nagai Y, Inui T, Popiel HA, Fujikake N, Hasegawa K, Urade Y, et al. A toxic monomeric conformer of the polyglutamine protein. Nat Struct Mol Biol. 2007;14(4):332-40.
141. Nagai Y, Fujikake N, Ohno K, Higashiyama H, Popiel HA, Rahadian J, et al. Prevention of polyglutamine oligomerization and neurodegeneration by the peptide inhibitor QBP1 in Drosophila. Hum Mol Genet. 2003;12(11):1253-9.
142. Popiel HA, Nagai Y, Fujikake N, Toda T. Protein transduction domain-mediated delivery of QBP1 suppresses polyglutamine-induced neurodegeneration in vivo. Mol Ther. 2007;15(2):303-9.
143. Popiel HA, Nagai Y, Fujikake N, Toda T. Delivery of the aggregate inhibitor peptide QBP1 into the mouse brain using PTDs and its therapeutic effect on polyglutamine disease mice. Neurosci Lett. 2009;449(2):87-92.

144. Chen X, Wu J, Luo Y, Liang X, Supnet C, Kim MW, et al. Expanded polyglutamine-binding peptoid as a novel therapeutic agent for treatment of Huntington's disease. Chem Biol. 2011;18(9):1113-25.
145. Arribat Y, Bonneaud N, Talmat-Amar Y, Layalle S, Parmentier ML, Maschat F. A huntingtin peptide inhibits polyQ-huntingtin associated defects. PLoS One. 2013;8(7):e68775.
146. Arribat Y, Talmat-Amar Y, Paucard A, Lesport P, Bonneaud N, Bauer C, et al. Systemic delivery of P42 peptide: a new weapon to fight Huntington's disease. Acta Neuropathol Commun. 2014;2:86.
147. Underwood BR, Rubinsztein DC. Spinocerebellar ataxias caused by polyglutamine expansions: a review of therapeutic strategies. Cerebellum. 2008;7(2):215-21.
148. Karpuj MV, Garren H, Slunt H, Price DL, Gusella J, Becher MW, et al. Transglutaminase aggregates huntingtin into nonamyloidogenic polymers, and its enzymatic activity increases in Huntington's disease brain nuclei. Proc Natl Acad Sci U S A. 1999;96(13):7388-93.
149. Karpuj MV, Becher MW, Springer JE, Chabas D, Youssef S, Pedotti R, et al. Prolonged survival and decreased abnormal movements in transgenic model of Huntington disease, with administration of the transglutaminase inhibitor cystamine. Nat Med. 2002;8(2):143-9.
150. Lesort M, Chun W, Johnson GV, Ferrante RJ. Tissue transglutaminase is increased in Huntington's disease brain. J Neurochem. 1999;73(5):2018-27.
151. Dedeoglu A, Kubilus JK, Jeitner TM, Matson SA, Bogdanov M, Kowall NW, et al. Therapeutic effects of cystamine in a murine model of Huntington's disease. J Neurosci. 2002;22(20):8942-50.
152. Zainelli GM, Ross CA, Troncoso JC, Muma NA. Transglutaminase cross-links in intranuclear inclusions in Huntington disease. J Neuropathol Exp Neurol. 2003;62(1):14-24.
153. Lesort M, Lee M, Tucholski J, Johnson GV. Cystamine inhibits caspase activity. Implications for the treatment of polyglutamine disorders. J Biol Chem. 2003;278(6):3825-30.
154. Borrell-Pages M, Canals JM, Cordelieres FP, Parker JA, Pineda JR, Grange G, et al. Cystamine and cysteamine increase brain levels of BDNF in Huntington disease via HSJ1b and transglutaminase. J Clin Invest. 2006;116(5):1410-24.
155. Horwich AL, Weissman JS. Deadly conformations–protein misfolding in prion disease. Cell. 1997;89(4):499-510.
156. Morimoto RI. Dynamic remodeling of transcription complexes by molecular chaperones. Cell. 2002;110(3):281-4.
157. Nollen EA, Morimoto RI. Chaperoning signaling pathways: molecular chaperones as stress-sensing 'heat shock' proteins. J Cell Sci. 2002;115(Pt 14):2809-16.
158. Schubert U, Anton LC, Gibbs J, Norbury CC, Yewdell JW, Bennink JR. Rapid degradation of a large fraction of newly synthesized proteins by proteasomes. Nature. 2000;404(6779):770-4.
159. Warrick JM, Paulson HL, Gray-Board GL, Bui QT, Fischbeck KH, Pittman RN, et al. Expanded polyglutamine protein forms nuclear inclusions and causes neural degeneration in Drosophila. Cell. 1998;93(6):939-49.
160. Warrick JM, Chan HY, Gray-Board GL, Chai Y, Paulson HL, Bonini NM. Suppression of polyglutamine-mediated neurodegeneration in Drosophila by the molecular chaperone HSP70. Nat Genet. 1999;23(4):425-8.
161. Williams AJ, Knutson TM, Colomer Gould VF, Paulson HL. In vivo suppression of polyglutamine neurotoxicity by C-terminus of Hsp70-interacting protein (CHIP) supports an aggregation model of pathogenesis. Neurobiol Dis. 2009;33(3):342-53.
162. Kobayashi Y, Kume A, Li M, Doyu M, Hata M, Ohtsuka K, et al. Chaperones Hsp70 and Hsp40 suppress aggregate formation and apoptosis in cultured neuronal cells expressing truncated androgen receptor protein with expanded polyglutamine tract. J Biol Chem. 2000;275(12):8772-8.

163. Huang S, Ling JJ, Yang S, Li XJ, Li S. Neuronal expression of TATA box-binding protein containing expanded polyglutamine in knock-in mice reduces chaperone protein response by impairing the function of nuclear factor-Y transcription factor. Brain. 2011;134(Pt 7):1943-58.
164. Zijlstra MP, Rujano MA, Van Waarde MA, Vis E, Brunt ER, Kampinga HH. Levels of DNAJB family members (HSP40) correlate with disease onset in patients with spinocerebellar ataxia type 3. Eur J Neurosci. 2010;32(5):760-70.
165. Li L, Saegusa H, Tanabe T. Deficit of heat shock transcription factor 1-heat shock 70 kDa protein 1A axis determines the cell death vulnerability in a model of spinocerebellar ataxia type 6. Genes Cells. 2009;14(11):1253-69.
166. Sakahira H, Breuer P, Hayer-Hartl MK, Hartl FU. Molecular chaperones as modulators of polyglutamine protein aggregation and toxicity. Proc Natl Acad Sci U S A. 2002;99 Suppl 4:16412-8.
167. Muchowski PJ, Wacker JL. Modulation of neurodegeneration by molecular chaperones. Nat Rev Neurosci. 2005;6(1):11-22.
168. Olshina MA, Angley LM, Ramdzan YM, Tang J, Bailey MF, Hill AF, et al. Tracking mutant huntingtin aggregation kinetics in cells reveals three major populations that include an invariant oligomer pool. J Biol Chem. 2010;285(28):21807-16.
169. Monsellier E, Redeker V, Ruiz-Arlandis G, Bousset L, Melki R. Molecular interaction between the chaperone Hsc70 and the N-terminal flank of huntingtin exon 1 modulates aggregation. J Biol Chem. 2015;290(5):2560-76.
170. Cummings CJ, Mancini MA, Antalffy B, DeFranco DB, Orr HT, Zoghbi HY. Chaperone suppression of aggregation and altered subcellular proteasome localization imply protein misfolding in SCA1. Nat Genet. 1998;19(2):148-54.
171. Cummings CJ, Sun Y, Opal P, Antalffy B, Mestril R, Orr HT, et al. Over-expression of inducible HSP70 chaperone suppresses neuropathology and improves motor function in SCA1 mice. Hum Mol Genet. 2001;10(14):1511-8.
172. Chai Y, Koppenhafer SL, Bonini NM, Paulson HL. Analysis of the role of heat shock protein (Hsp) molecular chaperones in polyglutamine disease. J Neurosci. 1999;19(23):10338-47.
173. Tsou WL, Ouyang M, Hosking RR, Sutton JR, Blount JR, Burr AA, et al. The deubiquitinase ataxin-3 requires Rad23 and DnaJ-1 for its neuroprotective role in Drosophila melanogaster. Neurobiol Dis. 2015;82:12-21.
174. Bailey CK, Andriola IF, Kampinga HH, Merry DE. Molecular chaperones enhance the degradation of expanded polyglutamine repeat androgen receptor in a cellular model of spinal and bulbar muscular atrophy. Hum Mol Genet. 2002;11(5):515-23.
175. Tsou WL, Hosking RR, Burr AA, Sutton JR, Ouyang M, Du X, et al. DnaJ-1 and karyopherin alpha3 suppress degeneration in a new Drosophila model of Spinocerebellar Ataxia Type 6. Hum Mol Genet. 2015.
176. Smith HL, Li W, Cheetham ME. Molecular chaperones and neuronal proteostasis. Semin Cell Dev Biol. 2015;40:142-52.
177. Zou J, Guo Y, Guettouche T, Smith DF, Voellmy R. Repression of heat shock transcription factor HSF1 activation by HSP90 (HSP90 complex) that forms a stress-sensitive complex with HSF1. Cell. 1998;94(4):471-80.
178. Kim HR, Kang HS, Kim HD. Geldanamycin induces heat shock protein expression through activation of HSF1 in K562 erythroleukemic cells. IUBMB Life. 1999;48(4):429-33.
179. Whitesell L, Mimnaugh EG, De Costa B, Myers CE, Neckers LM. Inhibition of heat shock protein HSP90-pp60v-src heteroprotein complex formation by benzoquinone ansamycins: essential role for stress proteins in oncogenic transformation. Proc Natl Acad Sci U S A. 1994;91(18):8324-8.

180. Hay DG, Sathasivam K, Tobaben S, Stahl B, Marber M, Mestril R, et al. Progressive decrease in chaperone protein levels in a mouse model of Huntington's disease and induction of stress proteins as a therapeutic approach. Hum Mol Genet. 2004;13(13):1389-405.
181. Sittler A, Lurz R, Lueder G, Priller J, Lehrach H, Hayer-Hartl MK, et al. Geldanamycin activates a heat shock response and inhibits huntingtin aggregation in a cell culture model of Huntington's disease. Hum Mol Genet. 2001;10(12):1307-15.
182. Fujikake N, Nagai Y, Popiel HA, Okamoto Y, Yamaguchi M, Toda T. Heat shock transcription factor 1-activating compounds suppress polyglutamine-induced neurodegeneration through induction of multiple molecular chaperones. J Biol Chem. 2008;283(38):26188-97.
183. Auluck PK, Meulener MC, Bonini NM. Mechanisms of Suppression of {alpha}-Synuclein Neurotoxicity by Geldanamycin in Drosophila. J Biol Chem. 2005;280(4):2873-8.
184. Waza M, Adachi H, Katsuno M, Minamiyama M, Sang C, Tanaka F, et al. 17-AAG, an Hsp90 inhibitor, ameliorates polyglutamine-mediated motor neuron degeneration. Nat Med. 2005;11(10):1088-95.
185. Tokui K, Adachi H, Waza M, Katsuno M, Minamiyama M, Doi H, et al. 17-DMAG ameliorates polyglutamine-mediated motor neuron degeneration through well-preserved proteasome function in an SBMA model mouse. Hum Mol Genet. 2009;18(5):898-910.
186. Katsuno M, Sang C, Adachi H, Minamiyama M, Waza M, Tanaka F, et al. Pharmacological induction of heat-shock proteins alleviates polyglutamine-mediated motor neuron disease. Proc Natl Acad Sci U S A. 2005;102(46):16801-6.
187. Neckers L, Ivy SP. Heat shock protein 90. Curr Opin Oncol. 2003;15(6):419-24.
188. Isaacs JS, Xu W, Neckers L. Heat shock protein 90 as a molecular target for cancer therapeutics. Cancer Cell. 2003;3(3):213-7.
189. Ronnen EA, Kondagunta GV, Ishill N, Sweeney SM, Deluca JK, Schwartz L, et al. A phase II trial of 17-(Allylamino)-17-demethoxygeldanamycin in patients with papillary and clear cell renal cell carcinoma. Invest New Drugs. 2006;24(6):543-6.
190. Modi S, Stopeck AT, Gordon MS, Mendelson D, Solit DB, Bagatell R, et al. Combination of trastuzumab and tanespimycin (17-AAG, KOS-953) is safe and active in trastuzumab-refractory HER-2 overexpressing breast cancer: a phase I dose-escalation study. J Clin Oncol. 2007;25(34):5410-7.
191. Chiosis G, Lucas B, Shtil A, Huezo H, Rosen N. Development of a purine-scaffold novel class of Hsp90 binders that inhibit the proliferation of cancer cells and induce the degradation of Her2 tyrosine kinase. Bioorg Med Chem. 2002;10(11):3555-64.
192. Chiosis G, Timaul MN, Lucas B, Munster PN, Zheng FF, Sepp-Lorenzino L, et al. A small molecule designed to bind to the adenine nucleotide pocket of Hsp90 causes Her2 degradation and the growth arrest and differentiation of breast cancer cells. Chem Biol. 2001;8(3):289-99.
193. Lundgren K, Zhang H, Brekken J, Huser N, Powell RE, Timple N, et al. BIIB021, an orally available, fully synthetic small-molecule inhibitor of the heat shock protein Hsp90. Mol Cancer Ther. 2009;8(4):921-9.
194. Taldone T, Chiosis G. Purine-scaffold Hsp90 inhibitors. Curr Top Med Chem. 2009;9(15):1436-46.
195. Brough PA, Aherne W, Barril X, Borgognoni J, Boxall K, Cansfield JE, et al. 4,5-diarylisoxazole Hsp90 chaperone inhibitors: potential therapeutic agents for the treatment of cancer. J Med Chem. 2008;51(2):196-218.
196. Gaspar N, Sharp SY, Eccles SA, Gowan S, Popov S, Jones C, et al. Mechanistic evaluation of the novel HSP90 inhibitor NVP-AUY922 in adult and pediatric glioblastoma. Mol Cancer Ther. 2010;9(5):1219-33.

197. Baldo B, Weiss A, Parker CN, Bibel M, Paganetti P, Kaupmann K. A screen for enhancers of clearance identifies huntingtin as a heat shock protein 90 (Hsp90) client protein. J Biol Chem. 2012;287(2):1406-14.
198. Labbadia J, Cunliffe H, Weiss A, Katsyuba E, Sathasivam K, Seredenina T, et al. Altered chromatin architecture underlies progressive impairment of the heat shock response in mouse models of Huntington disease. J Clin Invest. 2011;121(8):3306-19.
199. Rowinsky EK, Donehower RC. Paclitaxel (taxol). N Engl J Med. 1995;332(15):1004-14.
200. Zhu J, Chen W, Mi R, Zhou C, Reed N, Hoke A. Ethoxyquin prevents chemotherapy-induced neurotoxicity via Hsp90 modulation. Ann Neurol. 2013;74(6):893-904.
201. Ernst JT, Liu M, Zuccola H, Neubert T, Beaumont K, Turnbull A, et al. Correlation between chemotype-dependent binding conformations of HSP90alpha/beta and isoform selectivity-Implications for the structure-based design of HSP90alpha/beta selective inhibitors for treating neurodegenerative diseases. Bioorg Med Chem Lett. 2014;24(1):204-8.
202. Baptista MS, Duarte CB, Maciel P. Role of the ubiquitin-proteasome system in nervous system function and disease: using C. elegans as a dissecting tool. Cell Mol Life Sci. 2012.
203. Hershko A, Ciechanover A. The ubiquitin system. Annu Rev Biochem. 1998;67:425-79.
204. Dohm CP, Kermer P, Bahr M. Aggregopathy in neurodegenerative diseases: mechanisms and therapeutic implication. Neurodegener Dis. 2008;5(6):321-38.
205. Taylor JP, Hardy J, Fischbeck KH. Toxic proteins in neurodegenerative disease. Science. 2002;296(5575):1991-5.
206. Mayer RJ, Lowe J, Lennox G, Doherty F, Landon M. Intermediate filaments and ubiquitin: a new thread in the understanding of chronic neurodegenerative diseases. Prog Clin Biol Res. 1989;317:809-18.
207. Lowe J, Blanchard A, Morrell K, Lennox G, Reynolds L, Billett M, et al. Ubiquitin is a common factor in intermediate filament inclusion bodies of diverse type in man, including those of Parkinson's disease, Pick's disease, and Alzheimer's disease, as well as Rosenthal fibres in cerebellar astrocytomas, cytoplasmic bodies in muscle, and mallory bodies in alcoholic liver disease. J Pathol. 1988;155(1):9-15.
208. Bence NF, Sampat RM, Kopito RR. Impairment of the ubiquitin-proteasome system by protein aggregation. Science. 2001;292(5521):1552-5.
209. Zhou H, Cao F, Wang Z, Yu ZX, Nguyen HP, Evans J, et al. Huntingtin forms toxic NH2-terminal fragment complexes that are promoted by the age-dependent decrease in proteasome activity. J Cell Biol. 2003;163(1):109-18.
210. Wang J, Wang CE, Orr A, Tydlacka S, Li SH, Li XJ. Impaired ubiquitin-proteasome system activity in the synapses of Huntington's disease mice. J Cell Biol. 2008;180(6):1177-89.
211. Bennett EJ, Bence NF, Jayakumar R, Kopito RR. Global impairment of the ubiquitin-proteasome system by nuclear or cytoplasmic protein aggregates precedes inclusion body formation. Mol Cell. 2005;17(3):351-65.
212. Li X, Wang CE, Huang S, Xu X, Li XJ, Li H, et al. Inhibiting the ubiquitin-proteasome system leads to preferential accumulation of toxic N-terminal mutant huntingtin fragments. Hum Mol Genet. 2010;19(12):2445-55.
213. Maynard CJ, Bottcher C, Ortega Z, Smith R, Florea BI, Diaz-Hernandez M, et al. Accumulation of ubiquitin conjugates in a polyglutamine disease model occurs without global ubiquitin/proteasome system impairment. Proc Natl Acad Sci U S A. 2009;106(33):13986-91.
214. Durcan TM, Kontogiannea M, Bedard N, Wing SS, Fon EA. Ataxin-3 deubiquitination is coupled to Parkin ubiquitination via E2 ubiquitin-conjugating enzyme. J Biol Chem. 2012;287(1):531-41.

215. Durcan TM, Kontogiannea M, Thorarinsdottir T, Fallon L, Williams AJ, Djarmati A, et al. The Machado-Joseph disease-associated mutant form of ataxin-3 regulates parkin ubiquitination and stability. Hum Mol Genet. 2011;20(1):141-54.
216. Scaglione KM, Zavodszky E, Todi SV, Patury S, Xu P, Rodriguez-Lebron E, et al. Ube2w and ataxin-3 coordinately regulate the ubiquitin ligase CHIP. Mol Cell. 2011;43(4):599-612.
217. Hirabayashi M, Inoue K, Tanaka K, Nakadate K, Ohsawa Y, Kamei Y, et al. VCP/p97 in abnormal protein aggregates, cytoplasmic vacuoles, and cell death, phenotypes relevant to neurodegeneration. Cell Death Differ. 2001;8(10):977-84.
218. Doss-Pepe EW, Stenroos ES, Johnson WG, Madura K. Ataxin-3 interactions with rad23 and valosin-containing protein and its associations with ubiquitin chains and the proteasome are consistent with a role in ubiquitin-mediated proteolysis. Mol Cell Biol. 2003;23(18):6469-83.
219. Zhong X, Pittman RN. Ataxin-3 binds VCP/p97 and regulates retrotranslocation of ERAD substrates. Hum Mol Genet. 2006;15(16):2409-20.
220. Connell P, Ballinger CA, Jiang J, Wu Y, Thompson LJ, Hohfeld J, et al. The co-chaperone CHIP regulates protein triage decisions mediated by heat-shock proteins. Nat Cell Biol. 2001;3(1):93-6.
221. Jana NR, Dikshit P, Goswami A, Kotliarova S, Murata S, Tanaka K, et al. Co-chaperone CHIP associates with expanded polyglutamine protein and promotes their degradation by proteasomes. J Biol Chem. 2005;280(12):11635-40.
222. Kitada T, Asakawa S, Hattori N, Matsumine H, Yamamura Y, Minoshima S, et al. Mutations in the parkin gene cause autosomal recessive juvenile parkinsonism. Nature. 1998;392(6676):605-8.
223. Cemal CK, Carroll CJ, Lawrence L, Lowrie MB, Ruddle P, Al-Mahdawi S, et al. YAC transgenic mice carrying pathological alleles of the MJD1 locus exhibit a mild and slowly progressive cerebellar deficit. Hum Mol Genet. 2002;11(9):1075-94.
224. Wong HK, Bauer PO, Kurosawa M, Goswami A, Washizu C, Machida Y, et al. Blocking acid-sensing ion channel 1 alleviates Huntington's disease pathology via an ubiquitin-proteasome system-dependent mechanism. Hum Mol Genet. 2008;17(20):3223-35.
225. Anderson C, Crimmins S, Wilson JA, Korbel GA, Ploegh HL, Wilson SM. Loss of Usp14 results in reduced levels of ubiquitin in ataxia mice. J Neurochem. 2005;95(3):724-31.
226. Crimmins S, Jin Y, Wheeler C, Huffman AK, Chapman C, Dobrunz LE, et al. Transgenic rescue of ataxia mice with neuronal-specific expression of ubiquitin-specific protease 14. J Neurosci. 2006;26(44):11423-31.
227. Lee BH, Lee MJ, Park S, Oh DC, Elsasser S, Chen PC, et al. Enhancement of proteasome activity by a small-molecule inhibitor of USP14. Nature. 2010;467(7312):179-84.
228. Melendez A, Hall DH, Hansen M. Monitoring the role of autophagy in C. elegans aging. Methods Enzymol. 2008;451:493-520.
229. Yorimitsu T, Klionsky DJ. Autophagy: molecular machinery for self-eating. Cell Death Differ. 2005;12 Suppl 2:1542-52.
230. Xu M, Zhang HL. Death and survival of neuronal and astrocytic cells in ischemic brain injury: a role of autophagy. Acta Pharmacol Sin. 2011;32(9):1089-99.
231. Rubinsztein DC. Autophagy induction rescues toxicity mediated by proteasome inhibition. Neuron. 2007;54(6):854-6.
232. Rubinsztein DC, Gestwicki JE, Murphy LO, Klionsky DJ. Potential therapeutic applications of autophagy. Nat Rev Drug Discov. 2007;6(4):304-12.
233. Komatsu M, Waguri S, Chiba T, Murata S, Iwata J, Tanida I, et al. Loss of autophagy in the central nervous system causes neurodegeneration in mice. Nature. 2006;441(7095):880-4.
234. Hara T, Nakamura K, Matsui M, Yamamoto A, Nakahara Y, Suzuki-Migishima R, et al. Suppression of basal autophagy in neural cells causes neurodegenerative disease in mice. Nature. 2006;441(7095):885-9.

235. Lee SJ, Lim HS, Masliah E, Lee HJ. Protein aggregate spreading in neurodegenerative diseases: Problems and perspectives. Neurosci Res. 2011;70(4):339-48.
236. Levine B, Kroemer G. Autophagy in the pathogenesis of disease. Cell. 2008;132(1):27-42.
237. Cuervo AM, Stefanis L, Fredenburg R, Lansbury PT, Sulzer D. Impaired degradation of mutant alpha-synuclein by chaperone-mediated autophagy. Science. 2004;305(5688):1292-5.
238. Cuervo AM. Autophagy: in sickness and in health. Trends Cell Biol. 2004;14(2):70-7.
239. Ravikumar B, Vacher C, Berger Z, Davies JE, Luo S, Oroz LG, et al. Inhibition of mTOR induces autophagy and reduces toxicity of polyglutamine expansions in fly and mouse models of Huntington disease. Nat Genet. 2004;36(6):585-95.
240. Sarkar S, Ravikumar B, Floto RA, Rubinsztein DC. Rapamycin and mTOR-independent autophagy inducers ameliorate toxicity of polyglutamine-expanded huntingtin and related proteinopathies. Cell Death Differ. 2009;16(1):46-56.
241. Ravikumar B, Duden R, Rubinsztein DC. Aggregate-prone proteins with polyglutamine and polyalanine expansions are degraded by autophagy. Hum Mol Genet. 2002;11(9):1107-17.
242. Nixon RA, Wegiel J, Kumar A, Yu WH, Peterhoff C, Cataldo A, et al. Extensive involvement of autophagy in Alzheimer disease: an immuno-electron microscopy study. J Neuropathol Exp Neurol. 2005;64(2):113-22.
243. Webb JL, Ravikumar B, Atkins J, Skepper JN, Rubinsztein DC. Alpha-Synuclein is degraded by both autophagy and the proteasome. J Biol Chem. 2003;278(27):25009-13.
244. Berger Z, Ravikumar B, Menzies FM, Oroz LG, Underwood BR, Pangalos MN, et al. Rapamycin alleviates toxicity of different aggregate-prone proteins. Hum Mol Genet. 2006;15(3):433-42.
245. Menzies FM, Huebener J, Renna M, Bonin M, Riess O, Rubinsztein DC. Autophagy induction reduces mutant ataxin-3 levels and toxicity in a mouse model of spinocerebellar ataxia type 3. Brain. 2010;133(Pt 1):93-104.
246. Nascimento-Ferreira I, Santos-Ferreira T, Sousa-Ferreira L, Auregan G, Onofre I, Alves S, et al. Overexpression of the autophagic beclin-1 protein clears mutant ataxin-3 and alleviates Machado-Joseph disease. Brain. 2011.
247. Frake RA, Ricketts T, Menzies FM, Rubinsztein DC. Autophagy and neurodegeneration. J Clin Invest. 2015;125(1):65-74.
248. Vidal RL, Matus S, Bargsted L, Hetz C. Targeting autophagy in neurodegenerative diseases. Trends Pharmacol Sci. 2014;35(11):583-91.
249. Meijer AJ, Codogno P. Regulation and role of autophagy in mammalian cells. Int J Biochem Cell Biol. 2004;36(12):2445-62.
250. Yu WH, Cuervo AM, Kumar A, Peterhoff CM, Schmidt SD, Lee JH, et al. Macroautophagy - a novel beta-amyloid peptide-generating pathway activated in Alzheimer's disease. Journal of Cell Biology. 2005;171(1):87-98.
251. Menzies FM, Ravikumar B, Rubinsztein DC. Protective roles for induction of autophagy in multiple proteinopathies. Autophagy. 2006;2(3):224-5.
252. Sarkar S, Floto RA, Berger Z, Imarisio S, Cordenier A, Pasco M, et al. Lithium induces autophagy by inhibiting inositol monophosphatase. J Cell Biol. 2005;170(7):1101-11.
253. Xiong N, Jia M, Chen C, Xiong J, Zhang Z, Huang J, et al. Potential autophagy enhancers attenuate rotenone-induced toxicity in SH-SY5Y. Neuroscience. 2011;199:292-302.
254. Harron DW. Distinctive features of rilmenidine possibly related to its selectivity for imidazoline receptors. Am J Hypertens. 1992;5(4 Pt 2):91S-8S.
255. Montastruc JL, Macquin-Mavier I, Tran MA, Damase-Michel C, Koenig-Berard E, Valet P. Recent advances in the pharmacology of rilmenidine. Am J Med. 1989;87(3C):14S-7S.

256. Rose C, Menzies FM, Renna M, Acevedo-Arozena A, Corrochano S, Sadiq O, et al. Rilmenidine attenuates toxicity of polyglutamine expansions in a mouse model of Huntington's disease. Hum Mol Genet. 2010;19(11):2144-53.
257. Reid JL. Update on rilmenidine: clinical benefits. Am J Hypertens. 2001;14(11 Pt 2):322S-4S.
258. Sarkar S, Rubinsztein DC. Small molecule enhancers of autophagy for neurodegenerative diseases. Mol Biosyst. 2008;4(9):895-901.
259. Sarkar S, Perlstein EO, Imarisio S, Pineau S, Cordenier A, Maglathlin RL, et al. Small molecules enhance autophagy and reduce toxicity in Huntington's disease models. Nat Chem Biol. 2007;3(6):331-8.
260. Lin Y, Hubert L, Jr., Wilson JH. Transcription destabilizes triplet repeats. Mol Carcinog. 2009;48(4):350-61.
261. Okazawa H. Polyglutamine diseases: a transcription disorder? Cell Mol Life Sci. 2003;60(7):1427-39.
262. McCampbell A, Taylor JP, Taye AA, Robitschek J, Li M, Walcott J, et al. CREB-binding protein sequestration by expanded polyglutamine. Hum Mol Genet. 2000;9(14):2197-202.
263. Taylor JP, Taye AA, Campbell C, Kazemi-Esfarjani P, Fischbeck KH, Min KT. Aberrant histone acetylation, altered transcription, and retinal degeneration in a Drosophila model of polyglutamine disease are rescued by CREB-binding protein. Genes Dev. 2003;17(12):1463-8.
264. Li F, Macfarlan T, Pittman RN, Chakravarti D. Ataxin-3 is a histone-binding protein with two independent transcriptional corepressor activities. J Biol Chem. 2002;277(47):45004-12.
265. Li SH, Cheng AL, Zhou H, Lam S, Rao M, Li H, et al. Interaction of Huntington disease protein with transcriptional activator Sp1. Mol Cell Biol. 2002;22(5):1277-87.
266. Cohen-Carmon D, Meshorer E. Polyglutamine (polyQ) disorders: the chromatin connection. Nucleus. 2012;3(5):433-41.
267. Dunah AW, Jeong H, Griffin A, Kim YM, Standaert DG, Hersch SM, et al. Sp1 and TAFII130 transcriptional activity disrupted in early Huntington's disease. Science. 2002;296(5576):2238-43.
268. Hirose Y, Manley JL. RNA polymerase II and the integration of nuclear events. Genes Dev. 2000;14(12):1415-29.
269. Grewal SI, Moazed D. Heterochromatin and epigenetic control of gene expression. Science. 2003;301(5634):798-802.
270. Peserico A, Simone C. Physical and functional HAT/HDAC interplay regulates protein acetylation balance. J Biomed Biotechnol. 2011;2011:371832.
271. Haberland M, Montgomery RL, Olson EN. The many roles of histone deacetylases in development and physiology: implications for disease and therapy. Nature Reviews Genetics. 2009;10(1):32-42.
272. Steffan JS, Bodai L, Pallos J, Poelman M, McCampbell A, Apostol BL, et al. Histone deacetylase inhibitors arrest polyglutamine-dependent neurodegeneration in Drosophila. Nature. 2001;413(6857):739-43.
273. Ferrante RJ, Kubilus JK, Lee J, Ryu H, Beesen A, Zucker B, et al. Histone deacetylase inhibition by sodium butyrate chemotherapy ameliorates the neurodegenerative phenotype in Huntington's disease mice. J Neurosci. 2003;23(28):9418-27.
274. Hockly E, Richon VM, Woodman B, Smith DL, Zhou X, Rosa E, et al. Suberoylanilide hydroxamic acid, a histone deacetylase inhibitor, ameliorates motor deficits in a mouse model of Huntington's disease. Proc Natl Acad Sci U S A. 2003;100(4):2041-6.
275. Ying M, Xu R, Wu X, Zhu H, Zhuang Y, Han M, et al. Sodium butyrate ameliorates histone hypoacetylation and neurodegenerative phenotypes in a mouse model for DRPLA. J Biol Chem. 2006;281(18):12580-6.

276. Chou AH, Chen SY, Yeh TH, Weng YH, Wang HL. HDAC inhibitor sodium butyrate reverses transcriptional downregulation and ameliorates ataxic symptoms in a transgenic mouse model of SCA3. Neurobiol Dis. 2011;41(2):481-8.
277. Hahnen E, Hauke J, Trankle C, Eyupoglu IY, Wirth B, Blumcke I. Histone deacetylase inhibitors: possible implications for neurodegenerative disorders. Expert Opin Investig Drugs. 2008;17(2):169-84.
278. Minamiyama M, Katsuno M, Adachi H, Waza M, Sang C, Kobayashi Y, et al. Sodium butyrate ameliorates phenotypic expression in a transgenic mouse model of spinal and bulbar muscular atrophy. Hum Mol Genet. 2004;13(11):1183-92.
279. Latouche M, Lasbleiz C, Martin E, Monnier V, Debeir T, Mouatt-Prigent A, et al. A conditional pan-neuronal Drosophila model of spinocerebellar ataxia 7 with a reversible adult phenotype suitable for identifying modifier genes. J Neurosci. 2007;27(10):2483-92.
280. Chou AH, Yeh TH, Ouyang P, Chen YL, Chen SY, Wang HL. Polyglutamine-expanded ataxin-3 causes cerebellar dysfunction of SCA3 transgenic mice by inducing transcriptional dysregulation. Neurobiol Dis. 2008;31(1):89-101.
281. Richon VM, Emiliani S, Verdin E, Webb Y, Breslow R, Rifkind RA, et al. A class of hybrid polar inducers of transformed cell differentiation inhibits histone deacetylases. Proc Natl Acad Sci U S A. 1998;95(6):3003-7.
282. Richon VM, Sandhoff TW, Rifkind RA, Marks PA. Histone deacetylase inhibitor selectively induces p21(WAF1) expression and gene-associated histone acetylation. Proceedings of the National Academy of Sciences of the United States of America. 2000;97(18):10014-9.
283. Marks PA, Richon VM, Rifkind RA. Histone deacetylase inhibitors: inducers of differentiation or apoptosis of transformed cells. J Natl Cancer Inst. 2000;92(15):1210-6.
284. Munster PN, Rosen N, Rifkind R, Marks P, Richon V. The histone deacetylase inhibitor suberoylanilide hydroxamic acid (SAHA) induces differentiation of human breast cancer cells. Clinical Cancer Research. 2001;7(11):3725s-s.
285. Marks PA, Richon VM, Breslow R, Rifkind RA. Histone deacetylase inhibitors as new cancer drugs. Curr Opin Oncol. 2001;13(6):477-83.
286. Mielcarek M, Benn CL, Franklin SA, Smith DL, Woodman B, Marks PA, et al. SAHA Decreases HDAC 2 and 4 Levels In Vivo and Improves Molecular Phenotypes in the R6/2 Mouse Model of Huntington's Disease. PLoS ONE. 2011;6(11).
287. Scognamiglio A, Nebbioso A, Manzo F, Valente S, Mai A, Altucci L. HDAC-class II specific inhibition involves HDAC proteasome-dependent degradation mediated by RANBP2. Biochimica Et Biophysica Acta-Molecular Cell Research. 2008;1783(10):2030-8.
288. Ferrante RJ, Ryu H, Kubilus JK, D'Mello S, Sugars KL, Lee J, et al. Chemotherapy for the brain: the antitumor antibiotic mithramycin prolongs survival in a mouse model of Huntington's disease. J Neurosci. 2004;24(46):10335-42.
289. Zuccato C, Tartari M, Crotti A, Goffredo D, Valenza M, Conti L, et al. Huntingtin interacts with REST/NRSF to modulate the transcription of NRSE-controlled neuronal genes. Nat Genet. 2003;35(1):76-83.
290. Zuccato C, Ciammola A, Rigamonti D, Leavitt BR, Goffredo D, Conti L, et al. Loss of huntingtin-mediated BDNF gene transcription in Huntington's disease. Science. 2001;293(5529):493-8.
291. DeMarch Z, Giampa C, Patassini S, Bernardi G, Fusco FR. Beneficial effects of rolipram in the R6/2 mouse model of Huntington's disease. Neurobiol Dis. 2008;30(3):375-87.
292. Giampa C, Middei S, Patassini S, Borreca A, Marullo F, Laurenti D, et al. Phosphodiesterase type IV inhibition prevents sequestration of CREB binding protein, protects striatal parvalbumin interneurons and rescues motor deficits in the R6/2 mouse model of Huntington's disease. Eur J Neurosci. 2009;29(5):902-10.

293. Thomas EA. Involvement of HDAC1 and HDAC3 in the Pathology of Polyglutamine Disorders: Therapeutic Implications for Selective HDAC1/HDAC3 Inhibitors. Pharmaceuticals (Basel). 2014;7(6):634-61.
294. Thomas EA, Coppola G, Desplats PA, Tang B, Soragni E, Burnett R, et al. The HDAC inhibitor 4b ameliorates the disease phenotype and transcriptional abnormalities in Huntington's disease transgenic mice. Proc Natl Acad Sci U S A. 2008;105(40):15564-9.
295. Chen JY, Wang E, Galvan L, Huynh M, Joshi P, Cepeda C, et al. Effects of the Pimelic Diphenylamide Histone Deacetylase Inhibitor HDACi 4b on the R6/2 and N171-82Q Mouse Models of Huntington's Disease. PLoS Curr. 2013;5.
296. Jia H, Pallos J, Jacques V, Lau A, Tang B, Cooper A, et al. Histone deacetylase (HDAC) inhibitors targeting HDAC3 and HDAC1 ameliorate polyglutamine-elicited phenotypes in model systems of Huntington's disease. Neurobiol Dis. 2012;46(2):351-61.
297. Hubbert C, Guardiola A, Shao R, Kawaguchi Y, Ito A, Nixon A, et al. HDAC6 is a microtubule-associated deacetylase. Nature. 2002;417(6887):455-8.
298. Kovacs JJ, Murphy PJ, Gaillard S, Zhao X, Wu JT, Nicchitta CV, et al. HDAC6 regulates Hsp90 acetylation and chaperone-dependent activation of glucocorticoid receptor. Mol Cell. 2005;18(5):601-7.
299. Ren M, Leng Y, Jeong M, Leeds PR, Chuang DM. Valproic acid reduces brain damage induced by transient focal cerebral ischemia in rats: potential roles of histone deacetylase inhibition and heat shock protein induction. J Neurochem. 2004;89(6):1358-67.
300. Zhao Y, Sun H, Lu J, Li X, Chen X, Tao D, et al. Lifespan extension and elevated hsp gene expression in Drosophila caused by histone deacetylase inhibitors. J Exp Biol. 2005;208(Pt 4):697-705.
301. Kelly WK, O'Connor OA, Krug LM, Chiao JH, Heaney M, Curley T, et al. Phase I study of an oral histone deacetylase inhibitor, suberoylanilide hydroxamic acid, in patients with advanced cancer. J Clin Oncol. 2005;23(17):3923-31.
302. Rubin EH, Agrawal NG, Friedman EJ, Scott P, Mazina KE, Sun L, et al. A study to determine the effects of food and multiple dosing on the pharmacokinetics of vorinostat given orally to patients with advanced cancer. Clin Cancer Res. 2006;12(23):7039-45.
303. Garcia-Manero G, Assouline S, Cortes J, Estrov Z, Kantarjian H, Yang H, et al. Phase 1 study of the oral isotype specific histone deacetylase inhibitor MGCD0103 in leukemia. Blood. 2008;112(4):981-9.
304. Garcia-Manero G, Yang H, Bueso-Ramos C, Ferrajoli A, Cortes J, Wierda WG, et al. Phase 1 study of the histone deacetylase inhibitor vorinostat (suberoylanilide hydroxamic acid [SAHA]) in patients with advanced leukemias and myelodysplastic syndromes. Blood. 2008;111(3):1060-6.
305. Kriz J, Gowing G, Julien JP. Efficient three-drug cocktail for disease induced by mutant superoxide dismutase. Ann Neurol. 2003;53(4):429-36.
306. Selvi BR, Cassel JC, Kundu TK, Boutillier AL. Tuning acetylation levels with HAT activators: therapeutic strategy in neurodegenerative diseases. Biochim Biophys Acta. 2010;1799(10-12):840-53.
307. Gatchel JR, Zoghbi HY. Diseases of unstable repeat expansion: mechanisms and common principles. Nat Rev Genet. 2005;6(10):743-55.
308. Bennett JP. Free radicals, oxidative stress and the origin of Parkinson's disease. J Neurol Sci. 1999;170(2):75-6.
309. Alexi T, Hughes PE, Knusel B, Tobin AJ. Metabolic compromise with systemic 3-nitropropionic acid produces striatal apoptosis in Sprague-Dawley rats but not in BALB/c ByJ mice. Exp Neurol. 1998;153(1):74-93.
310. Alavi A, Dann R, Chawluk J, Alavi J, Kushner M, Reivich M. Positron emission tomography imaging of regional cerebral glucose metabolism. Semin Nucl Med. 1986;16(1):2-34.

311. Hayden MR, Hewitt J, Stoessl AJ, Clark C, Ammann W, Martin WR. The combined use of positron emission tomography and DNA polymorphisms for preclinical detection of Huntington's disease. Neurology. 1987;37(9):1441-7.
312. Young AB, Penney JB, Starosta-Rubinstein S, Markel DS, Berent S, Giordani B, et al. PET scan investigations of Huntington's disease: cerebral metabolic correlates of neurological features and functional decline. Ann Neurol. 1986;20(3):296-303.
313. Ciarmiello A, Cannella M, Lastoria S, Simonelli M, Frati L, Rubinsztein DC, et al. Brain white-matter volume loss and glucose hypometabolism precede the clinical symptoms of Huntington's disease. J Nucl Med. 2006;47(2):215-22.
314. Jenkins BG, Koroshetz WJ, Beal MF, Rosen BR. Evidence for impairment of energy metabolism in vivo in Huntington's disease using localized 1H NMR spectroscopy. Neurology. 1993;43(12):2689-95.
315. Koroshetz WJ, Jenkins BG, Rosen BR, Beal MF. Energy metabolism defects in Huntington's disease and effects of coenzyme Q10. Ann Neurol. 1997;41(2):160-5.
316. Brouillet E, Hantraye P, Ferrante RJ, Dolan R, Leroy-Willig A, Kowall NW, et al. Chronic mitochondrial energy impairment produces selective striatal degeneration and abnormal choreiform movements in primates. Proc Natl Acad Sci U S A. 1995;92(15):7105-9.
317. Gourfinkel-An I, Vila M, Faucheux B, Duyckaerts C, Viallet F, Hauw JJ, et al. Metabolic changes in the basal ganglia of patients with Huntington's disease: an in situ hybridization study of cytochrome oxidase subunit I mRNA. J Neurochem. 2002;80(3):466-76.
318. Sanchez-Pernaute R, Garcia-Segura JM, del Barrio Alba A, Viano J, de Yebenes JG. Clinical correlation of striatal 1H MRS changes in Huntington's disease. Neurology. 1999;53(4):806-12.
319. Acevedo-Torres K, Berrios L, Rosario N, Dufault V, Skatchkov S, Eaton MJ, et al. Mitochondrial DNA damage is a hallmark of chemically induced and the R6/2 transgenic model of Huntington's disease. DNA Repair (Amst). 2009;8(1):126-36.
320. Chen CM, Wu YR, Cheng ML, Liu JL, Lee YM, Lee PW, et al. Increased oxidative damage and mitochondrial abnormalities in the peripheral blood of Huntington's disease patients. Biochem Biophys Res Commun. 2007;359(2):335-40.
321. N. Kazachkova MR, R. Montiel, T. Cymbron, C. Bettencourt, A. Silva-Fernandes, S. Silva, P. Maciel & M. Lima. Patterns of mitochondrial DNA damage in blood and brain tissues of a transgenic mouse model of Machado–Joseph disease. Neurodegenerative Diseases. 2012.
322. Yu YC, Kuo CL, Cheng WL, Liu CS, Hsieh M. Decreased antioxidant enzyme activity and increased mitochondrial DNA damage in cellular models of Machado-Joseph disease. J Neurosci Res. 2009;87(8):1884-91.
323. Browne SE, Bowling AC, MacGarvey U, Baik MJ, Berger SC, Muqit MM, et al. Oxidative damage and metabolic dysfunction in Huntington's disease: selective vulnerability of the basal ganglia. Ann Neurol. 1997;41(5):646-53.
324. Perluigi M, Poon HF, Maragos W, Pierce WM, Klein JB, Calabrese V, et al. Proteomic analysis of protein expression and oxidative modification in r6/2 transgenic mice: a model of Huntington disease. Mol Cell Proteomics. 2005;4(12):1849-61.
325. Sorolla MA, Reverter-Branchat G, Tamarit J, Ferrer I, Ros J, Cabiscol E. Proteomic and oxidative stress analysis in human brain samples of Huntington disease. Free Radic Biol Med. 2008;45(5):667-78.
326. Cui L, Jeong H, Borovecki F, Parkhurst CN, Tanese N, Krainc D. Transcriptional repression of PGC-1alpha by mutant huntingtin leads to mitochondrial dysfunction and neurodegeneration. Cell. 2006;127(1):59-69.

327. Weydt P, Pineda VV, Torrence AE, Libby RT, Satterfield TF, Lazarowski ER, et al. Thermoregulatory and metabolic defects in Huntington's disease transgenic mice implicate PGC-1alpha in Huntington's disease neurodegeneration. Cell Metab. 2006;4(5):349-62.
328. Panov AV, Gutekunst CA, Leavitt BR, Hayden MR, Burke JR, Strittmatter WJ, et al. Early mitochondrial calcium defects in Huntington's disease are a direct effect of polyglutamines. Nat Neurosci. 2002;5(8):731-6.
329. Almeida S, Sarmento-Ribeiro AB, Januario C, Rego AC, Oliveira CR. Evidence of apoptosis and mitochondrial abnormalities in peripheral blood cells of Huntington's disease patients. Biochem Biophys Res Commun. 2008;374(4):599-603.
330. Panov A, Obertone T, Bennett-Desmelik J, Greenamyre JT. Ca(2+)-dependent permeability transition and complex I activity in lymphoblast mitochondria from normal individuals and patients with Huntington's or Alzheimer's disease. Ann N Y Acad Sci. 1999;893:365-8.
331. Milakovic T, Quintanilla RA, Johnson GV. Mutant huntingtin expression induces mitochondrial calcium handling defects in clonal striatal cells: functional consequences. J Biol Chem. 2006;281(46):34785-95.
332. Gizatullina ZZ, Lindenberg KS, Harjes P, Chen Y, Kosinski CM, Landwehrmeyer BG, et al. Low stability of Huntington muscle mitochondria against Ca2+ in R6/2 mice. Ann Neurol. 2006;59(2):407-11.
333. Brustovetsky N, LaFrance R, Purl KJ, Brustovetsky T, Keene CD, Low WC, et al. Age-dependent changes in the calcium sensitivity of striatal mitochondria in mouse models of Huntington's Disease. J Neurochem. 2005;93(6):1361-70.
334. Oliveira JM, Jekabsons MB, Chen S, Lin A, Rego AC, Goncalves J, et al. Mitochondrial dysfunction in Huntington's disease: the bioenergetics of isolated and in situ mitochondria from transgenic mice. J Neurochem. 2007;101(1):241-9.
335. Chen X, Wu J, Lvovskaya S, Herndon E, Supnet C, Bezprozvanny I. Dantrolene is neuroprotective in Huntington's disease transgenic mouse model. Mol Neurodegener. 2011;6:81.
336. Chen X, Tang TS, Tu H, Nelson O, Pook M, Hammer R, et al. Deranged calcium signaling and neurodegeneration in spinocerebellar ataxia type 3. J Neurosci. 2008;28(48):12713-24.
337. Liu J, Tang TS, Tu H, Nelson O, Herndon E, Huynh DP, et al. Deranged calcium signaling and neurodegeneration in spinocerebellar ataxia type 2. J Neurosci. 2009;29(29):9148-62.
338. Tabrizi SJ, Workman J, Hart PE, Mangiarini L, Mahal A, Bates G, et al. Mitochondrial dysfunction and free radical damage in the Huntington R6/2 transgenic mouse. Ann Neurol. 2000;47(1):80-6.
339. Browne SE, Ferrante RJ, Beal MF. Oxidative stress in Huntington's disease. Brain Pathol. 1999;9(1):147-63.
340. Perez-Severiano F, Rios C, Segovia J. Striatal oxidative damage parallels the expression of a neurological phenotype in mice transgenic for the mutation of Huntington's disease. Brain Res. 2000;862(1-2):234-7.
341. Sian J, Dexter DT, Lees AJ, Daniel S, Agid Y, Javoy-Agid F, et al. Alterations in glutathione levels in Parkinson's disease and other neurodegenerative disorders affecting basal ganglia. Ann Neurol. 1994;36(3):348-55.
342. Santamaria A, Perez-Severiano F, Rodriguez-Martinez E, Maldonado PD, Pedraza-Chaverri J, Rios C, et al. Comparative analysis of superoxide dismutase activity between acute pharmacological models and a transgenic mouse model of Huntington's disease. Neurochem Res. 2001;26(4):419-24.
343. Araujo J, Breuer P, Dieringer S, Krauss S, Dorn S, Zimmermann K, et al. FOXO4-dependent upregulation of superoxide dismutase-2 in response to oxidative stress is impaired in spinocerebellar ataxia type 3. Hum Mol Genet. 2011;20(15):2928-41.

344. Goswami A, Dikshit P, Mishra A, Mulherkar S, Nukina N, Jana NR. Oxidative stress promotes mutant huntingtin aggregation and mutant huntingtin-dependent cell death by mimicking proteasomal malfunction. Biochem Biophys Res Commun. 2006;342(1):184-90.
345. Wyttenbach A, Sauvageot O, Carmichael J, Diaz-Latoud C, Arrigo AP, Rubinsztein DC. Heat shock protein 27 prevents cellular polyglutamine toxicity and suppresses the increase of reactive oxygen species caused by huntingtin. Hum Mol Genet. 2002;11(9):1137-51.
346. Ferrante RJ, Andreassen OA, Jenkins BG, Dedeoglu A, Kuemmerle S, Kubilus JK, et al. Neuroprotective effects of creatine in a transgenic mouse model of Huntington's disease. J Neurosci. 2000;20(12):4389-97.
347. Dedeoglu A, Kubilus JK, Yang L, Ferrante KL, Hersch SM, Beal MF, et al. Creatine therapy provides neuroprotection after onset of clinical symptoms in Huntington's disease transgenic mice. J Neurochem. 2003;85(6):1359-67.
348. Verbessem P, Lemiere J, Eijnde BO, Swinnen S, Vanhees L, Van Leemputte M, et al. Creatine supplementation in Huntington's disease: a placebo-controlled pilot trial. Neurology. 2003;61(7):925-30.
349. Hersch SM, Gevorkian S, Marder K, Moskowitz C, Feigin A, Cox M, et al. Creatine in Huntington disease is safe, tolerable, bioavailable in brain and reduces serum 8OH2'dG. Neurology. 2006;66(2):250-2.
350. Beal MF, Henshaw DR, Jenkins BG, Rosen BR, Schulz JB. Coenzyme Q10 and nicotinamide block striatal lesions produced by the mitochondrial toxin malonate. Ann Neurol. 1994;36(6):882-8.
351. Jenkins BG, Brouillet E, Chen YC, Storey E, Schulz JB, Kirschner P, et al. Non-invasive neurochemical analysis of focal excitotoxic lesions in models of neurodegenerative illness using spectroscopic imaging. J Cereb Blood Flow Metab. 1996;16(3):450-61.
352. A randomized, placebo-controlled trial of coenzyme Q10 and remacemide in Huntington's disease. Neurology. 2001;57(3):397-404.
353. Hyson HC, Kieburtz K, Shoulson I, McDermott M, Ravina B, de Blieck EA, et al. Safety and tolerability of high-dosage coenzyme Q10 in Huntington's disease and healthy subjects. Mov Disord. 2010;25(12):1924-8.
354. Keene CD, Rodrigues CM, Eich T, Chhabra MS, Steer CJ, Low WC. Tauroursodeoxycholic acid, a bile acid, is neuroprotective in a transgenic animal model of Huntington's disease. Proc Natl Acad Sci U S A. 2002;99(16):10671-6.
355. Klivenyi P, Ferrante RJ, Gardian G, Browne S, Chabrier PE, Beal MF. Increased survival and neuroprotective effects of BN82451 in a transgenic mouse model of Huntington's disease. J Neurochem. 2003;86(1):267-72.
356. Fontaine MA, Geddes JW, Banks A, Butterfield DA. Effect of exogenous and endogenous antioxidants on 3-nitropionic acid-induced in vivo oxidative stress and striatal lesions: insights into Huntington's disease. J Neurochem. 2000;75(4):1709-15.
357. Bendheim PE, Poeggeler B, Neria E, Ziv V, Pappolla MA, Chain DG. Development of indole-3-propionic acid (OXIGON) for Alzheimer's disease. J Mol Neurosci. 2002;19(1-2):213-7.
358. Johnson JA, Johnson DA, Kraft AD, Calkins MJ, Jakel RJ, Vargas MR, et al. The Nrf2-ARE pathway: an indicator and modulator of oxidative stress in neurodegeneration. Ann N Y Acad Sci. 2008;1147:61-9.
359. Stack C, Ho D, Wille E, Calingasan NY, Williams C, Liby K, et al. Triterpenoids CDDO-ethyl amide and CDDO-trifluoroethyl amide improve the behavioral phenotype and brain pathology in a transgenic mouse model of Huntington's disease. Free Radic Biol Med. 2010;49(2):147-58.
360. Khanna S, Roy S, Ryu H, Bahadduri P, Swaan PW, Ratan RR, et al. Molecular basis of vitamin E action: tocotrienol modulates 12-lipoxygenase, a key mediator of glutamate-induced neurodegeneration. J Biol Chem. 2003;278(44):43508-15.

361. Osakada F, Hashino A, Kume T, Katsuki H, Kaneko S, Akaike A. Alpha-tocotrienol provides the most potent neuroprotection among vitamin E analogs on cultured striatal neurons. Neuropharmacology. 2004;47(6):904-15.
362. Conte V, Uryu K, Fujimoto S, Yao Y, Rokach J, Longhi L, et al. Vitamin E reduces amyloidosis and improves cognitive function in Tg2576 mice following repetitive concussive brain injury. J Neurochem. 2004;90(3):758-64.
363. Nakashima H, Ishihara T, Yokota O, Terada S, Trojanowski JQ, Lee VM, et al. Effects of alpha-tocopherol on an animal model of tauopathies. Free Radic Biol Med. 2004;37(2):176-86.
364. Berliocchi L, Bano D, Nicotera P. Ca2+ signals and death programmes in neurons. Philos Trans R Soc Lond B Biol Sci. 2005;360(1464):2255-8.
365. Dawson R, Jr., Beal MF, Bondy SC, Di Monte DA, Isom GE. Excitotoxins, aging, and environmental neurotoxins: implications for understanding human neurodegenerative diseases. Toxicol Appl Pharmacol. 1995;134(1):1-17.
366. Coyle JT, Schwarcz R. Lesion of striatal neurones with kainic acid provides a model for Huntington's chorea. Nature. 1976;263(5574):244-6.
367. McGeer EG, McGeer PL. Duplication of biochemical changes of Huntington's chorea by intrastriatal injections of glutamic and kainic acids. Nature. 1976;263(5577):517-9.
368. Giordano M, Ford LM, Brauckmann JL, Norman AB, Sanberg PR. MK801 prevents quinolinic acid-induced behavioral deficits and neurotoxicity in the striatum. Brain Res Bull. 1990;24(3):313-9.
369. Zhang H, Li Q, Graham RK, Slow E, Hayden MR, Bezprozvanny I. Full length mutant huntingtin is required for altered Ca2+ signaling and apoptosis of striatal neurons in the YAC mouse model of Huntington's disease. Neurobiol Dis. 2008;31(1):80-8.
370. Zeron MM, Chen N, Moshaver A, Lee AT, Wellington CL, Hayden MR, et al. Mutant huntingtin enhances excitotoxic cell death. Mol Cell Neurosci. 2001;17(1):41-53.
371. Nicholls DG. Mitochondrial dysfunction and glutamate excitotoxicity studied in primary neuronal cultures. Curr Mol Med. 2004;4(2):149-77.
372. Farooqui T, Farooqui AA. Aging: an important factor for the pathogenesis of neurodegenerative diseases. Mech Ageing Dev. 2009;130(4):203-15.
373. Duan W, Guo Z, Jiang H, Ware M, Li XJ, Mattson MP. Dietary restriction normalizes glucose metabolism and BDNF levels, slows disease progression, and increases survival in huntingtin mutant mice. Proc Natl Acad Sci U S A. 2003;100(5):2911-6.
374. Ferrer I, Goutan E, Marin C, Rey MJ, Ribalta T. Brain-derived neurotrophic factor in Huntington disease. Brain Res. 2000;866(1-2):257-61.
375. Gines S, Seong IS, Fossale E, Ivanova E, Trettel F, Gusella JF, et al. Specific progressive cAMP reduction implicates energy deficit in presymptomatic Huntington's disease knock-in mice. Hum Mol Genet. 2003;12(5):497-508.
376. Gines S, Bosch M, Marco S, Gavalda N, Diaz-Hernandez M, Lucas JJ, et al. Reduced expression of the TrkB receptor in Huntington's disease mouse models and in human brain. Eur J Neurosci. 2006;23(3):649-58.
377. Perez-Navarro E, Canudas AM, Akerund P, Alberch J, Arenas E. Brain-derived neurotrophic factor, neurotrophin-3, and neurotrophin-4/5 prevent the death of striatal projection neurons in a rodent model of Huntington's disease. J Neurochem. 2000;75(5):2190-9.
378. Allen SJ, Dawbarn D. Clinical relevance of the neurotrophins and their receptors. Clin Sci (Lond). 2006;110(2):175-91.
379. Bergerot A, Shortland PJ, Anand P, Hunt SP, Carlstedt T. Co-treatment with riluzole and GDNF is necessary for functional recovery after ventral root avulsion injury. Exp Neurol. 2004;187(2):359-66.

380. Katoh-Semba R, Asano T, Ueda H, Morishita R, Takeuchi IK, Inaguma Y, et al. Riluzole enhances expression of brain-derived neurotrophic factor with consequent proliferation of granule precursor cells in the rat hippocampus. FASEB J. 2002;16(10):1328-30.
381. Squitieri F, Ciammola A, Colonnese C, Ciarmiello A. Neuroprotective effects of riluzole in Huntington's disease. Eur J Nucl Med Mol Imaging. 2008;35(1):221-2.
382. Schiefer J, Landwehrmeyer GB, Luesse HG, Sprunken A, Puls C, Milkereit A, et al. Riluzole prolongs survival time and alters nuclear inclusion formation in a transgenic mouse model of Huntington's disease. Mov Disord. 2002;17(4):748-57.
383. Squitieri F, Orobello S, Cannella M, Martino T, Romanelli P, Giovacchini G, et al. Riluzole protects Huntington disease patients from brain glucose hypometabolism and grey matter volume loss and increases production of neurotrophins. Eur J Nucl Med Mol Imaging. 2009;36(7):1113-20.
384. Schilling G, Coonfield ML, Ross CA, Borchelt DR. Coenzyme Q10 and remacemide hydrochloride ameliorate motor deficits in a Huntington's disease transgenic mouse model. Neurosci Lett. 2001;315(3):149-53.
385. Kieburtz K, Feigin A, McDermott M, Como P, Abwender D, Zimmerman C, et al. A controlled trial of remacemide hydrochloride in Huntington's disease. Mov Disord. 1996;11(3):273-7.
386. Wang SE, Lin CL, Hsu CH, Sheu SJ, Chien CT, Wu CH. Treatment with a herbal formula B401 enhances neuroprotection and angiogenesis in the R6/2 mouse model of Huntington's disease. Drug Des Devel Ther. 2015;9:887-900.
387. Cho SR, Benraiss A, Chmielnicki E, Samdani A, Economides A, Goldman SA. Induction of neostriatal neurogenesis slows disease progression in a transgenic murine model of Huntington disease. J Clin Invest. 2007;117(10):2889-902.
388. Chintawar S, Hourez R, Ravella A, Gall D, Orduz D, Rai M, et al. Grafting neural precursor cells promotes functional recovery in an SCA1 mouse model. J Neurosci. 2009;29(42):13126-35.
389. Jin K, LaFevre-Bernt M, Sun Y, Chen S, Gafni J, Crippen D, et al. FGF-2 promotes neurogenesis and neuroprotection and prolongs survival in a transgenic mouse model of Huntington's disease. Proc Natl Acad Sci U S A. 2005;102(50):18189-94.
390. Ebert AD, Barber AE, Heins BM, Svendsen CN. Ex vivo delivery of GDNF maintains motor function and prevents neuronal loss in a transgenic mouse model of Huntington's disease. Exp Neurol. 2010;224(1):155-62.
391. Nakano KK, Dawson DM, Spence A. Machado disease. A hereditary ataxia in Portuguese emigrants to Massachusetts. Neurology. 1972;22(1):49-55.
392. Woods BT, Schaumburg HH. Nigro-spino-dentatal degeneration with nuclear ophthalmoplegia. A unique and partially treatable clinico-pathological entity. J Neurol Sci. 1972;17(2):149-66.
393. Rosenberg RN, Nyhan WL, Bay C. Autosomal dominant striatonigral degeneration: a clinical, pathological, and biochemical study of a new genetic disorder. Trans Am Neurol Assoc. 1976;101:78-80.
394. Coutinho P, Andrade C. Autosomal dominant system degeneration in Portuguese families of the Azores Islands. A new genetic disorder involving cerebellar, pyramidal, extrapyramidal and spinal cord motor functions. Neurology. 1978;28(7):703-9.
395. Lima L, Coutinho P. Clinical criteria for diagnosis of Machado-Joseph disease: report of a non-Azorena Portuguese family. Neurology. 1980;30(3):319-22.
396. Sequeiros J, Coutinho P. Epidemiology and clinical aspects of Machado-Joseph disease. Adv Neurol. 1993;61:139-53.
397. Rub U, Brunt ER, Del Turco D, de Vos RA, Gierga K, Paulson H, et al. Guidelines for the pathoanatomical examination of the lower brain stem in ingestive and swallowing disorders and its application to a dysphagic spinocerebellar ataxia type 3 patient. Neuropathol Appl Neurobiol. 2003;29(1):1-13.

398. Rosenberg RN. Machado-Joseph disease: an autosomal dominant motor system degeneration. Mov Disord. 1992;7(3):193-203.
399. Yamada M, Tan CF, Inenaga C, Tsuji S, Takahashi H. Sharing of polyglutamine localization by the neuronal nucleus and cytoplasm in CAG-repeat diseases. Neuropathol Appl Neurobiol. 2004;30(6):665-75.
400. Coutinho P, Sequeiros J. [Clinical, genetic and pathological aspects of Machado-Joseph disease]. J Genet Hum. 1981;29(3):203-9.
401. Rub U, de Vos RA, Brunt ER, Sebesteny T, Schols L, Auburger G, et al. Spinocerebellar ataxia type 3 (SCA3): thalamic neurodegeneration occurs independently from thalamic ataxin-3 immunopositive neuronal intranuclear inclusions. Brain Pathol. 2006;16(3):218-27.
402. Iwabuchi K, Tsuchiya K, Uchihara T, Yagishita S. Autosomal dominant spinocerebellar degenerations. Clinical, pathological, and genetic correlations. Rev Neurol (Paris). 1999;155(4):255-70.
403. Takiyama Y, Nishizawa M, Tanaka H, Kawashima S, Sakamoto H, Karube Y, et al. The gene for Machado-Joseph disease maps to human chromosome 14q. Nat Genet. 1993;4(3):300-4.
404. Ichikawa Y, Goto J, Hattori M, Toyoda A, Ishii K, Jeong SY, et al. The genomic structure and expression of MJD, the Machado-Joseph disease gene. J Hum Genet. 2001;46(7):413-22.
405. Bettencourt C, Santos C, Montiel R, Costa MD, Cruz-Morales P, Santos LR, et al. Increased transcript diversity: novel splicing variants of Machado-Joseph Disease gene (ATXN3). Neurogenetics. 2009.
406. Nishiyama K, Murayama S, Goto J, Watanabe M, Hashida H, Katayama S, et al. Regional and cellular expression of the Machado-Joseph disease gene in brains of normal and affected individuals. Ann Neurol. 1996;40(5):776-81.
407. Goto J, Watanabe M, Ichikawa Y, Yee SB, Ihara N, Endo K, et al. Machado-Joseph disease gene products carrying different carboxyl termini. Neurosci Res. 1997;28(4):373-7.
408. Burk K, Abele M, Fetter M, Dichgans J, Skalej M, Laccone F, et al. Autosomal dominant cerebellar ataxia type I clinical features and MRI in families with SCA1, SCA2 and SCA3. Brain. 1996;119 (Pt 5):1497-505.
409. Klockgether T, Skalej M, Wedekind D, Luft AR, Welte D, Schulz JB, et al. Autosomal dominant cerebellar ataxia type I. MRI-based volumetry of posterior fossa structures and basal ganglia in spinocerebellar ataxia types 1, 2 and 3. Brain. 1998;121 (Pt 9):1687-93.
410. Onodera O, Idezuka J, Igarashi S, Takiyama Y, Endo K, Takano H, et al. Progressive atrophy of cerebellum and brainstem as a function of age and the size of the expanded CAG repeats in the MJD1 gene in Machado-Joseph disease. Ann Neurol. 1998;43(3):288-96.
411. D'Abreu A, Franca MC, Jr., Yasuda CL, Campos BA, Lopes-Cendes I, Cendes F. Neocortical atrophy in Machado-Joseph disease: a longitudinal neuroimaging study. J Neuroimaging. 2012;22(3):285-91.
412. Seidel K, Siswanto S, Brunt ER, den Dunnen W, Korf HW, Rub U. Brain pathology of spinocerebellar ataxias. Acta Neuropathol. 2012;124(1):1-21.
413. Rub U, Brunt ER, Deller T. New insights into the pathoanatomy of spinocerebellar ataxia type 3 (Machado-Joseph disease). Curr Opin Neurol. 2008;21(2):111-6.
414. Romanul FC, Fowler HL, Radvany J, Feldman RG, Feingold M. Azorean disease of the nervous system. N Engl J Med. 1977;296(26):1505-8.
415. Klockgether T, Schols L, Abele M, Burk K, Topka H, Andres F, et al. Age related axonal neuropathy in spinocerebellar ataxia type 3/Machado-Joseph disease (SCA3/MJD). J Neurol Neurosurg Psychiatry. 1999;66(2):222-4.
416. Gilman S. The spinocerebellar ataxias. Clin Neuropharmacol. 2000;23(6):296-303.
417. Koeppen AH. The pathogenesis of spinocerebellar ataxia. Cerebellum. 2005;4(1):62-73.

418. Robitaille Y, Lopes-Cendes I, Becher M, Rouleau G, Clark AW. The neuropathology of CAG repeat diseases: review and update of genetic and molecular features. Brain Pathol. 1997;7(3):901-26.
419. Braak H, Rub U, Del Tredici K. Involvement of precerebellar nuclei in multiple system atrophy. Neuropathol Appl Neurobiol. 2003;29(1):60-76.
420. Rub U, Schultz C, Del Tredici K, Gierga K, Reifenberger G, de Vos RA, et al. Anatomically based guidelines for systematic investigation of the central somatosensory system and their application to a spinocerebellar ataxia type 2 (SCA2) patient. Neuropathol Appl Neurobiol. 2003;29(5):418-33.
421. Rub U, Brunt ER, Petrasch-Parwez E, Schols L, Theegarten D, Auburger G, et al. Degeneration of ingestion-related brainstem nuclei in spinocerebellar ataxia type 2, 3, 6 and 7. Neuropathol Appl Neurobiol. 2006;32(6):635-49.
422. Rub U, Brunt ER, Gierga K, Schultz C, Paulson H, de Vos RA, et al. The nucleus raphe interpositus in spinocerebellar ataxia type 3 (Machado-Joseph disease). J Chem Neuroanat. 2003;25(2):115-27.
423. Rub U, de Vos RA, Schultz C, Brunt ER, Paulson H, Braak H. Spinocerebellar ataxia type 3 (Machado-Joseph disease): severe destruction of the lateral reticular nucleus. Brain. 2002;125(Pt 9):2115-24.
424. Rub U, Seidel K, Ozerden I, Gierga K, Brunt ER, Schols L, et al. Consistent affection of the central somatosensory system in spinocerebellar ataxia type 2 and type 3 and its significance for clinical symptoms and rehabilitative therapy. Brain Res Rev. 2007;53(2):235-49.
425. Chai Y, Koppenhafer SL, Shoesmith SJ, Perez MK, Paulson HL. Evidence for proteasome involvement in polyglutamine disease: localization to nuclear inclusions in SCA3/MJD and suppression of polyglutamine aggregation in vitro. Hum Mol Genet. 1999;8(4):673-82.
426. Mori F, Nishie M, Piao YS, Kito K, Kamitani T, Takahashi H, et al. Accumulation of NEDD8 in neuronal and glial inclusions of neurodegenerative disorders. Neuropathol Appl Neurobiol. 2005;31(1):53-61.
427. Seidel K, den Dunnen WF, Schultz C, Paulson H, Frank S, de Vos RA, et al. Axonal inclusions in spinocerebellar ataxia type 3. Acta Neuropathol. 2010;120(4):449-60.
428. Hayashi M, Kobayashi K, Furuta H. Immunohistochemical study of neuronal intranuclear and cytoplasmic inclusions in Machado-Joseph disease. Psychiatry Clin Neurosci. 2003;57(2):205-13.
429. Seidel K, Meister M, Dugbartey GJ, Zijlstra MP, Vinet J, Brunt ER, et al. Cellular protein quality control and the evolution of aggregates in spinocerebellar ataxia type 3 (SCA3). Neuropathol Appl Neurobiol. 2012;38(6):548-58.
430. Taniwaki T, Sakai T, Kobayashi T, Kuwabara Y, Otsuka M, Ichiya Y, et al. Positron emission tomography (PET) in Machado-Joseph disease. J Neurol Sci. 1997;145(1):63-7.
431. Wullner U, Reimold M, Abele M, Burk K, Minnerop M, Dohmen BM, et al. Dopamine transporter positron emission tomography in spinocerebellar ataxias type 1, 2, 3, and 6. Arch Neurol. 2005;62(8):1280-5.
432. D'Abreu A, Franca M, Jr., Appenzeller S, Lopes-Cendes I, Cendes F. Axonal dysfunction in the deep white matter in Machado-Joseph disease. J Neuroimaging. 2009;19(1):9-12.
433. Kang JS, Klein JC, Baudrexel S, Deichmann R, Nolte D, Hilker R. White matter damage is related to ataxia severity in SCA3. J Neurol. 2014;261(2):291-9.
434. Schulz JB, Borkert J, Wolf S, Schmitz-Hubsch T, Rakowicz M, Mariotti C, et al. Visualization, quantification and correlation of brain atrophy with clinical symptoms in spinocerebellar ataxia types 1, 3 and 6. Neuroimage. 2010;49(1):158-68.
435. Eichler L, Bellenberg B, Hahn HK, Koster O, Schols L, Lukas C. Quantitative assessment of brain stem and cerebellar atrophy in spinocerebellar ataxia types 3 and 6: impact on clinical status. AJNR Am J Neuroradiol. 2011;32(5):890-7.

436. Reetz K, Costa AS, Mirzazade S, Lehmann A, Juzek A, Rakowicz M, et al. Genotype-specific patterns of atrophy progression are more sensitive than clinical decline in SCA1, SCA3 and SCA6. Brain. 2013;136(Pt 3):905-17.
437. Brown SD, Hancock JM, Gates H. Understanding mammalian genetic systems: the challenge of phenotyping in the mouse. PLoS Genet. 2006;2(8):e118.
438. Chadman KK, Yang M, Crawley JN. Criteria for validating mouse models of psychiatric diseases. Am J Med Genet B Neuropsychiatr Genet. 2009;150B(1):1-11.
439. Costa Mdo C, Luna-Cancalon K, Fischer S, Ashraf NS, Ouyang M, Dharia RM, et al. Toward RNAi therapy for the polyglutamine disease Machado-Joseph disease. Mol Ther. 2013;21(10):1898-908.
440. Bichelmeier U, Schmidt T, Hubener J, Boy J, Ruttiger L, Habig K, et al. Nuclear localization of ataxin-3 is required for the manifestation of symptoms in SCA3: in vivo evidence. J Neurosci. 2007;27(28):7418-28.
441. Torashima T, Koyama C, Iizuka A, Mitsumura K, Takayama K, Yanagi S, et al. Lentivector-mediated rescue from cerebellar ataxia in a mouse model of spinocerebellar ataxia. EMBO Rep. 2008;9(4):393-9.
442. Boy J, Schmidt T, Schumann U, Grasshoff U, Unser S, Holzmann C, et al. A transgenic mouse model of spinocerebellar ataxia type 3 resembling late disease onset and gender-specific instability of CAG repeats. Neurobiol Dis. 2010;37(2):284-93.
443. Jortner BS. The return of the dark neuron. A histological artifact complicating contemporary neurotoxicologic evaluation. Neurotoxicology. 2006;27(4):628-34.
444. Goncalves N, Simoes AT, Cunha RA, de Almeida LP. Caffeine and adenosine A(2A) receptor inactivation decrease striatal neuropathology in a lentiviral-based model of Machado-Joseph disease. Ann Neurol. 2013;73(5):655-66.
445. Nascimento-Ferreira I, Santos-Ferreira T, Sousa-Ferreira L, Auregan G, Onofre I, Alves S, et al. Overexpression of the autophagic beclin-1 protein clears mutant ataxin-3 and alleviates Machado-Joseph disease. Brain. 2011;134(Pt 5):1400-15.
446. Silva-Fernandes A, Duarte-Silva S, Neves-Carvalho A, Amorim M, Soares-Cunha C, Oliveira P, et al. Chronic Treatment with 17-DMAG Improves Balance and Coordination in A New Mouse Model of Machado-Joseph Disease. Neurotherapeutics. 2014.
447. Nobrega C, Nascimento-Ferreira I, Onofre I, Albuquerque D, Hirai H, Deglon N, et al. Silencing mutant ataxin-3 rescues motor deficits and neuropathology in Machado-Joseph disease transgenic mice. PLoS One. 2013;8(1):e52396.
448. Boudreau RL, Martins I, Davidson BL. Artificial microRNAs as siRNA shuttles: improved safety as compared to shRNAs in vitro and in vivo. Mol Ther. 2009;17(1):169-75.
449. Rodriguez-Lebron E, Costa M, Luna-Cancalon K, Peron TM, Fischer S, Boudreau RL, et al. Silencing mutant ATXN3 expression resolves molecular phenotypes in SCA3 transgenic mice. Mol Ther. 2013;21(10):1909-18.
450. Evers MM, Tran HD, Zalachoras I, Pepers BA, Meijer OC, den Dunnen JT, et al. Ataxin-3 protein modification as a treatment strategy for spinocerebellar ataxia type 3: removal of the CAG containing exon. Neurobiol Dis. 2013;58:49-56.
451. Krause T, Gerbershagen MU, Fiege M, Weisshorn R, Wappler F. Dantrolene–a review of its pharmacology, therapeutic use and new developments. Anaesthesia. 2004;59(4):364-73.
452. Wang HL, Hu SH, Chou AH, Wang SS, Weng YH, Yeh TH. H1152 promotes the degradation of polyglutamine-expanded ataxin-3 or ataxin-7 independently of its ROCK-inhibiting effect and ameliorates mutant ataxin-3-induced neurodegeneration in the SCA3 transgenic mouse. Neuropharmacology. 2013;70:1-11.

453. Chen JF, Sonsalla PK, Pedata F, Melani A, Domenici MR, Popoli P, et al. Adenosine A2A receptors and brain injury: broad spectrum of neuroprotection, multifaceted actions and "fine tuning" modulation. Prog Neurobiol. 2007;83(5):310-31.
454. Gomes CV, Kaster MP, Tome AR, Agostinho PM, Cunha RA. Adenosine receptors and brain diseases: neuroprotection and neurodegeneration. Biochim Biophys Acta. 2011;1808(5):1380-99.
455. Popoli P, Blum D, Martire A, Ledent C, Ceruti S, Abbracchio MP. Functions, dysfunctions and possible therapeutic relevance of adenosine A2A receptors in Huntington's disease. Prog Neurobiol. 2007;81(5-6):331-48.
456. Costa MD, Luna-Cancalon K, Fischer S, Ashraf NS, Ouyang M, Dharia RM, et al. Toward RNAi Therapy for the Polyglutamine Disease Machado-Joseph Disease. Molecular Therapy. 2013;21(10):1898-908.
457. Rodriguez-Lebron E, Costa MD, Luna-Cancalon K, Peron TM, Fischer S, Boudreau RL, et al. Silencing Mutant ATXN3 Expression Resolves Molecular Phenotypes in SCA3 Transgenic Mice. Molecular Therapy. 2013;21(10):1909-18.
458. Sakai T, Matsuishi T, Yamada S, Komori H, Iwashita H. Sulfamethoxazole-trimethoprim double-blind, placebo-controlled, crossover trial in Machado-Joseph disease: sulfamethoxazole-trimethoprim increases cerebrospinal fluid level of biopterin. J Neural Transm Gen Sect. 1995;102(2):159-72.
459. Correia M, Coutinho P, Silva MC, Guimaraes J, Amado J, Matos E. Evaluation of the effect of sulphametoxazole and trimethoprim in patients with Machado-Joseph disease. Rev Neurol. 1995;23(121):632-4.
460. Schulte T, Mattern R, Berger K, Szymanski S, Klotz P, Kraus PH, et al. Double-blind crossover trial of trimethoprim-sulfamethoxazole in spinocerebellar ataxia type 3/Machado-Joseph disease. Arch Neurol. 2001;58(9):1451-7.
461. Chan-Palay V. Indoleamine neurons and their processes in the normal rat brain and in chronic diet-induced thiamine deficiency demonstrated by uptake of 3H-serotonin. J Comp Neurol. 1977;176(4):467-93.
462. Wenthur CJ, Bennett MR, Lindsley CW. Classics in chemical neuroscience: fluoxetine (prozac). ACS Chem Neurosci. 2014;5(1):14-23.
463. Monte TL, Rieder CR, Tort AB, Rockenback I, Pereira ML, Silveira I, et al. Use of fluoxetine for treatment of Machado-Joseph disease: an open-label study. Acta Neurol Scand. 2003;107(3):207-10.
464. Lou JS, Goldfarb L, McShane L, Gatev P, Hallett M. Use of buspirone for treatment of cerebellar ataxia. An open-label study. Arch Neurol. 1995;52(10):982-8.
465. Trouillas P, Brudon F, Adeleine P. Improvement of cerebellar ataxia with levorotatory form of 5-hydroxytryptophan. A double-blind study with quantified data processing. Arch Neurol. 1988;45(11):1217-22.
466. Trouillas P, Xie J, Adeleine P. Buspirone, a serotonergic 5-HT1A agonist, is active in cerebellar ataxia. A new fact in favor of the serotonergic theory of ataxia. Prog Brain Res. 1997;114:589-99.
467. Trouillas P, Xie J, Adeleine P, Michel D, Vighetto A, Honnorat J, et al. Buspirone, a 5-hydroxytryptamine1A agonist, is active in cerebellar ataxia. Results of a double-blind drug placebo study in patients with cerebellar cortical atrophy. Arch Neurol. 1997;54(6):749-52.
468. Friedman JH. Machado-Joseph disease/spinocerebellar ataxia 3 responsive to buspirone. Mov Disord. 1997;12(4):613-4.
469. Takei A, Honma S, Kawashima A, Yabe I, Fukazawa T, Hamada K, et al. Beneficial effects of tandospirone on ataxia of a patient with Machado-Joseph disease. Psychiatry Clin Neurosci. 2002;56(2):181-5.
470. Takei A, Fukazawa T, Hamada T, Sohma H, Yabe I, Sasaki H, et al. Effects of tandospirone on "5-HT1A receptor-associated symptoms" in patients with Machado-Josephe disease: an open-label study. Clin Neuropharmacol. 2004;27(1):9-13.

471. Ientile R, Caccamo D, Macaione V, Torre V, Macaione S. NMDA-evoked excitotoxicity increases tissue transglutaminase in cerebellar granule cells. Neuroscience. 2002;115(3):723-9.
472. Liu CS, Hsu HM, Cheng WL, Hsieh M. Clinical and molecular events in patients with Machado-Joseph disease under lamotrigine therapy. Acta Neurol Scand. 2005;111(6):385-90.
473. Zesiewicz TA, Sullivan KL. Treatment of ataxia and imbalance with varenicline (chantix): report of 2 patients with spinocerebellar ataxia (types 3 and 14). Clin Neuropharmacol. 2008;31(6):363-5.
474. Zesiewicz TA, Sullivan KL, Freeman A, Juncos JL. Treatment of imbalance with varenicline Chantix(R): report of a patient with fragile X tremor/ataxia syndrome. Acta Neurol Scand. 2009;119(2):135-8.
475. Zesiewicz TA, Sullivan KL, Gooch CL, Lynch DR. Subjective improvement in proprioception in 2 patients with atypical Friedreich ataxia treated with varenicline (Chantix). J Clin Neuromuscul Dis. 2009;10(4):191-3.
476. Zesiewicz TA, Greenstein PE, Sullivan KL, Wecker L, Miller A, Jahan I, et al. A randomized trial of varenicline (Chantix) for the treatment of spinocerebellar ataxia type 3. Neurology. 2012;78(8):545-50.
477. Goodwin FK. Rationale for using lithium in combination with other mood stabilizers in the management of bipolar disorder. J Clin Psychiatry. 2003;64 Suppl 5:18-24.
478. Lin D, Mok H, Yatham LN. Polytherapy in bipolar disorder. CNS Drugs. 2006;20(1):29-42.
479. Wood NI, Morton AJ. Chronic lithium chloride treatment has variable effects on motor behaviour and survival of mice transgenic for the Huntington's disease mutation. Brain Res Bull. 2003;61(4):375-83.
480. Feng HL, Leng Y, Ma CH, Zhang J, Ren M, Chuang DM. Combined lithium and valproate treatment delays disease onset, reduces neurological deficits and prolongs survival in an amyotrophic lateral sclerosis mouse model. Neuroscience. 2008;155(3):567-72.
481. Jia DD, Zhang L, Chen Z, Wang CR, Huang FZ, Duan RH, et al. Lithium chloride alleviates neurodegeneration partly by inhibiting activity of GSK3beta in a SCA3 Drosophila model. Cerebellum. 2013;12(6):892-901.
482. Fornai F, Longone P, Cafaro L, Kastsiuchenka O, Ferrucci M, Manca ML, et al. Lithium delays progression of amyotrophic lateral sclerosis. Proc Natl Acad Sci U S A. 2008;105(6):2052-7.
483. Watase K, Gatchel JR, Sun Y, Emamian E, Atkinson R, Richman R, et al. Lithium therapy improves neurological function and hippocampal dendritic arborization in a spinocerebellar ataxia type 1 mouse model. PLoS Med. 2007;4(5):e182.
484. Saute JA, Castilhos RM, Monte TL, Schumacher-Schuh AF, Donis KC, D'Avila R, et al. A randomized, phase 2 clinical trial of lithium carbonate in Machado-Joseph disease. Mov Disord. 2014.
485. Saute JA, Donis KC, Serrano-Munuera C, Genis D, Ramirez LT, Mazzetti P, et al. Ataxia rating scales–psychometric profiles, natural history and their application in clinical trials. Cerebellum. 2012;11(2):488-504.
486. Kieling C, Morales Saute JA, Jardim LB. When ataxia is not just ataxia. Nat Clin Pract Neurol. 2007;3(5):E2.
487. Saute JA, de Castilhos RM, Monte TL, Schumacher-Schuh AF, Donis KC, D'Avila R, et al. A randomized, phase 2 clinical trial of lithium carbonate in Machado-Joseph disease. Mov Disord. 2014;29(4):568-73.

Objectives

Considering the lack of knowledge on pathogenic mechanisms underlying MJD and the currently inexistent therapies for this disorder, this thesis work has its main focus on hypothesis-based pharmacological pre-clinical trials, using the CMVMJD135 mouse model. Bearing this in mind we aimed to test the therapeutic efficacy of:

1. Inducing the load of molecular chaperones in the cell, using an Hsp90 inhibitor, 17-DMAG;
2. Increasing the autophagy process, using lithium chloride or a combination of lithium chloride and temsirolimus (CCI-779);
3. Targeting the ER stress response, using tauroursodeoxycholic acid (TUDCA), also known to have multiple actions in the cells (anti-apoptotic, anti-inflammatory, chemical chaperone) contributing to neuroprotection.
4. Increasing the energy status in the cell, using a natural nutrient, creatine.

Chapter 2

Chronic treatment with 17-DMAG improves balance and coordination in a new mouse model of Machado-Joseph disease

Neurotherapeutics (2014) 11:433–449
DOI 10.1007/s13311-013-0255-9

ORIGINAL ARTICLE

Chronic Treatment with 17-DMAG Improves Balance and Coordination in A New Mouse Model of Machado-Joseph Disease

Anabela Silva-Fernandes · Sara Duarte-Silva · Andreia Neves-Carvalho · Marina Amorim · Carina Soares-Cunha · Pedro Oliveira · Kenneth Thirstrup · Andreia Teixeira-Castro · Patrícia Maciel

Published online: 30 January 2014

Abstract Machado-Joseph disease (MJD) or spinocerebellar ataxia type 3 (SCA3) is a neurodegenerative disease currently with no treatment. We describe a novel mouse model of MJD which expresses mutant human ataxin-3 at near endogenous levels and manifests MJD-like motor symptoms that appear gradually and progress over time. CMVMJD135 mice show ataxin-3 intranuclear inclusions in the CNS and neurodegenerative changes in key disease regions, such as the pontine and dentate nuclei. Hsp90 inhibition has shown promising outcomes in some neurodegenerative diseases, but nothing is known about its effects in MJD. Chronic treatment of CMVMJD mice with Hsp90 inhibitor 17-DMAG resulted in a delay in the progression of their motor coordination deficits and, at 22 and 24 weeks of age, was able to rescue the uncoordination phenotype to wild-type levels; in parallel, a reduction in neuropathology was observed in treated animals. We observed limited induction of heat-shock proteins with treatment, but found evidence that 17-DMAG may be acting through autophagy, as LC3-II (both at mRNA and protein levels) and beclin-1 were induced in the brain of treated animals. This resulted in decreased levels of the mutant ataxin-3 and reduced intranuclear aggregation of this protein. Our data validate this novel mouse model as a relevant tool for the study of MJD pathogenesis and for pre-clinical studies, and show that Hsp90 inhibition is a promising therapeutic strategy for MJD.

Keywords Polyglutamine · animal models · ataxia · behavior · therapy · autophagy.

Anabela Silva-Fernandes and Sara Duarte-Silva contributed equally to this work

Electronic supplementary material The online version of this article (doi:10.1007/s13311-013-0255-9) contains supplementary material, which is available to authorized users.

A. Silva-Fernandes · S. Duarte-Silva · A. Neves-Carvalho · M. Amorim · C. Soares-Cunha · A. Teixeira-Castro · P. Maciel (✉)
Life and Health Sciences Research Institute (ICVS), School of Health Sciences, University of Minho, Braga, Portugal
e-mail: pmaciel@ecsaude.uminho.pt

A. Silva-Fernandes · S. Duarte-Silva · A. Neves-Carvalho · M. Amorim · C. Soares-Cunha · A. Teixeira-Castro · P. Maciel
ICVS/3B's - PT Government Associate Laboratory, Braga/Guimarães, Portugal

P. Oliveira
ICBAS - Abel Salazar Biomedical Sciences Institute, University of Porto, Porto, Portugal

K. Thirstrup
Dept. of Neurodegeneration, H. Lundbeck A/S, Valby, Denmark

Introduction

Machado-Joseph disease (MJD), also known as spinocerebellar ataxia type 3 (SCA3), is caused by a CAG repeat expansion (>55) [1] in the protein coding region of the *ATXN3* gene, located in chromosome 14q32.1 and encoding the protein ataxin-3. The main clinical features of MJD are ataxia and ophthalmoplegia, which can be associated to a variable degree with peripheral amyotrophy, intention fasciculation-like movements of facial and lingual muscles, rigidity, spasticity, dystonia and palpebral retraction, leading to the appearance of bulging eyes [2]. Ataxin-3 harboring the expanded polyQ tract has a strong tendency for aggregation, leading to the formation of inclusions in the nucleus and cytoplasm of neuronal cells, including axonal tracts [3, 4], the pathogenic relevance of which remains unclear.

Molecular chaperones are crucial for the maintenance of native protein conformation, and recent research has shown that defective chaperone action may have pathogenic consequences [5, 6]. Several studies demonstrated the involvement of the heat shock proteins in MJD [7–10]; co-localization of Hsp70, Hsp40 and Hsp90, but not other chaperones (Hsp27, Hsp60 and Hsp110) with aggregates formed by mutant ataxin-3 has been described, which might result in a depletion of these protective molecules [7, 9]. In order to promote the correct refolding of the pathogenic protein(s) and to reduce the formation of toxic aggregated forms, the use of compounds that promote increased expression of heat shock proteins (HSPs), leading to improved protein folding and/or clearance of the mutant protein by the ubiquitin proteasome system or through autophagy, has been proposed [11, 12]. Hsp90, by itself and/or associated with multichaperone complexes, is a major repressor of HSF-1 acting in a feedback regulation mechanism [13]. Pharmacologic inactivation of Hsp90 leads to the overexpression of several molecular chaperones, activating the heat-shock response (HSR) *via* the persistence of HSF-1 action [13, 14]. Potent Hsp90 inhibitors, such as 17-AAG or 17-DMAG, have been shown to reduce aggregate load and toxicity in cell, fly, nematode and mouse models of several neurodegenerative diseases, dependently on HSF-1 [15–20]. Concerning polyQ diseases, these two compounds have been shown to have beneficial effects only for SBMA [19–21]. Despite its high potency, 17-AAG showed poor solubility and stability and demonstrated moderate toxicity in several clinical trials [22]. In contrast, 17-DMAG is a more potent analog of 17-AAG [23], is more water soluble than 17-AAG and can be administered orally [24], which could be advantageous for clinical purposes.

Although mouse models have been a remarkable tool in human disease research, several criteria have to be achieved in order to validate a genetically manipulated mouse as a model of a disease [25]. Therapeutic trials need to be performed in animal models showing significant similarities to the human diseases, in order to better evaluate the therapeutic benefit of a specific compound. Although several transgenic mouse models have been generated for the study of MJD, it has been difficult to find in one single model the main features of this disorder (reviewed in [26]).

In this work, we generated a new transgenic mouse model expressing ATXN3 with 135 glutamines under the control of the CMV promoter. These mice develop a progressive neurological disease overlapping with the core clinical features of MJD and show relevant neuropathology as well as ubiquitin-positive ataxin-3 intranuclear inclusions in regions of the brain known to be involved in MJD, including the pontine and deep cerebellar nuclei. We used this model in a pre-clinical trial to validate Hsp90 inhibition as a therapeutic strategy for MJD, with encouraging results that suggest that this approach should be pursued.

Results

CMVMJD135 Mice Express the Expanded Human Ataxin-3 in the CNS

We have generated transgenic mice expressing the ATXN3c cDNA variant of the *ATXN3* gene carrying a repeat tract with the sequence $(CAG)_2CAAAAGCAGCAA(CAG)_{129}$, coding for 135 glutamines, under the regulation of the CMV promoter (Fig. 1A). Transgene mRNA quantification demonstrated that one lineage (hereafter designated CMVMJD135), expressed the human ATXN3 protein in the brain (Fig. 1B). This lineage, possessing two copies of the transgene, expressed the human *ATXN3* mRNA at near-endogenous levels in the cerebellum, brainstem, forebrain and spinal cord (Fig. 1C). When breeding these animals we observed intergenerational CAG repeat length variation, mostly towards contraction (Supplementary Fig. 1) (maternal meioses (n=24): mean=−1.46±2.74; range=[−7, +4]; paternal meioses (n=42): mean=−0,71±1,61; range=[−5, +1]). We chose to study animals with repeat lengths over 129. All the comparisons for the genotype factor were performed between CMVMJD135 mice and wild-type littermates since it has been previously shown that transgenic mice expressing human ataxin-3 carrying a normal CAG repeat tract did not display any differences in the phenotype or neuropathology in comparison with wild-type (wt) [27–30]. In addition, our previous data have shown that even expression of ataxin-3 with 83 glutamines under the CMV promoter caused no phenotype change [31].

CMVMJD135 Transgenic Mice Display Progressive Neurological Deficits

At 4 weeks of age, transgenic and control littermates were indistinguishable in their home cage; however, at 16 weeks of age transgenic animals started to present a visibly abnormal gait and at 40 weeks of age they showed an unhealthy appearance, an abnormal body posture, limb clasping and limb tonus deficit (Fig. 1D).

Female CMVMJD135 transgenic and control mice gained weight at a similar rate until 19 weeks of age (Fig. 1E); however, transgenic males showed a significantly lower body weight gain compared with control males at 19 weeks of age, and since this age, all transgenic animals demonstrated a decline in body weight, whereas their wt littermates continued to gain weight until 40 weeks of age (male: genotype x age, $F_{2,61}$=35.067, p<0.000; female: genotype x age, $F_{2,61}$=5.211, p=0.008).

In the balance beam test, CMVMJD135 mice showed a significantly worse performance already at 10 weeks of age traversing the medium square beam (male: genotype, $F_{1,40}$= 30.845, $p=2\times10^{-6}$, age, $F_{1,40}$=6.356, p=0.014; female: genotype, $F_{1,44}$=10.754, p=0.002) (Fig. 2B), as well as the medium (male: genotype, $F_{1,34}$=22.023, $p=4.3\times10^{-5}$; female:

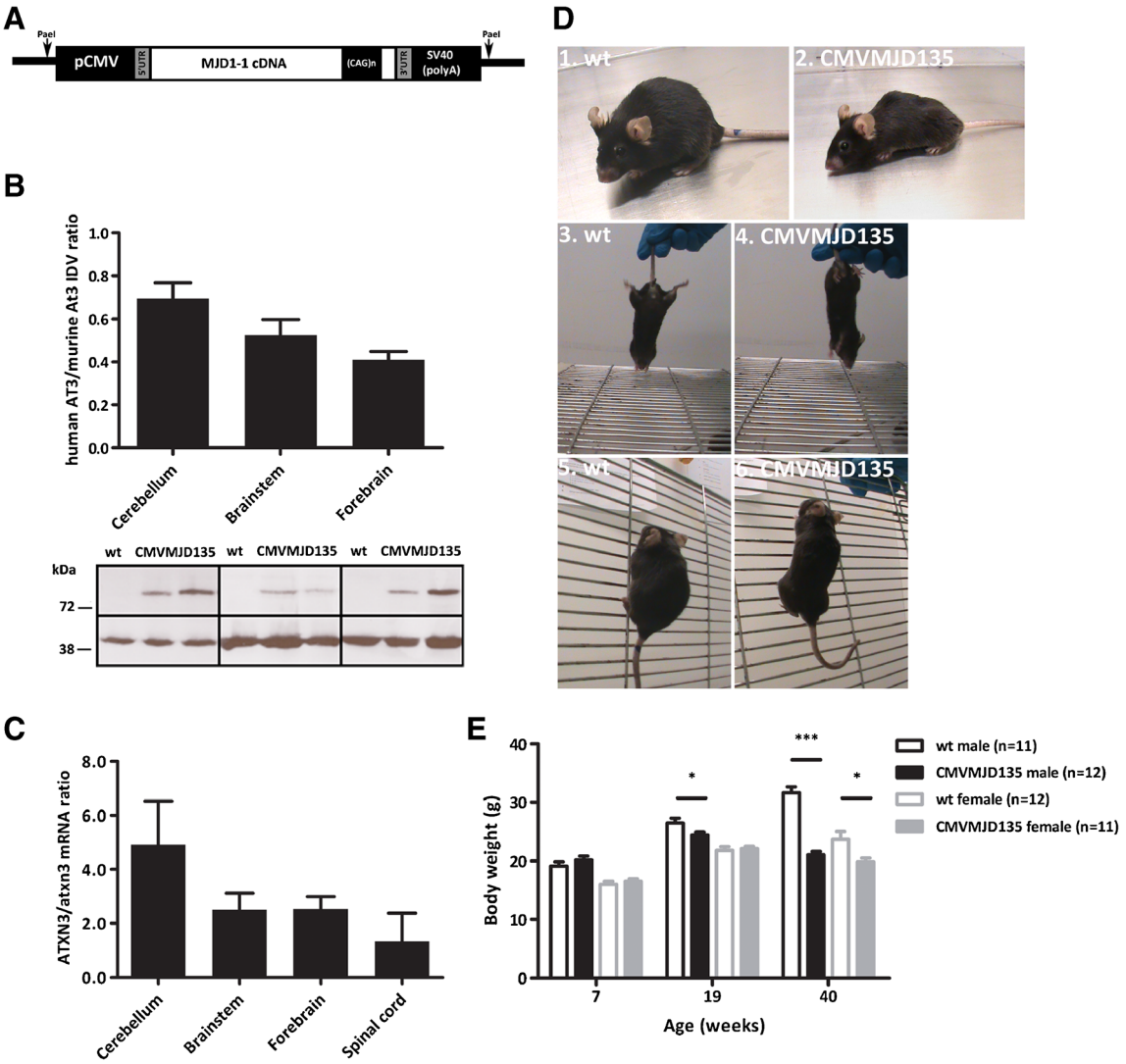

Fig. 1 Generation of a transgenic mouse model of MJD carrying the expanded ATXN3 with 135 CAGs. (A) Schematic diagram of the plasmid CMVMJDAT3Q135_1.5 used for the generation of cDNA MJD transgenic mice. (B) Western blot anti-ATXN3 in different CNS regions (cerebellum, forebrain and brainstem) of CMVMJD135 mice with 14–16 weeks of age. In all lanes, the endogenous mouse ataxin-3 (Atxn3) is detected at about 42 kDa. An approximately 80-kDa protein corresponding to expanded ATXN3 is detected in transgenic animal lysates. (C) qRT-PCR analysis of human ATXN3 and murine Atxn3 mRNA expression levels. Values are presented as mean ± SEM (n=4). (D) CMVMJD135 mice at 40 weeks of age presenting body posture deficit with lower pelvic elevation and hunchback (2), limb clasping (4) and reduced hindlimb tonus (6) in comparison with wt animals (1,3,5). (E) Assessment of body weight with age (n=11–12 for each group). Asterisks indicate significant differences between wt control and CMVMJD135 transgenic mice. *p<0.05, **p<0.01, ***p<0.001

genotype, $F_{1,37}$=4.859, p=0.034) (Fig. 2D) and the small round beams (male: genotype, $F_{1,31}$=18.486, p=1.58×10^{-4}; female: genotype, $F_{1,34}$=11.487, p=0.002, age, $F_{1,34}$=5.618, p=0.024) (Fig. 2E). With disease progression, CMVMJD135 mice demonstrated a higher frequency of foot slips and a flattened body posture in the beams. By 40 weeks of age, transgenic mice failed to maintain balance on the beams and fell off.

Footprint patterns of wt (41 weeks of age) and CMVMJD135 transgenic mice at 14, 28 and 41 weeks of age are illustrated in Fig. 3A. Dragging of the feet was observed in transgenic animals already at 14 weeks of age, progressing through age and becoming increasingly more severe (41 weeks: p=2.44×10^{-4}) (Fig. 3B). Additionally, beginning at 16 weeks of age, transgenic mice displayed a reduced paw overlap when compared with control animals, indicating an altered uniformity of step alternation (genotype, $F_{1,11}$=5.184, p=0.044) (Fig. 3C) as well as a significant decrease in the stride length (genotype, $F_{1,11}$=36.086, p=8.8×10^{-5}) (Fig. 3D).

CMVMJD135 mice swam significantly slower than control littermates at 22–25 weeks of age (genotype, $F_{1,21}$= 17.927, p=3.71×10^{-4}) and more so at 40 weeks (genotype, $F_{1,15}$=42.466, p=1.0×10^{-5}) (Fig. 4A). In addition, they displayed abnormalities in their swimming movements, adopting a twisted posture, and kicked in an uncoordinated

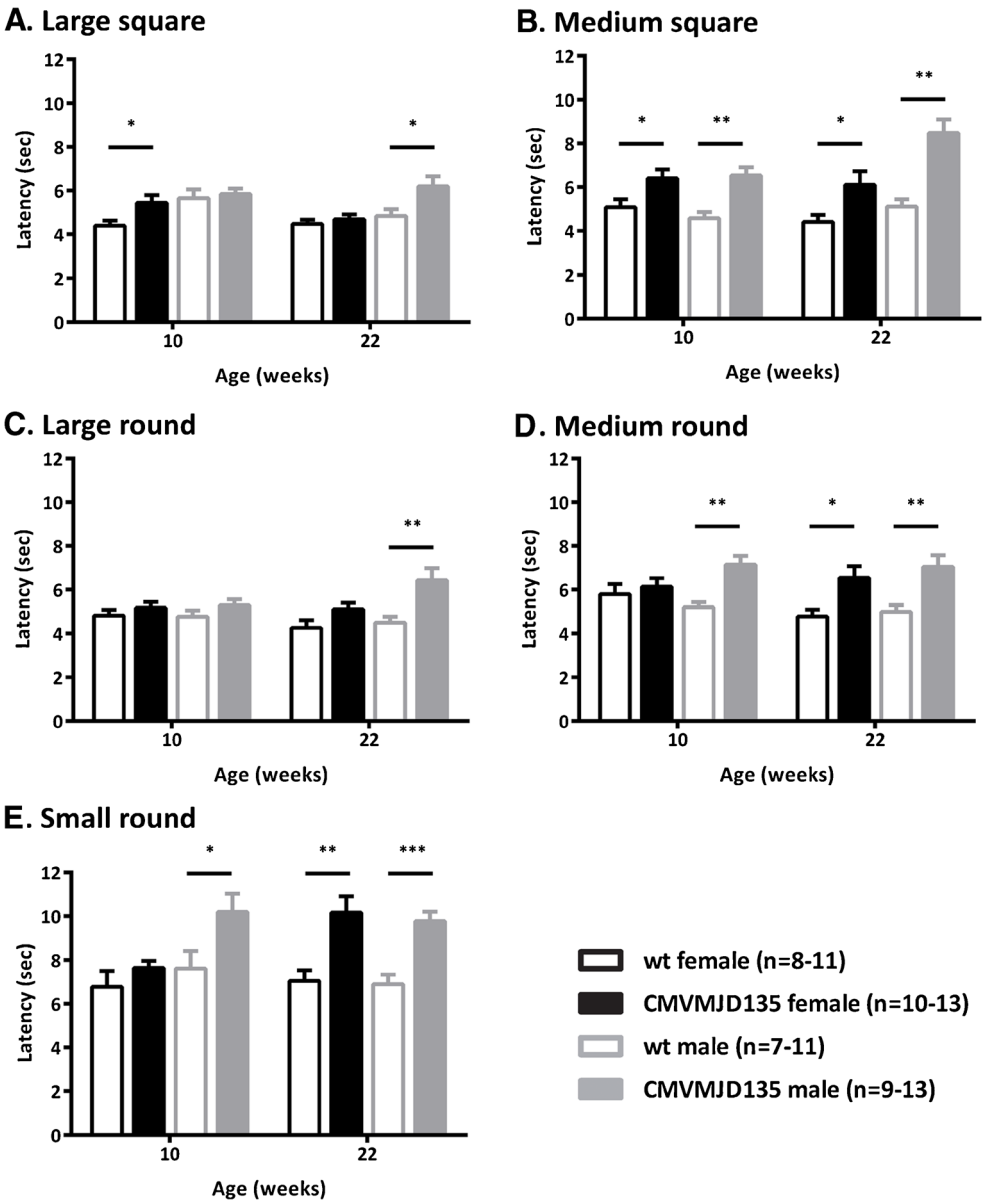

Fig. 2 Body balance impairment in CMVMJD135 mice. Balance beam test performance of wt and transgenic animals using square (A,B) and round beams (C–E) is depicted at 10 and 22 weeks of age. Values are presented as mean ± SEM (n=8–13 for each genotype and gender). *p<0.05, **p<0.01, ***p<0.001

manner with both hind- and forelimbs. In the rotarod paradigm, significant differences were observed from the age of 20 weeks (genotype, $F_{1,21}$=4.879, p=0.038) (Fig. 4B). At 40 weeks of age, transgenic animals showed a dramatic deterioration in their rotarod performance compared with littermate controls, both in the accelerating rod (genotype, $F_{1,17}$=20.234, p=3.17×10^{-4}) and at constant speeds (8 rpm: p=0.004; 15 rpm: p=0.002; 20 rpm: p=0.003; 24 rpm: p=0.002) (Fig. 4C).

At the first age of assessment with the SHIRPA protocol (7 weeks) CMVMJD135 transgenic mice revealed significant differences in performance in the hanging wire grip test, that became worse with age (male: genotype x age, $F_{1,42}$=30.331, p=2.0×10^{-6}; female: genotype x age, $F_{1,41}$=36.955, p<0.000) (Fig. 5A). At 19 weeks of age, a significant percentage of transgenic animals developed loss of hindlimb tonus resistance (male: p=1.07×10^{-4}; female: p=0.002) (Fig. 5B), a decrease in forelimb strength (male: p=0.003; female: p=0.006) (Fig. 5C) and hindlimb clasping (male: p=1.07×10^{-4}; female: p=0.006) (Fig. 5D). Furthermore, 40-week-old animals demonstrated a dramatic deterioration of the neurological symptoms observed at 19 weeks of age in the SHIRPA protocol, namely, the loss of hindlimb tonus, the tremors and the decreased locomotor and exploratory activity, among others (Supplementary Fig. 2A–D). From 40 weeks of age onwards, most CMVMJD135 mice were not able to traverse the beams or stay in the rotarod and their footprinting pattern was difficult to measure due to the severe dragging, which led us to halt the phenotype evaluation.

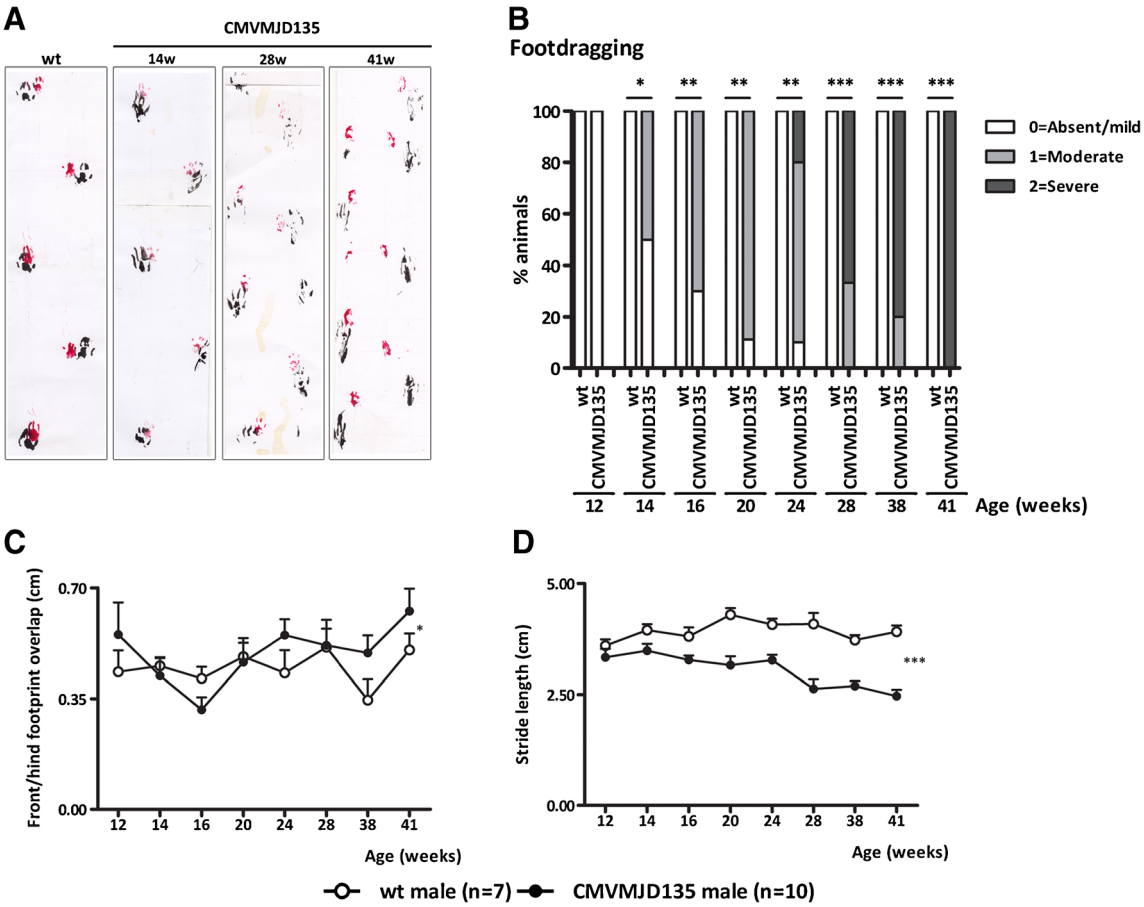

Fig. 3 Abnormal footprint pattern in transgenic mice. (A) Representative walking footprint patterns of 14-, 28- and 41-week-old CMVMJD135 mice. Qualitatively, the patterns generated clearly differ, showing that transgenic mice display foot-dragging. At late stages CMVMJD135 mice also demonstrate shorter strides and an irregular left–right step pattern as compared with the wt control mice. (B) Quantitative analysis of foot-dragging. Quantitative analysis of the footprint patterns of wt and transgenic mice, based on measurements of (C) distance between front and hind footprint overlap and (D) stride length through age. Values are presented as mean ± SEM (n=7 and 10 for wt and transgenic, respectively). *p<0.05, **p<0.01, ***p<0.001

A group of wt (n=9) and transgenic animals (n=13) were followed through life until they had to be sacrificed due to established humane endpoints (93 weeks of age). Although transgenic mice showed a progressive deterioration of the motor phenotype, no differences were observed in survival rate between both genotypes until this age, in the laboratory conditions used, which included lowering the food to an accessible level and hydrating it at ages when transgenic animals had difficulty reaching the food and drink compartments.

For cognitive assessment, the Morris Water Maze test was performed at 10 weeks of age, before the motor symptoms would interfere excessively with testing, and no differences were found (Supplementary Fig. 2E,F).

CMVMJD135 Mice Exhibit Reduced Brain Weight, Reduced Volume and Total Cell Number in Pontine Nuclei and Intranuclear Ataxin-3 Inclusions

The total brain weight of CMVMJD135 mice was slightly reduced (5 %) in comparison with control littermates at late stages of the disease (42–43 weeks) (p=2.74×10^{-4}) (Fig. 6A). However, we did not observe differences in brain weight in animals sacrificed at 20 weeks of age, suggesting that the motor phenotype begins before marked neuronal loss. Stereological evaluation of CMVMJD135 mice brains at 60 weeks of age revealed a significantly reduced volume as well as a decrease in total cell number in pontine nuclei indicating neuronal demise in this region, known to be affected in MJD (Fig. 6B). Interestingly, transgenic mice showed a significant volume reduction without cell loss in the dentate nuclei. In contrast, no differences were found in the locus coeruleus and in the substantia nigra (SN), although hyperchromatic cells and astrogliosis were observed in SN (Fig. 6C; Supplementary Fig. 3).

Immunohistochemistry showed the presence of ataxin-3 inclusions in the nucleus of neuronal cells in different regions of the CNS of CMVMJD135 mice at 20–35 weeks of age (Fig. 6C) including the pontine nuclei, reticulotegmental nucleus of the pons, spinal cord neurons, the facial nuclei, anterior olfactory nuclei, ventral tenia tecta, inferior olive,

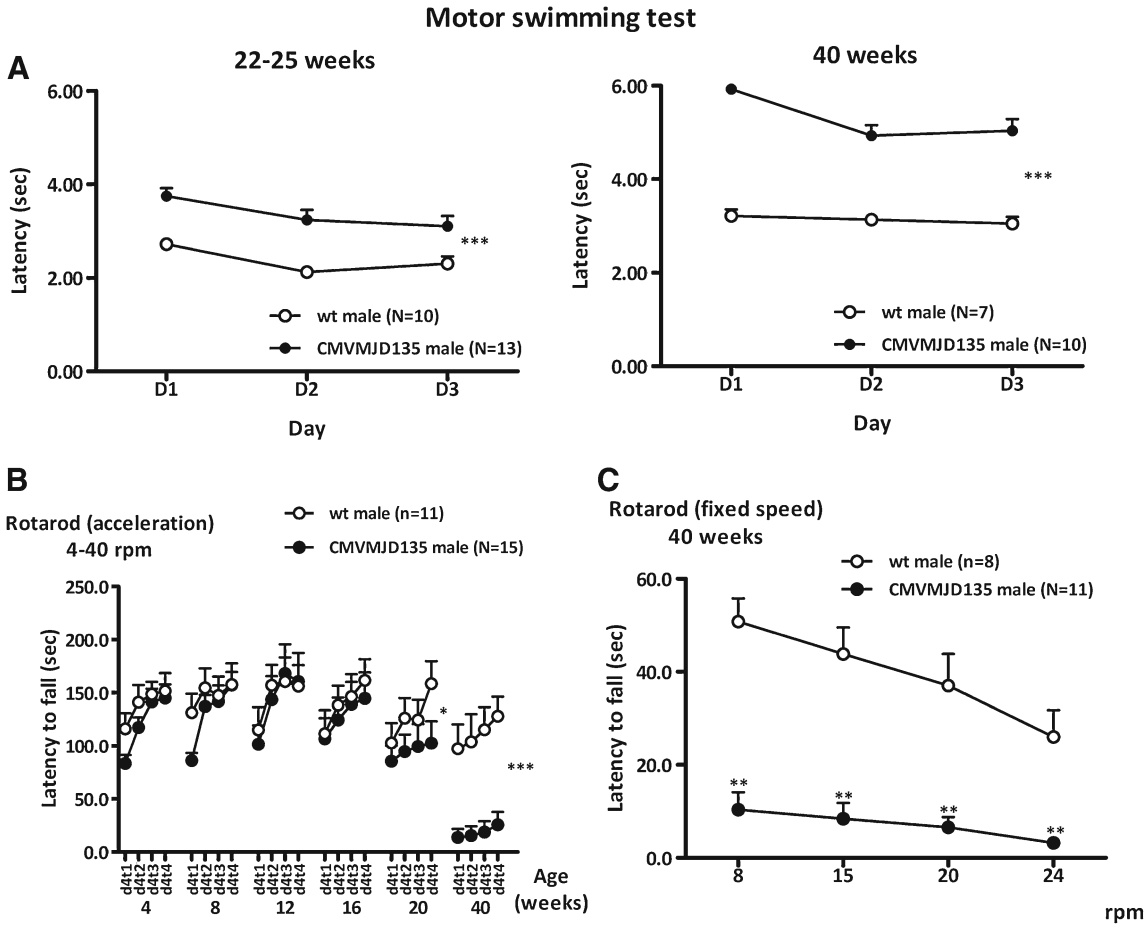

Fig. 4 Motor incoordination on the rotarod and in the swimming tank in CMVMJD135 mice. (A) 22–25- and 40-week-old wt and CMVMJD135 male mice (n=7–15) were tested for motor coordination in the swimming tank, by assessing the latency to swim over a 60-cm distance to a visible escape platform. Transgenic mice displayed swimming impairments given by a significant increase in the time spent to cross the 60-cm distance. Rotarod analysis of CMVMJD135 and wt animals were tested in (B) an accelerating rod (4–40 rpm) and (C) at constant speeds. The mean±SEM of the latency to fall at each speed level was recorded. Rotarod deficit was present at 20 weeks of age and older (shown for 40 weeks); CMVMJD135 transgenic mice displayed a progressive decline in performance on the rotarod with increasing rotation speed. *p<0.05, **p<0.01, ***p<0.001

the dentate nuclei, locus coeruleus and the cuneate nuclei. The evaluation of cell morphology by cresyl violet staining at 24 weeks of age showed an increased abundance of seemingly atrophic and hyperchromatic neurons in the pontine nuclei of CMVMJD135 mice (Fig. 6C,g–j).

17-DMAG Chronic Treatment Improved Several Features of the Motor Phenotype Observed in CMVMJD135 Mice

Given previous results suggesting that Hsp90 inhibition could be a useful therapeutic approach for polyQ disease, our own finding with 17-DMAG in a nematode model of MJD [32], and the lack of studies in vertebrate models of this disorder, we tested the effect of 17-DMAG in the CMVMJD135 mouse. All analyses in this pre-clinical trial were performed using male mice.

A pilot study was performed in wt animals in order to determine the effective dose of 17-DMAG which induces Hsp70 in the brain. Previous studies have shown increased oral availability of 17-DMAG in comparison with 17-AAG; however, above 10 mg/kg 17-DMAG has been described to be toxic in mice [33]. It has also been demonstrated that i.p. 17-DMAG administration leads to a better bioavailability than the oral route [24]. In our dose–response study using three i.p. injections per week on alternate days, with 17-DMAG at 5, 10 or 25 mg/kg, we observed that, 12 hours post-last injection, only with the dose of 25 mg/kg was the expression of Hsp-70 significantly induced in the brain, this dosage being thus selected for the chronic therapeutic study (Supplementary Fig. 4). With systemic administration of this dosage, the concentration of 17-DMAG in the brain 1 hour after treatment was 42 ng/g (drug quantity/brain weight) with a plasma/brain ration of 0,2.

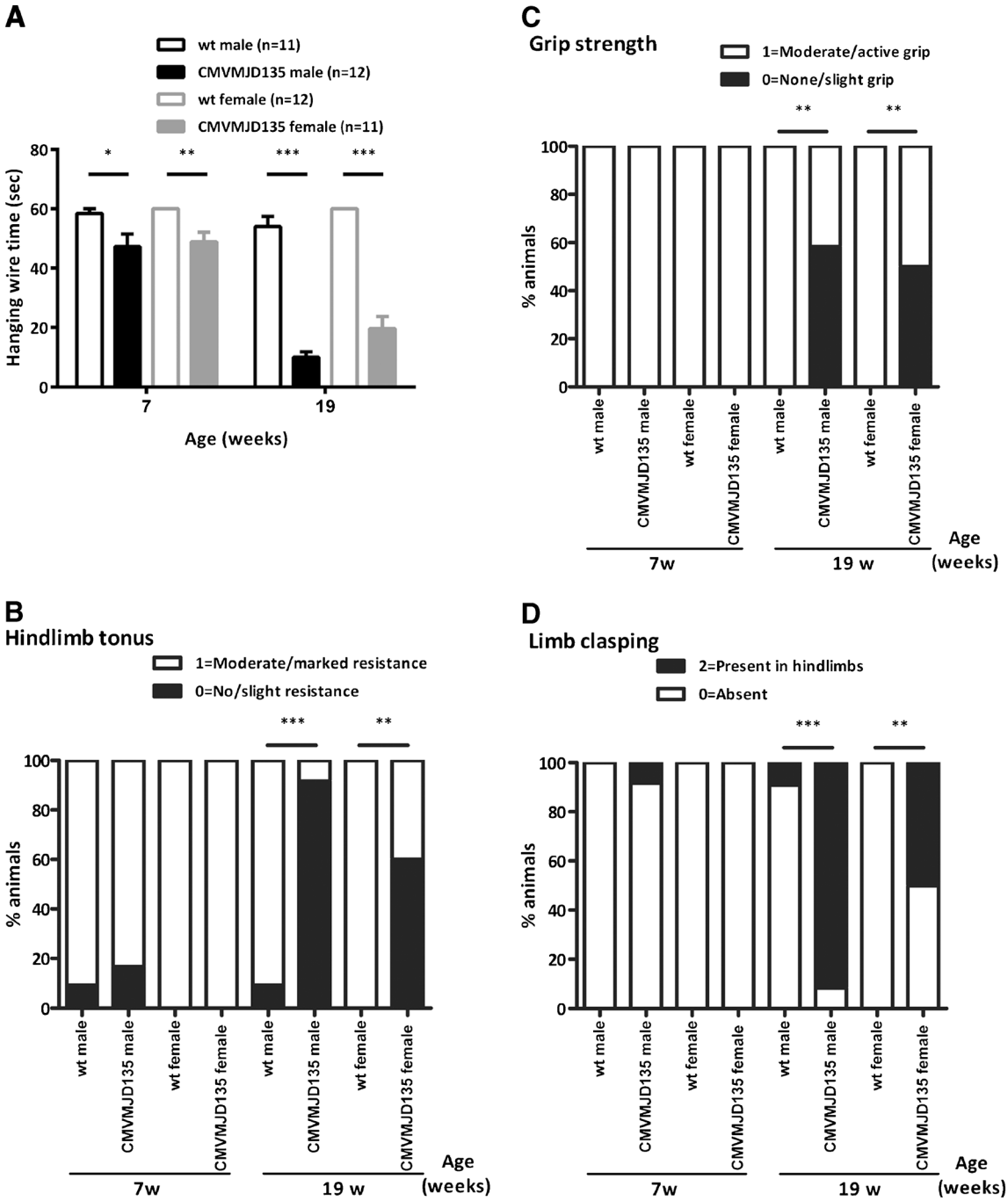

Fig. 5 Phenotype of CMVMJD135 mice detected in the SHIRPA protocol. (A) Strength and fine motor coordination evaluation in the hanging wire grip test, measured by the latency to fall off the grid. Values are presented as mean ± SEM (n=11–12 for each group). (B) At 19 weeks of age animals demonstrated hindlimb tonus alterations, (C) a decrease in forelimb grip strength and (D) a higher percentage of animals displaying clasping of the hindlimbs when compared to controls. Values are presented as percentage of animals with different scores in the SHIRPA protocol (n=11–12 for each group). *p<0.05, **p<0.01, ***p<0.001

In the therapeutic assay, we used four groups of animals: 17-DMAG- and vehicle-treated wt (n=10; n=10, respectively) and CMVMJD135 animals (n=10; n=12, respectively). In the motor swimming test, 17-DMAG treatment had a highly beneficial effect, being able to improve the phenotype of the transgenic animals almost to the performance level of wt animals at 16, 22 and 24 weeks of age (genotype x treatment, $F_{1,38}$=19.912, p=0.00007); this effect was lost at 30 weeks of age (Fig. 7A). 17-DMAG treatment also had a positive effect in the rotarod performance of CMVMJD135 animals, which was comparable to that of wt animals at 22 weeks of age (15 rpm: genotype x treatment, $F_{1,33}$=6.378, p=0.017); this

A

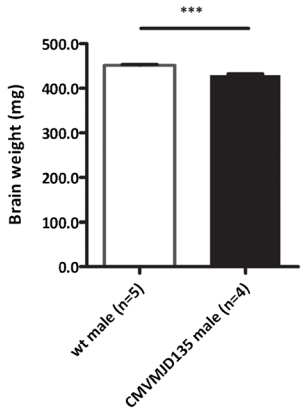

B

Genotype (n)	Brain region	Mean of total volume (μm^3) E+08 ± SD E+07	Mean of total cell number (±SD) E+04 ± SD E+03
wild-type (5)	Pontine nuclei	6,47 ± 0,752	33,5 ± 41,3
CMVMJD135 (9)		**5,63 ± 4,15***	**29,3 ± 24,0***
wild-type (4)	Dentate nuclei	1,45 ± 2,56	7,25 ± 3,94
CMVMJD135 (4)		**0,920 ± 1,01***	6,11 ± 8,81
wild-type (5)	Locus coeruleus	0,294 ± 0,569	2,49 ± 6,67
CMVMJD135 (5)		0,255 ± 0,496	2,09 ± 5,37
wild-type (5)	Substantia nigra	9,75 ± 12,1	40,4 ± 82,7
CMVMJD135 (5)		9,14 ± 16,7	39,9 ± 65,2

C

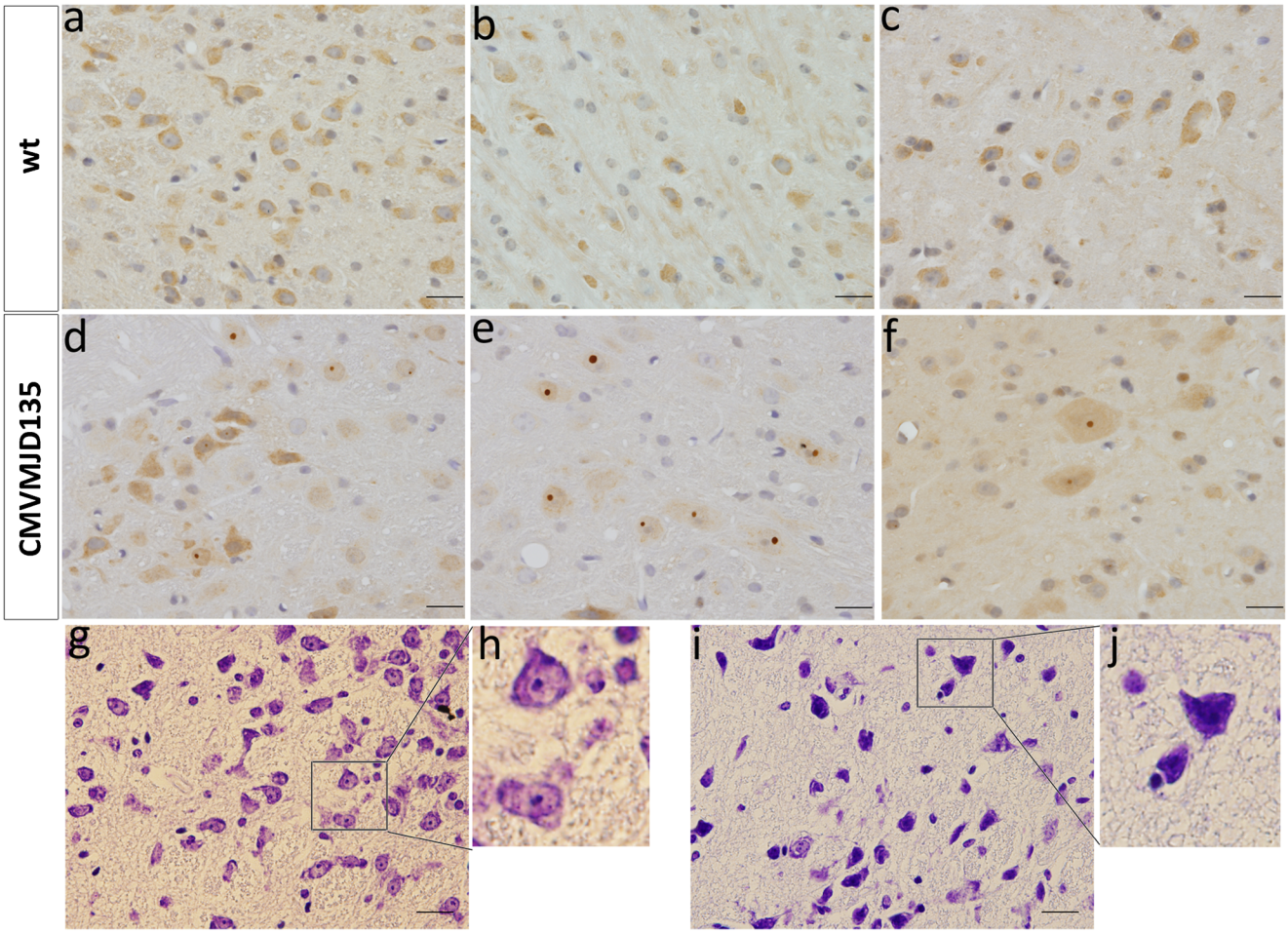

Fig. 6 Neuropathology of CMVMJD135 mice. (A) Brain weight analysis at 42–43 weeks of age of wt (n=5) and CMVMJD135 male mice (n=4). (B) Volume and total cell number quantification in different brain regions of transgenic (n=9) and control (n=5) male animals using stereological methods. (C) Anti-ataxin-3 immunohistochemistry (rabbit anti-MJD1.1) of wt (a-c) and CMVMJD135 mice (d-f) at approximately 20–35 weeks of age. CMVMJD135 mice exhibited nuclear and cytoplasmic inclusions positive for ataxin-3 in different regions of the CNS, namely, pontine nuclei (d), reticulotegmetal nucleus of pons (e) and spinal cord neurons (f); Cresyl violet brain sections in the pontine nuclei of wt (g) and in CMVMJD135 (i) mice. Higher magnification of neuronal cells in the wt (h) and transgenic mice (j). Images are representative of the results obtained for six animals per genotype, three each female and male. Scale bar: 20 μm

effect was no longer statistically significant at 24 and 30 weeks of age (Fig. 7B). At 22 and 24 weeks of age 17-DMAG-treated CMVMJD135 mice had a better performance in the balance beam test (Fig. 7C; Medium square 24 weeks—genotype: $F_{1,37}$=6.228, p=0.017; treatment: $F_{1,37}$=6.903, p=0.012. Small circle 22 weeks—genotype: $F_{1,37}$=7.45, p=0.01;

treatment: $F_{1,37}$=10.385, p=0.003. Small circle 24weeks—genotype: $F_{1,36}$=8.50, p=0.006; treatment: $F_{1,36}$=7.346, p=0.01), which was not maintained at 30 weeks of age, suggesting that 17-DMAG treatment is delaying the manifestation of loss of balance in these animals. Moreover, 17-DMAG was able to delay the onset and progression of the foot-dragging phenotype, since at any age the percentage of CMVMJD135 animals treated with 17-DMAG showing foot-dragging was less than in those not receiving treatment (p<0.05) (Fig. 7D). In summary, 17-DMAG chronic treatment was able to delay the motor deficits in the rotarod, motor swimming and balance beam test by approximately 8 weeks, which represents approximately 9 % of the median C57Bl/6 normal lifespan [34] (600 days), and to a lesser extent the foot-dragging (6 weeks, 7 % of the lifespan).

17-DMAG treatment failed to ameliorate other manifestations of the disease evaluated in the SHIRPA protocol, namely, those more related to weakness/hypotonia (hanging wire, hindlimb tonus), tremors and abnormal reflexes (limb clasping). Although we did not detect any improvement in the hanging wire test, in the total number of rears and body weight, the sample size we used (n=10–12) would be sufficient to detect an improvement of 50 % at several time points (see Supplementary Table). For the number of squares travelled in the arena, the required sample size for the observed mean difference to be significant would be much larger than the one we used (see Supplementary Table).

17-DMAG Treatment Reduces Neuropathology in the CNS of CMVMJD135 Mice

Transgenic vehicle-treated animals demonstrated the presence of shrunken and morphologically abnormal cells in the pontine nuclei. In contrast, 17-DMAG treated animals showed normal cell morphology, shrunken cells being almost undetectable in this brain region at 30 and 16 weeks of age (Supplementary Fig. 5). Quantification of the ataxin-3 nuclear inclusions present in the pontine nuclei of CMVMJD135 mice revealed a significant reduction of the number of cells containing these inclusions, also reflected in a reduced number of inclusions per area, in 17-DMAG-treated transgenic animals when compared to vehicle-treated ones (p=0.009) (Fig. 8A).

Mutant Ataxin-3 Levels are Reduced Through Autophagy in 17-DMAG-Treated CMVMJD135 Mice

No differences were found in ataxin-3 expression at mRNA level in the brainstem between the treatment groups, which allow us to conclude that 17-DMAG treatment is not affecting expression of ataxin-3 at the transcription level (Fig. 8B). Interestingly, however, the protein levels of mutant human ataxin-3 in the brainstem were dramatically reduced in 17-DMAG-treated animals at 16 (p=0.033) and 30 weeks of age (p=0.019), suggesting that this treatment is promoting mutant ataxin-3 degradation rather than refolding (Fig. 8C).

In an attempt to dissect the mechanism of action of the drug we analysed the levels of molecular chaperones in treated animals. Unexpectedly, at 20 weeks, mRNA expression levels of molecular chaperones Hsp-70 and −40 were not significantly increased upon 17-DMAG treatment in transgenic mice, while there was a trend towards increase in the controls (Fig. 9A). Hsp70 quantification in the forebrain at 16 and 30 weeks of age in CMVMJD135 mice demonstrated that chronic treatment with 17-DMAG led to a statistically non-significant trend towards increase in Hsp70 expression in this brain region in transgenic mice at 16 weeks of age, whereas at 30 weeks the opposite trend was present (Fig. 9B). These results suggest that HSR induction by chronic administration of 17-DMAG at 25 mg/kg may be compromised in the disease state, particularly at later stages. Since it was previously shown that 17-AAG and its analogue 17-DMAG are able to activate macroautophagy in different model systems [35–37], we also assessed activation of this pathway. We observed an increase in the beclin-1 protein levels in the brainstem of 16- and 30-week-old mice and of the LC3-II/LC3-I ratio at 30 weeks of age, after chronic 17-DMAG treatment (p=0.008, p=0.017, respectively) in transgenic mice but not in controls, confirming the specificity of this activation (Fig. 9C,D).

Discussion

The pathogenic mechanism of MJD, as well as of other polyQ disorders, is not well understood, and these disorders remain incurable to date. In this work, we have generated a new transgenic mouse model expressing at near the same cDNA variant of ataxin- 3 as in our previous CMVMJD94 model, ATXN3c- which corresponds to the most predominant variant of the protein in the brain [38], but with an increased number of glutamine residues (135Q). Moreover, we tested a potent Hsp90 inhibitor, 17-DMAG, that was able to improve the motor phenotype and the neuropathological features of CMVMJD135 mice.

Our results show that the CMVMJD135 mouse is a powerful model for pre-clinical trials in MJD. The behavioral evaluation of CMVMJD135 mice revealed the presence of several phenotypic abnormalities that gradually appear and progress during a lifespan of over one and a half years, namely, balance and motor coordination deficits, loss of limb strength, decreased locomotor and exploratory activity, abnormal gait and tremors, with many parameters assessable by objective tests. The first sign of neurological disease in the CMVMJD135 model was the presence of balance and grip abnormalities at 6 weeks of age. Cerebellar ataxia is one of the first clinical manifestations seen in MJD patients, and is due to unsteadiness or impaired balance. Although behavioral

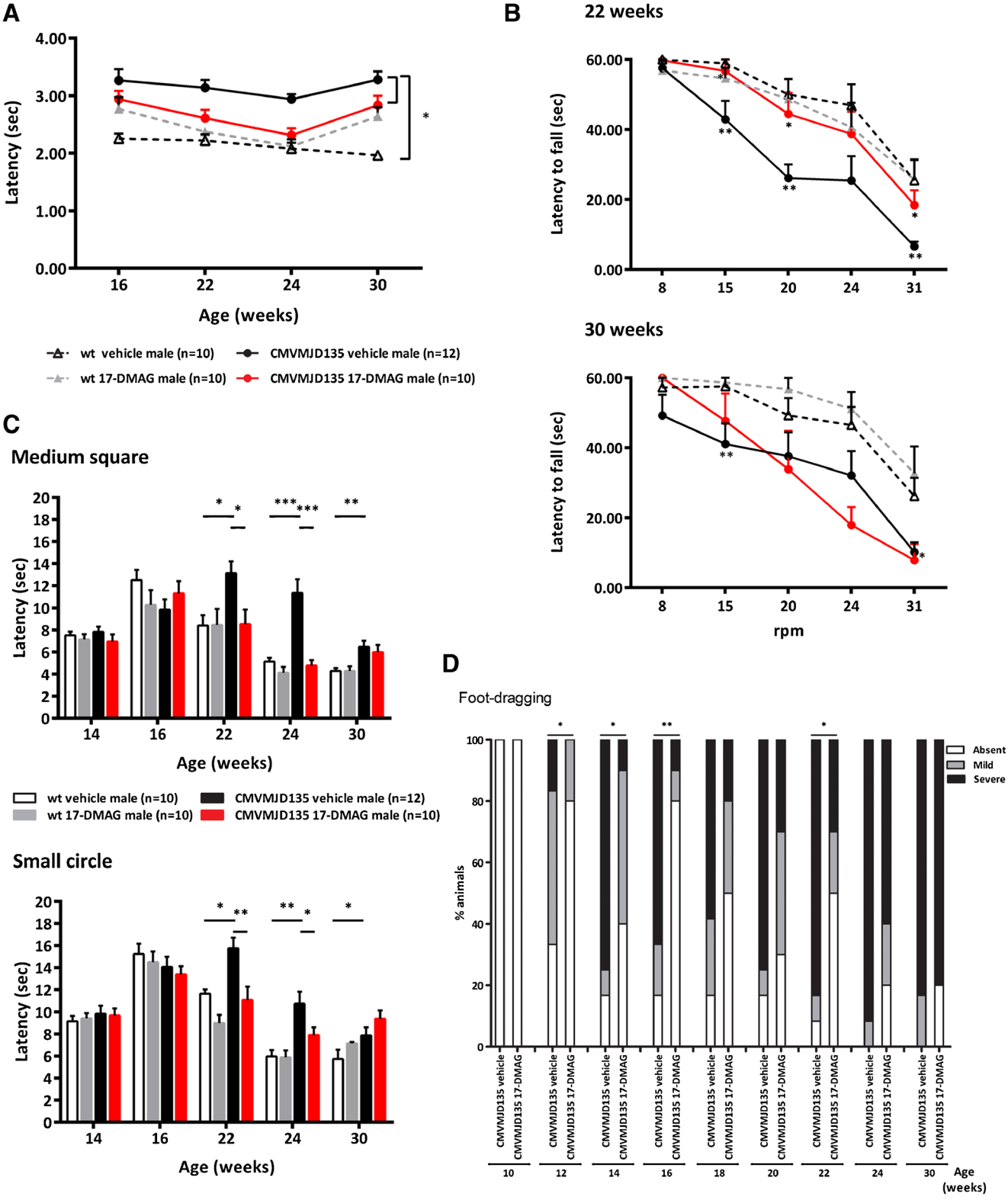

alterations suggestive of loss of coordination in CMVMJD135 mice were observed at 4 and 8 weeks of age, at these ages animals were indistinguishable from their wt littermates by simple observation in their home cage. At 16 weeks of age, however, signs of neurological abnormality were already observable in CMVMJD135 mice in their home cage, in particular a clearly abnormal gait. The footprinting pattern evaluation of CMVMJD135 mice clearly demonstrated foot-

◀ **Fig. 7** 17-DMAG improves motor coordination of CMVMJD135 mice. (A) Motor swimming test was performed at 16, 22, 24 and 30 weeks of age (n=10–12 animals for each tested group) and the mean latency of the third day test was analyzed. Transgenic mice displayed swimming impairments, given by a significant increase in the time spent to swim across 60 cm distance, and 17-DMAG treatment improved their performance. (B) Rotarod test was performed at 22 and 30 weeks of age (n=10–12 for each tested group) to evaluate motor coordination at constant speed in the rod (8, 15, 20, 24 and 31 rpm). 17-DMAG treatment was able to rescue this phenotype at 22 weeks of age. (C) Balance beam test was performed at 14, 16, 22, 24 and 30 weeks of age (n=10–12 for each tested group. 17-DMAG treatment significantly improved balance deficits at 22 and 24 weeks of age. Values are presented as mean ± SEM. (D) Quantitative analysis of the percentage of animals showing foot-dragging. 17-DMAG treatment delays the onset and progression of this symptom. *p<0.05, **p<0.01, ***p<0.001

dragging and, at later stages of the disease, a shortened step length and a decrease in the hind/ frontlimb overlap. Transgenic animals also showed a significant deficit in the accelerating rod at 20 weeks of age, which was further aggravated at 40 weeks of age, in the constant and accelerating rod. In the motor swimming test, the abnormal posture and inappropriate kicking movements exhibited by CMVMJD135 contrasted markedly with the coordinated synchronized paddling movements shown by wt mice.

The analysis of CAG repeat number through the generations of CMVMJD135 mice revealed that CAG tract length varied in approximately 54–79 % of the transmissions, frequently towards contractions. The genescan profile of the CAG tract obtained from mouse tail revealed that somatic mosaicism was also present. Thus, our new model seems to replicate this feature of the human disease as well.

The histological evaluation of CMVMJD135 mouse brains frequently revealed abnormal cell morphology in the pontine nuclei as well as gliosis in the substantia nigra at clearly symptomatic ages (24 weeks of age). The stereological analysis of pontine nuclei of CMVMJD135 brain at late stages (60 weeks of age) revealed a reduced volume and total cell number in this region and reduced volume in the dentate nuclei, two regions of high involvement in human patients. Moreover, we observed a total brain weight decrease, but only at late stages of the disease (42–43 weeks of age), which supports the hypothesis that major cell loss only occurs at these advanced stages. These results suggest that the early motor phenotype observed in our model is mostly attributable to dysfunction of the brain regions affected in MJD, clearly preceding neuronal cell death. In order to validate this hypothesis, it will be necessary to perform a longitudinal neuropathology analysis of the brain regions affected in MJD, to

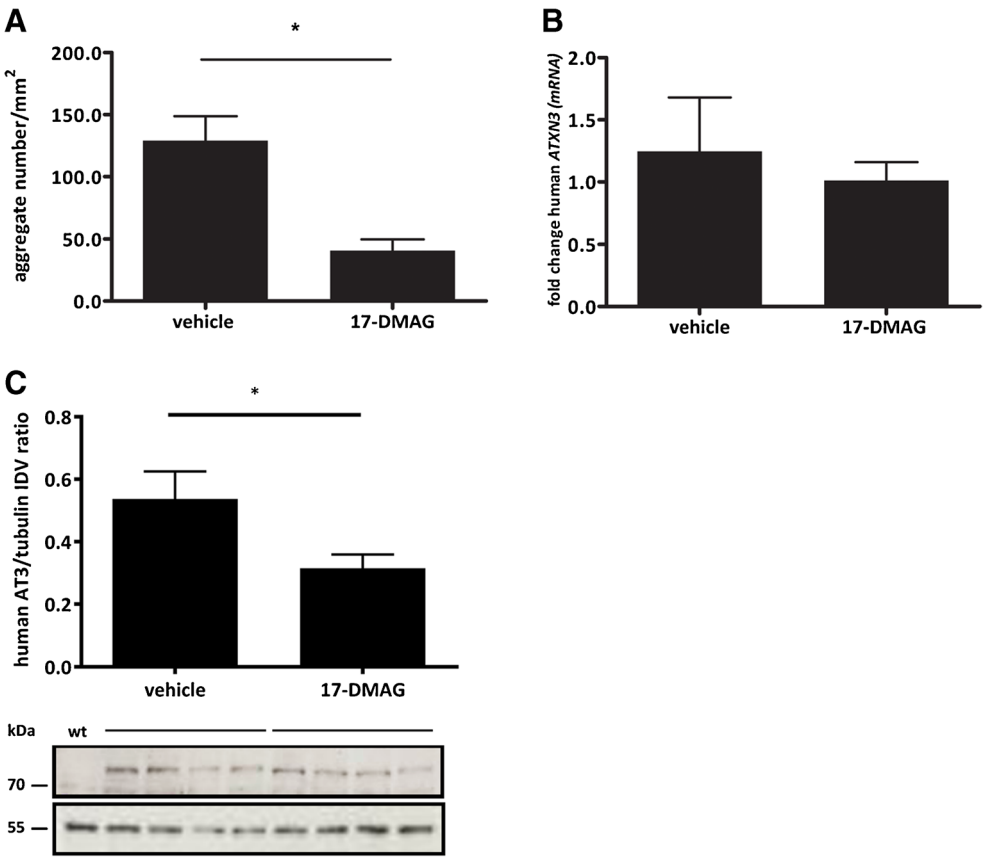

Fig. 8 17-DMAG treatment reduced the levels of human ataxin-3 and the aggregate load in CMVMJD135 mice brain. (A) Neuronal inclusions were counted in the pontine nuclei of 30-week-old animals treated with vehicle or 17-DMAG (n=3 for each condition). Four slides of each animal were used for the analysis. (B) qRT-PCR analysis of human ATXN3 mRNA expression levels (n=4). (C) Anti-ataxin-3 western-blot (rabbit anti-MJD1.1) of 30-week-old CMVMJD135 mice, either vehicle or treated with 17-DMAG (n=4 for each condition), were performed in the brainstem. Mutant human ataxin-3 has a molecular weight of approximately 80 kDa. Values are presented as mean ± SEM; *p<0.05, **p<0.01, ***p<0.001

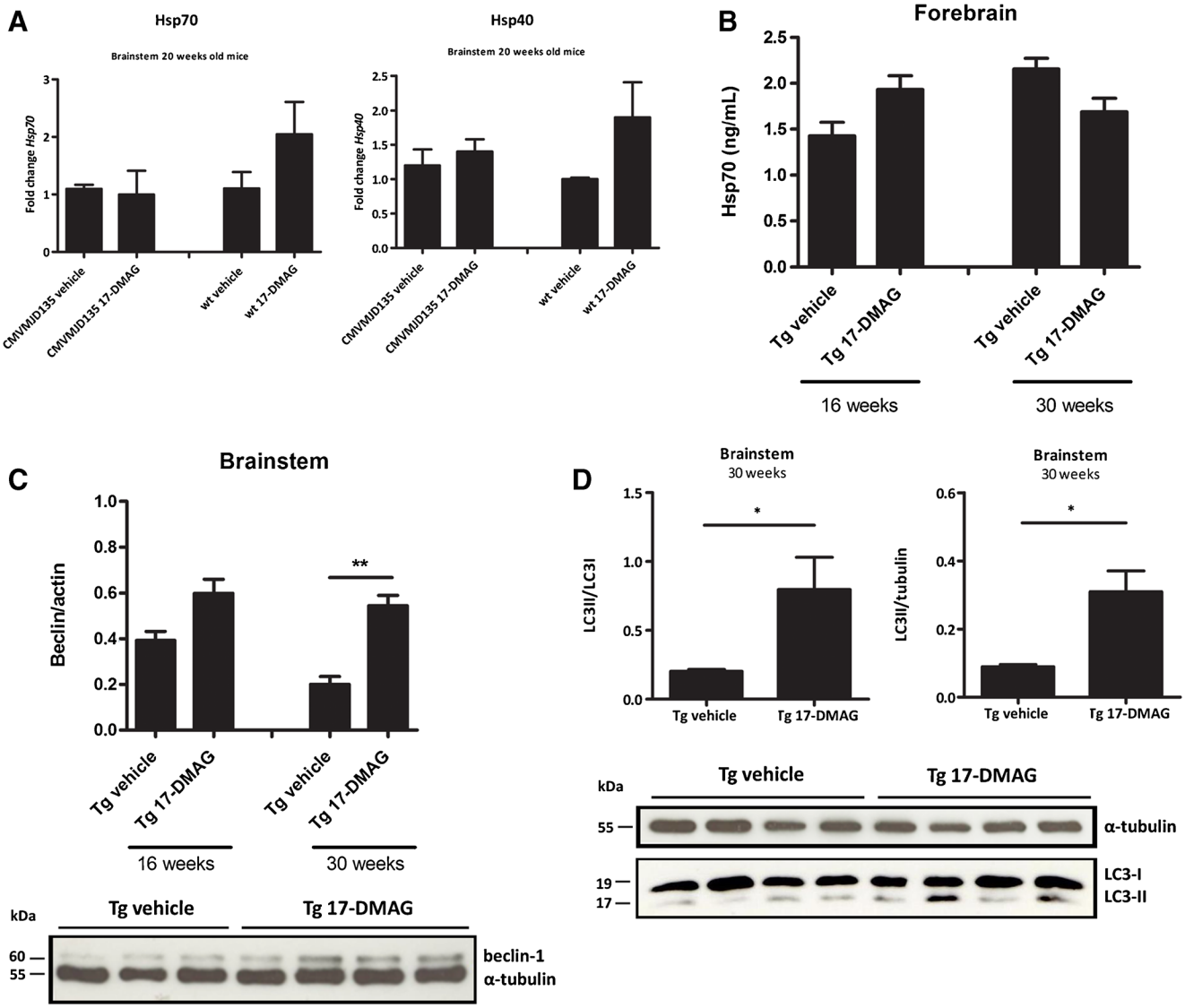

Fig. 9 17-DMAG is able to induce autophagy in CMVMJD135 animals. ELISA assays, western blots and qRT-PCR analysis of HSR and autophagy markers were performed in the brainstem or forebrain of 16-, 20- or 30-week-old wt and CMVMJD135 mice (n=4–5) treated with vehicle or 17-DMAG (25 mg/kg), 12 hours after the last treatment. (A) *Hsp70*, *Hsp40* mRNA expression levels were normalized for the housekeeping gene *HPRT*. (B) ELISA assay for Hsp70 quantification. Anti- Beclin-1 (C) and anti-LC3 (D) western-blots. LC3-II was normalized both for tubulin and LC3-I; Beclin-1 was normalized for tubulin. Values are presented as mean ± SEM; *p<0.05, **p<0.01, ***p<0.001

establish correlations between the phenotype here defined and the neurodegeneration pattern.

An important feature of MJD, as well as of other polyQ diseases, is the presence of neuronal inclusions containing the mutant protein. Our previous results have shown the presence of motor symptoms in a transgenic mouse model of MJD in the absence of intranuclear inclusions, suggesting that these are not essential for disease manifestation [31]. However, the nature and relevance of intermediate species of the aggregation process remains to be elucidated in this disorder. In this new transgenic mouse, intranuclear inclusions were present in the cells of affected brain regions, such as the pontine and deep cerebellar nuclei, but also in regions that are spared, such as the anterior olfactory nuclei and ventral tenia tecta. This is concordant with what is seen in human MJD patients, where neurodegeneration was not clearly correlated with the occurrence of ataxin-3 immunopositive inclusions [39]. Moreover, neuronal inclusions were observed already at 20 but not at 16 weeks of age, when several motor symptoms were already clearly present. This is in agreement with previous results obtained in other transgenic mouse models of MJD, in which symptoms appear before the detection of the inclusions [40].

Although the role of intranuclear inclusions, the end-product of the aggregation process in MJD pathogenesis, remains to be clarified, the presence of this pathological hallmark of disease in our model indicates that it successfully replicates the full aggregation process that happens in humans. The combination of clinical and neuropathologic features of

CMVMJD135 mice prompted us to start pre-clinical trials using different compounds, targeting different potential pathogenic mechanisms for MJD.

The chaperone machinery has the potential to neutralize the toxicity caused by misfolded and aggregated proteins, making the activation of molecular chaperones an attractive therapeutic strategy [21, 41]. Treatment of CMVMJD135 mice with 17-DMAG markedly improved motor performance, given by the results in the motor swimming, rotarod and beam balance tests, reduced the expression levels of human ataxin-3 at protein level and reduced the nuclear aggregate load in the pontine nuclei. Regarding neuropathology, 17-DMAG also led to a visible amelioration in cell morphology in affected brain areas, such as the pontine nuclei, at 16 and 30 weeks of age. Intriguingly, however, 17-DMAG had no beneficial effect in other neurological symptoms, for instance, limb weakness, tremor and abnormal reflexes, and the beneficial effects of 17-DMAG treatment were not maintained throughout disease progression. At 30 weeks of age, CMVMJD135 mice treated with 17-DMAG started to present MJD symptoms similar to those of mice treated with saline. Data from preclinical toxicity studies for 17-DMAG in animal models have recently become available [33], leading us to believe that it is possible to further increase 17-DMAG dose (higher than 25 mg/kg) while keeping outside its toxicity range; this should be tested in future studies.

In our study, and in spite of the therapeutic effects observed, the chronic administration of 17-DMAG failed to induce the HSR in CMVMJD135 mice, particularly at later stages of the disease. This is in agreement with what was recently described in a Huntington's disease mouse model treated with an Hsp90 inhibitor [42]. These authors tested the effectiveness of HSF-1 dissociation from the Hsp90 complex, its translocation to the nucleus and consequent hyperphosphorylation, features interfering with HSF-1 trimerization and its ability to induce HS gene expression [43], and concluded that all those processes were occurring normally upon treatment, suggesting that the problem was at the level of transcriptional activation of HSF1 targets due to excessive chromatin condensation. A similar phenomenon appears to be taking place in CMVMJD135 mice.

Since it was previously shown that 17-AAG and its analogue used in this study—17-DMAG—are able to activate the autophagy process in different model systems [35–37], and given that our results suggested degradation of ataxin-3 was occurring, we assessed known autophagy markers in 17-DMAG-treated animals. Our results suggest that autophagy is activated by the drug specifically in diseased animals. This is confirmed by an increase in the protein levels of Beclin-1 and LC3-II, detected only in 17-DMAG-treated CMVMJD135 mice. Although we could not observe an induction of HS genes at the age tested (20 and 30 weeks of age), this induction might still happen earlier in life, being no longer seen in later disease stages, when autophagy starts taking place as a compensatory mechanism. In addition to improving the major symptoms of disease, 17-DMAG reduced mutant protein levels and aggregate load in CMVMJD135 mice, which is a good additional proof of its beneficial effects. 17-DMAG is currently in Phase I of clinical trials for advanced solid tumors (www.clinicaltrials.gov), to test dosage, toxicity, pharmacokinetics and pharmacodynamics. So far, the most frequently observed collateral effects of this compound were fatigue, nausea, diarrhea and headache [44]. Although the effects of continuous activation of HSF-1 are not well understood, and it was suggested to be detrimental in some situations [45], our data show that 17-DMAG is a promising compound and Hsp90 an interesting molecular target for MJD therapy. There is a need to better understand the impairment of the HSR during aging in mice (since this study is not easy to perform in humans) which will help in the development of new drugs that can act synergistically with 17-DMAG in the improvement of proteostasis.

Materials and Methods

Generation of Transgenic Mice, Breeding, Genotyping, CAG Repeat Sizing and Mouse Maintenance

To generate transgenic MJD mice, we converted the ATXN3a cDNA variant carrying a repeat tract ($(CAG)_2CAAAAGCAGCAA(CAG)_{124}$), coding for 130 glutamines (plasmid pF25B3.3::AT3Q130::YFP) in the ATXN3c variant [18] into the pCMV vector (Fig. 1A). This plasmid, designated pCMVAT3Q135_1.5, was linearized by total digestion with PaeI (Fermentas), the fragment of interest (3150 bp) was then purified from an agarose gel using the QiaQuick gel extraction system (Qiagen, Hamburg, Germany) and microinjected into fertilized murine oocytes of the C57Bl/6 mouse strain (QTRN, Canada). To establish the lineage CMVMJD135, founder C was bred with C57Bl/6 females and the hemizygous progeny were bred with littermate wt animals to generate the experimental groups. DNA extraction, animal genotyping, transgene copy number and CAG repeat size analyses were performed as previously described [31].

All animal procedures were conducted in accordance with European regulations (European Union Directive 86/609/EEC). The animals were anesthetized with a mixture of ketamine hydrochloride (150 mg/kg) plus medetomidine (0.3 mg/kg). Animal facilities and the people directly involved in animal experiments (ASF, SDS, ANC) were certified by the Portuguese regulatory entity — Direcção Geral de Veterinária. All of the protocols performed were approved by the joint Animal Ethics Committee of the Life and Health Sciences Research Institute, University of Minho, and the Institute for

Molecular and Cell Biology, University of Porto. Health monitoring was performed according to FELASA guidelines [46], confirming the Specified Pathogen Free health status of sentinel animals maintained in the same animal room.

Behavioral Analysis

CMVMJD135 phenotypic characterization was performed during the diurnal period in groups of five animals per cage including CMVMJD135 hemizygous transgenic mice and wt littermates (n=11–15 per genotype and gender). The mean repeat size (±SD) for all mice used was (133±1). Animals were evaluated monthly in the rotarod [31] (beginning at 4 weeks of age until 40 weeks of age), by the modified SHIRPA protocol [31] (at 7, 19 and 40 weeks of age), using the balance beam test [47] (at 10 and 22 weeks of age) and the motor swimming test [47] (between 22–25 and 40 weeks of age). Rotarod tests and footprinting pattern were performed as previously described [31] as was the SHIRPA protocol, with the addition of the hanging wire grip test. To evaluate the severity of foot-dragging through age the footprinting patern of CMVMJD135 (n=10) and wt controls (n=7) was classified at each time point considering six consecutive steps (0=absent/mild, up to three steps; 1=moderate, more than three steps out of six; 2=severe, all steps out of six).

Hanging Wire Grip Test Each mouse was placed on a wire cage top, which was slowly inverted and suspended at approximately 30 cm to the floor. The time it took each mouse to fall from the cage top was recorded. Any mouse still gripping the cage top after 60 seconds was removed.

Balance Beam Test Motor coordination and balance of mice were assessed by measuring the ability of the mice to traverse a graded series of narrow beams to reach an enclosed safety platform as previously described [47]. The beams consisted of long strips of PVC (1 m) with a 27- and 11-square cross-section or a 28-, 15-, or 10-mm round diameter. During training, mice were placed at the start of the 11-mm square beam and trained over 3 days (3 trials per day) to traverse the beam to the safe platform.

Motor swimming test [47] and Morris water maze were performed as previously described [48, 49].

Western Blot

Protein isolation from mouse tissues and western blot were performed as previously described [31] homogenized in cold RIPA buffer and a mixture of protease inhibitors (Complete; Roche). The blots were blocked overnight at 4 °C with the primary Ab: rabbit anti-ataxin-3 serum (kindly provided by Dr. Henry Paulson) (1:10000); mouse anti-Hsp70 (1:2000 StressGene), rabbit anti-LC3 (1:500 Cell Signaling), rabbit anti-Beclin1 (1:1000 Cell signaling) and mouse anti-alpha-tubulin (1:100, DSHB). Band quantification was performed using ImageJ software according to the manufacturer's instructions using alpha-tubulin as the loading control.

qRTPCR

Total RNA was isolated from CMVMJD135 mice tissues using TRIZOL (Invitrogen, Calrsbad, CA, USA) according to the manufacturer's protocol. First-strand cDNA, synthesized using oligo-dT (Bio-rad), was amplified by quantitative reverse-transcriptase PCR (qRT-PCR) as previously described [31]. Human and mouse ataxin-3 primers were used for transgene expression quantification [31]: HSP40 (F: 5'CGCCGG ACGGGTATATAGAG3'; R: 5'GGCCCAGCGTCTGATA GTAG3'), HSP70 (F: 5'CCAACGCTGTCACTCAAACC 3'; R: 5'GCCCTTGTCCAGAACTCTCC3') and LC3 (F: 5'TTCTTCCTCCTGGTGAATGG3'; R: 5'GTGGGTGCCT ACGTTCTCAT3').

Neuropathology and Immunohistochemistry

Transgenic and wt littermate mice were deeply anesthetized and transcardially perfused with PBS followed by 4 % paraformaldehyde (PFA) in PBS. Brains were postfixed overnight in fixative solution and embedded in paraffin. Slides with 4-μm-thick paraffin sections were stained with cresyl violet or processed for immunohistochemistry with rabbit GFAP Ab (DAKO Corporation, Carpinteria, CA) (1:500) or rabbit anti-MJD1.1 [50] (1:40) or anti-ubiquitin (1:500) [31]. Ataxin-3 positive inclusions in the pontine nuclei of 30 weeks old animals either vehicle or 17-DMAG treated (n=3–4 for each condition, three slides per animal) were quantified and normalized for total area using the Olympus BX 51 stereological microscope and the Visiopharma integrator system software.

Stereological Analysis Neuronal number and volume were obtained by systematic random sampling in pontine nuclei from Bregma level −3.80 mm through 4.60 mm; substantia nigra from Bregma level −2.46 mm through 4.04 mm; locus coeruleus from Bregma level −5.34 mm through 5.80 mm and dentate nuclei from Bregma level −5.68 mm thourh 6.36, according to the Paxinos and Franklin mouse brain atlas of 2001. Every second section containing the region of interest was selected to obtain a sample in a systematic uniform and random manner (section sampling fraction; ssf = 0.5). Volume estimation was obtained according to Cavalieri's principle [51]. Each known area was multiplied by the represented thickness (30 μm x 2 sections). Average cell numbers were estimated using the optical fractionator method [52]. The area (a) of the counting frame was 400 μm^2 (20 μm x 20 μm), the area sampling fraction (asf) = a (frame)/ a (step length) was

0.004. The height (h: 15 μm) of the optical dissector was equivalent to the thickness of the section (t: 30 μm).

The measurements were performed using The Visiopharm Integrator System, version 2.12.3.0 and a camera (Pixelink PL-A622) attached to a motorized microscope (Olympus BX51).

17-DMAG Dose Determination

Wt animals were injected with 17-DMAG (InvivoGen) at different concentrations (5, 10 and 25 mg/kg, n=4 per dose) three times per week on alternate days, and 12 hours after the last injection the animals were sacrificed. Another set of animals (n=4) was injected with vehicle (saline NaCl 0,9 %) and sacrificed at the same time. The protein levels of Hsp70 were measured by western blot in the muscle and in the brain.

Determination of Blood/Plasma Ratio to Estimate 17-DMAG brain exposure

A total of six C57Bl/6 mice at approximately 6 months of age were used, in which two were injected intraperitoneally three times in a week with saline—0.9 % NaCl and four animals with 17-DMAG 25 mg/kg. Animals were anesthetized 1 hour post-injection and the blood was removed from the inferior vena cava, and after perfusion with PBS brains were dissected, weighted and immediately frozen at −80ºC. Brain tissue was homogenized in acetonitrile:H_20 (4:1 v/v). After centrifugation, plasma and brain supernatants were harvested and samples were frozen at −80 °C until bioanalysis. Brain and plasma samples were analysed for content of drug by use of UltraPerformance LC® (UPLC®) chromatography followed by tandem-MS (MS/MS) detection.

Hsp70 ELISA Assay

An Hsp70 ELISA kit (ADI-EKS-700B from ENZO life sciences, UK) was used to measure the Hsp70 concentration in brain tissue from mice. The analysis was carried out according to the manufacturer's instructions. Briefly, forebrain tissue protein extracts were obtained as described above and extraction reagent (ELISA kit) with phosphostop and protease inhibitor cocktail was added. The homogenate was spinned down at 20,000 g for 10 min and the supernantant was kept at −80 °C until analysis. The protein concentration was determined using a standard BCA Protein assay (Thermo scientific, Denmark), and upon ELISA analysis, 100 μg of protein was analysed per well according to the standard protocol. The developed plates were measured with a Spectramax 340PC (Molecular Devices Inc., USA) at 450 nm (reference 540 nm). Hsp70 concentration was calculated based on the standard curve and expressed as ng of Hsp70 per ml.

17-DMAG Treatment and Behavioral Assessment

CMVMJD135 and littermate mice (n=10−12 for each group) were intraperitoneally injected three times a week since 5 weeks of age (one week before the onset of symptoms) with 17-DMAG at 25 mg/kg (for a mean mouse weight of 25 g) or with a 0.9 % saline solution. The animals were evaluated every two weeks in the balance beam test and using the SHIRPA protocol since 6 weeks of age. Foot-dragging was evaluated as described above and at the age of 16, 22, 24 and 30 weeks the animals were also tested in the rotarod and in the motor swimming test. Behavior analysis methods were described above.

Statistical Analysis

Power analysis was used to determine the sample size [53]. Considering the different variables under study, such as weight, time held in the hanging wire, rotarod and swimming latency, assuming a power of 0.8 and a significance level of 0.05, different required sample sizes were obtained, depending on the specified smallest detectable difference and the variability within the four populations under study (wt vehicle, wt 17-DMAG, tg vehicle and tg 17-DMAG). Based on these calculations and bearing in mind that as the age of the animals increases also the mean differences increase and, possibly, the standard deviations, a sample size ranging between five and ten animals was obtained and, therefore, a sample of ten animals was chosen. Sample size calculations of each behavioral test were also assessed assuming a power of 0.8 and a significance level of 0.05 (Supplementary Table). The effect size was calculated taking into account an improvement of 50 %, using mean and standard deviation values previously obtained for transgenic and control groups for the different behavioral tests.

Behavioral data were analyzed by the non-parametric Mann–Whitney U-test when variables were non-continuous or when a continuous variable did not present a normal distribution (Kolmogorov-Smirnov (K-S) test $p<0.05$). Continuous variables with normal distributions (K-S test $p>0.05$) were analyzed with the Student's t-test and two-way ANOVA (factors: genotype and age for basal behavioral characterization of the CMVMJD135 mice; factors: genotype and treatment in the 17-DMAG preclinical trial). For the motor swimming test, repeated-measures ANOVA was performed considering two factors: genotype and treatment. All statistical analyses were performed using SPSS 22.0 (SPSS Inc., Chicago, IL). A critical value for significance of two-tailed $p<0.05$ was used throughout the study.

Acknowledgements We would like to thank to Dr. Henry Paulson for providing the anti-ataxin-3 serum, Dr. Mónica Sousa for the pCMV vector and to Eng. Lucília Goreti Pinto, Luís Martins, Miguel Carneiro and Celina Barros for technical assistance. This work was supported by Fundação para a Ciência e Tecnologia through the projects FEDER/FCT, POCI/SAU-MMO/60412/2004 and PTDC/SAU-GMG/64076/2006.

This work was supported by Fundação para a Ciência e Tecnologia through fellowships SFRH/BPD/91562/2012 to A.S-F., SFRH/BD/78388/2011 to S.D-S., SFRH/BD/51059/2010 to A.N-C., and SFRH/BPD/79469/2011 to A.T-C..

References

1. Maciel P, Costa MC, Ferro A, Rousseau M, Santos CS, Gaspar C et al. Improvement in the molecular diagnosis of Machado-Joseph disease. Arch Neurol. 2001;58(11):1821–7.
2. Coutinho P, Andrade C. Autosomal dominant system degeneration in Portuguese families of the Azores Islands. A new genetic disorder involving cerebellar, pyramidal, extrapyramidal and spinal cord motor functions. Neurology. 1978;28(7):703–9.
3. Seidel K, den Dunnen WF, Schultz C, Paulson H, Frank S, de Vos RA et al. Axonal inclusions in spinocerebellar ataxia type 3. Acta Neuropathol. 2010;120(4):449–60.
4. Paulson HL, Perez MK, Trottier Y, Trojanowski JQ, Subramony SH, Das SS et al. Intranuclear inclusions of expanded polyglutamine protein in spinocerebellar ataxia type 3. Neuron. 1997;19(2):333–44.
5. Huang S, Ling JJ, Yang S, Li XJ, Li S. Neuronal expression of TATA box-binding protein containing expanded polyglutamine in knock-in mice reduces chaperone protein response by impairing the function of nuclear factor-Y transcription factor. Brain. 2011;134(Pt 7):1943–58.
6. Zijlstra MP, Rujano MA, Van Waarde MA, Vis E, Brunt ER, Kampinga HH. Levels of DNAJB family members (HSP40) correlate with disease onset in patients with spinocerebellar ataxia type 3. Eur J Neurosci. 2010;32(5):760–70.
7. Chai Y, Koppenhafer SL, Bonini NM, Paulson HL. Analysis of the role of heat shock protein (Hsp) molecular chaperones in polyglutamine disease. J Neurosci. 1999;19(23):10338–47.
8. Williams AJ, Knutson TM, Colomer Gould VF, Paulson HL. In vivo suppression of polyglutamine neurotoxicity by C-terminus of Hsp70-interacting protein (CHIP) supports an aggregation model of pathogenesis. Neurobiol Dis. 2009;33(3):342–53.
9. Yoshida H, Yoshizawa T, Shibasaki F, Shoji S, Kanazawa I. Chemical chaperones reduce aggregate formation and cell death caused by the truncated Machado-Joseph disease gene product with an expanded polyglutamine stretch. Neurobiol Dis. 2002;10(2):88–99.
10. Warrick JM, Chan HY, Gray-Board GL, Chai Y, Paulson HL, Bonini NM. Suppression of polyglutamine-mediated neurodegeneration in Drosophila by the molecular chaperone HSP70. Nat Genet. 1999;23(4):425–8.
11. Kaushik S, Cuervo AM. Chaperones in autophagy. Pharmacol Res. 2012;66(6):484–93.
12. Lamark T, Johansen T. Aggrephagy: selective disposal of protein aggregates by macroautophagy. Int J Cell Biol. 2012;2012:736905.
13. Zou J, Guo Y, Guettouche T, Smith DF, Voellmy R. Repression of heat shock transcription factor HSF1 activation by HSP90 (HSP90 complex) that forms a stress-sensitive complex with HSF1. Cell. 1998;94(4):471–80
14. Kim HR, Kang HS, Kim HD. Geldanamycin induces heat shock protein expression through activation of HSF1 in K562 erythroleukemic cells. IUBMB Life. 1999;48(4):429–33.
15. Hay DG, Sathasivam K, Tobaben S, Stahl B, Marber M, Mestril R et al. Progressive decrease in chaperone protein levels in a mouse model of Huntington's disease and induction of stress proteins as a therapeutic approach. Hum Mol Genet. 2004;13(13):1389–405.
16. Sittler A, Lurz R, Lueder G, Priller J, Lehrach H, Hayer-Hartl MK et al. Geldanamycin activates a heat shock response and inhibits huntingtin aggregation in a cell culture model of Huntington's disease. Hum Mol Genet. 2001;10(12):1307–15.
17. Auluck PK, Meulener MC, Bonini NM. Mechanisms of suppression of {alpha}-synuclein neurotoxicity by geldanamycin in Drosophila. J Biol Chem. 2005;280(4):2873–8.
18. Teixeira-Castro A, Ailion M, Jalles A, Brignull HR, Vilaca JL, Dias N et al. Neuron-specific proteotoxicity of mutant ataxin-3 in C. elegans: rescue by the DAF-16 and HSF-1 pathways. Hum Mol Genet. 2011;20(15):2996–3009.
19. Waza M, Adachi H, Katsuno M, Minamiyama M, Sang C, Tanaka F et al. 17-AAG, an Hsp90 inhibitor, ameliorates polyglutamine-mediated motor neuron degeneration. Nat Med. 2005;11(10):1088–95.
20. Tokui K, Adachi H, Waza M, Katsuno M, Minamiyama M, Doi H et al. 17-DMAG ameliorates polyglutamine-mediated motor neuron degeneration through well-preserved proteasome function in an SBMA model mouse. Hum Mol Genet. 2009;18(5):898–910.
21. Katsuno M, Sang C, Adachi H, Minamiyama M, Waza M, Tanaka F et al. Pharmacological induction of heat-shock proteins alleviates polyglutamine-mediated motor neuron disease. Proc Natl Acad Sci USA. 2005;102(46):16801–6.
22. Ronnen EA, Kondagunta GV, Ishill N, Sweeney SM, Deluca JK, Schwartz L et al. A phase II trial of 17-(Allylamino)-17-demethoxygeldanamycin in patients with papillary and clear cell renal cell carcinoma. Invest New Drugs. 2006;24(6):543–6.
23. Smith V, Sausville EA, Camalier RF, Fiebig HH, Burger AM. Comparison of 17-dimethylaminoethylamino-17-demethoxygeldanamycin (17DMAG) and 17-allylamino-17-demethoxygeldanamycin (17AAG) in vitro: effects on Hsp90 and client proteins in melanoma models. Cancer Chemother Pharmacol. 2005;56(2):126–37.
24. Egorin MJ, Lagattuta TF, Hamburger DR, Covey JM, White KD, Musser SM et al. Pharmacokinetics, tissue distribution, and metabolism of 17-(dimethylaminoethylamino)-17-demethoxygeldanamycin (NSC 707545) in CD2F1 mice and Fischer 344 rats. Cancer Chemother Pharmacol. 2002;49(1):7–19.
25. Chadman KK, Yang M, Crawley JN. Criteria for validating mouse models of psychiatric diseases. Am J Med Genet B Neuropsychiatr Genet. 2009;150B(1):1–11.
26. Costa Mdo C, Paulson HL. Toward understanding Machado-Joseph disease. Prog Neurobiol. 2012;97(2):239–57.
27. Bichelmeier U, Schmidt T, Hubener J, Boy J, Ruttiger L, Habig K et al. Nuclear localization of ataxin-3 is required for the manifestation of symptoms in SCA3: in vivo evidence. J Neurosci. 2007;27(28):7418–28.
28. Cemal CK, Carroll CJ, Lawrence L, Lowrie MB, Ruddle P, Al-Mahdawi S et al. YAC transgenic mice carrying pathological alleles of the MJD1 locus exhibit a mild and slowly progressive cerebellar deficit. Hum Mol Genet. 2002;11(9):1075–94.
29. Chou AH, Yeh TH, Ouyang P, Chen YL, Chen SY, Wang HL. Polyglutamine-expanded ataxin-3 causes cerebellar dysfunction of SCA3 transgenic mice by inducing transcriptional dysregulation. Neurobiol Dis. 2008;31(1):89–101.
30. Goti D, Katzen SM, Mez J, Kurtis N, Kiluk J, Ben-Haiem L et al. A mutant ataxin-3 putative-cleavage fragment in brains of Machado-Joseph disease patients and transgenic mice is cytotoxic above a critical concentration. J Neurosci. 2004;24(45):10266–79.
31. Silva-Fernandes A, Costa Mdo C, Duarte-Silva S, Oliveira P, Botelho CM, Martins L et al. Motor uncoordination and neuropathology in a transgenic mouse model of Machado-Joseph disease lacking intranuclear inclusions and ataxin-3 cleavage products. Neurobiol Dis. 2010;40(1):163–76.
32. Teixeira-Castro A, Ailion M, Jalles A, Brignull HR, Vilaca JL, Dias N et al. Neuron-specific proteotoxicity of mutant ataxin-3 in C. elegans: rescue by the DAF-16 and HSF-1 pathways. Hum Mol Genet. 2011; 20(15):2996–3009.
33. Hollingshead M, Alley M, Burger AM, Borgel S, Pacula-Cox C, Fiebig HH et al. In vivo antitumor efficacy of 17-DMAG (17-

dimethylaminoethylamino-17-demethoxygeldanamycin hydrochloride), a water-soluble geldanamycin derivative. Cancer Chemother Pharmacol. 2005;56(2):115–25.
34. Curtis HJ. Genetic factors in aging. Adv Genet. 1971;16:305–24.
35. Palacios C, Martin-Perez R, Lopez-Perez AI, Pandiella A, Lopez-Rivas A. Autophagy inhibition sensitizes multiple myeloma cells to 17-dimethylaminoethylamino-17-demethoxygeldanamycin-induced apoptosis. Leuk Res. 2010;34(11):1533–8.
36. Rusmini P, Simonini F, Crippa V, Bolzoni E, Onesto E, Cagnin M et al. 17-AAG increases autophagic removal of mutant androgen receptor in spinal and bulbar muscular atrophy. Neurobiol Dis. 2011;41(1):83–95.
37. Riedel M, Goldbaum O, Schwarz L, Schmitt S, Richter-Landsberg C. 17-AAG induces cytoplasmic alpha-synuclein aggregate clearance by induction of autophagy. PLoS One. 2010;5(1):e8753.
38. Harris GM, Dodelzon K, Gong L, Gonzalez-Alegre P, Paulson HL. Splice isoforms of the polyglutamine disease protein ataxin-3 exhibit similar enzymatic yet different aggregation properties. PLoS One. 2010;5(10):e13695.
39. Rub U, de Vos RA, Brunt ER, Sebesteny T, Schols L, Auburger G et al. Spinocerebellar ataxia type 3 (SCA3): thalamic neurodegeneration occurs independently from thalamic ataxin-3 immunopositive neuronal intranuclear inclusions. Brain Pathol. 2006;16(3):218–27.
40. Boy J, Schmidt T, Schumann U, Grasshoff U, Unser S, Holzmann C et al. A transgenic mouse model of spinocerebellar ataxia type 3 resembling late disease onset and gender-specific instability of CAG repeats. Neurobiol Dis. 2010;37(2):284–93.
41. Herbst M, Wanker EE. Small molecule inducers of heat-shock response reduce polyQ-mediated huntingtin aggregation. A possible therapeutic strategy. Neurodegener Dis. 2007;4(2–3):254–60.
42. Labbadia J, Cunliffe H, Weiss A, Katsyuba E, Sathasivam K, Seredenina T et al. Altered chromatin architecture underlies progressive impairment of the heat shock response in mouse models of Huntington disease. J Clin Invest. 2011;121(8):3306–19.
43. Akerfelt M, Morimoto RI, Sistonen L. Heat shock factors: integrators of cell stress, development and lifespan. Nat Rev Mol Cell Biol. 2010;11(8):545–55.
44. Ramanathan RK, Egorin MJ, Erlichman C, Remick SC, Ramalingam SS, Naret C et al. Phase I pharmacokinetic and pharmacodynamic study of 17-dimethylaminoethylamino-17-demethoxygeldanamycin, an inhibitor of heat-shock protein 90, in patients with advanced solid tumors. J Clin Oncol. 2010;28(9):1520–6.
45. Feder JH, Rossi JM, Solomon J, Solomon N, Lindquist S. The consequences of expressing hsp70 in Drosophila cells at normal temperatures. Genes Dev. 1992;6(8):1402–13.
46. Nicklas W, Baneux P, Boot R, Decelle T, Deeny AA, Fumanelli M et al. Recommendations for the health monitoring of rodent and rabbit colonies in breeding and experimental units. Lab Anim. 2002;36(1):20–42.
47. Carter RJ, Lione LA, Humby T, Mangiarini L, Mahal A, Bates GP et al. Characterization of progressive motor deficits in mice transgenic for the human Huntington's disease mutation. J Neurosci. 1999;19(8):3248–57.
48. Morris R. Developments of a water-maze procedure for studying spatial learning in the rat. J Neurosci Methods. 1984;11(1):47–60.
49. Cerqueira JJ, Mailliet F, Almeida OF, Jay TM, Sousa N. The prefrontal cortex as a key target of the maladaptive response to stress. J Neurosci. 2007;27(11):2781–7.
50. Ferro A, Carvalho AL, Teixeira-Castro A, Almeida C, Tome RJ, Cortes L et al. NEDD8: a new ataxin-3 interactor. Biochim Biophys Acta. 2007;1773(11):1619–27.
51. Gundersen HJ, Bendtsen TF, Korbo L, Marcussen N, Moller A, Nielsen K et al. Some new, simple and efficient stereological methods and their use in pathological research and diagnosis. APMIS. 1988;96(5):379–94.
52. West MJ, Slomianka L, Gundersen HJ. Unbiased stereological estimation of the total number of neurons in thesubdivisions of the rat hippocampus using the optical fractionator. Anat Rec. 1991;231(4):482–97.
53. Zar JH. Biostatistical Analysis, 4th edn. Prentice Hall, 1999.

Supplementary material

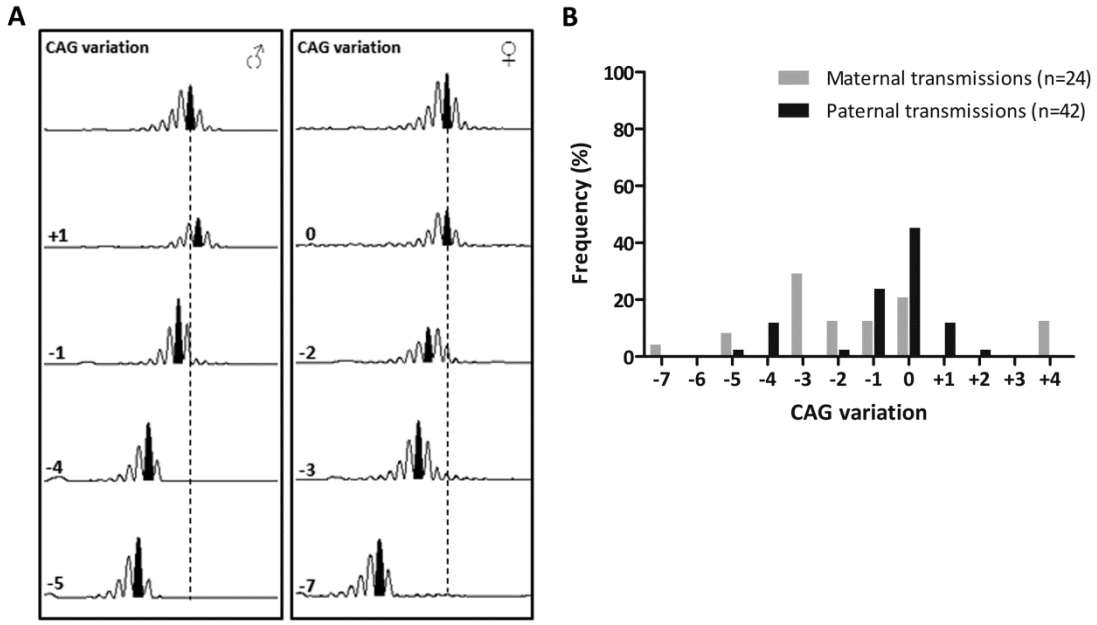

Supplementary Fig. 1. Intergenerational instability of the CAG repeat in MJD mice. **(A)** Representative Genescan tract diagrams showing the variation of the CAG repeat tract in maternal and paternal meioses of CMVMJD135 mice. **(B)** Differential pattern of CAG repeat variation in CMVMJD135 male ($n = 42$) and female meioses ($n = 24$). Values are presented as frequency (%).

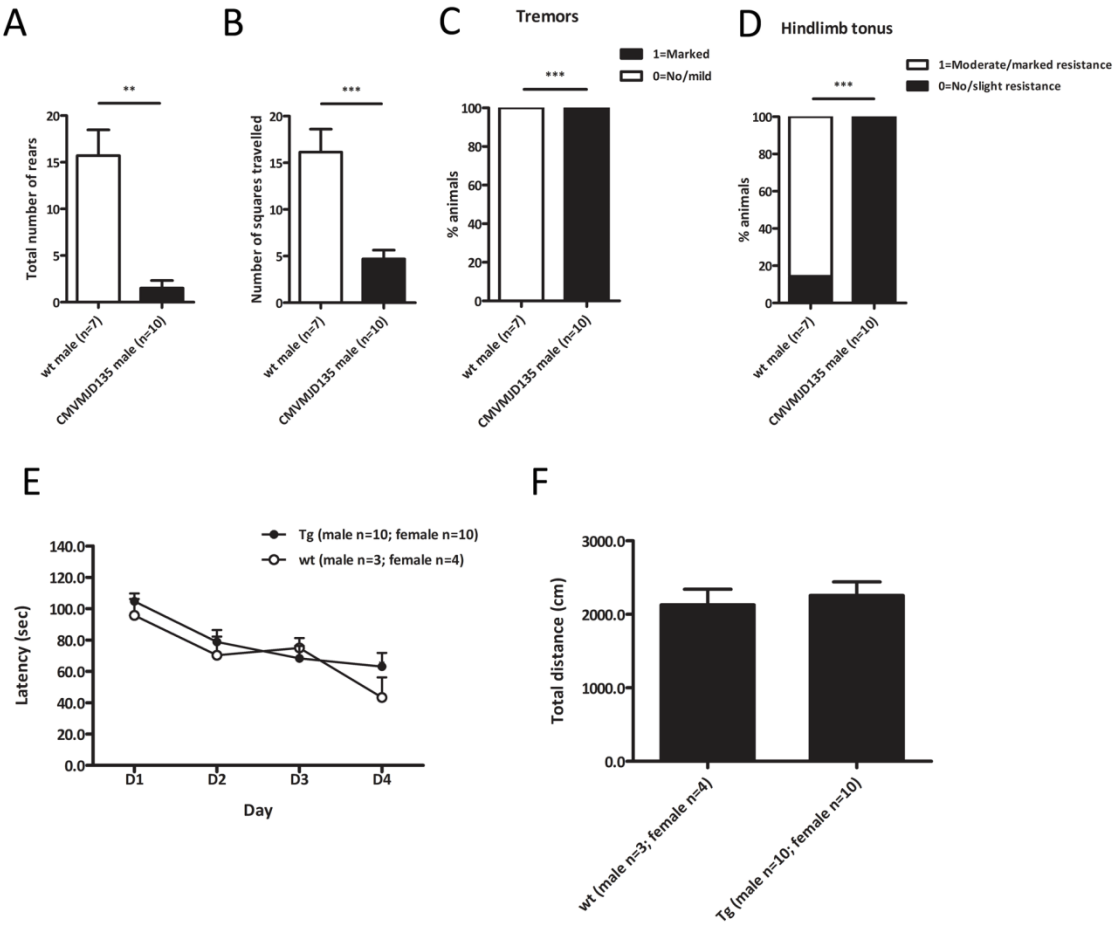

Supplementary Fig. 2. Evaluation of the progression of the disease at 40 weeks of age in the SHIRPA protocol. Spatial cognitive performance in CMVMJD135 mice at 10 weeks of age. **(A)** Exploratory behavior given by the number of rears was dramatically decreased in CMVMJD135 mice as well as the spontaneous locomotor activity **(B).** In addition, at 40 weeks of age animals demonstrate severe tremors **(C)** and hindlimb tonus resistance decrease (n = 7–10) **(D). (E)** Morris water maze test (MWM) was performed in wt ($n = 7$) and CMVMJD135 mice ($n = 20$) in five consecutive days and the time and distance travelled was recorded. **(F)** To exclude a motor influence in this spatial memory task the open-field test was performed one week after the MWM test and no differences were found between controls and transgenic animals indicating that the cognitive function is preserved in this model, as in MJD patients. MWM testing at later ages was not possible due to motor impairments. $^{*}p < 0.05$, $^{**}p < 0.01$, $^{***}p < 0.001$.

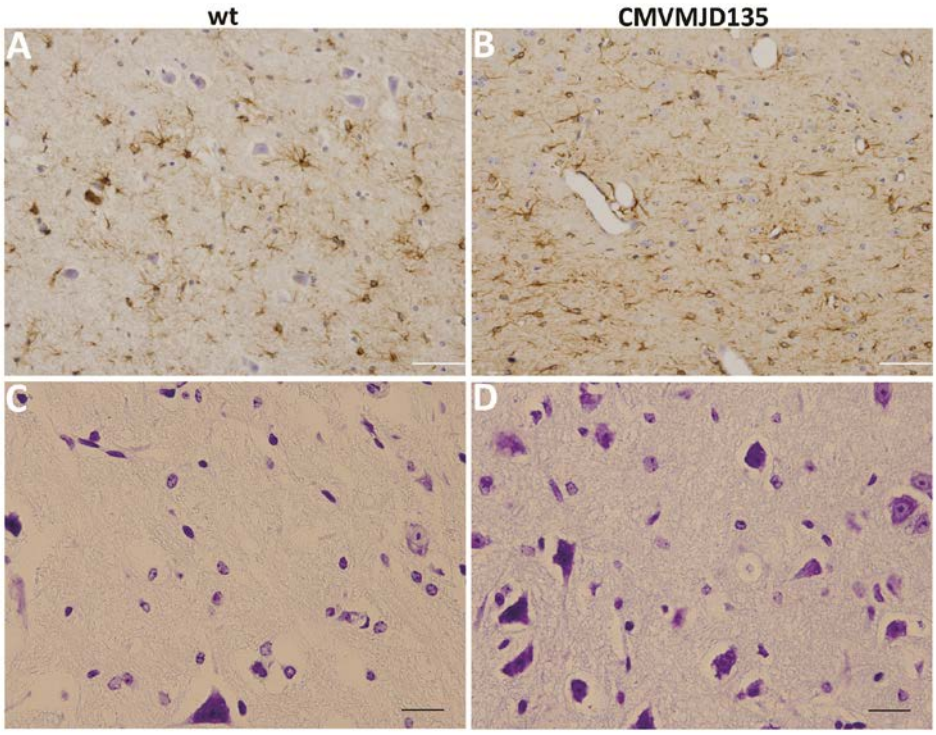

Supplementary Fig. 3. Neuropathology of substantia nigra in CMVMJD135 mice. Anti-GFAP immunohistochemistry in the substantia nigra of wt **(A)** and CMVMJD135 **(B)** mice (n = 3–4). Scale bar: 50 μm. Cresyl violet staining of the susbtantia nigra in wt **(C)** and transgenic mice **(D).** Scale bar: 20 μm.

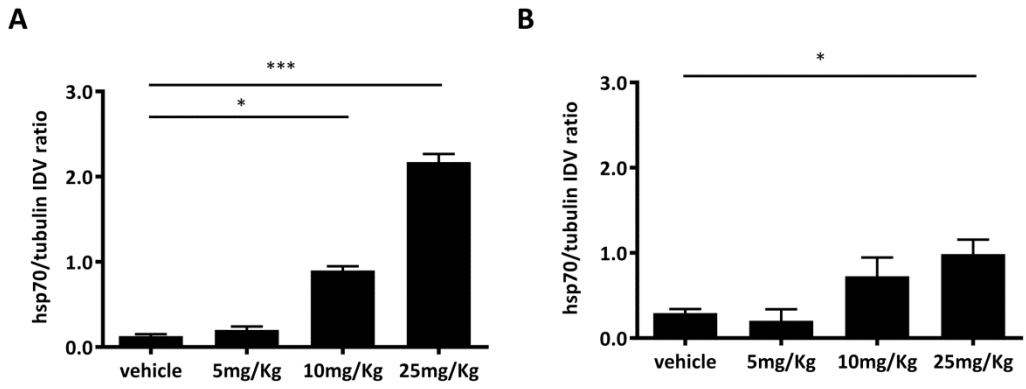

Supplementary Fig. 4. One-week of 17-DMAG treatment increases Hsp70 protein levels in the muscle **(A)** and in the brain (brainstem) **(B)** in a dose-dependent manner. Male wt mice were injected three times during a week with different concentrations of 17-DMAG: 5, 10 and 25 mg/kg ($n = 4$ for each dosage). 12 hours after the last injection mice were sacrificed and Hsp70 proteins levels were measured. In brain tissue, as in muscle, there was a dose-dependent response in Hsp70 induction by 17-DMAG, although the increase in expression was only statistically significant at 25 mg/kg ($p < 0.05$) which we selected for the therapeutic study. With systemic administration of this dosage, the concentration of 17-DMAG in the brain 1 hour after treatment was 42 ng/g (drug quantity/brain weight) with a plasma/brain ratio of 0,2. *$p < 0.05$, **$p < 0.01$, ***$p < 0.001$.

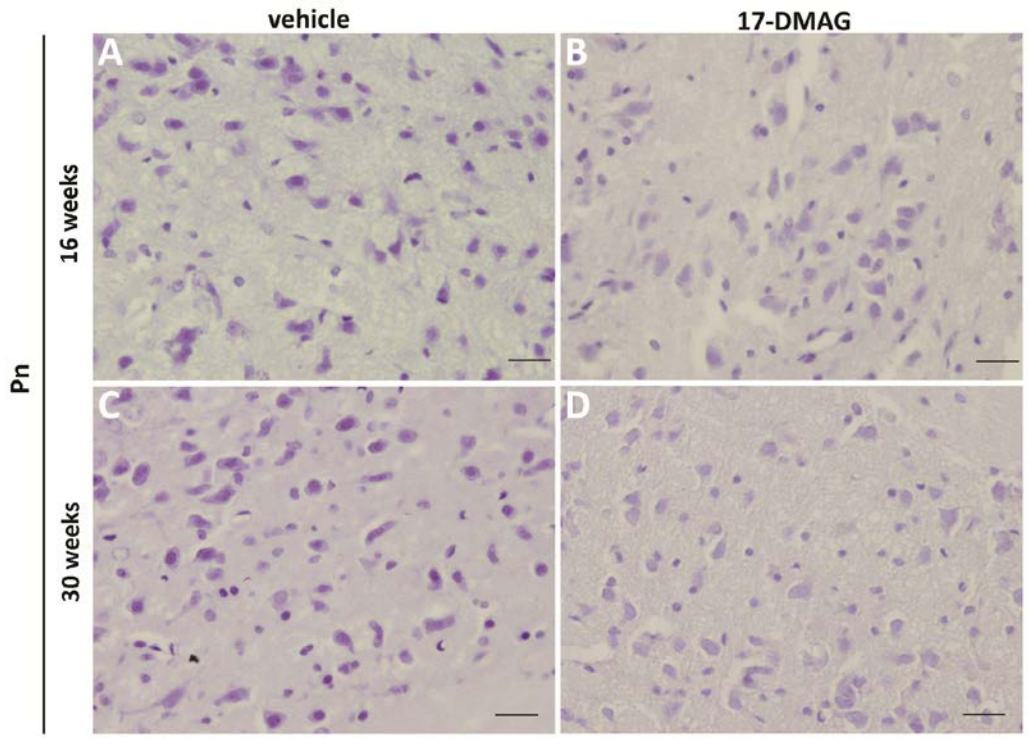

Supplementary Fig. 5. Decreased neuropathology in CMVMJD135 mice treated with 17-DMAG. Comparative sections of pontine nuclei of male CMVMJD135 mice treated with vehicle **(A and C)** or 17-DMAG **(B and D)** at 16 weeks of age **(A and B)** and 30 weeks of age **(C and D)** stained with cresyl violet (n = 3 for each group); 17-DMAG-treated mice present a decrease in the number of pyknotic cells in the pontine nuclei at both ages. Scale bar: 20 μm.

Supplementary Table 1. Sample size calculations for each behavioral test assuming a power of 0.8 and a significance level of 0.05.

			Age (weeks)	6	8	10	12	14	16	20	22	24	28	30	38	40-41
	WEIGHT		Effect size							0,70	1,00	2,50				2,75
			n							18,00	9,00	3,00				2,00
BEHAVIORAL TESTS	REARINGS (NUMBER OF REARS)		Effect size									2,00				2,75
			n									3,00				2,00
	LOCOMOTOR ACTIVITY (NUMBER OF QUADRANTS)		Effect size							0,80	0,60	0,50				2,00
			n							14,00	25,00	35,00				3,00
	HANGING WIRE TEST (LATENCY)		Effect size	0,80	1,00	1,25	2,50	3,50	4,00	4,50	1,50	1,25				9,00
			n	14,00	9,00	6,00	3,00	2,00	2,00	2,00	5,00	6,00				2,00
	STRIDE LENGTH		Effect size					0,50	0,80	1,00		1,00	1,25		1,50	1,50
			n					35,00	16,00	9,00		9,00	6,00		5,00	5,00
	BALANCE BEAM TEST (LATENCY)	MEDIUM SQUARE	Effect size								0,70	0,80		0,70		
			n								18,00	14,00		18,00		
		SMALL CIRCLE	Effect size								0,70	0,80		0,50		
			n								18,00	14,00		35,00		
	MOTOR SWIMMING TEST		Effect size								1,00	1,50		1,50		1,50
			n								9,00	5,00		5,00		5,00
	ROTAROD (LATENCY)	8 rpm	Effect size								0,20	0,10		0,25		1,25
			n								90,00	90,00		90,00		6,00
		15 rpm	Effect size								0,50	0,25		0,50		1,25
			n								35,00	90,00		35,00		6,00
		20 rpm	Effect size								1,00	0,20		0,25		1,75
			n								9,00	90,00		90,00		4,00
		24 rpm	Effect size								0,50	0,50		0,40		3,00
			n								35,00	35,00		50,00		2,00
		31 rpm	Effect size								2,25	1,00		1,00		
			n								3,00	9,00		9,00		

Chapter 3

Lithium Chloride therapy fails to improve motor function in a transgenic mouse model of Machado-Joseph disease

Cerebellum (2014) 13:713–727
DOI 10.1007/s12311-014-0589-9

ORIGINAL PAPER

Lithium Chloride Therapy Fails to Improve Motor Function in a Transgenic Mouse Model of Machado-Joseph Disease

Sara Duarte-Silva · Andreia Neves-Carvalho · Carina Soares-Cunha · Andreia Teixeira-Castro · Pedro Oliveira · Anabela Silva-Fernandes · Patrícia Maciel

Published online: 12 August 2014

Abstract The accumulation of misfolded proteins in neurons, leading to the formation of cytoplasmic and nuclear aggregates, is a common theme in age-related neurodegenerative diseases, possibly due to disturbances of the proteostasis and insufficient activity of cellular protein clearance pathways. Lithium is a well-known autophagy inducer that exerts neuroprotective effects in different conditions and has been proposed as a promising therapeutic agent for several neurodegenerative diseases. We tested the efficacy of chronic lithium (10.4 mg/kg) treatment in a transgenic mouse model of Machado-Joseph disease, an inherited neurodegenerative disease, caused by an expansion of a polyglutamine tract within the protein ataxin-3. A battery of behavioral tests was used to assess disease progression. In spite of activating autophagy, as suggested by the increased levels of Beclin-1, Atg7, and LC3-II, and a reduction in the p62 protein levels, lithium administration showed no overall beneficial effects in this model concerning motor performance, showing a positive impact only in the reduction of tremors at 24 weeks of age. Our results do not support lithium chronic treatment as a promising strategy for the treatment of Machado-Joseph disease (MJD).

Keywords Polyglutamine · Spinocerebellar ataxia · Lithium · Autophagy · Therapy · Triplet repeats

Introduction

Lithium, a monovalent cation and a FDA-approved drug with the ability to cross the blood–brain barrier, has been used in the past 6 decades for the treatment of bipolar disorder(BD) and also adjunctively with mood stabilizers and antidepressants to enhance, prolong, and facilitate treatment response and remission of mood disorders [1, 2]. Although its therapeutic mechanisms remain unclear, strong in vivo and in vitro evidence suggests that lithium has neurotrophic/neuroprotective properties toward a wide range of insults, and also in neurodegenerative diseases [3, 4]. Lithium inhibits glycogen synthase kinase-3 [5, 6] and increases the protein levels of the brain-derived neurotrophic factor (BDNF) [7, 8], leading to an enhanced cell survival. Lithium also regulates calcium homeostasis and suppresses calcium-dependent activation of pro-apoptotic signaling pathways [9], and it can protect against endoplasmic reticulum (ER) stress [10], associated with impaired synaptic plasticity and pathology in neurodegenerative conditions, such as Alzheimer's disease (AD) [11]. In order to be effective, lithium requires long-term treatment, and its effects are not reverted immediately after discontinuation. For this reason, it is thought that lithium acts at the gene expression level. Indeed, lithium is able to upregulate the expression of important molecules such as HSP70 [12, 13], BCL-2 [9, 14, 15], BDNF [7, 8, 16], HSF1 [13], and CREB [4], among others. Moreover, lithium decreases inositol 1,4,5-trisphosphate by inhibiting phosphoinositol phosphatases [17, 18]; this was proposed as a

Electronic supplementary material The online version of this article (doi:10.1007/s12311-014-0589-9) contains supplementary material, which is available to authorized users.

S. Duarte-Silva · A. Neves-Carvalho · C. Soares-Cunha · A. Teixeira-Castro · A. Silva-Fernandes · P. Maciel (✉)
Life and Health Sciences Research Institute (ICVS), School of Health Sciences, University of Minho, Campus Gualtar, 4710-057 Braga, Portugal
e-mail: pmaciel@ecsaude.uminho.pt

S. Duarte-Silva · A. Neves-Carvalho · C. Soares-Cunha · A. Teixeira-Castro · A. Silva-Fernandes · P. Maciel
ICVS/3B's - PT Government Associate Laboratory, Braga/Guimarães, Portugal

P. Oliveira
ICBAS - Abel Salazar Biomedical Sciences Institute, University of Porto, Porto, Portugal

novel mechanism to induce autophagy [19–21]. Macroautophagy, commonly referred to as autophagy, is an important process for the degradation of proteins and organelles and plays a major role in cellular stress conditions [22]. It is also involved in neuronal and astrocytic cell survival and function [23]. The process of autophagy begins with the formation of double-membrane structures called autophagosomes that fuse with lysosomes (autolysosomes) and lately degrade their contents by lysosomal hydrolytic enzymes [24, 25]. Autophagy recycles cytoplasmic proteins in normal conditions and recycles nutrients when necessary, for instance, under starvation. The accumulation of misfolded proteins in cells is a common feature in aging and in several neurodegenerative disorders [26], which makes autophagy a prominent target for the treatment of such diseases; these include amyotrophic lateral sclerosis (ALS), Parkinson disease (PD), AD, Huntington's disease (HD), and Machado-Joseph disease (MJD) [27–37]. Drugs that potentially modulate autophagy are increasingly being used in clinical trials, and screens are being performed for the discovery of new compounds that induce autophagy. Autophagy is modulated by several signaling pathways and is directly inhibited by the serine/threonine protein kinase mammalian target of rapamycin (mTOR) [38]. Administration of rapamycin has been demonstrated to be beneficial in different animal models of neurodegenerative disorders, by enhancing autophagic function [24, 29, 36, 39, 40]. Autophagy can also be regulated independently of mTOR, which can be achieved through lithium, sodium valproate, and carbamazepine, compounds that lower myo-inositol-1,4,5-triphosphate levels [20, 41]. Lithium acts as an autophagy enhancer or inhibitor, depending on the dosage. At higher doses, it inhibits GSK3β, which suppresses autophagy [42]; in contrast, at lower doses, it inhibits IMPAse, inducing autophagy [20].

Chronic lithium treatment was tested in several models of neurodegenerative diseases. Lithium was shown to have beneficial effects in patients and also in an ALS mouse model [43, 44]. The study in the mouse model demonstrated neuroprotection by lithium, which delayed disease onset and duration and increased lifespan. In the clinical trial, a randomized study of adults with ALS showed that none of the patients treated with lithium died during the 15 months of the follow-up, and the disease progression was markedly attenuated [44]. In a mouse model of HD, this treatment had variable effects; lithium improved the motor performance and reduced depressive-like behavior, but only when administered post-symptomatically [45]; furthermore, it had no effect on survival in this model [45]. Chronic treatment with lithium also improved neurological function and hippocampal dendritic arborization in a mouse model of SCA1 [46]. More recently, chronic lithium treatment was shown to ameliorate the phenotype of a MJD *Drosophila* model, partially by inhibiting GSK3β [47].

Taking into account the beneficial effects of lithium and its autophagy induction properties, and considering that little is known about its possible effects in MJD, we performed chronic lithium treatment in the CMVMJD135 mouse model [48]. Our results show limited beneficial effects of lithium treatment; although it subtly improved a few of the symptoms observed at specific time points, it was not able to globally improve motor function in this model. These findings do not support the idea that lithium is a good candidate to treat MJD. This is of clinical relevance, since one may avoid the collateral effects of trying lithium therapy in MJD patients.

Material and Methods

Transgenic Mice We used the CMVMJD135 mice [48], which express an expanded version of the human MJD1-1 cDNA (the 3 UIMs-containing variant of ATXN3) under the regulation of the CMV promoter (ubiquitous expression) at near-endogenous levels. All animals were maintained under standard laboratory conditions: an artificial 12-h light/dark cycle (lights on from 8:00 to 20:00 h), with an ambient temperature of 21±1 °C and a relative humidity of 50–60 %; the mice were given a standard diet (4RF25 during the gestation and postnatal periods, and 4RF21 after weaning, Mucedola SRL, Settimo Milanese, Italy) and water ad libitum. All procedures were conducted in accordance with European regulations (European Union Directive 86/609/EEC). Animal facilities and the people directly involved in animal experiments (S.D.S, A.N.C) were certified by the Portuguese regulatory entity—Direcção Geral de Veterinária. All the protocols performed were approved by the joint Animal Ethics Committee of the Life and Health Sciences Research Institute, University of Minho. Health monitoring was performed according to FELASA guidelines [49], confirming the Specified Pathogen Free health status of sentinel animals maintained in the same animal room. Humane endpoints for experiment were defined (20 % reduction of the body weight, inability to reach food and water, presence of wounds in the body, dehydration), but not needed as the study period was conceived to include ages at which animals do not reach these endpoints.

Mouse Genotyping The progenies produced by mating MJD transgenic with wild-type animals were genotyped at weaning by PCR, as previously described [50].

Drug Treatment and Behavioral Tests Male mice were used in the study since they show less variability than females in behavioral tests, due to the more variable hormonal female status. Transgenic and non-transgenic, drug- and vehicle-treated animals were housed at weaning in groups of five animals per cage. The experiment started at 4 weeks and

ended at 24 weeks of age. At 4 weeks of age, we screened the overall status of the animals by the SHIRPA protocol before starting the treatment with lithium chloride (LiCl, Merck, Massachusetts, USA). The treatment started at the asymptomatic age of 5 weeks, 1 week before the previously observed onset of symptoms [48].

We used a total of 40 animals, which were housed according to the drug administered, since the experiment was carried out by a single experimenter, which was only blind to the genetic status of the animals. The animals were intraperitoneally injected three times per week, except in the week of behavioral tests. Transgenic and non-transgenic littermates (n=10 for each genotype) were treated with 10.4 mg/kg of lithium chloride as previously described [44, 45]. Control littermate animals were given a vehicle injection of buffer (0.15 M NaCl, 5 % Tween-20, and 5 % PEG 400) with the same frequency. The animals were evaluated at 20 and 24 weeks of age in the Beam Walk Balance test. The SHIRPA protocol was performed at all ages tested. For a detailed description of behavioral testing, see below.

Body Weight All mice were weighed a week before the start of the drug treatment (4 weeks) and then at 5, 6, 8, 9, 10, 12, 13, 14, 16, 17, 18, and 20 weeks of age.

Beam Walk Balance Test The beam walk balance test assesses balance but is also sensitive to fine motor coordination. This test measures the ability of the animal to stay upright and to walk on an elevated beam without falling to the cushioned pads below, or slipping to one side of the beam. The beams are 70 cm long and made of smooth wood with a square (12 mm wide) or a round (11- and 17-mm diameter) shape. The beam is placed at the height of 50 cm. The test has different levels of difficulty obtained by varying the shape and width of the beams. The animals were trained during 3 days in the square beam (12 mm). In the fourth day, they were tested in the training beam and also in two round beams (17 and 11 mm).

The animal is placed on one end of the beam and then allowed to walk along the beam and reach the opposite end (which has a "safe" dark box). At the end of the training days, the animals should be capable of performing the task in less than 20 s. By day 4, animals were tested using two beams of different width and shape (square and round). If the animal fell or turned around in the beam, this was considered one failed trial. Each animal had the opportunity to fail two times in each beam. The time the animal took to cross the beam was counted, and time was discounted if the animal stopped in the beam.

SHIRPA Protocol We established a protocol for phenotypic assessment based on the primary screen of the SHIRPA protocol, which mimics the diagnostic process of general neurological and psychiatric examination in humans [51]. Each mouse was placed in a viewing jar (15-cm diameter) for 5 min and transferred to a 15-labeled-squares arena (55×33×18 cm), and then a series of anatomical and behavioral features were registered. The full details of the SHIRPA protocol are available at the site http://empress.har.mrc.ac.uk/browser/?sop_id=10_002_0. In addition, we included the footprint pattern test (see below) to assess gait [52] and the counting of rears over 5 min in the viewing jar, as a measure of spontaneous vertical exploratory activity. The protocol was adjusted in order to minimize animal handling and to generate uniformity in waiting times between the tests [53].

Footprint Pattern The footprint test was used to evaluate the foot dragging of the animals. To obtain footprints, the hindpaws and forepaws of the mice were coated with black and red non-toxic paints, respectively. A clean rectangular paper sheet was placed on the floor of the runway for each run. The animals were then allowed to walk along a 100 cm long×4.2 cm width×10 cm height corridor in the direction of an enclosed black box. Each animal was allowed to achieve one valid trial per age. To evaluate the presence of foot dragging through age, the footprinting pattern of CMVMJD135 and wild-type (wt) vehicle- and lithium-treated (n=10 per group) was analyzed at each time point considering six consecutive steps (absent, no dragging; present, at least one step out of six shows dragging).

Assessment of Autophagy Activation The animals that were chronically treated with LiCl for 19 weeks and were killed 12 h after the last injection as previously described [48], and the brain and muscle tissue were immediately frozen in dry ice. We also injected wild-type animals with LiCl (10.4 mg/kg) three times in 1 week in alternate days and performed the killing at different time points after the last injection: 6, 14, 16, 18, and 24 h for determination of acute effects. Another set of animals was injected with the vehicle and killed at the same time points.

Western Blot Brain tissue was homogenized in cold 0.1 M Tris–HCl, pH 7.5, 0.1 M EDTA, and a mixture of protease inhibitors (Complete, Roche, Swiss) and was sonicated for 10 s. Protein concentration was determined using the Bradford assay (Biorad, CA, USA). Samples were heated for 5 min at 100 °C and microfuged for 10 s before loading. For each sample, 15 μg of total protein was loaded into SDS-PAGE gels and then transferred to nitrocellulose membranes (Amersham GE Healthcare, UK). After incubation with the primary antibodies—rabbit anti-LC3 (1:1,000 Novus Biologicals, Littleton, CO), rabbit anti-IMPA1 (1:1,000, Abcam, Cambridge, UK), rabbit anti-p62 (1:50, Abcam, Cambridge, UK), rabbit anti-Beclin-1 (1:1,000, Cell signaling, Beverly, MA), rabbit anti-Atg7 (1:1000, Cell signaling, Beverly, MA), mouse anti-alpha-tubulin (1:100, DSHB, University of Iowa, Iowa), and mouse anti-beta-actin (1:100, DSHB, University of Iowa, IA)—the secondary antibodies were incubated at the

following dilutions: anti-rabbit (1:10.000, Santa Cruz, Dallas, TX, USA) and anti-mouse (1:10.000, Santa Cruz, Dallas, TX, USA). Antibody affinity was detected by chemiluminescence (ECL kit, Santa Cruz, Dallas, Texas, USA). Band quantification was performed using the ImageJ software according to the manufacturer's instructions, using alpha-tubulin as the loading control.

Determination of Lithium Plasma Levels The plasma lithium levels were measured applying the LITH assay using the Dimension Vista® System (LITH Flex® reagent cartridge)–SIEMENS.

Statistical Analysis Power analysis was used to determine the sample size [54]. Considering the different variables under study, such as weight and time held in the hanging wire, assuming a power of 0.8 and a significance level of 0.05, different required sample sizes were obtained, depending on the specified smallest detectable difference and the variability of the experimental groups. Based on these calculations and bearing in mind that as the age of the animals increases, also the mean differences increase and, possibly, the standard deviations, a sample size ranging between five and ten animals was obtained, and therefore, a sample of ten animals was chosen. For specific behavioral tests and time points of analysis, see Supplementary Table S1.

Continuous variables with normal distributions (K-S test $p>0.05$) were analyzed with the Student's t test or two-way ANOVA (factors: genotype and treatment). Behavioral data were subjected to the non-parametric Mann–Whitney U test when variables were non-continuous or when a continuous variable did not present a normal distribution (Kolmogorov-Smirnov test $p<0.05$). Categorical variables in the SHIRPA protocol were analyzed by contingency tables (Fisher's exact test). All statistical analyses were performed using SPSS 22.0 (SPSS Inc., Chicago, IL). A critical value for significance of $p<0.05$ was used throughout the study.

Results

In the CMVMJD135 transgenic mouse model, mutant ataxin-3 expression is close to the endogenous levels and the MJD-like symptoms are progressive in life, as observed in human patients [48]. In the current study, we confirmed the onset of the neurological phenotype at 6 weeks of age, with loss of grip strength, measured using the hanging wire test. At 20 weeks of age, the animals showed a deficit in balance on the beam test. It was also possible to observe tremors, foot dragging, and limb clasping. Furthermore, they exhibited decreased locomotor and exploratory behavior late in life. This model does not show premature death, allowing long-treatment periods—in the present case, treatment was administered for 19 weeks, i.e., until the age of 24 weeks, when animals display overt symptoms and a full-blown neurological phenotype.

Autophagy Is not Altered in the Brain of CMVMJD135 Mice

At basal conditions, autophagic activity in 24-month-old CMVMJD135 mouse brains did not differ from that of littermate controls (Fig. 1a). Autophagy was assessed by the measurement of protein levels of LC3-II (Fig. 1b), an autophagosome marker; of Beclin-1 (Fig. 1c), a protein involved in the nucleation step of autophagy; of Atg7 (Fig. 1d) involved in the elongation step of this process; of p62 (Fig. 1e), an autophagy substrate; and of IMPA1 (Fig. 1f), an enzyme responsible for the provision of inositol required for synthesis of phosphatidylinositol and polyphosphoinositides. Our results suggest that autophagy is neither impaired nor over-activated in this transgenic mouse model of MJD.

Lithium Chloride Induces Autophagy in the Mouse Brain

In order to verify if lithium chloride could induce autophagy at the dosage we planned to administer (10.4 mg/kg), similar to that used by Fornai et al. [44 and Wood and Morton 45], we used a group of wild-type mice, injected them with lithium chloride [45] three times per week, and measured the levels of autophagy markers in the brain at different time points after the last injection (6, 14, 16, 18, and 24 h post-injection). In these mice, in which the mean plasma lithium concentration achieved was 0.3±0.09 mmol/L, we were able to observe an increase in the LC3-II/LC3-I ratio (Fig. 2a) and a decrease in IMPA1 (Fig. 2b), an enzyme whose expression is directly inhibited by lithium. According to the *Guidelines for the use and interpretation of assays for monitoring autophagy in higher eukaryotes* [55], LC3 is the only marker for autophagosomes, but in mammalian cells, total LC3 protein levels may not be altered after a cellular challenge; the most probable finding is the increase in the conversion of LC3-I to LC3-II. LC3-I is abundant and stable in the central nervous system, which is a parameter to take in consideration in this type of measurements [55]. Importantly, the LC3-II/LC3-I ratio was increased at the protein level in the brain of lithium-treated mice (Fig. 2a). We also found an increase in LC3-II/LC3-I ratio in muscle tissue (data not shown). Consistently, Beclin-1, a protein involved in the nucleation step of the autophagosome formation [56], was also increased in animals treated with LiCl, supporting autophagy induction by this treatment (Fig. 2b). Furthermore, the levels of Atg7, a protein involved in the elongation step of autophagosome formation, were also increased in the LiCl-treated animals (Fig. 2c). The decrease in p62 levels confirms that autophagy was occurring without blockage (Fig. 2d). The levels of IMPA1 were, as expected, decreased (Fig. 2e).

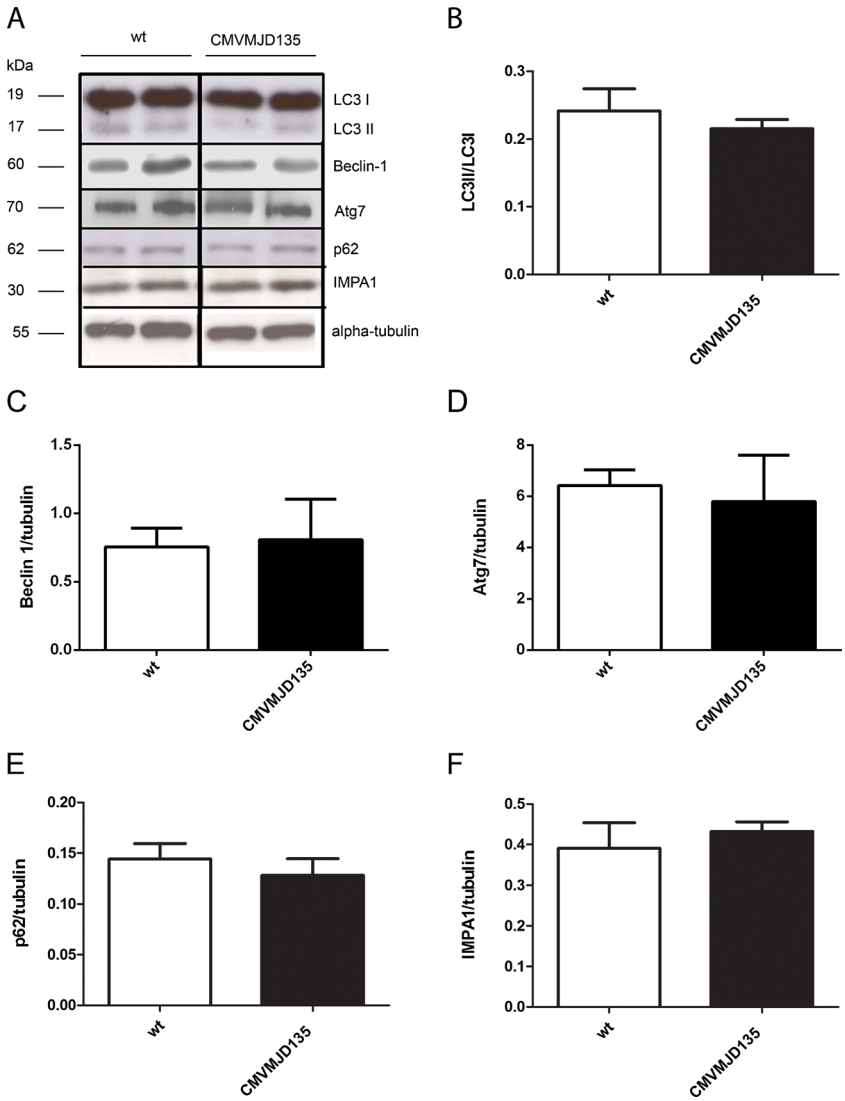

Fig. 1 Autophagy basal levels in CMVMJD135 mice. **a** Representative Western blot probed with LC3, Beclin-1, Atg7, p62, IMPA1, and tubulin antibodies. At least three technical replicates were performed. **b**–**f** LC3-II, Beclin-1, Atg7, p62, and IMPA1 protein levels were measured in brain lysates of CMVMJD135 mice (n=5) and their littermate wild type (n=5) at 24 months of age. LC3-II protein levels were normalized both for LC3-I and α-tubulin; Beclin-1, Atg7, p62, and IMPA1 were normalized for α-tubulin. *p<0.05; **p<0.01; ***p<0.001 (Student's t test)

To complement these analyses, we measured the levels of autophagy markers in the brain of the transgenic animals that were chronically treated with LiCl, namely, the LC3-II/LC3-I ratio (Fig. 3a), as well as protein levels of Beclin-1 (Fig. 3b), Atg7 (Fig. 3c), p62 (Fig. 3d), and IMPA1 (Fig. 3e), and the results were similar to those observed for the acute LiCl treatment, confirming that autophagy remains induced in the chronically treated animals.

Intriguingly, and despite the efficacy of LiCl to induce autophagy, it did not reduce the protein levels of mutant human ataxin-3 in the brain of LiCl-treated animals, which were comparable to those of vehicle-treated mice (Supplementary Fig. S1).

Lithium Did not Improve Body Weight Loss in CMVMJD135 Mice

We assessed the phenotype of the mice from 4 to 24 weeks of age (Fig. 4a). Animals were weighed at 4 (before the treatment) 5, 6, 8, 9, 10, 12, 13, 14, 16, 17, 18, and 20 weeks of age. One of the known collateral effects of lithium treatment in human patients is weight gain [57], but we did not observe this in our study. Chronic administration of LiCl had no effect on body weight in wt animals, compared with wt animals treated with vehicle. At 12 weeks of age, vehicle-treated CMVMJD135 mice started to lose weight compared to the vehicle-treated wt animals (p=0.024) as previously observed for this model [48] (genotype: $F_{1,40}$=9.919; p=0.003) and as it is known to occur in human patients [58]; this body weight reduction was progressive in time, as shown in Fig. 4b. No differences were found between vehicle- and lithium-treated transgenic animals, i.e., lithium treatment did not improve this body weight reduction.

Lithium Treatment Had no Major Effect on Neurological Deficits Present in CMVMJD135 Mice

We analyzed all the animals using the SHIRPA protocol [51] before the treatment onset, at 4 weeks of age, and no

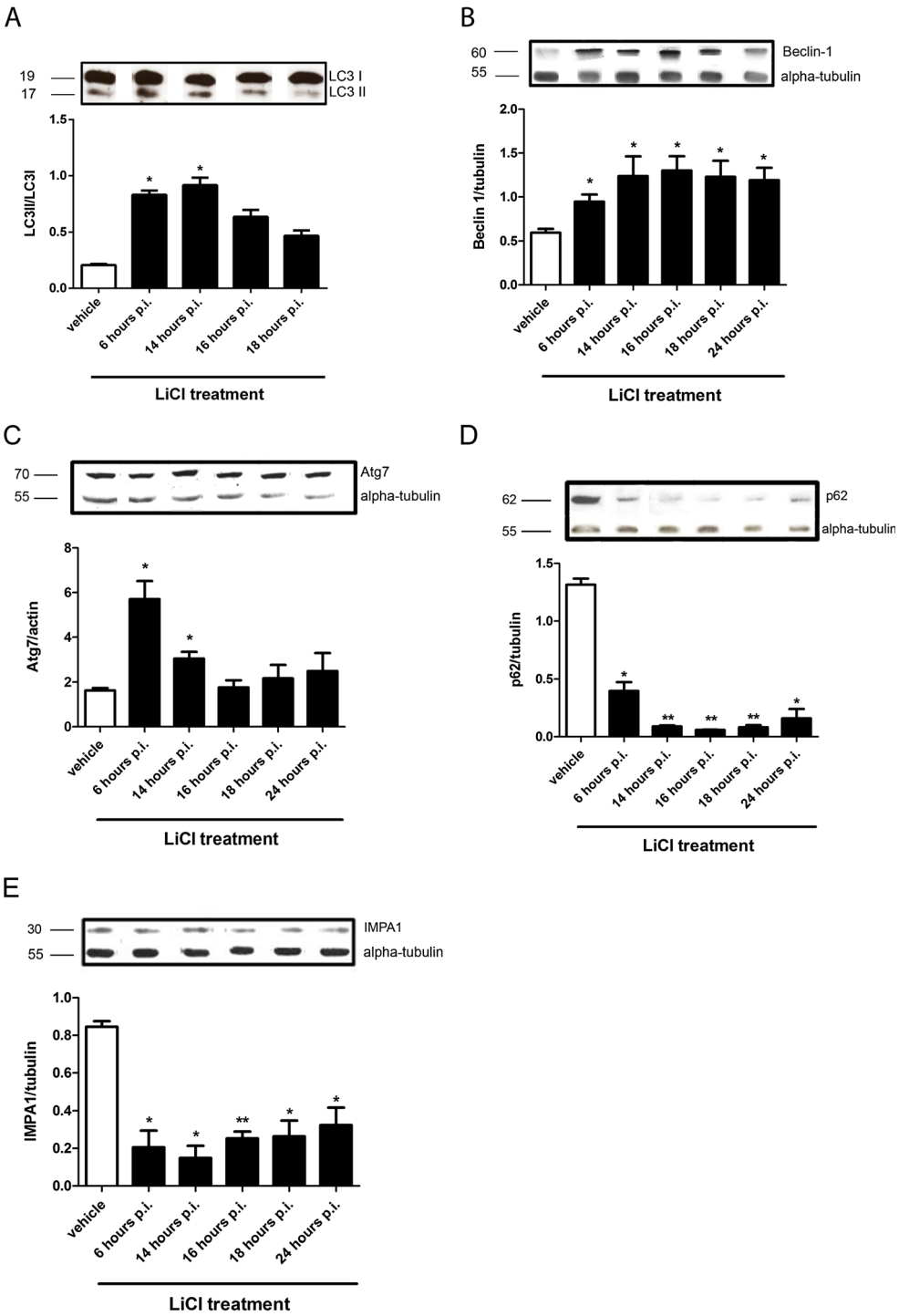

Fig. 2 Autophagy induction by acute lithium treatment. **a** Anti-LC3 Western blot of brain lysates of wild-type animals injected with vehicle (n=4) or lithium 10.4 mg/kg (n=4 for each time point); **b** Beclin-1 Western blot of brain lysates of wild-type animals injected with vehicle (n=4) or lithium 10.4 mg/kg (n=4 for each time point); **c** Atg7 Western blot of brain lysates of wild-type animals injected with vehicle (n=4) or lithium 10.4 mg/kg (n=4 for each time point); **d** p62 Western blot of brain lysates of wild-type animals injected with vehicle (n=4) or lithium 10.4 mg/kg (n=4 for each time point); **e** anti-IMPA1 Western blot analysis of brain lysates of wild-type animals injected with vehicle (n=4) or lithium 10.4 mg/kg (n=4 for each time point); lithium-injected animals were killed at different time points as shown in the *graph*; vehicle animals were killed 6 h post-injection. Alpha-tubulin or beta-actin was used as loading control. *p<0.05; **p<0.01; (Student's t test)

differences were found between wt and CMVMJD135 animals (data not shown), meaning that at this time point, the transgenic animals did not show any symptoms of disease.

The first disease manifestation in the CMVMJD135 model is the loss of limb strength given by the hanging wire test, which measures the time the mouse is able to hold a grid with its hindlimbs and, mostly, forelimbs, before falling. Whereas wild-type animals—treated and vehicle groups—were almost always able to complete the task (hanging in the grid for the maximum time, 2 min), transgenic animals—both LiCl- and vehicle-treated groups—showed a decreased latency to fall from the grid, worsening with age (genotype: $F_{1,39}$=324.589; $p=1.6628\times10^{-20}$) (Fig. 4c).

At 16 weeks and subsequent ages, CMVMJD135 vehicle-treated animals showed a decrease in exploratory behavior, given by the infrequent rearing behavior, which progressed to

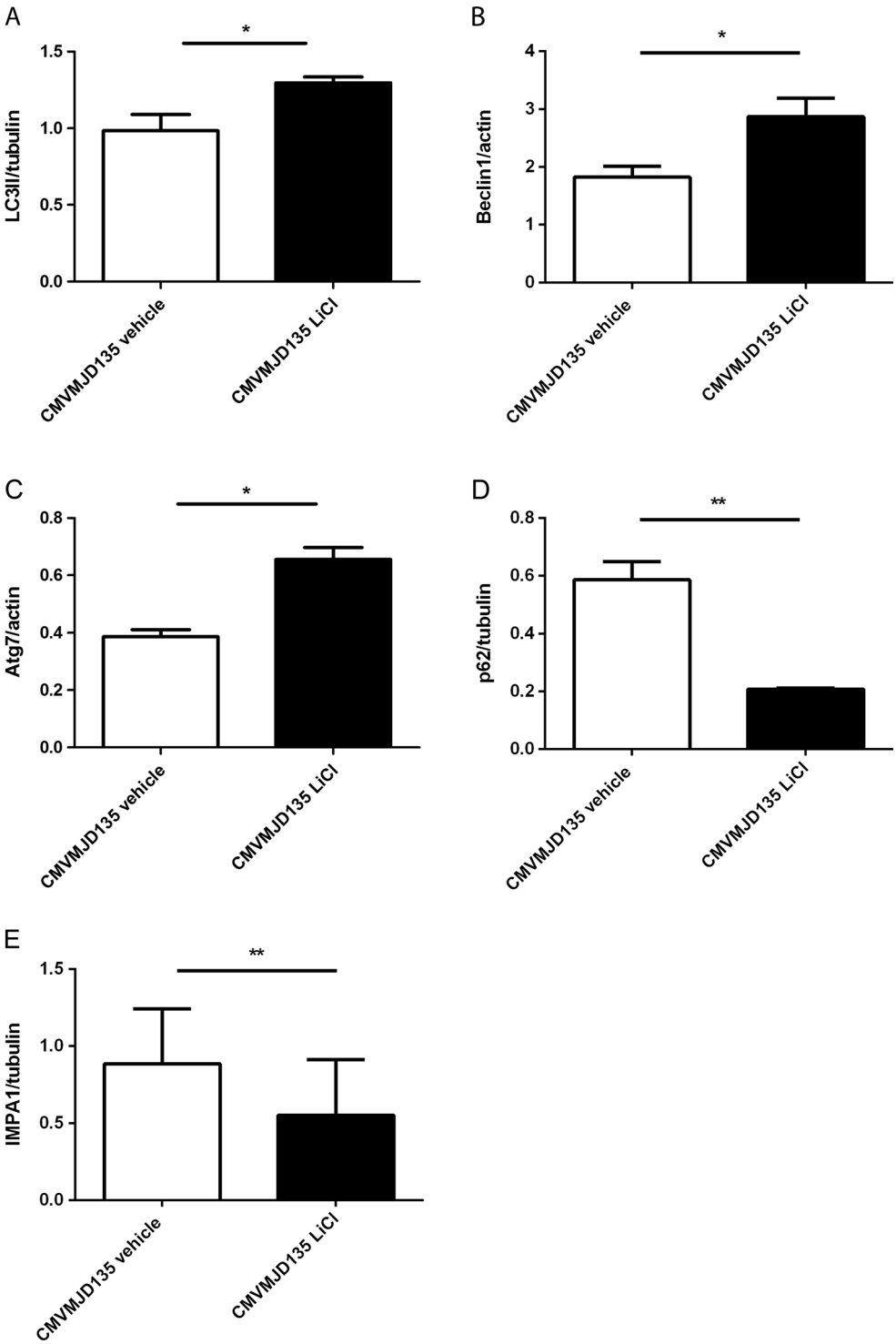

Fig. 3 Autophagy induction by lithium in chronically treated transgenic mice at 24 weeks of age. **a** Anti-LC3 Western blot of brain lysates of transgenic animals injected with vehicle (n=4) or lithium 10.4 mg/kg (n=4); **b** Beclin-1 Western blot of brain lysates of transgenic animals injected with vehicle (n=4) or lithium 10.4 mg/kg (n=4); **c** Atg7 Western blot of brain lysates of transgenic animals injected with vehicle (n=4) or lithium 10.4 mg/kg (n=4); **d** p62 Western blot of brain lysates of transgenic animals injected with vehicle (n=4) or lithium 10.4 mg/kg (n=4); **e** anti-IMPA1 Western blot analysis of brain lysates of transgenic animals injected with vehicle (n=4) or lithium 10.4 mg/kg (n=4); alpha-tubulin or beta-actin was used as loading control. *p<0.05; **p<0.01; (Student's t test)

almost no rearing at the age of 24 weeks (p<0.05). At 8 weeks of age, lithium-treated CMVMJD135 animals showed an increase in exploratory behavior when compared with vehicle-treated CMVMJD135 animals, given by the increase in number of rears in the viewing jar (p=0.026). This activity reached that of the vehicle-treated wt animals at this age, but at later stages, the improvement was no longer seen (Fig. 5a). To further test exploratory locomotor activity, we counted the number of squares travelled in the arena used in the SHIRPA protocol. CMVMJD135 treated with vehicle showed a decrease in the number of squares travelled in the arena at 20 and 24 weeks of age (p=0.003 and p=0.002, respectively), which was not improved by chronic lithium treatment (Fig. 5b).

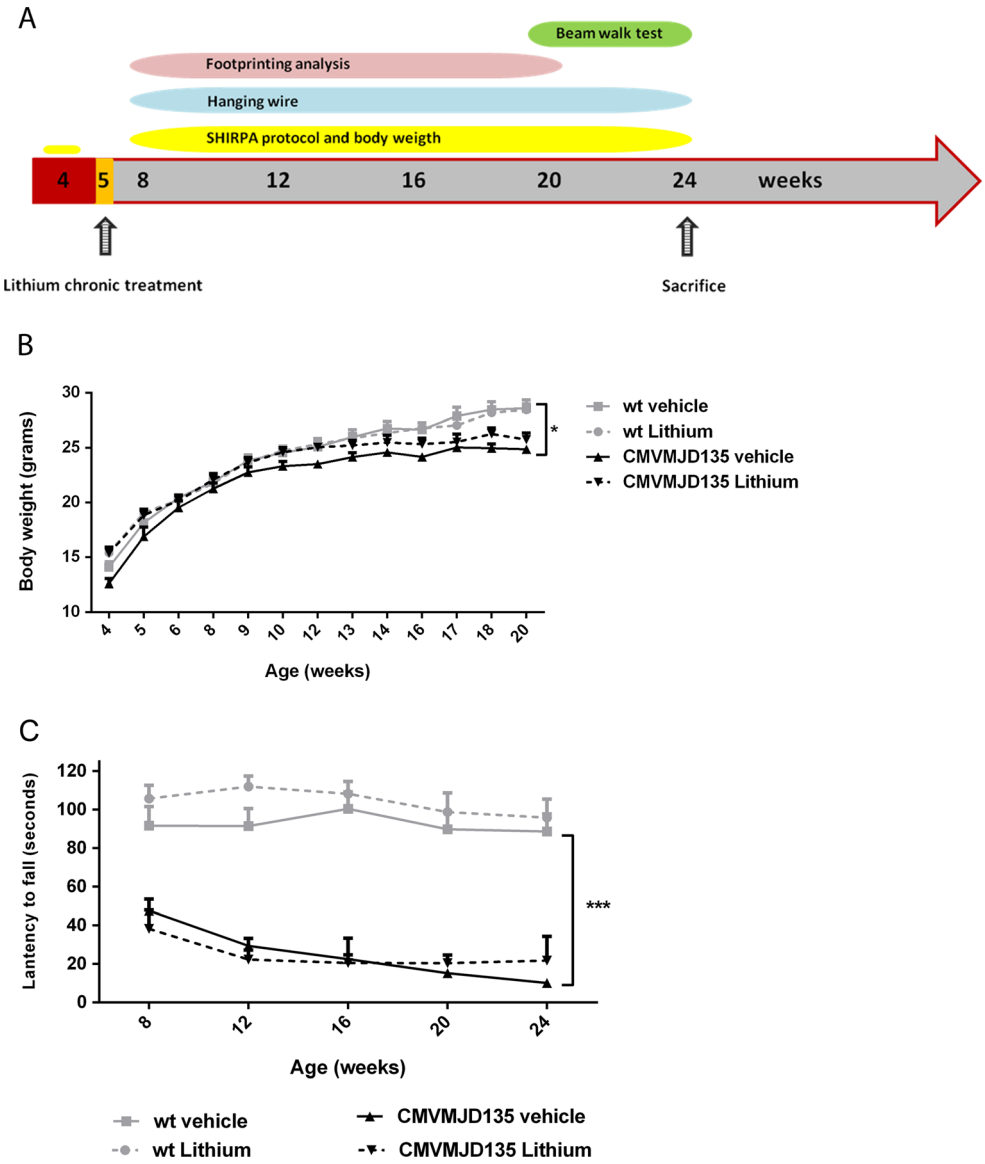

Fig. 4 Effect of lithium treatment on body weight and strength of CMVMJD135 and wt mice. **a** Schematic timeline for the behavioral analysis of lithium pre-clinical trial. **b** The body weight in grams between 8 and 20 weeks of age was depicted for wt and CMVMJD135 mice treated with LiCl or vehicle (n=10 for each group). **c** Hanging wire test—all transgenic animals display a worse performance in holding the grid with age (from 8 to 24 weeks of age). A maximum time of 2 min was given to each animal and the time that they took to fall was registered (n=10 for each group). *Symbols* represent mean ± SEM of the different groups. *p<0.05; ***p<0.001, for genotype factor (two-way ANOVA)

We also performed qualitative analysis of the gait in the open arena as described by Rogers et al. [51]. We scored the animals with 0 when their gait was normal, 1 when the animal had a fluid stepping but an abnormal walking, and 2 when the animal had limited walking [51]. CMVMJD135 animals started to have significantly worse gait scores at the age of 20 weeks (p=0.029), and at 24 weeks of age, 100 % of the animals had a visibly abnormal gait (80 % of the animals were scored as 1, 10 % as 2, and 10 % as 0, p=0.000017) (Fig. 5c). There was a trend toward improvement with lithium treatment, but only at 24 weeks of age (80 % of the vehicle transgenic animals were scored as having abnormal gait, in contrast with 67 % of the treated transgenic animals, p=0.054) (Fig. 5c). Additionally, we performed a semi-quantitative analysis of the foot dragging observed in the mice (Fig. 5d). We found no significant differences in the footstep measurements between the four groups at the ages tested, but it was possible to observe that CMVMJD135 animals presented foot dragging at 12 weeks (p=0.00002) and that this symptom progressed in severity with age (p<0.05). At 20 weeks of age, all CMVMJD135 mice (100 %, $p=2\times10^{-5}$) dragged their feet while walking. Lithium was not able to rescue this phenotype.

When mice are picked up by the tail and suspended toward a surface, their normal reflex is to extend all the four paws to anticipate the ground [59]. The paw clasping phenotype, in which the animals contract the paws instead of extending them, is observed in several mouse models with damage in the cerebellum [60, 61] or in the basal ganglia [62, 63], and also in models of AD [64–66]. In CMVMJD135 mice, this paw clasping phenotype was detected at 24 weeks of age ($p=2\times10^{-6}$), whereas wt animals never presented this abnormal reflex (Fig. 6a). Lithium treatment was not able to rescue this aspect of the phenotype (Fig. 6a).

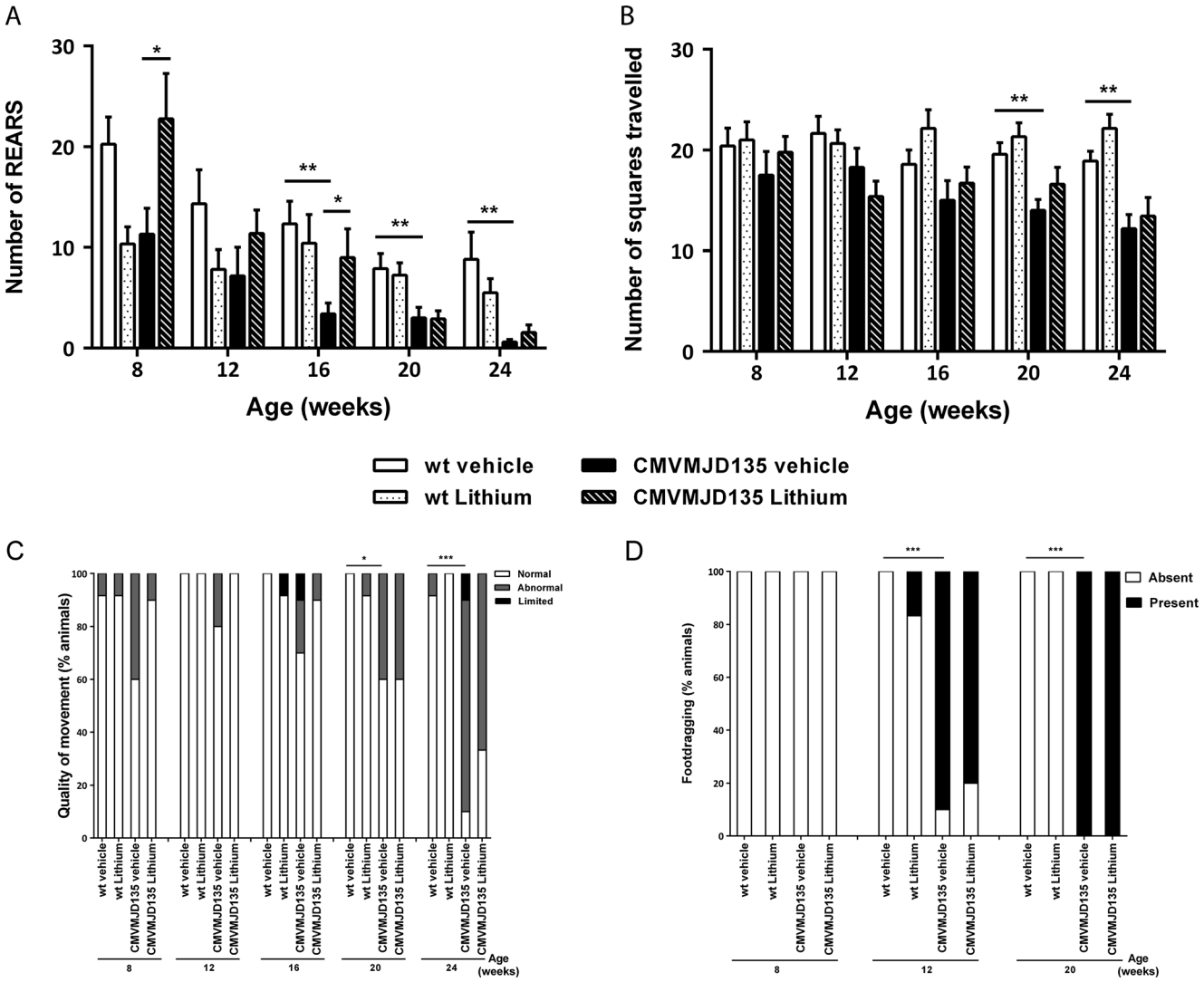

Fig. 5 Effect of lithium treatment upon spontaneous exploratory activity and gait quality. **a** Transgenic animals display decreased vertical locomotor activity at 16 weeks of age and subconsequent ages (n=10 for each group); **b** Transgenic animals travel less in the arena than wild-type animals at 20 and 24 weeks of age; lithium treatment had no effect in this phenotype (n=10 for each group). **c** CMVMJD135 animals have abnormal gait at 20 and 24 weeks of age (qualitative assessment) that is slightly reverted by LiCl at 24 weeks, although not statistical significant (n=10 for each group). **d** Quantitative analysis of the foot dragging: Presence/absence of dragging demonstrated that transgenic animals drag their feet since 12 weeks of age, which was not ameliorated by LiCl (n=10 for each group). *p<0.05; **p<0.01; ***p<0.001

We also observed an increase in the percentage of transgenic animals presenting tremors through age, starting at 16 weeks of age (p<0.05), which was, surprisingly, ameliorated with lithium treatment, this improvement being significant only after a long period of administration (24 weeks of age, p=0.02) (Fig. 6b).

Lithium Fails to Rescue Balance and Fine Motor Deficits in CMVMJD135 Mice

The balance beam test depends on the mouse's ability to maintain balance while traversing a narrow beam to reach a safe platform [67] and was used to test the balance and fine motor coordination capabilities in CMVMJD135 and wt animals, treated with LiCl or with the vehicle. At 20 weeks, CMVMJD135 animals were slower to traverse the round beams with 17 mm (genotype: $F_{1,31}$=8.96; p=0.005; genotype×treatment: $F_{1,31}$=5.260; p=0.029) and 11 mm of diameter (genotype: $F_{1,36}$=4.447; p=0.042), but not significantly slower in the 12-mm square beam, in which they had been trained; the difficulty in performing this task was confirmed at 24 weeks of age, when transgenic animals were slower in traversing the 12-mm square beam (genotype: $F_{1,37}$=6.412; p=0.016), the 17-mm round beam ($F_{1,30}$=5.315; p=0.028), and the 11-mm round beam (genotype: $F_{1,33}$=5.041; p=0.032) (Fig. 7). In the 11-mm round beam, transgenic mice showed a "crawling behavior" (when the animal's thorax and abdomen are in contact with the beam surface) and dragged

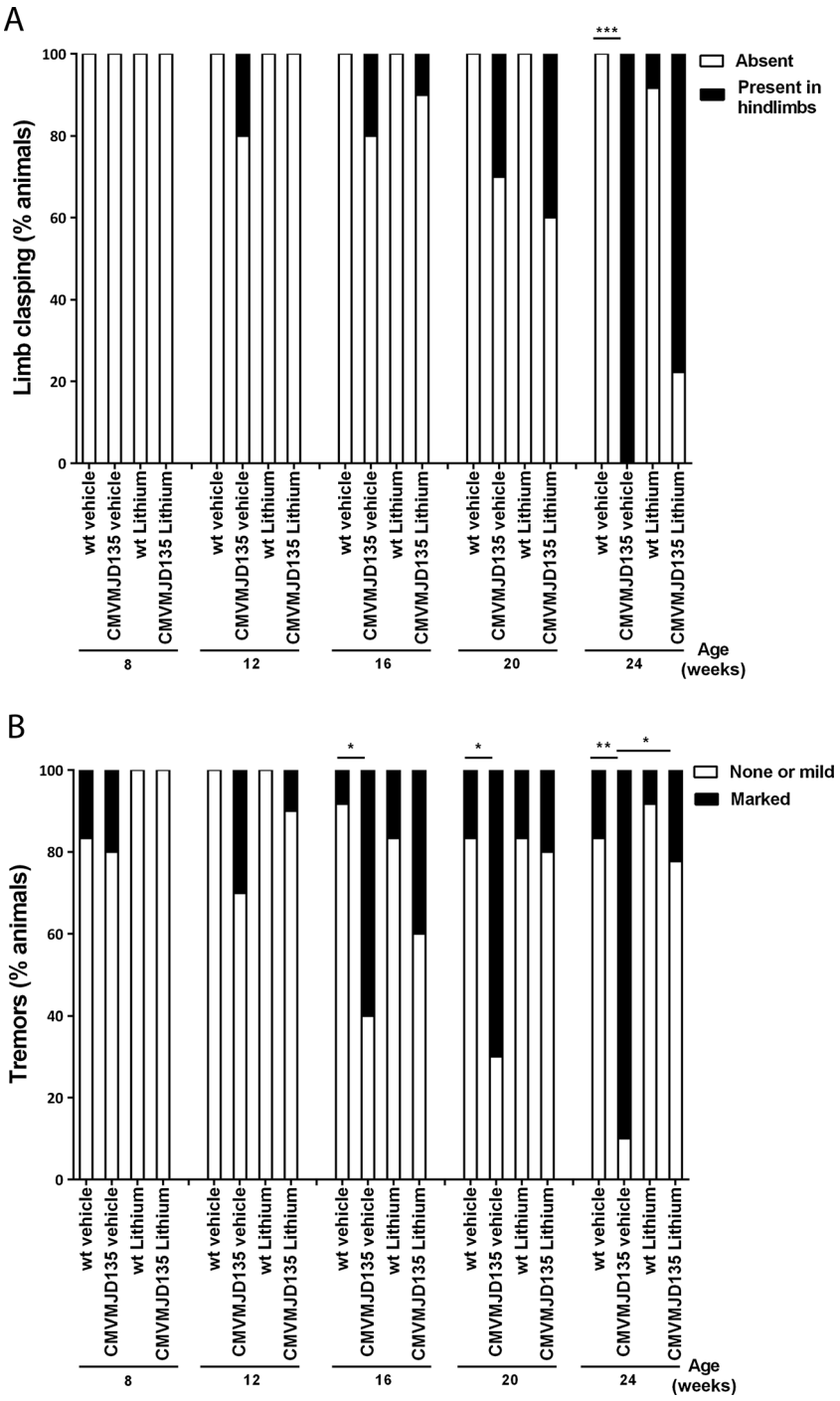

Fig. 6 Effect of lithium treatment on limb clasping and tremors. **a** Limb clasping is observed in transgenic animals—treated and non-treated—at 24 weeks of age (n=10 for each group). **b** CMVMJD135 mice presented tremors since 16 weeks of age; LiCl is able to decrease tremors in transgenic animals at 24 weeks of age (n=10 for each group). *p<0.05; **p<0.01; ***p<0.001 (Fisher's exact test)

themselves across the beam. Lithium had no significant effects in the performance in the beam of either wt or CMVMJD135 mice.

Discussion

One promising therapeutic strategy in diseases associated with misfolded protein accumulation is the stimulation of cellular degradation pathways such as macroautophagy. Here we have tested the effect of authophagy activation by lithium in a mouse model of MJD, beginning at a pre-symptomatic age.

In this study, we confirmed the progressive neurologic phenotype of the CMVMJD135 mouse model, through observation of the group of vehicle-treated animals, which behaved as previously described [48]. Chronic lithium treatment was, however, not able to rescue the neurological phenotype of these mice. The disease-causing polyQ CAG repeat

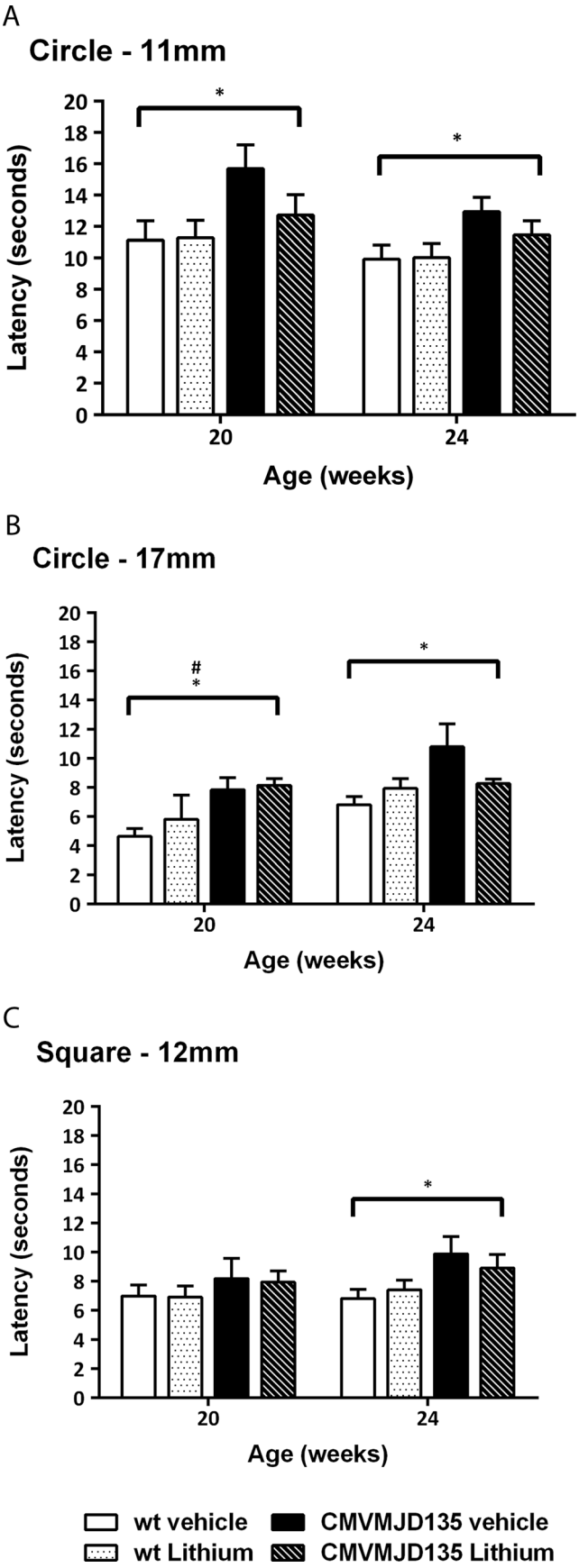

◀ **Fig. 7** Effect of lithium treatment on balance and motor coordination. Each *bar* corresponds to the mean of two consecutive trials in each beam. The time to traverse the beam was videotaped and then measured by the same experimenter. Ten to 12 animals were used for each condition. *$p<0.05$ for genotype factor (two-way ANOVA); #$p<0.05$ for genotype×treatment factor (two-way ANOVA)

expansion in ataxin-3 might cause neurotoxicity both through a toxic gain of function and a loss of the wild-type ataxin-3 normal function(s) [68]. Several molecular pathways might be involved in MJD neuropathology, although the precise pathogenic mechanism(s) is (are) not known [69, 70]. Decreased autophagy is a cellular process that might be included in these mechanisms [36, 37, 71]. An autophagy impairment was recently proposed to occur in a mouse model of MJD, as well as in the brain of MJD patients [37]. MJD pathogenesis has been modeled through the expression of mutant ataxin-3 that causes aggregate formation and toxicity, in cell models and in vivo [72], and autophagy has been shown to be an effective cellular strategy for the clearance of these aggregated proteins [73, 74]. Menzies and colleagues demonstrated that autophagy induction by rapamycin could improve rotarod performance in a transgenic mouse model of MJD [36]; however, the MJD model used in this study presented a very mild phenotype (not significantly different from control mice from a statistical standpoint), and the authors proposed that this hypothesis should be further confirmed in a model with more marked phenotype. Also, in this study, the authors suggest that it would be of great importance to test other compounds that can induce autophagy, such as lithium. Here, we provide a complete behavioral analysis of the CMVMJD135 mouse model chronically treated with lithium chloride.

At basal conditions, it was not possible to observe significant differences in protein levels of LC3-II, Beclin-1, Atg7, p62, and IMPA autophagy markers when comparing CMVMJD135 with wild-type animals at 24 weeks of age (when they have a well-established phenotype), suggesting that, in spite of the neurodegenerative changes they show [48], the autophagy process is functioning normally in the brain of these mice. This is in contrast with the findings in another transgenic mouse model of MJD, characterized by more marked overexpression of ataxin-3 and a faster disease progression [75], where it has been proposed that autophagy was over-activated but functional only at early stages of the disease [37].

Given the previous results in other related neurodegenerative diseases and our own results with 17-DMAG, which delayed disease progression the CMVMJD135 mouse and induced autophagy [48], we reasoned that even if autophagy is normal in these mice, it might be useful to boost the cells' capacity to eliminate toxic ataxin-3 aggregates; hence, we proceeded with chronic lithium treatment in the CMVMJD135 mice. In this study we selected to use a dosage

at the lower limit of the therapeutic range in order to avoid cerebellar toxicity as much as possible. The efficacy of lithium as an autophagy inducer in the brain was validated by the decrease in protein levels of IMPA-1, induction of Beclin-1 and Atg7 protein levels, increased LC3-II/LC3-I ratio, and decrease in p62 in treated CMVMJD135 mice. Our reason for studying treatment of the CMVMJD135 mice before onset of the symptoms was to have the strongest effect possible in the disease progression and to see if we could prevent or delay the onset of the disease rather than treat it once established, as mechanistically, we anticipated that it would be harder to remove the larger nuclear inclusions than smaller cytoplasmic aggregates. Considering the availability of a genetic test for MJD patients, this early stage treatment design could be feasible for mutation carriers even before they present clinical symptoms.

At the phenotypic level, LiCl treatment did not rescue the loss of body weight observed in CMVMJD135 animals. Progressive weight loss is observed in MJD patients [58], despite a normal appetite [76] and also in HD patients [77]. It has been reported previously that treatment with LiCl pre-symptomatically caused loss of body weight in a HD mouse model, whereas a gain of body weight was observed when LiCl treatment was performed in post-symptomatic animals [45]. We have not observed loss or gain of body weight as result of the treatment here performed, which was initiated 1 week before symptom onset. Intriguingly, at 8 weeks of age, lithium-treated CMVMJD135 animals showed an increase in exploratory behavior when compared with vehicle-treated CMVMJD135 animals, given by the increase in number of rears in the viewing jar. This activity reached the levels of vehicle-treated wt animals. We believe that this apparent (and transient) amelioration might have been due to an improved reaction to the novelty of the test (i.e., an effect in mood) and not because lithium was having benefic effects at the motor level, since this rescue of hypoactivity was not manifested in other motor parameters and was not maintained through life.

The tremors observed in CMVMJD135 mice were ameliorated with lithium treatment, this improvement being statistically significant only after a long period of lithium administration. This is an intriguing finding because tremors are often observed in BD patients taking lithium for long periods [78], being a side effect of this drug. Additionally, tremors are not a major symptom in MJD patients, but rather a rare manifestation [79–81] that can be treated with levodopa or dopamine agonists [82]. Thus, the tremor rescue by lithium treatment that we observed in CMVMJD135 mice at one of the time points of analysis might not have a major impact in human patients.

Gait analysis was performed using qualitative analysis, given by the "the way animals walk" in the arena—scored by the experimenter, as part of the SHIRPA protocol [51]—and by the footprinting analysis [52], respectively. In the qualitative gait analysis, vehicle-treated CMVMJD135 animals showed visible deficits in gait at 20 and 24 weeks of age. In the last time point of analysis (at 24 weeks), LiCl treatment appeared to improve the visible quality of gait, but this effect was not statistically significant.

Regarding balance (balance beam test), abnormal reflexes (limb clasping), and strength/fine motor coordination (hanging wire test), it was also not possible to observe any amelioration of CMVMJD135 mice with lithium treatment. Of notice, the number of animals used in the study allowed detection of a 50 % effect size for all tests for at least one age, with the exception of the medium square and small circle beams in the balance beam test and the exploratory locomotor activity in the SHIRPA protocol (Supplementary Table S1).

Lithium was shown to have beneficial effects in motor performance (given by rotarod analysis) in a transgenic mouse model of SCA1 [46] but had no effect in motor performance in a HD mouse model when administered pre-symptomatically [45]. The current study demonstrates that long-term peri-symptomatically initiated lithium treatment had no major effects in a mouse model of MJD. Depending on the concentration, lithium has well-established collateral effects. At least, in mice, these side effects may be the result of differences in the ability of some individual mice to clear LiCl from the plasma. In humans, at a dose of 1.5 mEq/L the side effects are considered mild, but anorexia [83], tremors [84], nausea, diarrhea, vertigo, confusion (American Psychiatric Association 2002), and cognitive impairment can occur [85]. Of relevance to this pathology, irreversible cerebellar toxicity due to lithium intoxication has long been recognized and can lead to ataxia, nystagmus, and dysarthria [86]. The pathophysiology of lithium-related ataxia appears to be related with loss of Purkinje cells in the cerebellum, with sparing of the surrounding basket cells [87]. Clinicians are aware of these risks and monitor lithium plasma levels of the patients' closely. Side effects need to be carefully analyzed since lithium can cause cerebellar toxicity even at so-called therapeutic levels [88].

While completing the experiments for this article, a human clinical trial with lithium carbonate was performed in MJD patients (http://clinicaltrials.gov/ct2/show/record/NCT01096082). This study demonstrated that lithium (at a dose of 0.5–0.8 mEq/L) was safe and well tolerated by patients during the trial period, but the disease progression was not improved after 48 weeks of follow-up, given by the Neurological Examination Score for the Assessment of Spinocerebellar Ataxia (NESSCA) and the Scale for the Assessment and Rating of Ataxia (SARA) scales. However, the authors were able to show that the patients treated with lithium had a slightly slower progression concerning two quantitative ataxia assessment tools, the mean PATA rate and the Click Test, as well as in the spinocerebellar ataxia functional index (SCAFI) and composite cerebellar functional score (CCFS),

when compared to patients receiving placebo. Considering this minor improvement in a few ataxia measures, the authors proposed that a larger number of patients should be enrolled in a new clinical trial to clarify these results [89]. Although the dosage used in our study is considerably lower than that used in the human study, and our treatment was initiated 1 week before symptom onset, this clinical trial is in accordance with the present study, where we could not find improvement by chronic LiCl treatment in the coordination and ataxia measurements, although some behavioral parameters, such as tremors and gait quality, were slightly ameliorated. Furthermore, we used similar doses as those administered in studies showing beneficial effects in mouse models of ALS and HD [44, 45] and confirmed that this dosage induced the expected biological effects, namely concerning autophagy induction.

Conclusion

In conclusion, the present study, demonstrates that chronic lithium treatment is not able to rescue the CMVMJD135 mouse phenotype; our results do not support lithium treatment as a good approach for MJD, particularly as the above mentioned side effects must be taken in consideration.

Acknowledgments We would like to thank the animal caretaker Celina Barros for technical support. We thank Dr. Alexandra Estrada and Dra. Mónica Macedo from the Clinical and Pathological laboratory of Braga Hospital for the cooperation in the determination of plasma lithium levels. This work was supported by Fundação para a Ciência e Tecnologia through the projects [FEDER/FCT, POCI/SAU-MMO/60412/2004], and [PTDC/SAU-GMG/64076/2006]. This work was supported by Fundação para a Ciência e Tecnologia through fellowships [SFRH/BD/78388/2011 to S.D-S., SFRH/BPD/91562/2012 to A.S-F., SFRH/BD/51059/2010 to A.N-C., SFRH/BPD/79469/2011 to A.T-C.]. Sara Duarte-Silva states that she had full access to all of the data in the study and take responsibility for the integrity of the data and the accuracy of the data analysis.

Conflict of Interest The authors do not report any conflict of interest.

References

1. Lin D, Mok H, Yatham LN. Polytherapy in bipolar disorder. CNS drugs. 2006;20(1):29–42.
2. Goodwin FK. Rationale for using lithium in combination with other mood stabilizers in the management of bipolar disorder. J Clin Psychiatr. 2003;64 Suppl 5:18–24.
3. Gao XM, Fukamauchi F, Chuang DM. Long-term biphasic effects of lithium treatment on phospholipase C-coupled M3-muscarinic acetylcholine receptors in cultured cerebellar granule cells. Neurochem Int. 1993;22(4):395–403.
4. Ozaki N, Chuang DM. Lithium increases transcription factor binding to AP-1 and cyclic AMP-responsive element in cultured neurons and rat brain. J Neurochem. 1997;69(6):2336–44.
5. Klein PS, Melton DA. A molecular mechanism for the effect of lithium on development. Proc Natl Acad Sci U S A. 1996;93(16):8455–9.
6. Ryves WJ, Harwood AJ. Lithium inhibits glycogen synthase kinase-3 by competition for magnesium. Biochem Biophys Res Commun. 2001;280(3):720–5. doi:10.1006/bbrc.2000.4169.
7. Hashimoto R, Takei N, Shimazu K, Christ L, Lu B, Chuang DM. Lithium induces brain-derived neurotrophic factor and activates TrkB in rodent cortical neurons: an essential step for neuroprotection against glutamate excitotoxicity. Neuropharmacology. 2002;43(7):1173–9.
8. Fukumoto T, Morinobu S, Okamoto Y, Kagaya A, Yamawaki S. Chronic lithium treatment increases the expression of brain-derived neurotrophic factor in the rat brain. Psychopharmacol (Berl). 2001;158(1):100–6. doi:10.1007/s002130100871.
9. Chen RW, Chuang DM. Long term lithium treatment suppresses p53 and Bax expression but increases Bcl-2 expression. A prominent role in neuroprotection against excitotoxicity. J Biol Chem. 1999;274(10):6039–42.
10. Hiroi T, Wei H, Hough C, Leeds P, Chuang DM. Protracted lithium treatment protects against the ER stress elicited by thapsigargin in rat PC12 cells: roles of intracellular calcium, GRP78 and Bcl-2. Pharmacogenomics J. 2005;5(2):102–11. doi:10.1038/sj.tpj.6500296.
11. Mattson MP, LaFerla FM, Chan SL, Leissring MA, Shepel PN, Geiger JD. Calcium signaling in the ER: its role in neuronal plasticity and neurodegenerative disorders. Trends Neurosci. 2000;23(5):222–9.
12. Bijur GN, De Sarno P, Jope RS. Glycogen synthase kinase-3beta facilitates staurosporine- and heat shock-induced apoptosis. Protection by lithium. J Biol Chem. 2000;275(11):7583–90.
13. Ren M, Senatorov VV, Chen RW, Chuang DM. Postinsult treatment with lithium reduces brain damage and facilitates neurological recovery in a rat ischemia/reperfusion model. Proc Natl Acad Sci U S A. 2003;100(10):6210–5. doi:10.1073/pnas.0937423100.
14. Wei H, Leeds PR, Qian Y, Wei W, Chen R, Chuang D. Beta-amyloid peptide-induced death of PC 12 cells and cerebellar granule cell neurons is inhibited by long-term lithium treatment. Eur J Pharmacol. 2000;392(3):117–23.
15. Rohn TT, Vyas V, Hernandez-Estrada T, Nichol KE, Christie LA, Head E. Lack of pathology in a triple transgenic mouse model of Alzheimer's disease after overexpression of the anti-apoptotic protein Bcl-2. J Neurosci. 2008;28(12):3051–9. doi:10.1523/JNEUROSCI.5620-07.2008.
16. Jacobsen JP, Mork A. The effect of escitalopram, desipramine, electroconvulsive seizures and lithium on brain-derived neurotrophic factor mRNA and protein expression in the rat brain and the correlation to 5-HT and 5-HIAA levels. Brain Res. 2004;1024(1–2):183–92. doi:10.1016/j.brainres.2004.07.065.
17. Berridge MJ, Downes CP, Hanley MR. Neural and developmental actions of lithium: a unifying hypothesis. Cell. 1989;59(3):411–9.
18. Quiroz JA, Gould TD, Manji HK. Molecular effects of lithium. Mol Interv. 2004;4(5):259–72. doi:10.1124/mi.4.5.6.
19. Phiel CJ, Klein PS. Molecular targets of lithium action. Annu Rev Pharmacol Toxicol. 2001;41:789–813. doi:10.1146/annurev.pharmtox.41.1.789.
20. Sarkar S, Floto RA, Berger Z, Imarisio S, Cordenier A, Pasco M, et al. Lithium induces autophagy by inhibiting inositol monophosphatase. J Cell Biol. 2005;170(7):1101–11. doi:10.1083/jcb.200504035.
21. Sarkar S, Rubinsztein DC. Inositol and IP3 levels regulate autophagy: biology and therapeutic speculations. Autophagy. 2006;2(2):132–4.
22. Melendez A, Hall DH, Hansen M. Monitoring the role of autophagy in *C. elegans* aging. Methods Enzymol. 2008;451:493–520. doi:10.1016/S0076-6879(08)03229-1.

23. Xu M, Zhang HL. Death and survival of neuronal and astrocytic cells in ischemic brain injury: a role of autophagy. Acta Pharmacol Sin. 2011;32(9):1089–99. doi:10.1038/aps.2011.50.
24. Rubinsztein DC. Autophagy induction rescues toxicity mediated by proteasome inhibition. Neuron. 2007;54(6):854–6. doi:10.1016/j.neuron.2007.06.005.
25. Rubinsztein DC, Gestwicki JE, Murphy LO, Klionsky DJ. Potential therapeutic applications of autophagy. Nat Rev Drug Discov. 2007;6(4):304–12. doi:10.1038/nrd2272.
26. Lee SJ, Lim HS, Masliah E, Lee HJ. Protein aggregate spreading in neurodegenerative diseases: problems and perspectives. Neurosci Res. 2011;70(4):339–48. doi:10.1016/j.neures.2011.05.008.
27. Levine B, Kroemer G. Autophagy in the pathogenesis of disease. Cell. 2008;132(1):27–42. doi:10.1016/j.cell.2007.12.018.
28. Cuervo AM, Stefanis L, Fredenburg R, Lansbury PT, Sulzer D. Impaired degradation of mutant alpha-synuclein by chaperone-mediated autophagy. Science. 2004;305(5688):1292–5. doi:10.1126/science.1101738.
29. Cuervo AM. Autophagy: in sickness and in health. Trends Cell Biol. 2004;14(2):70–7. doi:10.1016/j.tcb.2003.12.002.
30. Ravikumar B, Vacher C, Berger Z, Davies JE, Luo S, Oroz LG, et al. Inhibition of mTOR induces autophagy and reduces toxicity of polyglutamine expansions in fly and mouse models of Huntington disease. Nat Genet. 2004;36(6):585–95. doi:10.1038/ng1362.
31. Sarkar S, Ravikumar B, Floto RA, Rubinsztein DC. Rapamycin and mTOR-independent autophagy inducers ameliorate toxicity of polyglutamine-expanded huntingtin and related proteinopathies. Cell Death Differ. 2009;16(1):46–56. doi:10.1038/cdd.2008.110.
32. Ravikumar B, Duden R, Rubinsztein DC. Aggregate-prone proteins with polyglutamine and polyalanine expansions are degraded by autophagy. Hum Mol Genet. 2002;11(9):1107–17.
33. Nixon RA, Wegiel J, Kumar A, Yu WH, Peterhoff C, Cataldo A, et al. Extensive involvement of autophagy in Alzheimer disease: an immuno-electron microscopy study. J Neuropathol Exp Neurol. 2005;64(2):113–22.
34. Webb JL, Ravikumar B, Atkins J, Skepper JN, Rubinsztein DC. Alpha-synuclein is degraded by both autophagy and the proteasome. J Biol Chem. 2003;278(27):25009–13. doi:10.1074/jbc.M300227200.
35. Berger Z, Ravikumar B, Menzies FM, Oroz LG, Underwood BR, Pangalos MN, et al. Rapamycin alleviates toxicity of different aggregate-prone proteins. Hum Mol Genet. 2006;15(3):433–42. doi:10.1093/hmg/ddi458.
36. Menzies FM, Huebener J, Renna M, Bonin M, Riess O, Rubinsztein DC. Autophagy induction reduces mutant ataxin-3 levels and toxicity in a mouse model of spinocerebellar ataxia type 3. Brain : J Neurol. 2010;133(Pt 1):93–104. doi:10.1093/brain/awp292.
37. Nascimento-Ferreira I, Santos-Ferreira T, Sousa-Ferreira L, Auregan G, Onofre I, Alves S et al. Overexpression of the autophagic beclin-1 protein clears mutant ataxin-3 and alleviates Machado-Joseph disease. Brain. 2011. doi:10.1093/brain/awr047.
38. Meijer AJ, Codogno P. Regulation and role of autophagy in mammalian cells. Int J Biochem Cell Biol. 2004;36(12):2445–62. doi:10.1016/j.biocel.2004.02.002.
39. Yu WH, Cuervo AM, Kumar A, Peterhoff CM, Schmidt SD, Lee JH, et al. Macroautophagy—a novel beta-amyloid peptide-generating pathway activated in Alzheimer's disease. J Cell Biol. 2005;171(1):87–98. doi:10.1083/jcb.200505082.
40. Menzies FM, Ravikumar B, Rubinsztein DC. Protective roles for induction of autophagy in multiple proteinopathies. Autophagy. 2006;2(3):224–5.
41. Xiong N, Jia M, Chen C, Xiong J, Zhang Z, Huang J, et al. Potential autophagy enhancers attenuate rotenone-induced toxicity in SH-SY5Y. Neuroscience. 2011;199:292–302. doi:10.1016/j.neuroscience.2011.10.031.
42. Stambolic V, Ruel L, Woodgett JR. Lithium inhibits glycogen synthase kinase-3 activity and mimics wingless signalling in intact cells. Curr Biol. 1996;6(12):1664–8.
43. Feng HL, Leng Y, Ma CH, Zhang J, Ren M, Chuang DM. Combined lithium and valproate treatment delays disease onset, reduces neurological deficits and prolongs survival in an amyotrophic lateral sclerosis mouse model. Neuroscience. 2008;155(3):567–72. doi:10.1016/j.neuroscience.2008.06.040.
44. Fornai F, Longone P, Cafaro L, Kastsiuchenka O, Ferrucci M, Manca ML et al. Lithium delays progression of amyotrophic lateral sclerosis. Proceedings of the National Academy of Sciences of the United States of America. 2008;105(6):2052-7. doi:10.1073/pnas.0708022105
45. Wood NI, Morton AJ. Chronic lithium chloride treatment has variable effects on motor behaviour and survival of mice transgenic for the Huntington's disease mutation. Brain Res Bull. 2003;61(4):375–83.
46. Watase K, Gatchel JR, Sun Y, Emamian E, Atkinson R, Richman R, et al. Lithium therapy improves neurological function and hippocampal dendritic arborization in a spinocerebellar ataxia type 1 mouse model. PLoS Med. 2007;4(5):e182. doi:10.1371/journal.pmed.0040182.
47. Jia DD, Zhang L, Chen Z, Wang CR, Huang FZ, Duan RH et al. Lithium chloride alleviates neurodegeneration partly by inhibiting activity of GSK3beta in a SCA3 *Drosophila* model. Cerebellum. 2013. doi:10.1007/s12311-013-0498-3.
48. Silva-Fernandes A, Duarte-Silva S, Neves-Carvalho A, Amorim M, Soares-Cunha C, Oliveira P et al. Chronic treatment with 17-DMAG improves balance and coordination in a new mouse model of Machado-Joseph disease. Neurotherapeutics : the journal of the American Society for Experimental NeuroTherapeutics. 2014. doi:10.1007/s13311-013-0255-9.
49. Nicklas W, Baneux P, Boot R, Decelle T, Deeny AA, Fumanelli M, et al. Recommendations for the health monitoring of rodent and rabbit colonies in breeding and experimental units. Lab Anim. 2002;36(1):20–42.
50. Silva-Fernandes A, Costa MD, Duarte-Silva S, Oliveira P, Botelho CM, Martins L et al. Motor uncoordination and neuropathology in a transgenic mouse model of Machado-Joseph disease lacking intranuclear inclusions and ataxin-3 cleavage products. Neurobiol Dis. 2010. doi:10.1016/j.nbd.2010.05.021.
51. Rogers DC, Fisher EM, Brown SD, Peters J, Hunter AJ, Martin JE. Behavioral and functional analysis of mouse phenotype: SHIRPA, a proposed protocol for comprehensive phenotype assessment. Mamm Genome : Off J Int Mamm Genome Soc. 1997;8(10):711–3.
52. Carter RJ, Lione LA, Humby T, Mangiarini L, Mahal A, Bates GP, et al. Characterization of progressive motor deficits in mice transgenic for the human Huntington's disease mutation. J Neurosci : Off J Soc Neurosci. 1999;19(8):3248–57.
53. Rafael JA, Nitta Y, Peters J, Davies KE. Testing of SHIRPA, a mouse phenotypic assessment protocol, on Dmd(mdx) and Dmd(mdx3cv) dystrophin-deficient mice. Mamm Genome. 2000;11(9):725–8. doi:10.1007/s003350010149.
54. JH Z. Biostatistical analysis (4th Edition). Prentice Hall; 1999
55. Klionsky DJ, Abeliovich H, Agostinis P, Agrawal DK, Aliev G, Askew DS, et al. Guidelines for the use and interpretation of assays for monitoring autophagy in higher eukaryotes. Autophagy. 2008;4(2):151–75.
56. Itakura E, Kishi C, Inoue K, Mizushima N. Beclin 1 forms two distinct phosphatidylinositol 3-kinase complexes with mammalian Atg14 and UVRAG. Mol Biol Cell. 2008;19(12):5360–72. doi:10.1091/mbc.E08-01-0080.
57. Baptista T, Teneud L, Contreras Q, Alastre T, Burguera JL, de Burguera M, et al. Lithium and body weight gain. Pharmacopsychiatry. 1995;28(2):35–44. doi:10.1055/s-2007-979586.

58. Saute JAM, da Silva ACF, Souza GN, Russo AD, Donis KC, Vedolin L, et al. Body mass index is inversely correlated with the expanded CAG repeat length in SCA3/MJD patients. Cerebellum. 2012;11(3):771–4.
59. Lalonde R, Strazielle C. Brain regions and genes affecting limb-clasping responses. Brain Res Rev. 2011;67(1–2):252–9. doi:10.1016/j.brainresrev.2011.02.005.
60. Chou AH, Yeh TH, Ouyang P, Chen YL, Chen SY, Wang HL. Polyglutamine-expanded ataxin-3 causes cerebellar dysfunction of SCA3 transgenic mice by inducing transcriptional dysregulation. Neurobiol Dis. 2008;31(1):89–101. doi:10.1016/j.nbd.2008.03.011.
61. Cemal CK, Carroll CJ, Lawrence L, Lowrie MB, Ruddle P, Al-Mahdawi S, et al. YAC transgenic mice carrying pathological alleles of the MJD1 locus exhibit a mild and slowly progressive cerebellar deficit. Hum Mol Genet. 2002;11(9):1075–94.
62. Mangiarini L, Sathasivam K, Seller M, Cozens B, Harper A, Hetherington C, et al. Exon 1 of the HD gene with an expanded CAG repeat is sufficient to cause a progressive neurological phenotype in transgenic mice. Cell. 1996;87(3):493–506.
63. Fernagut PO, Diguet E, Bioulac B, Tison F. MPTP potentiates 3-nitropropionic acid-induced striatal damage in mice: reference to striatonigral degeneration. Exp Neurol. 2004;185(1):47–62.
64. Wirths O, Weis J, Kayed R, Saido TC, Bayer TA. Age-dependent axonal degeneration in an Alzheimer mouse model. Neurobiol Aging. 2007;28(11):1689–99. doi:10.1016/j.neurobiolaging.2006.07.021.
65. Lalonde R, Dumont M, Staufenbiel M, Strazielle C. Neurobehavioral characterization of APP23 transgenic mice with the SHIRPA primary screen. Behav Brain Res. 2005;157(1):91–8. doi:10.1016/j.bbr.2004.06.020.
66. Lalonde R, Lewis TL, Strazielle C, Kim H, Fukuchi K. Transgenic mice expressing the betaAPP695SWE mutation: effects on exploratory activity, anxiety, and motor coordination. Brain Res. 2003;977(1):38–45.
67. Brooks SP, Dunnett SB. Tests to assess motor phenotype in mice: a user's guide. Nat Rev Neurosci. 2009;10(7):519–29. doi:10.1038/nrn2652.
68. Riess O, Rub U, Pastore A, Bauer P, Schols L. SCA3: neurological features, pathogenesis and animal models. Cerebellum. 2008;7(2):125–37. doi:10.1007/s12311-008-0013-4.
69. Costa MD, Paulson HL. Toward understanding Machado-Joseph disease. Prog Neurobiol. 2011. doi:10.1016/j.pneurobio.2011.11.006
70. Matos CA, de Macedo-Ribeiro S, Carvalho AL. Polyglutamine diseases: the special case of ataxin-3 and Machado-Joseph disease. Prog Neurobiol. 2011;95(1):26–48. doi:10.1016/j.pneurobio.2011.06.007.
71. Xiao H, Tang J, Hu Z, Tan J, Tang B, Jiang Z. [Polyglutamine-expanded ataxin-3 is degraded by autophagy]. Zhonghua Yi Xue Yi Chuan Xue Za Zhi. 2010;27(1):23-8. doi:10.3760/cma.j.issn.1003-9406.2010.01.005.
72. Paulson HL, Perez MK, Trottier Y, Trojanowski JQ, Subramony SH, Das SS, et al. Intranuclear inclusions of expanded polyglutamine protein in spinocerebellar ataxia type 3. Neuron. 1997;19(2):333–44.
73. Cheung ZH, Ip NY. Autophagy deregulation in neurodegenerative diseases—recent advances and future perspectives. J Neurochem. 2011;118(3):317–25. doi:10.1111/j.1471-4159.2011.07314.x.
74. Mizushima N, Levine B, Cuervo AM, Klionsky DJ. Autophagy fights disease through cellular self-digestion. Nature. 2008;451(7182):1069–75. doi:10.1038/nature06639.
75. Goti D, Katzen SM, Mez J, Kurtis N, Kiluk J, Ben-Haiem L, et al. A mutant ataxin-3 putative-cleavage fragment in brains of Machado-Joseph disease patients and transgenic mice is cytotoxic above a critical concentration. J Neurosci : Off J Soc Neurosci. 2004;24(45):10266–79. doi:10.1523/JNEUROSCI.2734-04.2004.
76. Schmitt I, Brattig T, Gossen M, Riess O. Characterization of the rat spinocerebellar ataxia type 3 gene. Neurogenetics. 1997;1(2):103–12.
77. Sanberg PR, Fibiger HC, Mark RF. Body weight and dietary factors in Huntington's disease patients compared with matched controls. Med J Aust. 1981;1(8):407–9.
78. Gelenberg AJ, Jefferson JW. Lithium tremor. J Clin Psychiatry. 1995;56(7):283–7.
79. Bettencourt C, Santos C, Coutinho P, Rizzu P, Vasconcelos J, Kay T, et al. Parkinsonian phenotype in Machado-Joseph disease (MJD/SCA3): a two-case report. BMC Neurol. 2011;11:131. doi:10.1186/1471-2377-11-131.
80. Coutinho P, Sequeiros J. Clinical, genetic and pathological aspects of Machado-Joseph disease. J Genet Hum. 1981;29(3):203–9.
81. Ishida C, Sakajiri K, Yoshikawa H, Sakashita Y, Okino S, Yamaguchi K, et al. Lower limb tremor in Machado-Joseph disease. Neurology. 1998;51(4):1225–6.
82. Nandagopal R, Moorthy SG. Dramatic levodopa responsiveness of dystonia in a sporadic case of spinocerebellar ataxia type 3. Postgrad Med J. 2004;80(944):363–5.
83. Savvopoulos S, Golaz J, Bouras C, Constantinidis J, Tissot R. Huntington chorea. Anatomoclinical and genetic study of 17 cases. Encéphale. 1990;16(4):251–9.
84. Miodownik C, Witztum E, Lerner V. Lithium-induced tremor treated with vitamin B6: a preliminary case series. Int J Psychiatry Med. 2002;32(1):103–8.
85. Tremont G, Stern RA. Minimizing the cognitive effects of lithium therapy and electroconvulsive therapy using thyroid hormone. Int J Neuropsychopharmacol. 2000;3(2):175–86. doi:10.1017/S1461145700001838.
86. Grignon S, Bruguerolle B. Cerebellar lithium toxicity: a review of recent literature and tentative pathophysiology. Therapie. 1996;51(2):101–6.
87. Peiffer J. Clinical and neuropathological aspects of long-term damage to the central nervous system after lithium medication. Arch Psychiatr Nervenkr. 1981;231(1):41–60.
88. Niethammer M, Ford B. Permanent lithium-induced cerebellar toxicity: three cases and review of literature. Mov Disord. 2007;22(4):570–3. doi:10.1002/mds.21318.
89. Saute JA, Machado de Castilhos R, Monte TL, Schumacher-Schuh AF, Donis KC, D'Avila R et al. A randomized, phase 2 clinical trial of lithium carbonate in Machado-Joseph disease. Movement disorders : official journal of the Movement Disorder Society. 2014. doi:10.1002/mds.25803.

Supplementary material

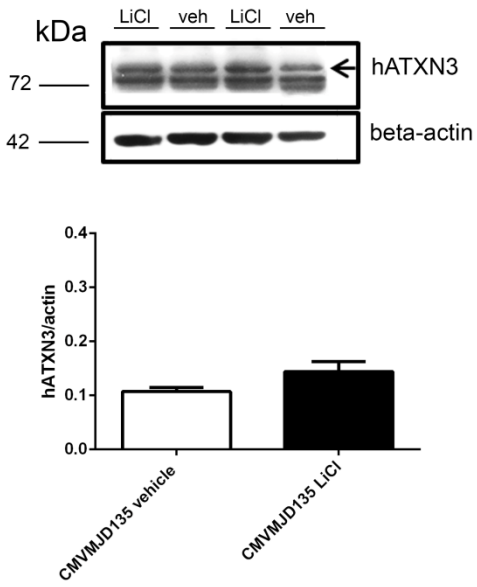

Supplementary figure 1: Levels of human ataxin-3 in LiCl-treated animals. Anti-ataxin-3 western-blot of brain lysates of transgenic animals injected with vehicle (veh) (n = 4) or lithium chloride (LiCl) 10.4 mg/Kg (n = 4) at 24 weeks of age. Actin was used as loading control (test-t student).

Supplementary Table 1. Sample size calculations for each behavioral test assuming a power of 0.8 and a significance level of 0.05.

Age (weeks)				4	5	6	8	9	10	12	13	14	16	17	18	20	24
BEHAVIORAL TESTS	WEIGHT		Effect size							2,35	2,20	3,64	3,83	4,07	4,35	5,18	
			n							3,00	3,00	3,00	3,00	3,00	3,00	3,00	
	REARINGS (NUMBER OF REARS)		Effect size										0,50			0,95	1,84
			n										35,00			9,00	5,00
	LOCOMOTOR ACTIVITY (NUMBER OF SQUARES)		Effect size													0,53	0,61
			n													50,00	25,00
	HANGING WIRE TEST (LATENCY)		Effect size				2,30			6,34			9,27			8,87	3,12
			n				3,00			3,00			3,00			3,00	3,00
	BALANCE BEAM TEST (LATENCY)	MEDIUM SQUARE	Effect size														0,55
			n														30,00
		CIRCLE 17 MM	Effect size													0,41	2,31
			n													50,00	3,00
		CIRCLE 11 MM	Effect size													0,56	0,59
			n													25,00	35,00

Chapter 4

Combined therapy with m-TOR-dependent and –independent autophagy inducers causes neurotoxicity in a mouse model of Machado-Joseph disease

Combined therapy with m-TOR-dependent and –independent autophagy inducers causes neurotoxicity in a mouse model of Machado-Joseph disease

Sara Duarte-Silva[a,b], Anabela Silva-Fernandes[a,b], Andreia Neves-Carvalho[a,b], Carina Soares-Cunha[a,b], Andreia Teixeira-Castro[a,b] and Patrícia Maciel[*a,b]

a) Life and Health Sciences Research Institute (ICVS), School of Health Sciences, University of Minho, Braga, Portugal;
b) ICVS/3B's - PT Government Associate Laboratory, Braga/Guimarães, Portugal

[*] Corresponding author: Patrícia Maciel, PhD. Life and Health Sciences Research Institute (ICVS), School of Health Sciences, ICVS/3B's – PT Government Associate Laboratory, University of Minho, Campus Gualtar, 4710-057 Braga, Portugal. Telephone: 351-253-604824, Fax: 351-253-604820. E-mail: pmaciel@ecsaude.uminho.pt

Abstract

A major pathological hallmark in several human neurodegenerative disorders, like Parkinson's disease (PD) and polyglutamine (polyQ) disorders, including Machado-Joseph disease (MJD), is the formation of intra-neuronal protein aggregates. MJD is an inherited neurodegenerative disease, caused by a CAG repeat expansion in the *ATXN3* gene, resulting in an abnormal protein, which is prone to misfolding and forms cytoplasmic and nuclear aggregates within neurons, ultimately inducing neurodegeneration.

Treatment of proteinopathies with drugs that up-regulate autophagy, like rapamycin, has shown promising results in cell, fly and mouse models of polyQ diseases. Temsirolimus (Cell Cycle inhibitor-779, CCI-779) is an analogue of rapamycin that inhibits the mammalian target of rapamycin (m-TOR), while lithium chloride acts by inhibiting inositol monophosphatase (IMPase), reducing free inositol and IP3 levels, both compounds being able to induce autophagy.

We have previously shown that chronic treatment with lithium chloride (10.4 mg/Kg) had limited effects in a transgenic MJD mouse model. Also, others have shown that temsirolimus had mild positive effects in a different mouse model of the disease. It has been suggested that the combination of mTOR-dependent and –independent autophagy inducers could be a more effective therapeutic approach. To further explore this avenue towards therapy, we treated CMVMJD135 transgenic mice with a conjugation of temsirolimus and lithium, both at concentrations known to induce autophagy and not to be toxic. Surprisingly, this combined treatment proved to be deleterious to both wild-type and transgenic animals, failing to rescue their neurological symptoms and actually exerting neurotoxic effects.

These results highlight the possible dangers of manipulating autophagy in the nervous system and suggest that a better understanding of the potential disruption in the autophagy pathway in SCA3/MJD are required before successful long-term autophagy modulating therapies can be developed.

Keywords: Polyglutamine diseases, animal models, ataxia, behavior, therapy, autophagy

Introduction

Machado-Joseph disease (MJD), also known as Spinocerebellar Ataxia type 3 (SCA3), is the most common autosomal dominant ataxia worldwide (1), and is caused by a CAG repeat expansion within the coding region of the *ATXN3* gene (2). The clinical severity and the age at onset of the disease depend on the length of the expanded repeat (3, 4). MJD is characterized by motor uncoordination and amyotrophy, spasticity, gait ataxia, difficulty with speech and swallowing, altered eye movements, double vision, and frequent urination (5, 6).

MJD shares many features with other polyglutamine diseases, such as the formation of cytoplasmic and nuclear inclusion bodies within neurons by the mutant protein (7, 8). It is assumed that the common toxic gain-of-function mechanisms for the polyglutamine-containing protein depend on aggregation and deposition of misfolded proteins leading to neuronal dysfunction and eventually cell death (9).

Despite the well-described clinical and pathological phenotypes, the molecular and cellular events underlying neurodegeneration in these disorders are still poorly understood. Compelling evidence points to major aetiological roles for interference with transcriptional regulation, protein aggregation and clearance, the ubiquitin-proteasome system and alterations of calcium homeostasis in the neuronal loss observed during the neurodegenerative process. These pathways could act independently or, more likely, interact and enhance each other, triggering the accumulation of cellular damage that eventually leads to dysfunction and death (10). This suggests that simultaneous targeting of several pathways may be therapeutically necessary to prevent neurodegeneration and preserve neuronal function. Understanding how dysregulation of these pathways mediates disease progression is leading to the first attempts of obtaining effective therapeutic strategies *in vivo*, which may prove beneficial in the treatment of polyQ diseases. One such pathway is autophagy, a process that encompasses lysosomal degradation of cytoplasmic material, such as defective organelles and unfolded/aggregated proteins. Autophagy is morphologically defined by the appearance of numerous cytosolic autophagosomes, which are formed by the assembly and expansion of double layered, membrane bound structures of unknown origin around whole organelles and isolated proteins. The autophagosomes encapsulate cytosolic materials and subsequently dock and fuse with lysosomes or other vacuoles, resulting in the degradation of their contents (11). In several neurological diseases, the pathological accumulation of autophagosomes/ autophagosome-like structures and abnormalities in the endosomal-lysosomal pathway has been documented by electron microscopy (EM) in human *post mortem* brain tissue (12-16). While initially this was interpreted as evidence of death triggered by

autophagy, the currently predominant perspective is that this vesicle accumulation reflects impaired autophagy completion, which is emerging as a common element to several neurodegenerative disorders (17, 18). Autophagy induction has therefore been advanced as a promising therapeutic strategy for these diseases (19, 20), and in the particular case of MJD, genetic approaches in lentiviral overexpression models have supported this conclusion (21).

The mammalian target of rapamycin (mTOR) kinase is a master negative regulator of autophagy (22). mTOR is a central sensor of energy status, growth factors and nutrient signals, and can be inhibited by rapamycin (23) and related small molecules (24). Besides this pathway, autophagy can also be regulated independently of mTOR (25). Inhibition of inositol monophosphatase (IMPase) reduces free inositol and IP3 levels, which leads to an upregulation of autophagy. Rapamycin has been shown to reduce aggregation of expanded polyQ in transfected cells (26), to protect against neurodegeneration in a fly model of Huntington disease (HD), and to improve motor performance and decrease aggregate formation in a mouse model of HD (27). Lithium, an mTOR-independent autophagy inducer has been shown to improve motor performance and depressive-like behavior in a mouse model of HD, as well as to improve neuropathology and motor function in a SCA1 mouse model (28, 29). We have recently shown that 19 weeks of lithium chloride (10.4 mg/Kg) treatment in the CMVMJD135 mouse model (30), had limited effects on the motor phenotype of these animals, despite its ability to induce autophagy both in the chronic and acute treatment (30). Temsirolimus (cell cycle inhibitor-779), a less toxic rapamycin analogue, was recently approved by the Food and Drug Administration (FDA) for the treatment of renal cell carcinoma (31, 32). This drug was shown to reduce mutant ataxin-3 levels and toxicity, as well as ameliorate the disease symptoms in a transgenic mouse model of MJD (19). Additionally, Menzies and colleagues suggested that the use of combined lithium and temsirolimus would be an interesting approach to explore (33). The theoretical basis for this combinatory approach would be the fact that lithium can act both as autophagy inducer or inhibitor, depending on the dose used (25, 34). At higher dosages lithium is actually able to inhibit GSK3, which suppresses autophagy via phosphorylation of mTOR (34, 35); thus, a combinatory therapy with another mTOR-dependent autophagy inducer could counteract this effect. The main goal of this work was to test the potential of this combinatory treatment in a MJD. We treated MJD transgenic animals (36, 37) chronically with a combination of temsirolimus and lithium – LiCl+CCI-779 (m-TOR-dependent and independent pathways, respectively). We show that the combinatory treatment using lithium and temsirolimus improved locomotion defects of a transgenic *C.elegans* model of MJD. However, our results show that the simultaneous administration of LiCl and CCI-779 was ineffective in rescuing the motor impairments

of CMVMJD135 mice and had deleterious effects both in CMVMJD135 and wild-type (wt) animals at the doses used in this pre-clinical trial.

Material and methods

Nematode strains and general methods. Standard methods were used for culturing and observing *C. elegans* (38). Briefly, nematodes were grown on nematode growth medium (NGM) plates seeded with *Escherichia coli* OP50 strain at 20°C. The transgenic AT3q130 strain used in this work was previously described by Teixeira-Castro et al (37). All assays were performed at room temperature (20 °C) on 4-days old synchronized animals grown at 20°C.

C. elegans **drug treatment and motility assay.** AT3q130 animals were grown in liquid culture in a 96-well plate format, with the combination of lithium and CCI779. Four day old animals were transferred from the 96-well plates onto an unseeded NGM plate (equilibrated at 20°C). Plates were allowed to dry for 1 hour before starting the assays. Motility assays were performed at 20°C as previously described (37, 39). Animals remaining inside a 1-cm circle after one min were scored as locomotion defective. Motor behavior assays were run in triplicates or quadruplicates (n=3 or 4), with a total of at least 150 animals tested per compound concentration. Compound preparation: Stock solution of 200 mM LiCl (1.05679-0100, Merck) was prepared in water. CCI779 (T8040, LC-laboratories) 48.5 mM stock solution was prepared in EtOH.

Ethics statement. All procedures with mice were conducted in accordance with European regulations (European Union Directive 2010/63/EU). Animal facilities and the people directly involved in animal experiments (S.D.S, A.N.C) were certified by the Portuguese regulatory entity — Direcção Geral de Alimentação e Veterinária.

All of the protocols performed were approved by the Animal Ethics Committee of the Life and Health Sciences Research Institute, University of Minho.

Mouse strains, maintenance and general methods. Male CMVMJD135 mice (background C57BL/6) (40) were used in the study since they were expected to show less variability than females in behavioral tests, due to the hormonal female status. Transgenic and non-transgenic drug- and placebo- treated animals were sequentially assigned and housed at weaning in groups of 5

animals in filter-topped polysulfone cages 267 × 207 × 140 mm (370 cm^2 floor area) (Tecniplast, Buguggiate, Italy), with corncob bedding (Scobis Due, Mucedola SRL, Settimo Milanese, Italy) in a conventional animal facility. The progeny produced by mating MJD transgenic with wild-type animals were genotyped at weaning by PCR, as we previously described (41). The experiment started at 4 weeks and ended at 24 weeks of age. All animals were maintained under standard laboratory conditions: an artificial 12 h light/dark cycle (lights on from 8:00 to 20:00 h), with an ambient temperature of 21±1 °C and a relative humidity of 50–60%; the mice were given a standard diet (4RF25 during the gestation and postnatal periods, and 4RF21 after weaning, Mucedola SRL, Settimo Milanese, Italy) and water *ad libitum*. Health monitoring was performed according to FELASA guidelines (42), confirming the Specified Pathogens status of sentinel animals maintained in the same animal room. Humane endpoints for experiment were defined (20% reduction of the body weight, inability to reach food and water, presence of wounds in the body, dehydration), but not needed in practice as the study period was conceived to include ages at which animals do not reach these endpoints. The animals were sacrificed by decapitation. The timeline used in this study is shown in Fig. 2A.

Drug treatment. In order to conduct this pre-clinical trial we used a combination of two FDA-approved compounds, lithium (LiCl, Merck) and temsirolimus (CCI-779, LC Laboratories). Mice were allocated to vehicle and LiCl+CCI-779-treated groups. The final numbers of animals in each group were: vehicle-treated CMVMJD135, n = 12; LiCl+CCI-779-treated CMVMJD135, n=10; vehicle-treated wt, n = 12; LiCl+CCI-779-treated wt, n=15. The treatment started at the asymptomatic age of 5 weeks. Animals were intraperitoneally injected three times a week in the testing room and immediately placed in their home cage, except in the week of behavioral tests. Transgenic and non-transgenic animals were treated with 10.4 mg/kg of lithium and 20 mg/kg of temsirolimus (doses and routes as previously described by (27-30)). Lithium stock solutions were prepared at a concentration of 25mg/kg in 0.15 M NaCl, 5% Tween-20 and 5% PEG 400 and Temsirolimus at 50 mg/kg in absolute ethanol. Control animals were given a placebo injection of buffer (0.15 M NaCl, 5% Tween-20 and 5% PEG 400) with the same frequency.

Body weight. All mice were weighed a week before the start of the drug treatment (4 weeks) and then at 8, 12, 16, 20 and 24 weeks of age.

Behavioral tests*.* The behavioral tests herein shown were performed as previously described (30). At 4 weeks of age we tested the motor performance and screened the overall health status of the animals using the SHIRPA protocol (43), before starting the treatment with the combined compounds. The SHIRPA protocol was applied at 4, 8, 12 and 16, 20 and 24 weeks of age (protocol details are

available at the site: http://empress.har.mrc.ac.uk/browser/?sop_id=10_002_0). In addition, we included the footprint pattern test (44). The protocol was adjusted in order to minimize animal handling and to generate uniformity in waiting times between the tests (45). To analyze the foot dragging phenotype (at 8, 12 and 20 weeks of age), six consecutive steps were evaluated and the presence or absence of foot dragging phenotype was registered as previously described (30).

The beam walk test, which assesses balance but is also sensitive to motor coordination was performed as previously described at 20 and 24 weeks of age (30). The time animals took to cross the beam was counted, and time was discounted if animals stopped in the beam.

Western-blot

Mouse brain tissue was homogenized in cold 0.1 M Tris-HCl, pH 7.5, 0.1 M EDTA, in the presence of a mixture of protease inhibitors (Complete; Roche, Swiss). Protein concentration was determined using the Bradford assay (Biorad, California, USA). Samples were heated for 5 minutes at 100°C, and microfuged for 10 seconds before loading. For each sample, 50 micrograms of total protein were loaded into SDS-Page gels and then transferred to nitrocellulose membranes (Biorad, California, USA). After, the membranes were incubated with the primary antibodies: rabbit anti-p62 (1:50, Abcam, Cambridge, UK) and rabbit anti-Beclin-1 (1:1000, Cell signaling, Beverly, MA), mouse anti-beta-actin (Ambion, 1:5000, Life Technologies, CA, USA), rabbit anti-LC3 (1:1000 Novus Biologicals, Littleton, CO) and rabbit anti-ataxin3 serum (1:5000; kindly provided by Dr. Henry Paulson). The secondary antibodies were incubated at the following dilutions: anti-rabbit (1:10.000, Biorad, California, USA) and anti-mouse (1:10.000, Biorad, California, USA). Antibody affinity was detected by chemiluminescence (Clarity ECL kit, Biorad, California, USA). Western-blot quantifications were performed using the Chemidoc XRS Software with ImageLab Software (Biorad, USA) according to the manufacturer's instructions and using beta-actin as the loading control.

Statistical analysis

The experimental unit used in this study was a single animal. Power analysis was used to determine the sample size as previously described (36). The estimates of required number of animals for specific behavioral tests and time-points of analysis are described in (30). Continuous variables with normal distributions (K-S test $p>0.05$) were analyzed with the Student t-test or two-way ANOVA (Factors: genotype and treatment). Behavioral data were subjected to the non-parametric Mann-Whitney U-test

when variables were non-continuous or when a continuous variable did not present a normal distribution (Kolmogorov-Smirnov test $p<0.05$). Categorical variables in the SHIRPA protocol were analyzed by contingency tables (Fisher's exact test). All statistical analyses were performed using SPSS 22.0 (SPSS Inc., Chicago, IL). A critical value for significance of $p< 0.05$ was used throughout the study.

Results

LiCl+CCI779 treatment improved locomotion deficits in a transgenic *C.elegans* model of MJD

We evaluated compound efficacy to rescue neuronal dysfunction in a *C. elegans* model of MJD pathogenesis, in which expression of mutant ATXN3 (AT3q130) in all neuronal cells results in locomotion defects (37). AT3q130 animals grown in liquid medium with or without drug for four days were tested for defects in locomotion, by employing a motility assay. Treatment with LiCl and CCI779 resulted in a partial rescue of locomotion impairment (Fig. 1). Taking these results in consideration, we pursued with this potential combinatory treatment by performing a pre-clinical trial in an MJD mouse model.

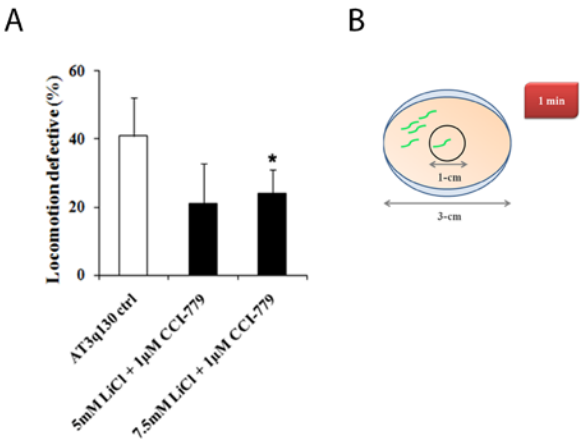

Figure 1. AT3q130 animals treatment with the small molecules targeting autophagy. (A) AT3q130 animals treated with 7.5mM of LiCl plus CCI-779 at 1 μM showed a significant reduction in locomotion defects given by the motility assay. **(B)** Schematic representation of the motility assay for *C.elegans*. Data are the mean ± SD, at least 150 animals per data point. Student's t-test, *p< 0.05.

The CMVMJD135 transgenic mice, expressing full-length human ataxin-3 with an expanded polyQ repeat of 135 glutamines ubiquitously and at near endogenous levels, have previously been shown to develop a slowly progressive motor and neuropathological phenotype resembling MJD (36). We treated these mice with LiCl+CCI-779 at dosages previously described, for each compound individually, to activate autophagy and not to be toxic (10.4 and 20 mg/Kg respectively) (27, 28, 30). We started the treatment regimen at 5 weeks of age (one week before the onset of the symptoms) and followed the animals until they reached 24 weeks, performing a monthly extensive characterization of

the animals using the SHIRPA protocol and the Beam walk test. The study design is summarized in Fig. 2A. Before the beginning of injections, at 4 weeks of age, mice were evaluated using the SHIRPA protocol, and no differences were observed between wild-type and transgenic animals.

Survival and general health

Survival is not a useful readout in pre-clinical trials using the CMVMJD135 model, because animals, although very sick, survive until quite late ages; however, during this pre-clinical trial three transgenic animals treated with LiCl+CCI-779 died (while none of the untreated animals died, p=0.006), which we attribute to the toxicity of the compounds when administered together. At the end of the experiment, both CMVMJD135 and wt mice treated with LiCl+CCI-779 presented an unhealthy appearance, but were still able to move and feed.

Administration of LiCl+CCI-779 to wt mice caused a significant decrease in the body weight in comparison to the vehicle group (p=0.002). This drug combination treatment also diminished significantly the already reduced body weight of CMVMJD135 mice when compared to the vehicle-treated transgenic group (p=0.001) (Fig. 2B).

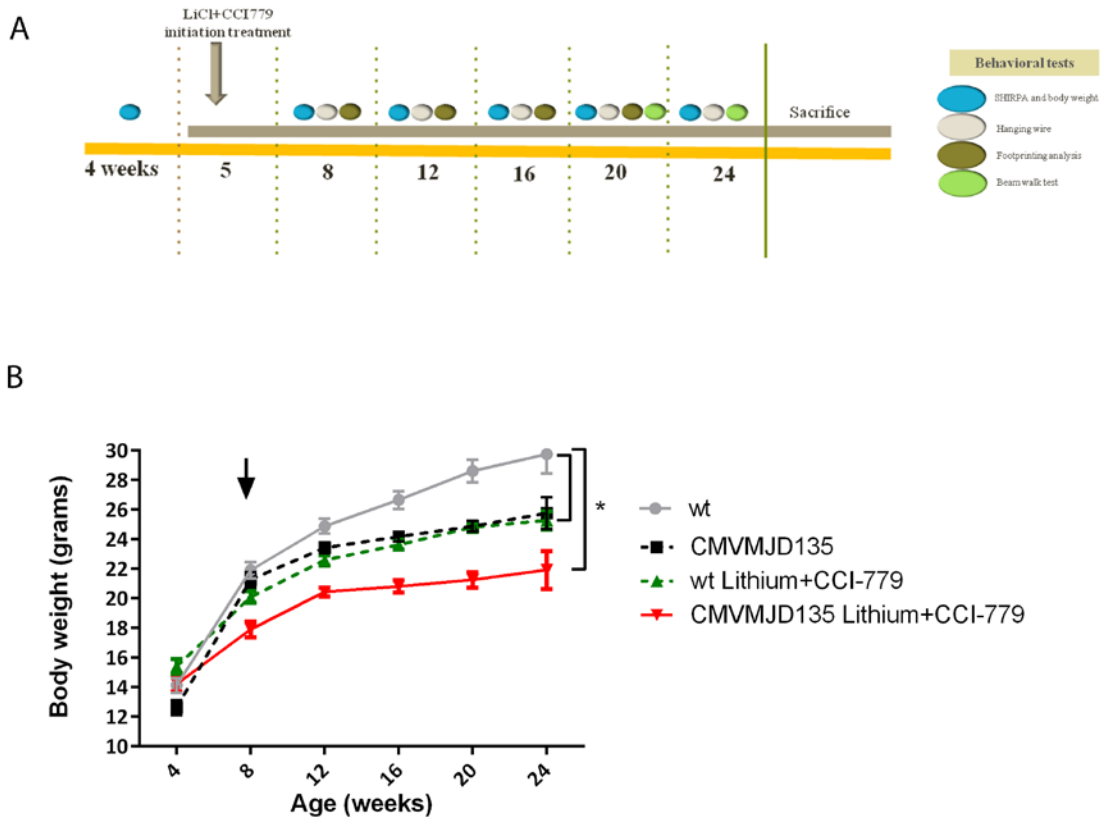

Figure 2. Effect of LiCl+CCI779 treatment on body weight of CMVMJD135 and wild-type mice. (A) Schematic timeline for the behavioral analysis of Lithium+CCI779 pre-clinical trial. **(B)** The body weight in grams between 8 to 24 weeks of age is depicted for wt and CMVMJD135 mice treated with LiCl+CCI779 or vehicle (n=10-12 for each group). Symbols represent mean ± SEM of the different groups. * represent the $p< 0.05$, for genotype factor (two-way ANOVA). Vertical arrow represents the onset of the phenotype.

SHIRPA protocol

At 8, 16, 20 and 24 weeks of age, we observed a decreased exploratory activity in vehicle-treated CMVMJD135 mice, while transgenic animals treated with LiCl+CCI-779 showed an increased exploratory activity at 8, 16 and 24 weeks of age, given by the significant increase in the number of rears in the viewing jar ($p=0.001$, $p=0.04$ and $p=0.003$ respectively), reaching a comparable performance to the wt vehicle-treated group (Fig. 3A). However, at eight weeks of age, there was an increase in exploratory behavior in wild-type mice treated with LiCl+CCI-779, suggesting a non-specific effect (Fig. 3A).

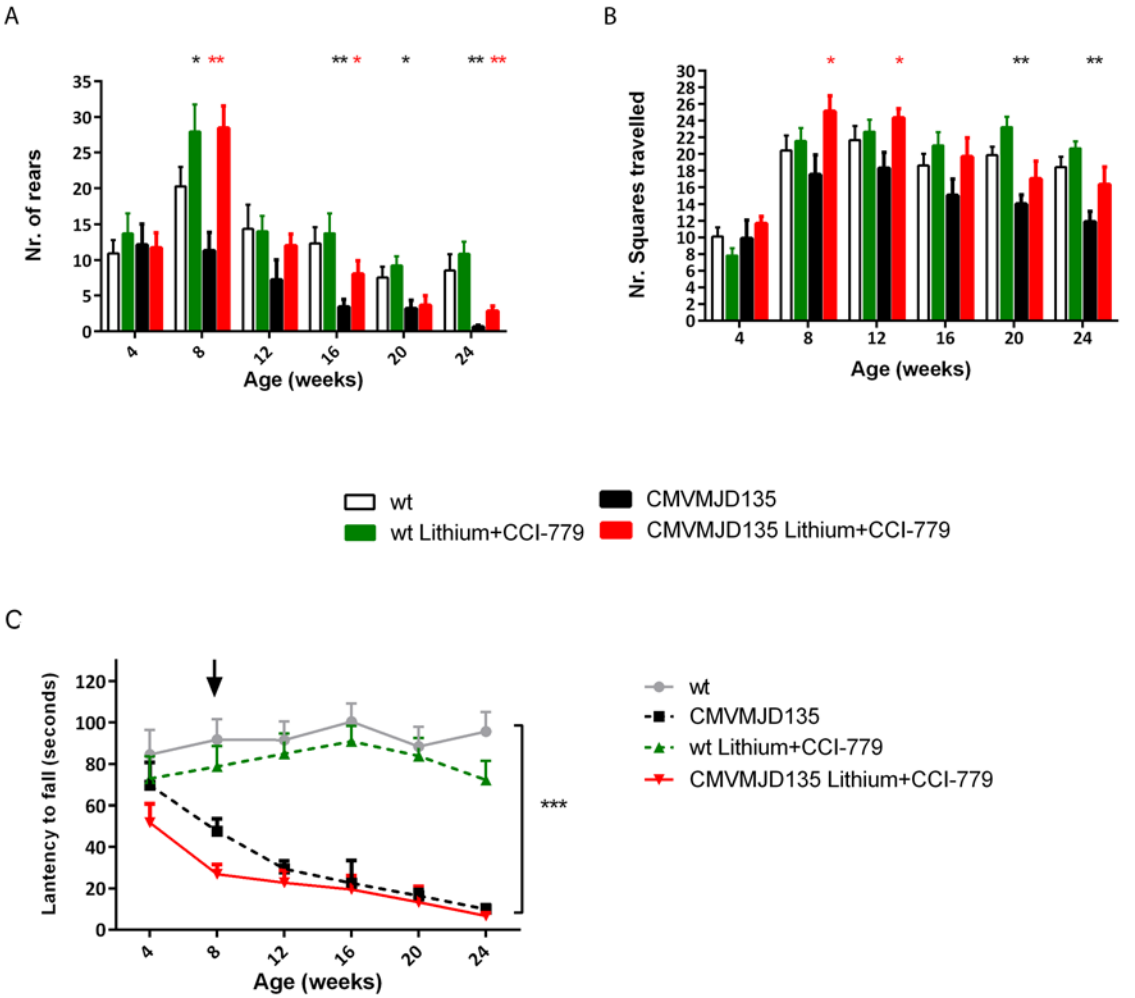

Figure 3. LiCl+CCI779 treatment effect on spontaneous exploratory activity and hindlimb strength. (A) Transgenic animals displayed decreased vertical locomotor activity at 8 weeks of age and subsequent ages, while CMVMJD135-treated mice showed an increased activity at 8, 16 and 24 weeks of age (n=10-12 for each group). **(B)** Transgenic animals traveled less in the arena than wild-type animals at 20 and 24 weeks of age; lithium+CCI779 treatment increased locomotor activity at 8 and 12 weeks of age (n=10-12 for each group). **(C)** On the hanging wire test all transgenic animals displayed a worse performance in holding the grid with age (from 8 to 24 weeks of age). A maximum time of 2 minutes was given to each animal and the time that they took to fall was registered (n=10-12 for each group). Symbols represent mean ± SEM of the different groups. *, **, *** represent the $p< 0.05$, 0.01 or 0.001, respectively, for genotype factor (two-way ANOVA). Red asterisks represent factor treatment in the analysis (CMVMJD135 mice *vs* CMVMJD135-treated mice). Vertical arrow represents the onset of the phenotype.

CMVMJD135 mice treated with LiCl+CCI-779 also demonstrated a significant increase in the locomotor activity when compared to vehicle-treated CMVMJD135 animals at 8 and 12 weeks of age ($p=0.022$ and $p=0.016$, respectively) (Fig. 3B). Of notice, at the age of 12 weeks we could not observe statistically significant differences between wt and CMVMJD135 vehicle-treated groups, meaning that the phenotype was not yet installed for these parameters (exploratory behavior and locomotor activity).

No effect of the LiCl+CCI-779 treatment was observed in the hanging wire test in CMVMJD135 mice (Fig. 3C). The grip strength (hanging wire test) of LiCl+CCI-779-treated wt animals was always worse than that of vehicle-treated wt animals. Regarding tremors, we observed a slight improvement in CMVMJD135 mice at 24 weeks of age (p=0.038) (Fig. 4A), as seen previously with lithium chloride treatment (30). We observed no therapeutic effect of LiCl+CCI-779 treatment on gait quality and limb clasping (Fig. 4B, C). The limb clasping reflex increased with disease progression, being statistically different only at 24 weeks of age. Importantly, at 16 and 20 weeks of age, the LiCl+CCI-779 treatment actually worsened limb clasping in the transgenic animals when compared to CMVMJD135-vehicle animals (Fig. 4C, labeled with #) (p=0.05 and 0.008 respectively).

Foot printing test

Footprint patterns of wt and CMVMJD135 transgenic mice treated with vehicle or LiCl+CCI-779 were analyzed for the presence of foot dragging. In agreement with previous observations (30, 36), at 12 weeks of age this phenotype was established in the CMVMJD135-vehicle animals ($p=2x10^{-5}$), while the wt-vehicle animals never presented foot dragging. LiCl+CCI-779 treatment was not able to improve foot dragging, and actually showed a trend to worsen the phenotype, given by the presence of foot dragging in the wt-treated animals and a higher percentage of LiCl+CCI-779-treated CMVMJD135 mice with this phenotype at 12 weeks of age (90% of CMVMJD135-vehicle animals vs. 100% of CMVMJD135-treated animals showed foot dragging) (Fig. 4D). At 20 weeks of age all the transgenic animals analyzed presented this phenotype ($p=2x10^{-5}$).

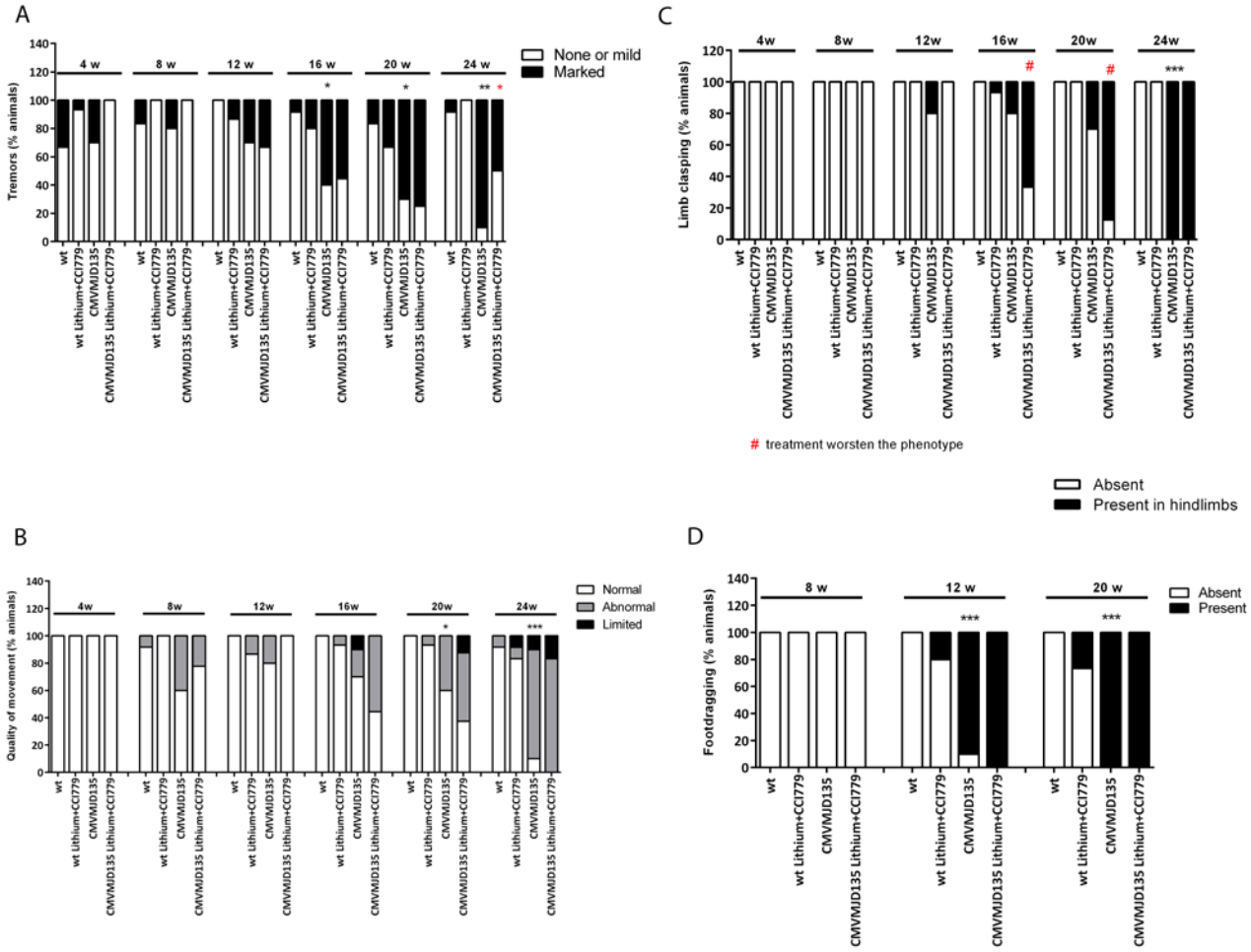

Figure 4. Effect of LiCl+CCI779 treatment on limb clasping, tremors and gait quality. (A) CMVMJD135 mice presented tremors from 16 weeks of age on. In the last time-point analyzed (24 weeks) LiCl+CCI779 treatment slightly improved this phenotype (n=10-12 for each group). **(B)** CMVMJD135 animals had abnormal gait at 20 and 24 weeks of age (qualitative assessment) which was not reverted by LiCl+CCI779 (n=10-12 for each group). **(C)** Limb clasping was observed in CMVMJD135 mice at 24 weeks of age; LiCl+CCI779 treatment anticipated the onset of this symptom, starting in the CMVMJD135-treated group at 16 weeks of age. Red # represents a worse phenotype observed in the treated group. **(D)** CMVMJD135 mice drag their feet since 12 weeks of age, which was not improved by LiCl+CCI779 treatment (n=10-12 for each group). Symbols represent mean ± SEM of the different groups. *, **, *** represent the p< 0.05; 0.01 or 0.001, respectively (Fisher's exact test).

Beam walk test

The beam walk test was performed at 20 and 24 weeks of age, when the phenotype of CMVMJD135 mice in this motor test is well established (36). In this particular pre-clinical trial, most of the transgenic animals treated with LiCl+CCI-779 were unable to perform the task, as shown in Fig. 5. At 20 weeks of age in the 11 mm circle beam, only three (in a total of ten animals) were able to cross the beam (Fig. 5A); these animals performed well in terms of latency to cross the square beam (12

mm), where seven animals concluded the task, but at this time-point we did not observe statistically significant differences among wt and CMVMJD135-vehicle animals, and no differences for treated animals (Fig. 5B). Later on, at 24 weeks of age, none of the CMVMJD135-treated mice were able to perform the beam walk test, either in the square or the round beams. Taking this into consideration, it is reasonable to consider that LiCl+CCI-779 treatment had detrimental effects on the transgenic animals, reflected in this balance-dependent task.

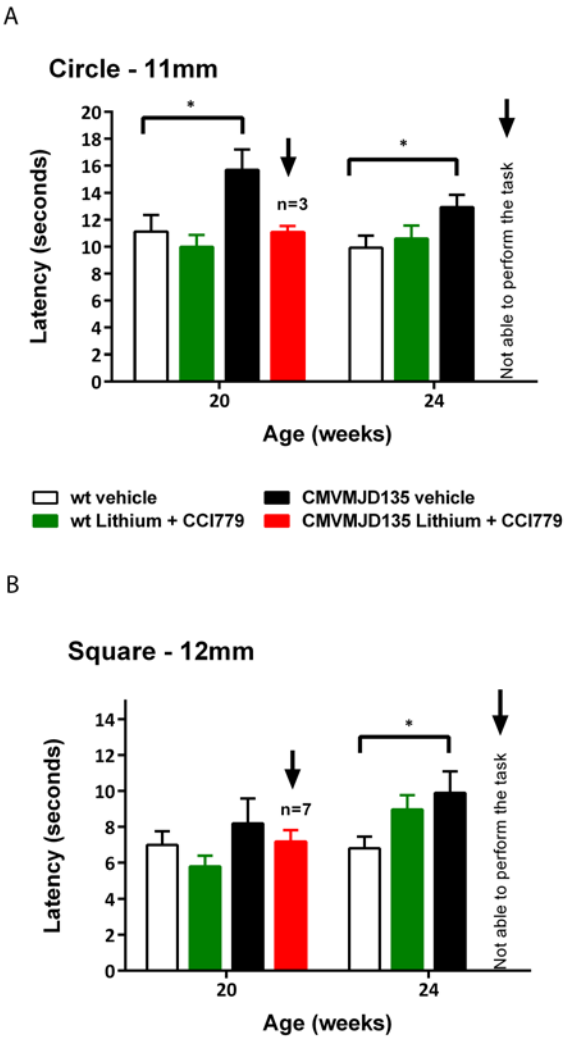

Figure 5. Effect of LiCl+CCI779 treatment on balance and motor coordination. Each bar corresponds to the mean of two consecutive trials in **(A)** circle and **(B)** square beams. The time to traverse the beam was videotaped and then measured by the same experimenter. 10-12 animals were used for each condition. CMVMJD135-treated mice showed severe difficulties in performing this task. * represents the $p<0.05$ for genotype factor (two-way ANOVA). Black arrows highlight the low or null number of CMVMJD135-treated mice able to perform the task.

Autophagy induction after LiCl+CCI-779 chronic treatment

In order to verify autophagy induction after LiCl+CCI-779 combination treatment, we measured in the brainstem of transgenic animals the levels of the autophagy markers LC3 (the classical marker of the autophagosomes; by analyzing the conversion of LC3I to LC3II (46), Beclin-1 (a protein involved in the nucleation step of the autophagosome formation) (47) and p62 (a scavenger protein that signals ubiquitylated proteins towards the autophagic machinery that directly interacts with LC3, being itself

degraded by autophagy) (48) (Fig. 6A, B and C, respectively). Similarly to what we observed for LiCl treatment alone (30), this combined treatment was able to increase the expression of Beclin-1 (p=0.006), which is associated with autophagy initiation, to increase the LC3II/LC3I ratio, and to decrease the protein levels of the autophagy substrate p62 (p=0.02), confirming increased autophagic flux. The degree of autophagy induction was, however, not significantly different between LiCl and LiCl+CCI-779 treatments when considering Beclin-1 and p62 autophagy markers (Fig. 6). Due to technical issues, we were not able to perform the western-blotting analysis for LC3 using the combined and single treatment samples in the same blot membrane. Nevertheless, the assessment using the LC3-II/LC3I ratio actually suggests the opposite, as we saw an increase of 136% in this ratio, whereas in our previous study with LiCl only (30) we had seen a 31% increase. So the results with different autophagy markers are not fully concordant regarding the relative extent of activation of autophagy of the combined versus single treatment.

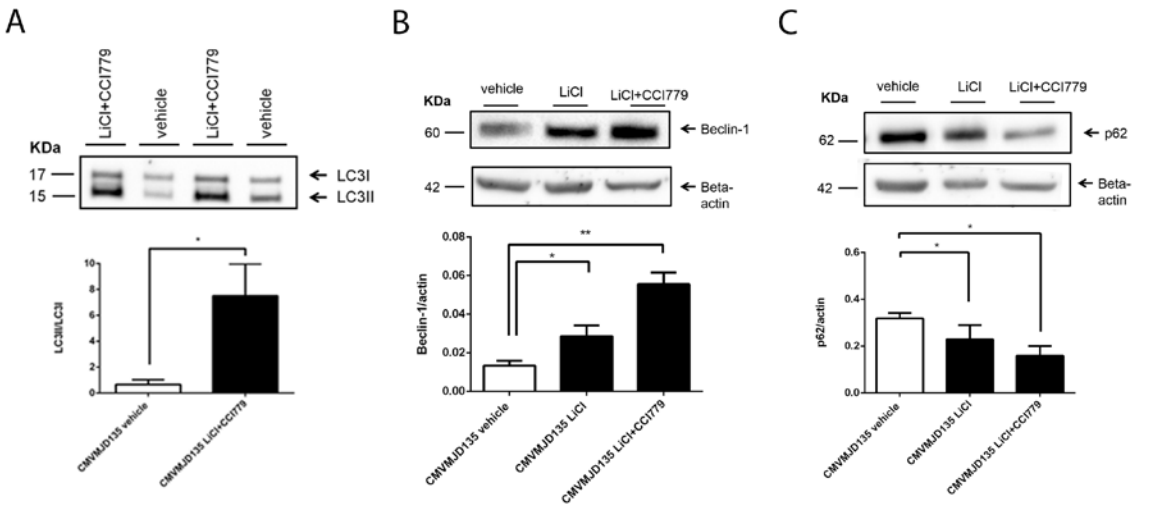

Figure 6. Autophagy induction by the chronic treatment with LiCl+CCI-779. (A) Anti-LC3 western-blot of brainstem lysates of transgenic animals injected with vehicle (n=3) or LiCl+CCI-779, at 10.4 and 20 mg/Kg respectively (n=3); **(B)** Anti-Beclin-1 western-blot of brainstem lysates of transgenic animals injected with vehicle (n=3), LiCl at 10.4 mg/Kg (n=3) or LiCl+CCI-779, at 10.4 and 20 mg/Kg respectively (n=3); **(C)** Anti-p62 western-blot of brainstem lysates of transgenic animals injected with vehicle (n=3), LiCl at 10.4 mg/Kg (n=3) or LiCl+CCI-779 at 10.4 and 20 mg/Kg respectively (n=3); beta-actin was used as loading control. At least 3 technical replicates were performed. *, **, represents the p< 0.05 or 0.01 respectively (Student t-test).

To test the effect of the combinatory drug treatment on steady-state ataxin-3 levels we performed western-blot analysis. The levels of mutant ataxin-3 in the brainstem of CMVMJD135 showed to be reduced upon LiCl+CCI779 chronic treatment (Fig. 7) (p=0.04).

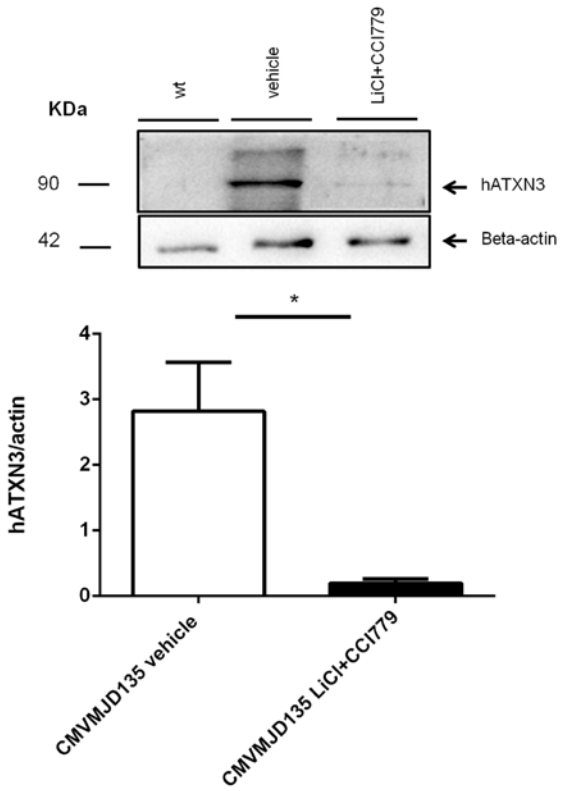

Figure 7. LiCl+CCI-779 treatment effect on ataxin-3 protein levels. Anti-ataxin-3 western-blot of brainstem lysates of transgenic animals injected with vehicle (n=4) or LiCl+CCI-779, at 10.4 and 20 mg/Kg respectively (n=4); beta-actin was used as loading control. * represents the $p< 0.05$ (t-test student).

Discussion

Based on the concept of autophagy induction as a potential therapeutic strategy for neurodegenerative diseases, here we have tested the effect of treatment with a combination of lithium and CCI-779 in a mouse model of MJD. It has been demonstrated in another mouse model of this disease that CCI-779 treatment, at the same dosage as used in this work (20mg/Kg), resulted in an improvement of motor coordination (19). However, the mouse model used had a very mild phenotype, observable only in the Rotarod and non-significantly different from the controls. The CMVMJD135 mouse model allowed us to further test this type of therapeutic strategy, due to its more severe phenotype and broad range of disease features. Furthermore, the combination of an autophagy-inducing compound with an mTOR-dependent and another with an mTOR-independent mode of action was used to test the therapeutic value of simultaneously modifying these complementary pathways.

Our first significant observation was that both wt and transgenic animals treated with LiCl+CCI-779 had a significant decrease in body weight during the treatment period. The body weight loss in both groups could be due to an exacerbated activation of autophagy in some tissues by the combination of these two drugs (although, unexpectedly, this enhanced induction was not observed with all autophagy markers in the brain), and/or it could reflect some systemic toxicity of this drug combination, also patent in the death of 30% of the treated animals, even though the doses used in this work for autophagy activation had already been tested in mice and shown not to be toxic, when administered separately (27, 28, 30). In fact, the lithium chloride dosage used here can be considered low (LiCl plasma levels of 0.3±0.09 mmol/L, as estimated previously by us (30)), being below the therapeutic range used in humans with bipolar disorder (30, 49).

Concerning the neurological phenotype, the effects of the combination therapy were generally not positive. The first manifestation of the disease in the CMVMJD135 model is loss of limb strength, which severely progresses with age (36). Chronic LiCl+CCI-779 treatment did not improve this muscular strength deficit, in accordance to other treatments previously performed in same model (30, 36). Since this phenotype starts early in life and progresses dramatically fast, the treatment regimen that we performed (starting one week before the appearance of the loss of muscular strength) may have been insufficient in terms of duration to rescue this deficit. Furthermore, the combined treatment herein tested appeared to have detrimental effects even in the wt animals, which performed worse in this task than vehicle-treated wt mice (although the difference did not reach statistical significance).

Results concerning other neurological parameters also point to very limited therapeutic effects and even some neurotoxicity of the drug combination, namely concerning limb clasping and gait quality,

for which the treated transgenic mice presented a more severe phenotype than the vehicle-treated CMVMJD135 animals. Furthermore, the combination of LiCl+CCI-779 had a negative impact on the foot printing pattern of wt animals, since it was possible to detect dragging of the paws in these animals, which did not occur in vehicle-treated wt animals. LiCl+CCI-779-treated CMVMJD135 animals also showed severe difficulties in the beam walk test; at 24 weeks of age these animals were not able to perform the task in the easier beam (square), while vehicle-treated CMVMJD135 animals at the same age were able to cross this beam (albeit taking longer than wt animals, due to motor deficits associated with the disease). In addition, when difficulty was enhanced by using the round narrower beam, this worsening of the phenotype became detectable at 20 weeks of age. In fact, the neurotoxic effect of the LiCl+CCI-779 combination treatment is strongly visible in this behavioral test, not allowing the comparative analysis between CMVMJD135 mice (treated *vs* vehicle).

Intriguingly, chronic treatment with LiCl+CCI-779 increased the vertical exploratory behavior in both wt and CMVMJD135 mice. Similar effects, also occurring in wt and CMVMJD135-treated animals, were detected in the spontaneous activity, given by the number of squares travelled in the arena. We had previously shown that LiCl treatment resulted in increased exploratory behavior in these mice (30), suggesting that the increase observed in the current study may be due to non-specific effects of this drug, most likely not disease-related.

We also observed a slight improvement of the tremors, which is in agreement with our previous result using LiCl alone in these mice (30), suggesting that this improvement might be due to that component of the treatment regimen. The presence of tremors in human patients is a rare event and can be treated with levodopa (5, 50-52), so this improvement may not be very relevant in the disease context.

In summary, these results demonstrate the negative impact of the combination of these two autophagy-inducing compounds when administered simultaneously, even in dosages that, upon single compound administration, were safe for mice (27, 28, 30). Thus, if any future LiCl+CCI-779 combination therapy is to be considered for MJD or other polyglutamine disorders, it would be necessary to adjust the doses of both compounds to avoid neurotoxicity.

Acknowledgements:

We would like to acknowledge Prof. Pedro Oliveira for statistical analysis support and the animal house caretaker Ms. Celina Barros for technical assistance. This work was supported by Fundação para a Ciência e Tecnologia through the projects [FEDER/FCT,

POCI/SAU-MMO/60412/2004], [PTDC/SAU-GMG/64076/2006]. This work was supported by Fundação para a Ciência e Tecnologia through fellowships [SFRH/BD/78388/2011 to S.D-S., SFRH/BPD/91562/2012 to A.S-F., SFRH/BD/51059/2010 to A.N-C., SFRH / BD / 51992 / 2012 to C.S-C and SFRH/BPD/79469/2011 to A.TC.].

References

1. Maciel P, Gaspar C, DeStefano AL, Silveira I, Coutinho P, Radvany J, et al. Correlation between CAG repeat length and clinical features in Machado-Joseph disease. Am J Hum Genet. 1995;57(1):54-61.

2. Kawaguchi Y, Okamoto T, Taniwaki M, Aizawa M, Inoue M, Katayama S, et al. CAG expansions in a novel gene for Machado-Joseph disease at chromosome 14q32.1. Nat Genet. 1994;8(3):221-8.

3. Paulson HL. Protein fate in neurodegenerative proteinopathies: polyglutamine diseases join the (mis)fold. Am J Hum Genet. 1999;64(2):339-45.

4. Gusella JF, MacDonald ME. Molecular genetics: unmasking polyglutamine triggers in neurodegenerative disease. Nat Rev Neurosci. 2000;1(2):109-15.

5. Coutinho P, Sequeiros J. [Clinical, genetic and pathological aspects of Machado-Joseph disease]. J Genet Hum. 1981;29(3):203-9.

6. Sequeiros J, Coutinho P. Epidemiology and clinical aspects of Machado-Joseph disease. Adv Neurol. 1993;61:139-53.

7. Becher MW, Kotzuk JA, Sharp AH, Davies SW, Bates GP, Price DL, et al. Intranuclear neuronal inclusions in Huntington's disease and dentatorubral and pallidoluysian atrophy: correlation between the density of inclusions and IT15 CAG triplet repeat length. Neurobiol Dis. 1998;4(6):387-97.

8. Wolozin B, Behl C. Mechanisms of neurodegenerative disorders: Part 1: protein aggregates. Arch Neurol. 2000;57(6):793-6.

9. Winklhofer KF, Tatzelt J, Haass C. The two faces of protein misfolding: gain- and loss-of-function in neurodegenerative diseases. EMBO J. 2008;27(2):336-49.

10. Duenas AM, Goold R, Giunti P. Molecular pathogenesis of spinocerebellar ataxias. Brain. 2006;129(Pt 6):1357-70.

11. Kelekar A. Autophagy. Ann N Y Acad Sci. 2005;1066:259-71.

12. Nixon RA, Wegiel J, Kumar A, Yu WH, Peterhoff C, Cataldo A, et al. Extensive involvement of autophagy in Alzheimer disease: an immuno-electron microscopy study. J Neuropathol Exp Neurol. 2005;64(2):113-22.

13. Yu WH, Cuervo AM, Kumar A, Peterhoff CM, Schmidt SD, Lee JH, et al. Macroautophagy - a novel beta-amyloid peptide-generating pathway activated in Alzheimer's disease. Journal of Cell Biology. 2005;171(1):87-98.

14. Anglade P, Vyas S, Javoy-Agid F, Herrero MT, Michel PP, Marquez J, et al. Apoptosis and autophagy in nigral neurons of patients with Parkinson's disease. Histol Histopathol. 1997;12(1):25-31.

15. Cataldo AM, Hamilton DJ, Barnett JL, Paskevich PA, Nixon RA. Properties of the endosomal-lysosomal system in the human central nervous system: Disturbances mark most neurons in populations at risk to degenerate in Alzheimer's disease. Journal of Neuroscience. 1996;16(1):186-99.

16. Moreira PI, Siedlak SL, Wang X, Santos MS, Oliveira CR, Tabaton M, et al. Autophagocytosis of mitochondria is prominent in Alzheimer disease (vol 66, pg 525, 2007). Journal of Neuropathology and Experimental Neurology. 2007;66(7):674-.

17. Martinez-Vicente M, Talloczy Z, Wong E, Tang G, Koga H, Kaushik S, et al. Cargo recognition failure is responsible for inefficient autophagy in Huntington's disease. Nat Neurosci. 2010;13(5):567-76.

18. Boland B, Kumar A, Lee S, Platt FM, Wegiel J, Yu WH, et al. Autophagy induction and autophagosome clearance in neurons: relationship to autophagic pathology in Alzheimer's disease. J Neurosci. 2008;28(27):6926-37.

19. Menzies FM, Huebener J, Renna M, Bonin M, Riess O, Rubinsztein DC. Autophagy induction reduces mutant ataxin-3 levels and toxicity in a mouse model of spinocerebellar ataxia type 3. Brain. 2010;133(Pt 1):93-104.

20. Spilman P, Podlutskaya N, Hart MJ, Debnath J, Gorostiza O, Bredesen D, et al. Inhibition of mTOR by rapamycin abolishes cognitive deficits and reduces amyloid-beta levels in a mouse model of Alzheimer's disease. PLoS One. 2010;5(4):e9979.

21. Nascimento-Ferreira I, Santos-Ferreira T, Sousa-Ferreira L, Auregan G, Onofre I, Alves S, et al. Overexpression of the autophagic beclin-1 protein clears mutant ataxin-3 and alleviates Machado-Joseph disease. Brain. 2011;134(Pt 5):1400-15.

22. Levine B, Klionsky DJ. Development by self-digestion: molecular mechanisms and biological functions of autophagy. Dev Cell. 2004;6(4):463-77.

23. Rubinsztein DC, Gestwicki JE, Murphy LO, Klionsky DJ. Potential therapeutic applications of autophagy. Nat Rev Drug Discov. 2007;6(4):304-12.

24. Zhang L, Yu J, Pan H, Hu P, Hao Y, Cai W, et al. Small molecule regulators of autophagy identified by an image-based high-throughput screen. Proc Natl Acad Sci U S A. 2007;104(48):19023-8.

25. Sarkar S, Floto RA, Berger Z, Imarisio S, Cordenier A, Pasco M, et al. Lithium induces autophagy by inhibiting inositol monophosphatase. J Cell Biol. 2005;170(7):1101-11.

26. Ravikumar B, Duden R, Rubinsztein DC. Aggregate-prone proteins with polyglutamine and polyalanine expansions are degraded by autophagy. Hum Mol Genet. 2002;11(9):1107-17.

27. Ravikumar B, Vacher C, Berger Z, Davies JE, Luo S, Oroz LG, et al. Inhibition of mTOR induces autophagy and reduces toxicity of polyglutamine expansions in fly and mouse models of Huntington disease. Nat Genet. 2004;36(6):585-95.

28. Wood NI, Morton AJ. Chronic lithium chloride treatment has variable effects on motor behaviour and survival of mice transgenic for the Huntington's disease mutation. Brain Res Bull. 2003;61(4):375-83.

29. Watase K, Gatchel JR, Sun Y, Emamian E, Atkinson R, Richman R, et al. Lithium therapy improves neurological function and hippocampal dendritic arborization in a spinocerebellar ataxia type 1 mouse model. PLoS Med. 2007;4(5):e182.

30. Duarte-Silva S, Neves-Carvalho A, Soares-Cunha C, Teixeira-Castro A, Oliveira P, Silva-Fernandes A, et al. Lithium chloride therapy fails to improve motor function in a transgenic mouse model of Machado-Joseph disease. Cerebellum. 2014;13(6):713-27.

31. Bergmann L, Maute L, Guschmann M. Temsirolimus for advanced renal cell carcinoma. Expert Rev Anticancer Ther. 2014;14(1):9-21.

32. Kwitkowski VE, Prowell TM, Ibrahim A, Farrell AT, Justice R, Mitchell SS, et al. FDA approval summary: temsirolimus as treatment for advanced renal cell carcinoma. Oncologist. 2010;15(4):428-35.

33. Sarkar S, Ravikumar B, Floto RA, Rubinsztein DC. Rapamycin and mTOR-independent autophagy inducers ameliorate toxicity of polyglutamine-expanded huntingtin and related proteinopathies. Cell Death Differ. 2009;16(1):46-56.

34. Stambolic V, Ruel L, Woodgett JR. Lithium inhibits glycogen synthase kinase-3 activity and mimics wingless signalling in intact cells. Curr Biol. 1996;6(12):1664-8.

35. Chiu CT, Chuang DM. Molecular actions and therapeutic potential of lithium in preclinical and clinical studies of CNS disorders. Pharmacol Ther. 2010;128(2):281-304.

36. Silva-Fernandes A, Duarte-Silva S, Neves-Carvalho A, Amorim M, Soares-Cunha C, Oliveira P, et al. Chronic Treatment with 17-DMAG Improves Balance and Coordination in A New Mouse Model of Machado-Joseph Disease. Neurotherapeutics. 2014.

37. Teixeira-Castro A, Ailion M, Jalles A, Brignull HR, Vilaca JL, Dias N, et al. Neuron-specific proteotoxicity of mutant ataxin-3 in C. elegans: rescue by the DAF-16 and HSF-1 pathways. Hum Mol Genet. 2011;20(15):2996-3009.

38. Brenner S. The genetics of Caenorhabditis elegans. Genetics. 1974;77(1):71-94.

39. Gidalevitz T, Ben-Zvi A, Ho KH, Brignull HR, Morimoto RI. Progressive disruption of cellular protein folding in models of polyglutamine diseases. Science. 2006;311(5766):1471-4.

40. Silva-Fernandes A, Duarte-Silva S, Neves-Carvalho A, Amorim M, Soares-Cunha C, Oliveira P, et al. Chronic treatment with 17-DMAG improves balance and coordination in a new mouse model of Machado-Joseph disease. Neurotherapeutics. 2014;11(2):433-49.

41. Silva-Fernandes A, Costa Mdo C, Duarte-Silva S, Oliveira P, Botelho CM, Martins L, et al. Motor uncoordination and neuropathology in a transgenic mouse model of Machado-Joseph disease lacking intranuclear inclusions and ataxin-3 cleavage products. Neurobiol Dis. 2010;40(1):163-76.

42. Nicklas W, Baneux P, Boot R, Decelle T, Deeny AA, Fumanelli M, et al. Recommendations for the health monitoring of rodent and rabbit colonies in breeding and experimental units. Lab Anim. 2002;36(1):20-42.

43. Rogers DC, Fisher EM, Brown SD, Peters J, Hunter AJ, Martin JE. Behavioral and functional analysis of mouse phenotype: SHIRPA, a proposed protocol for comprehensive phenotype assessment. Mamm Genome. 1997;8(10):711-3.

44. Carter RJ, Lione LA, Humby T, Mangiarini L, Mahal A, Bates GP, et al. Characterization of progressive motor deficits in mice transgenic for the human Huntington's disease mutation. J Neurosci. 1999;19(8):3248-57.

45. Rafael JA, Nitta Y, Peters J, Davies KE. Testing of SHIRPA, a mouse phenotypic assessment protocol, on Dmd(mdx) and Dmd(mdx3cv) dystrophin-deficient mice. Mamm Genome. 2000;11(9):725-8.

46. Klionsky DJ, Abdalla FC, Abeliovich H, Abraham RT, Acevedo-Arozena A, Adeli K, et al. Guidelines for the use and interpretation of assays for monitoring autophagy. Autophagy. 2012;8(4):445-544.

47. Itakura E, Kishi C, Inoue K, Mizushima N. Beclin 1 forms two distinct phosphatidylinositol 3-kinase complexes with mammalian Atg14 and UVRAG. Mol Biol Cell. 2008;19(12):5360-72.

48. Bjorkoy G, Lamark T, Brech A, Outzen H, Perander M, Overvatn A, et al. p62/SQSTM1 forms protein aggregates degraded by autophagy and has a protective effect on huntingtin-induced cell death. J Cell Biol. 2005;171(4):603-14.

49. Lin D, Mok H, Yatham LN. Polytherapy in bipolar disorder. CNS Drugs. 2006;20(1):29-42.

50. Bettencourt C, Santos C, Coutinho P, Rizzu P, Vasconcelos J, Kay T, et al. Parkinsonian phenotype in Machado-Joseph disease (MJD/SCA3): a two-case report. BMC Neurol. 2011;11:131.

51. Ishida C, Sakajiri K, Yoshikawa H, Sakashita Y, Okino S, Yamaguchi K, et al. Lower limb tremor in Machado-Joseph disease. Neurology. 1998;51(4):1225-6.

52. Nandagopal R, Moorthy SG. Dramatic levodopa responsiveness of dystonia in a sporadic case of spinocerebellar ataxia type 3. Postgrad Med J. 2004;80(944):363-5.

Chapter 5

TUDCA reduces neuroinflammation and improves motor symptoms in a transgenic mouse model of Machado-Joseph disease

TUDCA reduces neuroinflammation and improves motor symptoms in a transgenic mouse model of Machado-Joseph disease

Sara Duarte-Silva[1,2], Andreia Neves-Carvalho[1,2], Anabela Silva-Fernandes[1,2] and Patrícia Maciel[*1,2]

1) Life and Health Sciences Research Institute (ICVS), School of Health Sciences, University of Minho, Braga, Portugal;
2) ICVS/3B's - PT Government Associate Laboratory, Braga/Guimarães, Portugal;

[*] Corresponding author: Patrícia Maciel, PhD. Life and Health Sciences Research Institute (ICVS), School of Health Sciences, ICVS/3B's – PT Government Associate Laboratory, University of Minho, Campus Gualtar, 4710-057 Braga, Portugal. Telephone: 351-253-604824, Fax: 351-253-604820. E-mail: pmaciel@ecsaude.uminho.pt

Abstract

Machado-Joseph disease (MJD) is an autosomal dominant neurodegenerative disorder for which no effective treatment is currently available. We have generated a new transgenic mouse model expressing human ataxin-3 with an expanded CAG tract ubiquitously and at near-endogenous levels. CMVMJD135 mice develop a severe and progressive neurologic phenotype, with intranuclear inclusions in neurons and brain pathology consistent with the human disease. Tauroursodeoxycholic acid (TUDCA) is a bile acid (BA) with neuroprotective action, through its anti-amyloidogenic and chemical chaperone activities and its ability to modulate apoptotic pathways. This BA is orally bioavailable, BBB permeable, and has a very low toxicity profile. In addition, TUDCA has been approved by FDA for chronic use in humans to treat liver disorders. TUDCA has been shown to be beneficial in several models of different neurodegenerative diseases. The objective of this work was to test the therapeutic efficacy of TUDCA on the motor phenotype and neuropathology of CMVMJD135 mice, and to understand the mechanism of action of this compound in the brain. Four groups of animals were used: CMVMJD135 and wt littermates (C57Bl6) under normal or supplemented diet with 0.4% of TUDCA; treatment lasted from 5 to 34 weeks of age. A battery of motor and non-motor behavior tests was applied every two weeks.

Our results show that food supplementation with TUDCA delayed the onset of disease and improved the motor phenotype of CMVMJD135 mice, including balance, motor coordination and gait parameters. Furthermore, TUDCA administration ameliorated neurological reflexes, exploratory movement deficits and partially rescued muscular strength problems.

We also observed that TUDCA treatment was not able to reduce the ataxin-3 aggregate load in the pontine nuclei and LRT. Nevertheless, TUDCA normalized the mRNA levels of TNF-α, Il1β and Il10 in the brainstem and reduced the astrogliosis in the substantia nigra and brainstem. Furthermore, TUDCA treatment had neuroprotective effects, by restoring the calbindin positive phenotype of Purkinje cells in the cerebellum.

These results demonstrate the therapeutic efficacy of TUDCA supplementation in a mammalian model of MJD, and show a strong contribution of the anti-inflammatory properties of TUDCA. For this effect TUDCA could have important applications for therapy of neurodegenerative diseases, including MJD.

Introduction

Machado-Joseph disease (MJD), also known as Spinocerebellar Ataxia type 3 (SCA3), is the most common autosomal dominant ataxia worldwide and is caused by ataxin-3 with an expanded polyglutamine (polyQ) stretch (1). Clinically, MJD is characterized by gait ataxia, diplopia, dysarthria and spastic gait (2), without cognitive decline. *In vivo* brain imaging and *post-mortem* analysis show a widespread neuropathology in the brain of MJD patients, with atrophy of several brain regions, including cerebellum, medulla oblongata, pons, cranial nerves III to XII as well as substantia nigra. Other affected areas include the thalamus, basal ganglia and cerebral cortex. The atrophy of these brain regions associate both with neuronal and myelin losses and reactive astrogliosis is also a common finding (3, 4). Nuclear and cytoplasmic protein aggregates are found in affected and unaffected brain regions (3, 5-7). Interestingly, ataxin-3 (ATXN-3) inclusions were also found in axons, specifically in affected tracts (8). Despite the knowledge of clinical and pathologic features of MJD, the mechanisms that lead to disease are poorly understood and constitute a topic of investigation towards the identification of new therapy targets. Currently, clinicians address the therapy of MJD patients by attempting to improve symptoms such as the restless legs syndrome, cramps and fatigue (9). No current therapy exists that slows disease progression or prevents disease onset.

Potential therapeutic targets for MJD and other polyQ disorders can be divided into (i) those that are directed at the polyQ proteins themselves, namely gene silencing, attempts to enhance mutant protein degradation or inhibition/prevention of aggregation; or (ii) those that intercept the toxic downstream effects of the polyQ protein, such as mitochondrial dysfunction and oxidative stress, transcriptional abnormalities, UPS impairment, excitotoxicity, or activation of apoptotic pathways. In fact, some of these potential targets have already been tested in animal models of the disease and in some cases, a beneficial effect was found (10-21). For example, we have shown that treatment with 17-DMAG, described as an Hsp90 inhibitor able to increase chaperone expression, had positive, but transient effects in CMVMJD135 mouse model, and failed to increase chaperone load in the brain but rather increased autophagy (15). Yet, the translation of these pre-clinical trials to human patients is still very limited, mainly due to safety reasons. Testing FDA-approved compounds in MJD models allows the avoidance of these issues and could be a good strategy for faster translation results in patients. Considering the multisystemic pathologic and clinical features of this disease, another interesting approach would be the use of combinatory treatments of compounds with multiple cellular targets.

Ursodeoxycholic acid (UDCA) and its taurine conjugate Tauroursodeoxycholic acid (TUDCA) are endogenous bile acids known to cross the blood-brain barrier and to exert neuroprotection (22). They

are synthesized from cholesterol in the liver and are the major constituents of the bile, being responsible for the solubilization of dietary fats and some vitamins (23). In addition to being used in the clinic to treat primary biliary cirrhosis, TUDCA was recently tested as a therapeutic agent in Amyotrophic Lateral Sclerosis (ALS) patients, showing to be well tolerated and to slow disease progression (24). TUDCA acts upon multiple cellular targets and was also shown to reduce toxic aggregates and improve disease symptoms in different models of neurodegenerative disorders, including Familial Amyloidotic Polyneuropathy (FAP) (25), Alzheimer's disease (AD) (26-28), Huntington disease (HD) (29) and Parkinson's disease (PD) (30). The cytoprotective effects of TUDCA have been attributed to its anti-apoptotic and anti-oxidant properties (25, 29, 30), to prevention of mitochondrial toxicity (31) and to anti-inflammatory effects (26, 28, 32).

In this study, we used the CMVMJD135 mouse model of MJD (15) which presents several quantifiable traits reflecting aspects of the human condition at the behavioral and neuropathological levels, thus constituting an excellent model for pre-clinical interventions. Chronic treatment with TUDCA significantly improved motor dysfunction of the CMVMJD135 mice, and had an anti-inflammatory effect, counteracting astrocytic overactivation in the brain of these mice.

Methods

Ethics statement. All procedures were conducted in accordance with European regulations (European Union Directive 2010/63/EU). Animal facilities and the people directly involved in animal experiments (S.D.S, A.N.C) were certified by the Portuguese regulatory entity — Direcção Geral de Alimentação e Veterinária.

All of the protocols performed were approved by the Animal Ethics Committee of the Life and Health Sciences Research Institute, University of Minho.

Animals

Female CMVMJD135 (background C57BL/6) mice were used in the study. Transgenic and non-transgenic drug- and placebo- treated animals were alternately assigned and housed at weaning in groups of 5 animals in filter-topped polysulfone cages 267 × 207 × 140 mm (370 cm^2 floor area) (Tecniplast, Buguggiate, Italy), with corncob bedding (Scobis Due, Mucedola SRL, Settimo Milanese, Italy) in a conventional animal facility. The progeny produced by mating MJD transgenic with wild-type animals were genotyped at weaning by PCR, as we previously described (33). The experiment started at 4 weeks and ended at 34 weeks of age. All animals were maintained under standard laboratory conditions: an artificial 12 h light/dark cycle (lights on from 8:00 to 20:00 h), with an ambient temperature of 21±1°C and a relative humidity of 50–60%; the mice were given a standard diet (4RF25 during the gestation and postnatal periods, and 4RF21 after weaning, Mucedola SRL, Settimo Milanese, Italy) and water *ad libitum*. Health monitoring was performed according to FELASA guidelines (34), confirming the Specified Pathogens status of sentinel animals maintained in the same animal room. Humane endpoints for the experiment were defined (20% reduction of the body weight, inability to reach food and water, presence of wounds in the body, dehydration), but not needed in practice as the study period was conceived to include ages at which animals do not reach these endpoints. The animals were sacrificed by different methods according to the final purpose: either by decapitation or exsanguination perfusion with saline or PFA 4%; in this case, the animals were deeply anesthetized with a mixture of ketamine hydrochloride (150 mg/kg) plus medetomidine (0.3 mg/kg). The timeline of this study is shown in Fig. 1A.

Mouse genotyping.

The progeny produced by mating hemizygous MJD transgenics with wild-type animals were genotyped at weaning by PCR, as previously described (33). The mean CAG repeat size (±SD) for all mice used was 139 ± 3.

TUDCA treatment

CMVMJD135 and wt female mice were distributed and housed in groups of 5 animals per cage. TUDCA was supplemented in the standard diet at 0.4% (4RF21, Mucedola SRL, purchased at Ultragene, Portugal) as previously described (28). At 5 weeks of age the animals were sequentially assigned by cage into four groups of 15 animals each: CMVMJD135 and wt under normal diet and CMVMJD135 and wt under diet supplemented with TUDCA 0.4%. The treatment had the duration of 29 weeks, until the animals reached 34 weeks of age. This endpoint was chosen based on the fact that CMVMJD135 mice under standard diet were still able to reach the food in the cage and perform most of the behavioral tests used in the study; from our knowledge of the model, after this period of time these animals may no longer be able to reach the food alone and/or to perform some of the behavioral tests. TUDCA treatment was started at 5 weeks of age due to the previous knowledge that the phenotype onset in this model starts at 6 weeks of age (35). An extra group of animals (wt, CMVMJD135, CMVMJD135-TUDCA, n=5 per group) was generated to study the molecular effects of a less prolonged treatment in the brain of these animals.

Body weight. All mice were weighted from 4 to 34 weeks of age every two weeks.

Behavioral analysis

Beam walk balance test. This test assesses balance but is also sensitive to fine motor coordination. The test was performed as previously described (36). The animals were trained during 3 days in the square beam (12 mm). In the fourth day, they were tested in the training beam and also in one round beam (17 mm). If the animal fell or turned around in the beam, this was considered one failed trial. Each animal had the opportunity to fail 2 times in each beam. The time the animal took to cross the beam was counted, and time was discounted if the animal stopped in the beam.

Motor swimming test. To analyse voluntary locomotion, the mice were trained for 2 consecutive days (3 trials each animal) to traverse a clear perspex water tank to a safe platform at the end. The perspex tank was 100 cm long and the platform at the end was made from black perspex. The latency to cross the water tank was measured from a distance of 60 cm (the tank was labeled with a blue line to mark the initiation). The water temperature was monitored to 23 °C using a thermostat (36). The mice were tested for 3 consecutive days (2 trials per animal) and the latency to traverse the tank registered by the experimenter.

Vertical movement assessment (Rears). Each mouse was placed in a viewing jar (15 cm diameter) for 5 minutes, and the number of vertical movements (including movements on and off-the wall) was registered.

Spontaneous activity. The mice were transferred to a 15-labeled-squares arena (55×33×18 cm), and then a series of anatomical and behavioral features were registered. The number of squares travelled in the arena for 1 minute was counted. The gait quality was assessed by the same experimenter.

Footprint analysis. The footprint pattern was performed to assess gait as described in (36). To obtain footprints, the hind- and forepaws of the mice were coated with black and red non-toxic paints, respectively. A clean rectangular paper sheet was placed on the floor of the runway for each run. The animals were then allowed to walk along a 100-cm-long×4.2 cm width×10 cm height corridor in the direction of an enclosed black box. An inclined corridor was used instead of a horizontal one, since mice have the tendency to run upwards to escape. Each animal was allowed to achieve one valid trial per age. To evaluate the severity of foot dragging through age the foot printing pattern of CMVMJD135 and wt controls was classified at each time point considering six consecutive steps (0=absent/mild, up to three steps; 1=mild, more than three steps out of six; 2=severe, all steps out of six). The stride length was measured manually as the distance between two pawprints. Three values were measured for three consecutive steps.

Hanging wire grip test. The mice were placed on the top of a metallic grid and inverted 180° towards the surface of the bench. The latency to fall from the grid was registered by the experimenter. The maximum time of the test was 120 seconds.

Western-blot. Brain tissue was homogenized in cold 0.1 M Tris-HCl, pH 7.5, 0.1 M EDTA, and a mixture of protease inhibitors (Complete; Roche, Swiss) and was sonicated for 10 seconds. Protein concentration was determined using the Bradford assay (Biorad, California, USA). Samples were heated for 5 minutes at 100°C, and microfuged for 10 seconds before loading. For each sample, 15 micrograms of total protein were loaded into SDS-Page gels and then transferred to nitrocellulose membranes (Biorad, California, USA). After incubation with the primary antibodies: rabbit anti-ataxin-3 (1:10.000), rabbit anti-GFAP (1:500, Dako, Denmark), mouse anti-alpha-tubulin (1:200, DSHB, University of Iowa, Iowa) and mouse anti-beta-actin (1:100, DSHB, University of Iowa, Iowa); the secondary antibodies were incubated at the following dilutions: anti-rabbit (1:10.000, Biorad, California, USA) and anti-mouse (1:10.000, Biorad, California, USA). Antibody affinity was detected by

chemiluminescence (Clarity Western ECL, Biorad, California, USA). Band quantification was performed using the Image Lab software according to the manufacturer's instructions.

qRT-PCR. Total RNA was isolated from mouse tissues using TRIZOL (Invitrogen, Calrsbad, CA, USA) according to the manufacturer's protocol. First-strand cDNA, synthesized using oligo-dT (Biorad), was amplified by quantitative reverse-transcriptase PCR (qRT-PCR) according to the guidelines (Biorad). Human and mouse ataxin-3 primers were used for transgene expression quantification (37). The primers used were based on literature (15) or designed using PRIMER-BLAST (http://www.ncbi.nlm.nih.gov/tools/primer-blast/).

Neuropathology and immunohistochemistry. Transgenic and wt littermate mice were deeply anesthetized and transcardially perfused with PBS followed by 4% paraformaldehyde (PFA) in PBS. Brains were post fixed overnight in fixative solution and embedded in paraffin. Slides with 4-µm-thick paraffin sections were stained with cresyl violet or processed for immunohistochemistry with rabbit GFAP (1:500, DAKO Corporation), rabbit anti-ataxin-3 (1:1000) and rabbit anti-calbindin D-28K (1:1000, Millipore).

Ataxin-3 positive inclusions in the pontine nuclei (PN) and Lateral reticular nucleus of the medulla (LRt), and calbindin positive cells in the cerebellum of 34 weeks old animals either under standard or TUDCA supplemented diets were quantified and normalized for total area using the Fiji software (Image J).

Statistical analysis. The experimental unit used in this study was a single animal. Power analysis was used to determine the sample size as previously described (35). The estimates of required number of animals for specific behavioral tests and time-points of analysis are described in (16). Continuous variables with normal distributions (K-S test $p>0.05$) were analyzed with the Student t-test or two-way ANOVA (Factors: genotype and treatment). Behavioral data were subjected to the non-parametric Mann-Whitney U-test when variables were non-continuous or when a continuous variable did not present a normal distribution (Kolmogorov-Smirnov test $p<0.05$). Categorical variables in the SHIRPA protocol were analyzed by contingency tables (Fisher's exact test). All statistical analyses were performed using SPSS 22.0 (SPSS Inc., Chicago, IL). A critical value for significance of $p< 0.05$ was used throughout the study.

Results

At 4 weeks of age, a pre-symptomatic age, all the animals used in this pre-clinical trial were tested for motor function and limb strength parameters and no differences were observed between groups. At 5 weeks of age, TUDCA supplemented diet was given to wild-type (wt) and CMVMJD135 animals, while the vehicle groups (wt and CMVMJD135) remained under standard diet. TUDCA chronic treatment was kept until the animals reached 34 weeks of age. TUDCA had no impact on body and total brain weight of CMVMJD135 treated-mice (Fig. S1 A, B respectively), and had no effect on wt animals (Table S1). Importantly, the mean food consumption per cage was not different between standard and TUDCA diets (Fig. S1 C).

TUDCA enhances motor function and gait in CMVMJD135 mice

Chronic treatment with TUDCA for 29 weeks improved motor function and gait quality in CMVMJD135 mice. In the beam balance test, the motor deficits started manifesting at 14 weeks of age in untreated mice, both in the square and round beams. TUDCA had significant impact on this behavior since 24 weeks until 30 weeks of age on the square beam (Fig. 1B). Interestingly, in the narrowest beam, where difficulty is higher, CMVMJD135 animals under TUDCA treatment were able to perform the task at a later age (26 weeks), while transgenic animals on standard diet were not (Fig. 1C). Another way to test motor function is to assess the ability of mice to swim. Remarkably, TUDCA treatment had a strong effect on this task, and the motor improvement was observed since the onset of this symptom until the end of the trial, with a 76% reduction of the impairment at the age of 34 weeks (Fig. 1D). Gait analysis demonstrated a significant improvement of the footdragging phenotype since 12 weeks of age (at the onset of the symptom), which lasted for 10 weeks. After this period of treatment, CMVMJD135 mice under TUDCA diet had the same performance as CMVMJD135 animals under a standard diet (Fig 2A). Additionally, qualitative analysis of the gait quality showed a transient beneficial effect of TUDCA (Fig. 2B). In contrast, TUDCA had no effect on stride length (data not shown).

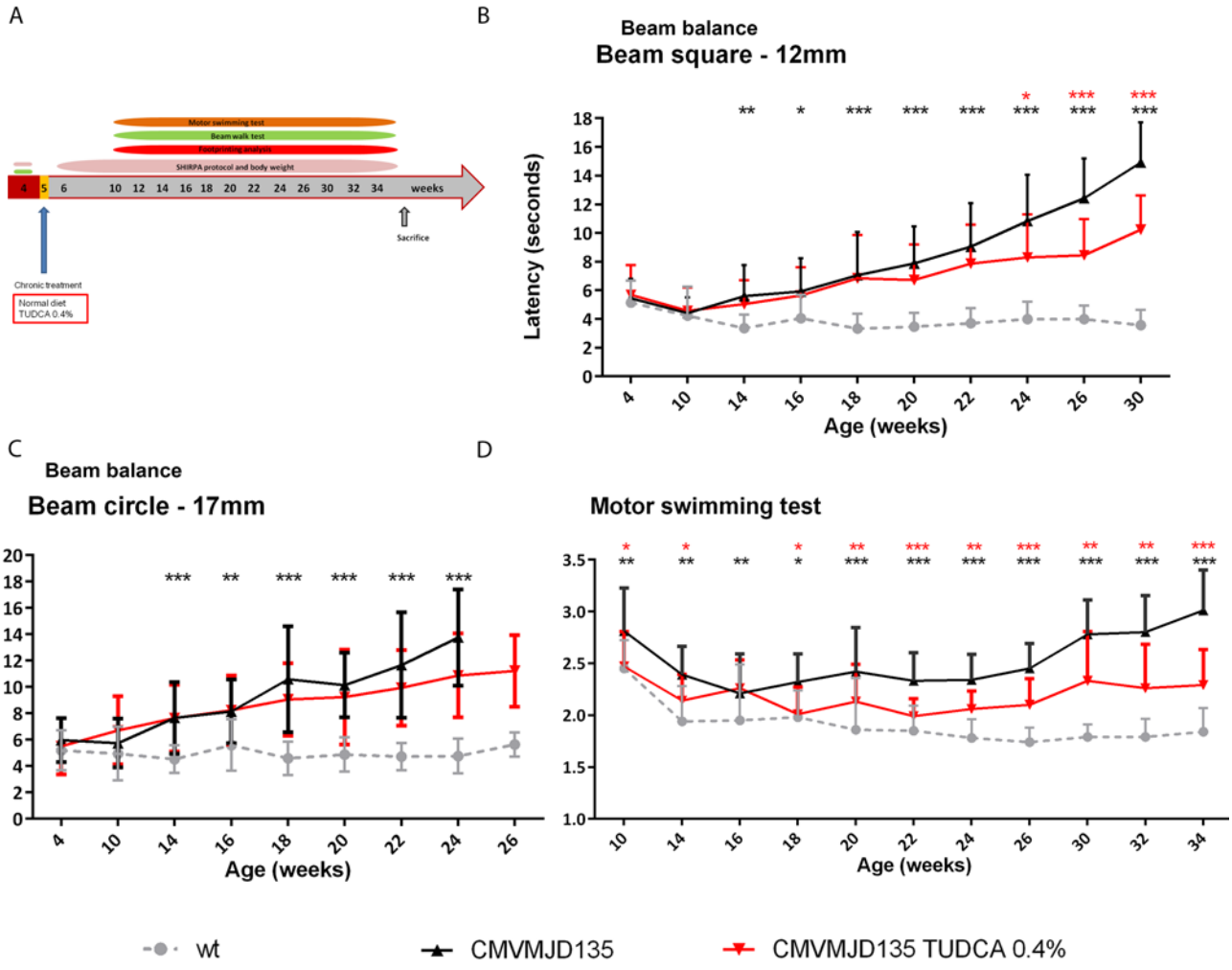

Figure 1. TUDCA treatment improved the coordination deficits of the CMVMJD135 mice (A) Schematic timeline for the behavioral analysis of TUDCA pre-clinical trial. CMVMJD135 mice have a better performance on the beam walk test both in the **(B)** square and in the **(C)** round beams. In the motor swimming test **(D)** this improvement is even more pronounced during disease progression until the end of the trial at 34 weeks of age. n=15-17 for each group used. Symbols represent mean ± SD of the different groups. *, **, *** represent the p< 0.05; 0.01 and 0.001 respectively. Repeated measures ANOVA was used considering genotype and treatment factors.

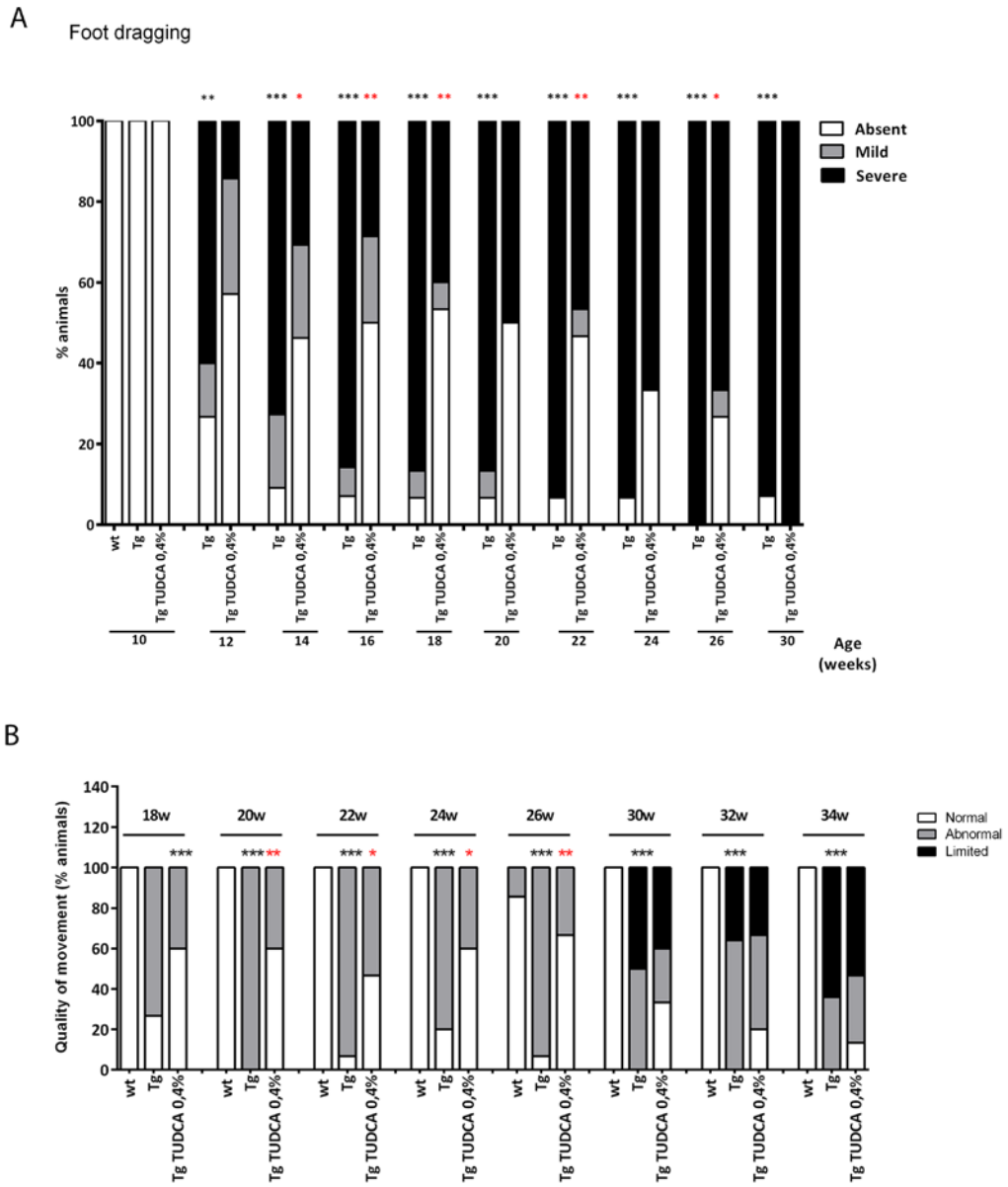

Figure 2. Gait is partially ameliorated by chronic TUDCA treatment. (A) Foot dragging was analyzed since 10 to 30 weeks of age. CMVMJD135 drag their feet since 12 weeks of age and TUDCA improved this phenotype since the onset until 22 weeks of age. Upon this age this improvement is no longer observed (Mann-Whitney U test). **(B)** Gait quality was evaluated in an open arena being the onset of abnormal gait observed at 18 weeks. TUDCA improved this phenotype parameter until 26 weeks of age (Fisher's exact test). Symbols represent mean ± SD of the different groups. *, **, *** represent the $p< 0.05$; 0.01 and 0.001 respectively.

Muscular strength is slightly improved by TUDCA treatment

Loss of limb strength is the first disease symptom observed in the CMVMJD135 mice, and it progresses dramatically with age (15). In fact, similarly to what was observed in other pre-clinical trials performed in this mouse model (15, 16), TUDCA had no major effect on the hanging wire test (Fig. 3A). Interestingly, however, the qualitative parameters of muscular strength, such as the hindlimb tonus and the forelimb strength to grab a grid scores were significantly improved by TUDCA after a long period of treatment (Fig. 3B, C respectively).

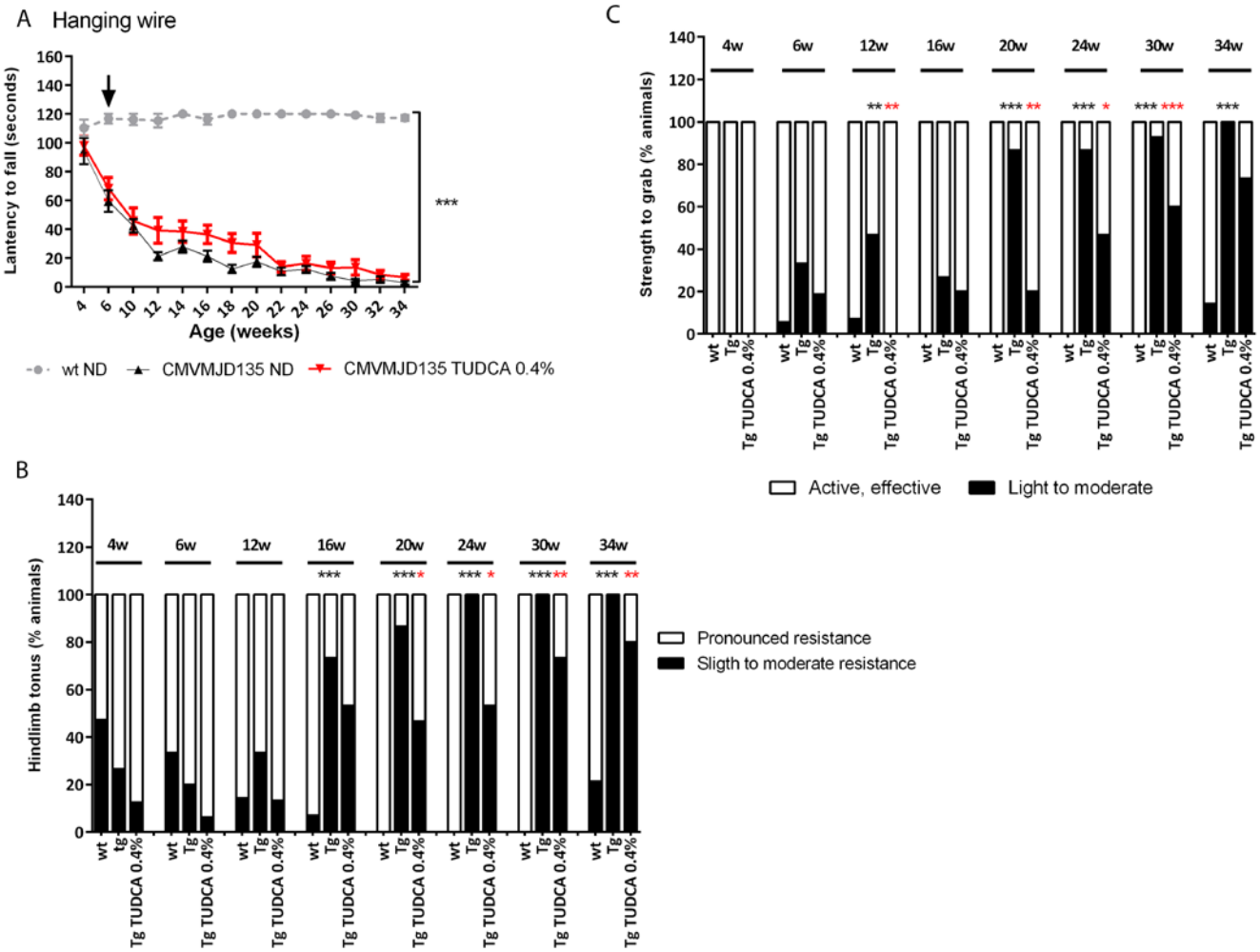

Figure 3. Muscular strength is slightly improved by TUDCA. (A) The hanging wire test was performed to evaluate limb strength; the phenotype onset occured at 6 weeks of age (black arrow). TUDCA had no significant impact on this test (Repeated measures ANOVA was used considering genotype and treatment factors). **(B)** The hindlimb tonus was evaluated and TUDCA treatment started to have a detectable positive effect 4 weeks after the onset of this phenotype, at 20 weeks of age, that was maintained until the end of the trial (Fisher's exact test). **(C)** The animals' strength to grab a grid evaluates the forelimb strength. CMVMJD135 mice started to shw reduced forelimb strength at 12 weeks of age and TUDCA treatment improved this loss of strength since the onset (Fisher's exact test). n=15-17 for each group used. Symbols represent mean ± SD of the different groups. *, **, *** represent the p< 0.05; 0.01 and 0.001 respectively.

TUDCA ameliorates tremors and abnormal neurological reflexes but not the spontaneous activity

The reduction of vertical movements, analysed by the number of rears on the wall of a cylinder, are a late manifesting aspect of the phenotype of the CMVMJD135 mice. Although TUDCA had limited effects on this parameter (Fig. 4A), we noticed that TUDCA-treated animals were still able to hold on their hindlimb paws during assessment of vertical exploratory activity at 34 weeks of age while CMVMJD135 mice under standard diet were unable to rise at this age, being completely immobile on the cylinder. Moreover, the horizontal movement analysed by the number of squares travelled in the arena for 1 minute showed no improvement by TUDCA (Fig 4B). Regarding other neurologic parameters, TUDCA treatment significantly improved the tremors and limb clasping displayed by CMVMJD135 mice (Fig. 4C, D respectively) comcumitantly with the appearance of these symptoms in the CMVMJD135 mice.

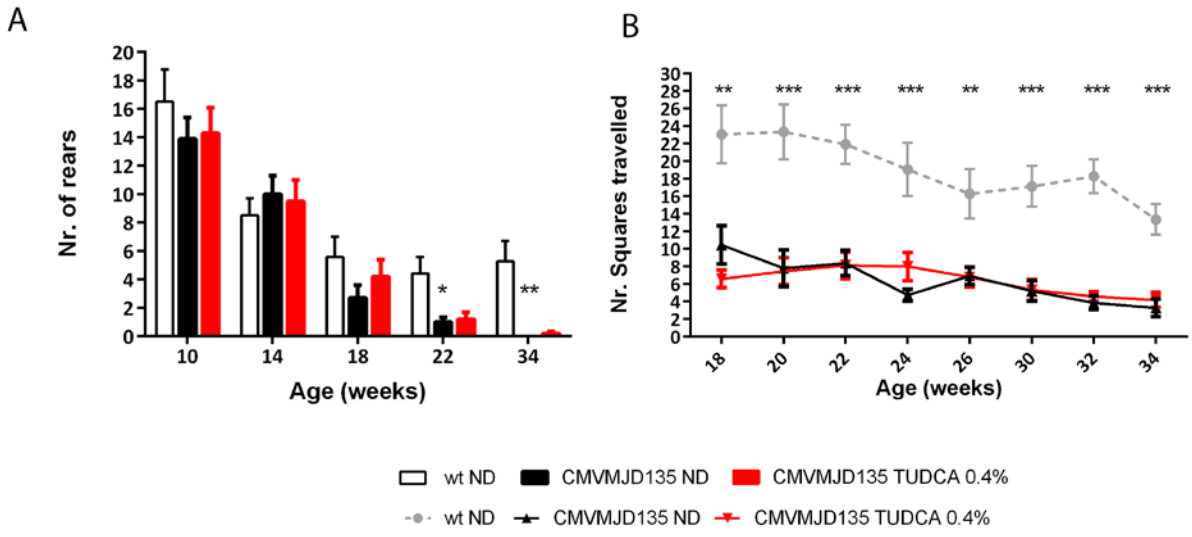

Figure 4. Continues next page.

Figure 4. Continued

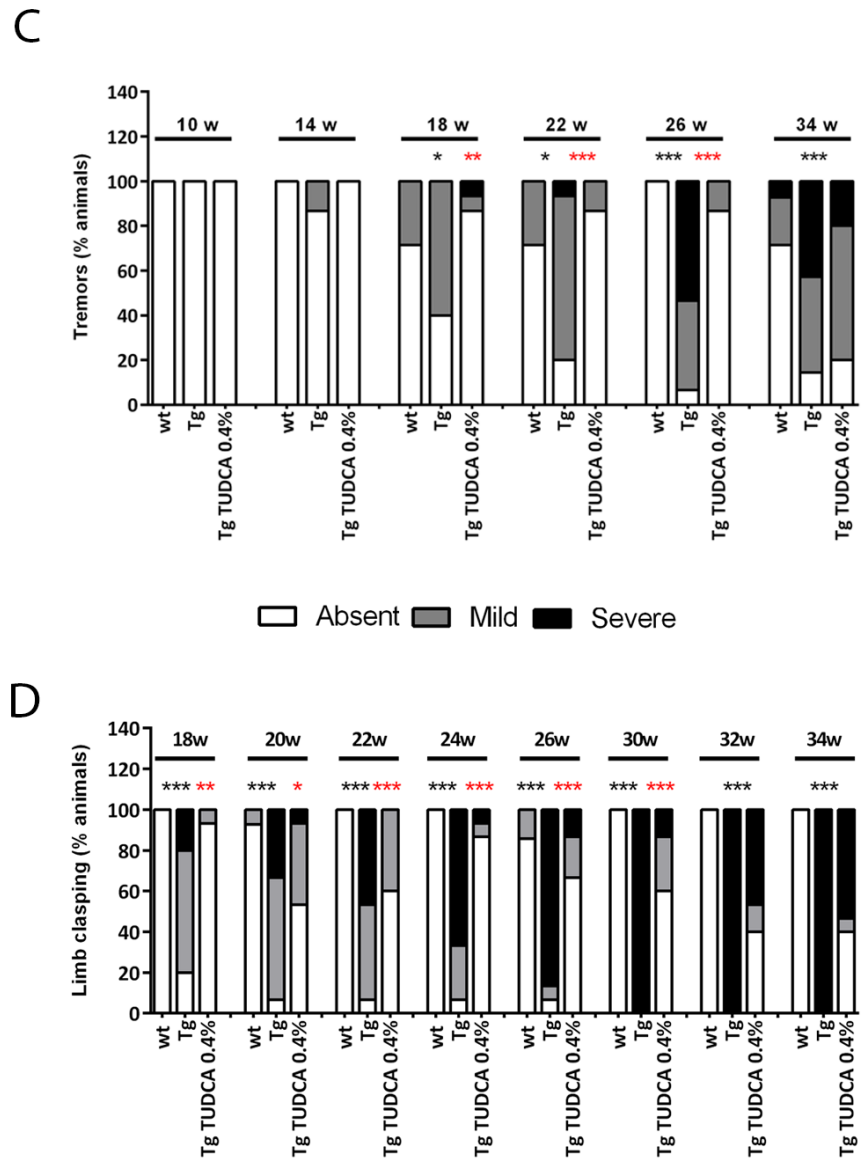

Figure 4. TUDCA had no major impact on exploratory activity but strongly reduced tremors and limb clasping. Spontaneous activity measured by the number of vertical movements (REARS) (Mann-Whitney U test) **(A)** and by the number of squares travelled in an open arena for 1 minute (Repeated measures ANOVA) **(B)** was not improved by TUDCA treatment. The tremors **(C)** and limb clasping **(D)** observed in the CMVMJD135 mice were significantly improved by chronic treatment (Fisher's exact test). n=15-17 for each group used. Symbols represent mean ± SD of the different groups. *, **, *** represent the p< 0.05; 0.01 and 0.001 respectively.

TUDCA treatment increases the Calbindin D28-K staining the Purkinje cell layer of the cerebellum of the CMVMJD135 mice

A decreased calbindin staining in the Purkinje cell layer of the cerebellum was previously described by others in transgenic mouse models of MJD (38, 39). We have also found a mild decrease in calbindin D28-K staining in the Purkinje cell layer of the cerebellum in the CMVMJD135 mice (40). TUDCA treatment increased the Calbindin D28-K staining in the Purkinje cell layer of the cerebellum ($p=0.005$) (Fig. 5A and B).

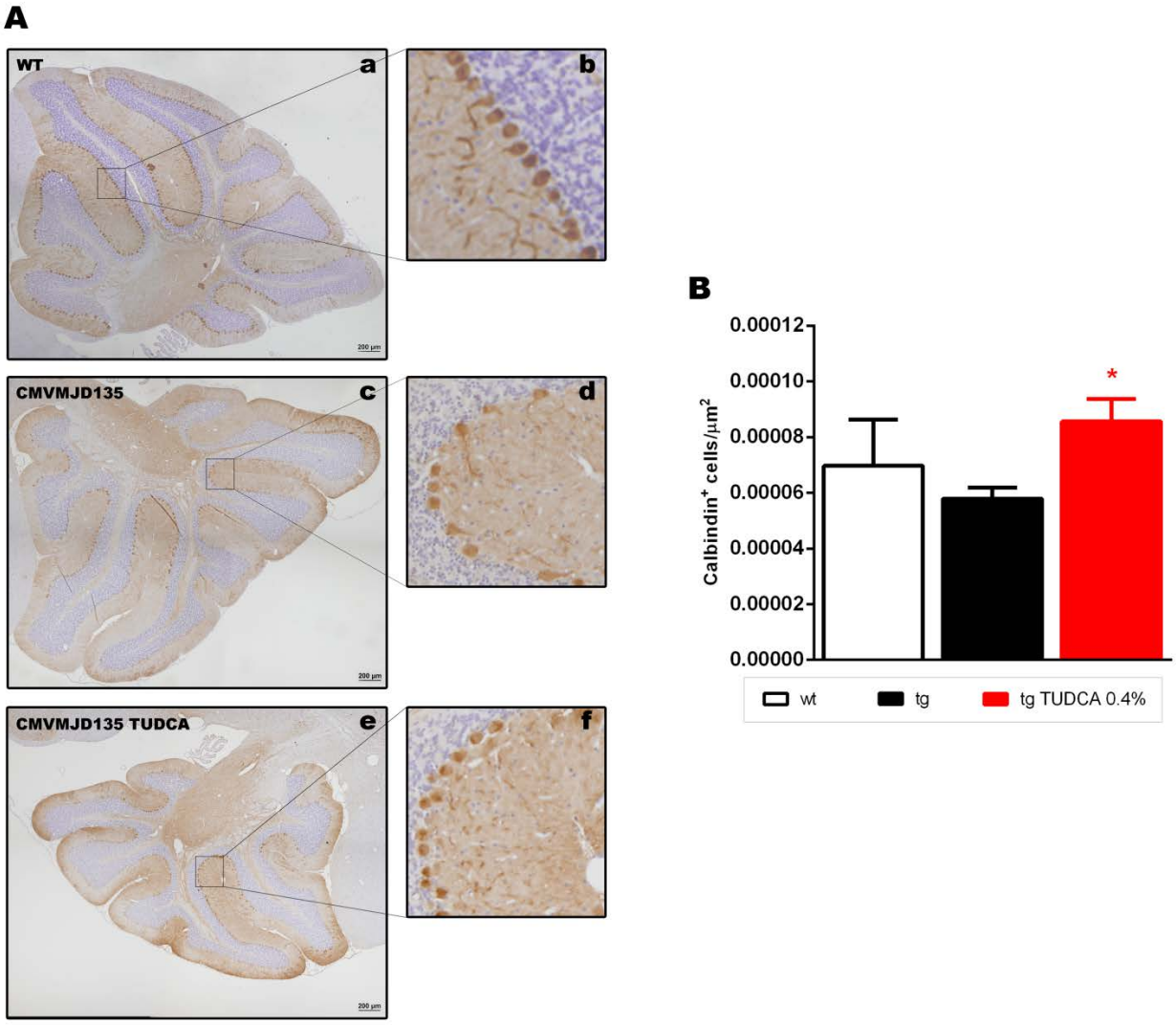

Figure 5. TUDCA treatment increases the Calbindin D28-K staining the Purkinje cell layer of the cerebellum of the CMVMJD135 mice. (A) representative images of Calbindin D28-K staining in wild-type (a-b), CMVMJD135 (c-d) and CMVMJD135-treated animals (e-f) (n=4 per group, 4 slides per animals were analyzed) and **(B)** quantitative analysis of Calbindin D28-K staining * represent the $p< 0.05$. The Calbindin D28-K positive cells were counted using the Fiji software (Image J). Scale bar 200µm.

Effects of TUDCA treatment on mutant ataxin-3

The presence of nuclear aggregates is a pathological hallmark of the disease in patients as well as in mouse models is (5, 15, 38, 41). Next, we quantified the number of ATXN3 positive nuclear inclusions in the brainstem of CMVMJD135 animals under standard and TUDCA diets. We found no effects of the treatment on ATXN3 aggregate load both on the pontine nuclei and lateral reticular nucleus (LRt) sub-regions of the brainstem (Fig.6 A, B respectively).

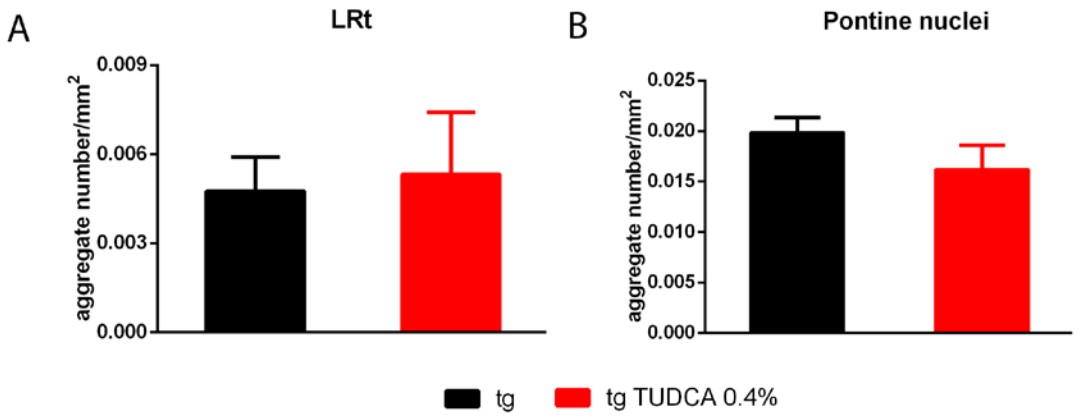

Figure 6. TUDCA treatment did not reduce the aggregate load in the brain of CMVMJD135 mice. Neuronal inclusions were counted in the LRt **(A)** and **(B)** pontine nuclei of 34-week-old animals under normal diet or TUDCA supplementation (n=3 for each condition). Four slides of each animal were used for the analysis (Student's t test). Values are presented as mean ± SEM; *p<0.05.

Molecular mechanism (s) of TUDCA action on the brain of CMVMJD135 mice

To dissect the mechanism(s) underlying the positive effects of TUDCA on CMVMJD135 mice neurological function, we performed an exploratory study addressing known modes of action of TUDCA in cells. This screen was first performed in the brainstem of animals that were subjected to 29 weeks of TUDCA treatment (i.e. 34 weeks old). Expression levels of molecules involved in the heat-shock response, autophagy, anti-oxidative response, ER stress and other neuroprotection pathways were measured and no differences were found between groups (Fig. 7A-E). Interestingly, molecules involved in inflammation were significantly influenced by TUDCA treatment. An up-regulation of TNF-a, Il-1b and Il10 (pro and anti-inflammatory cytokines) was found in CMVMJD135 mice, and the levels of these molecules were normalized by TUDCA treatment (Fig. 7F). No differences were found in other inflammation-related molecules such as Il-6, iNOS and lipocalin-2. Intriguingly, a similar analysis was performed in mice after a shorter time of TUDCA supplementation (18 weeks) and no statistically significant differences in expression were found for any the molecular pathways evaluated (Fig. S2 A-D),

neither between wt and CMVMJD135 mice nor between vehicle and TUDCA-treated transgenic mice. This suggests that neuroinflammation may be a late component rather than a primary determinant of the disease process in CMVMJD135 mice. We also measured the levels of some of the proteostasis-related genes in the spinal cord of 34 weeks old mice. We found no statistically differences in Hsp60, GRP75, BDNF, LC3 and GFAP. Consistently to the previous results, we found increased mRNA levels of TNF-α and Il1-β that were circumvented by TUDCA treatment (Fig. 8). Further studies should be conducted in younger animals to better understand the role of inflammation in the spinal cord and other brain regions besides the brainstem.

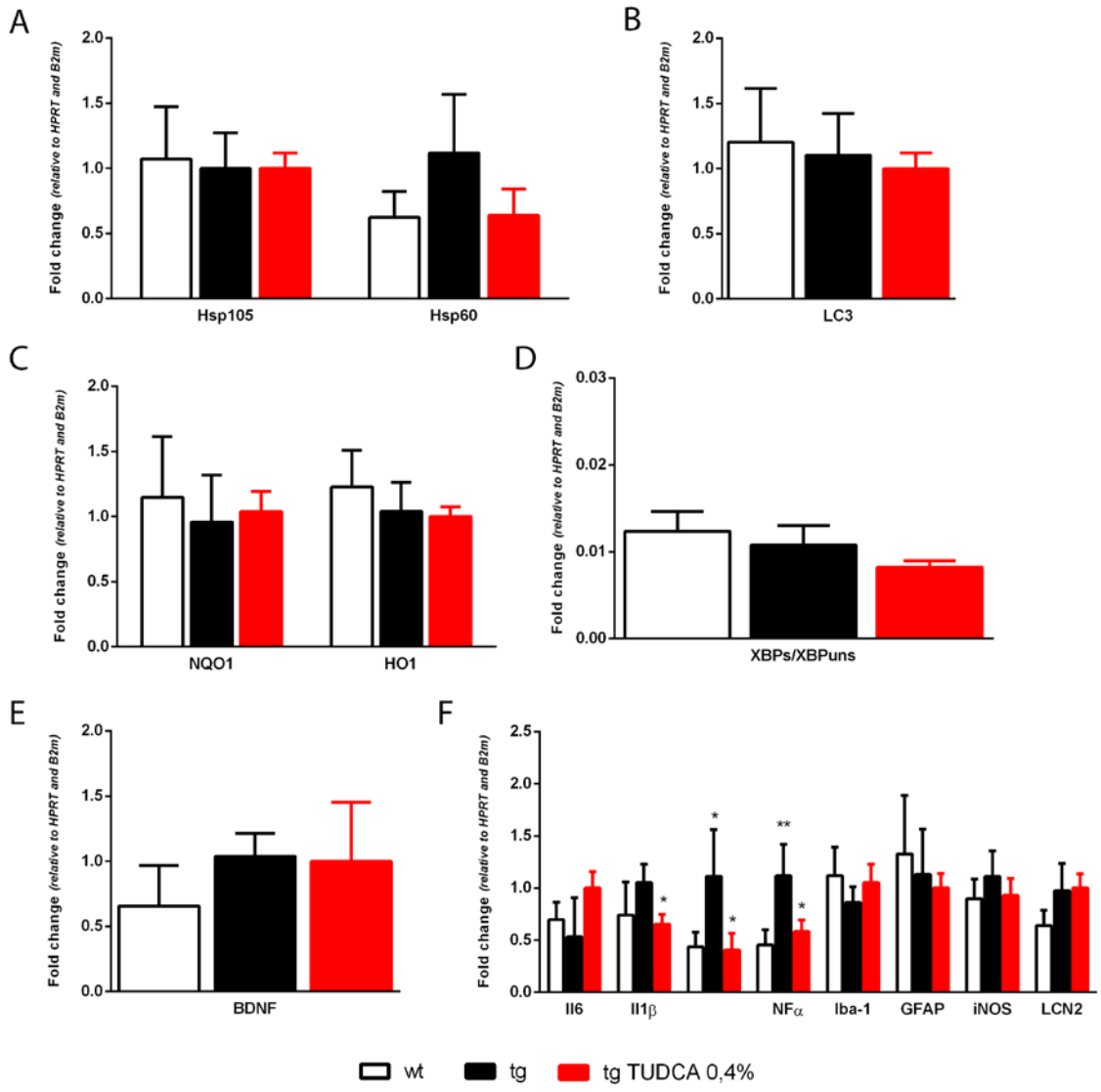

Figure 7. Effect of TUDCA treatment on mRNA expression of different proteostasis and inflammation-related genes. The expression levels of genes related to proteostasis such as **(A)** molecular chaperones, **(B)** autophagy, **(C)** anti-oxidative response, **(D)** ER stress, **(E)** neuroprotection and **(F)** inflammation were analyzed in the brainstem of 34 weeks-old wt and CMVMJD135 mice under normal and TUDCA diets. n=5-6 per group and two technical replicates were performed. Fold change (ΔΔCT method) is represented using B2m and HPRT as housekeepings genes (Student's t test). TUDCA was able to normalize the exacerbated inflammatory response of the CMVMJD135 mice. *, **, represent the p< 0.05; 0.01, respectively.

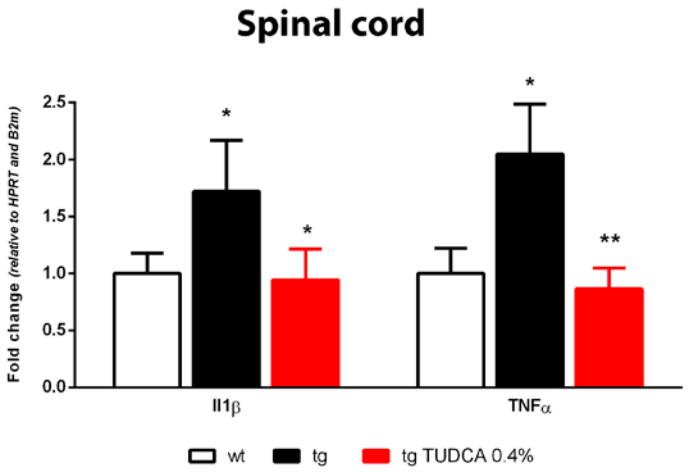

Figure 8. Effect of TUDCA treatment on mRNA expression of inflammation-related genes. The expression levels of TNF-α and Il1-β were analyzed in the spinal cord of 34 weeks-old wt and CMVMJD135 mice under normal and TUDCA diets. n=5-6 per group and two technical replicates were performed. Fold change (ΔΔCT method) is represented using B2m and HPRT as housekeeping genes (Student's t test). TUDCA was able to normalize the exacerbated inflammatory response of the CMVMJD135 mice in the spinal cord. *, **, represent the $p< 0.05$; 0.01, respectively.

Although, when we evaluated the mRNA levels of GFAP and Iba-1 (astrocytes and microglia markers respectively) we found no change in the mRNA expression levels of these markers (Fig. 7F), to further explore glial cell activation we measured the protein levels of GFAP in the total brainstem and found that GFAP was increased in CMVMJD135 mice and that the levels of this astrocytic marker were restored by TUDCA supplementation (Fig. 9A). Consistently, immunohistochemistry analysis of astrocytes in the substantia nigra showed a decreased GFAP staining intensity by TUDCA treatment (Fig. 9B). GFAP staining intensity was also quantified in the hilus of the hippocampus (unaffected region) and white matter of the cerebellum (potentially affected region), but no differences were found between groups (Fig. S3 A and B, respectively).

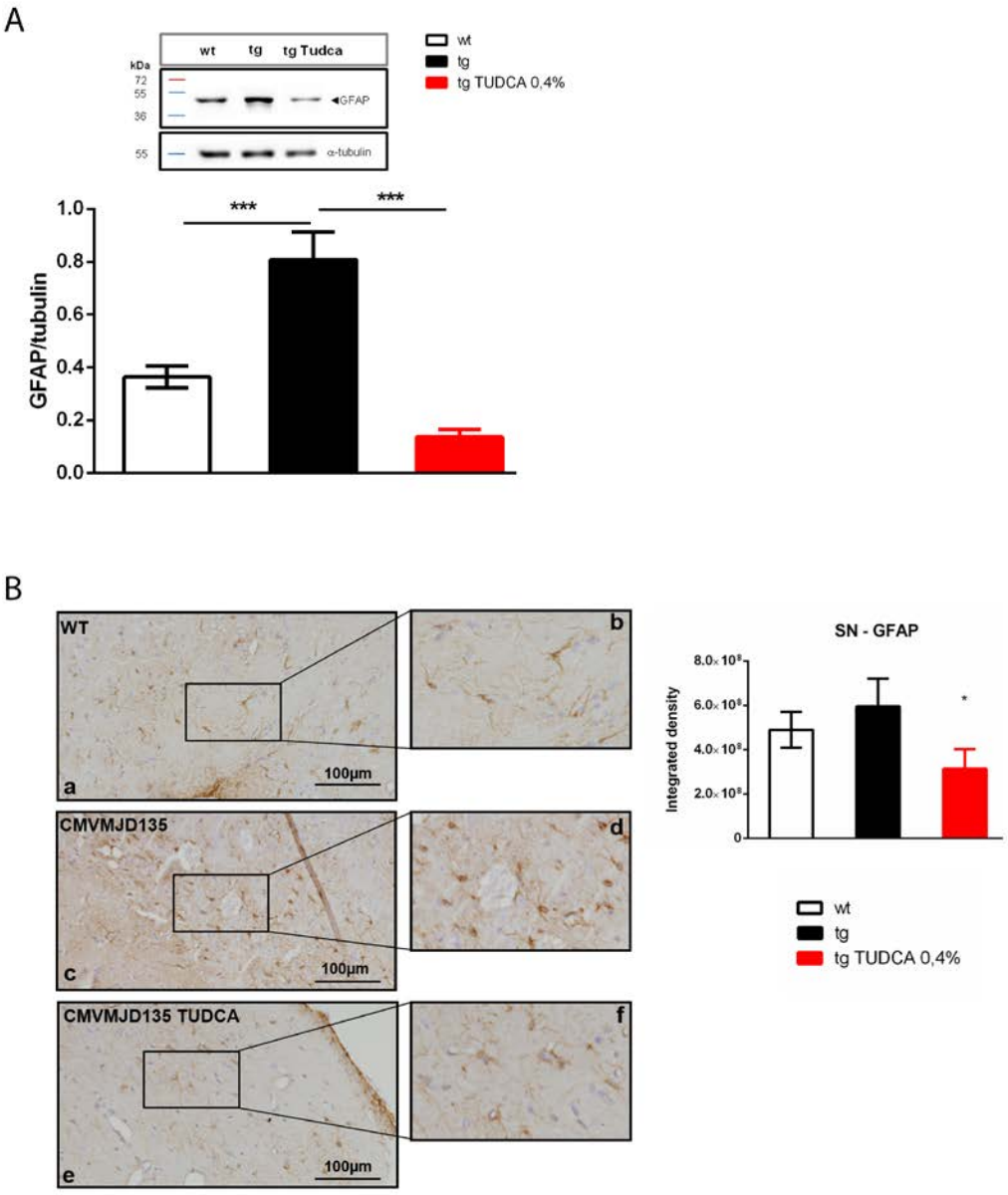

Figure 9. TUDCA decreases astrogliosis in the brainstem of the CMVMJD135 mice. TUDCA was able to **(A)** reduce the total protein levels of GFAP (astrocyte marker) in the brainstem of 34 weeks-old CMVMJD135 animals (n=4 per group, at least 3 technical replicates were performed) and **(B)** reduce the GFAP staining in the substantia nigra of the CMVMJD135 mice (n=4 per group, 4 slides per animals were analyzed). Representative images of the substantia nigra at 34 weeks of age of: (a-b) wild-type, (c-d) CMVMJD135 and (e-f) CMVMJD135 treated mice *, *** represent the $p< 0.05$ and 0.001 respectively. α-tubulin was used as loading control (Student's t test). The staining intensity was measured using the Fiji software (Image J).

Discussion

The neuroprotective effects of TUDCA, a nontoxic, endogenously produced bile acid, have been described in several models of neurodegenerative diseases (25, 27-30, 32) and this compound was already shown to have promising effects in ALS patients (24) without major adverse events. These findings make TUDCA and eventually other bile acids attractive candidate drugs for neurodegenerative diseases that require new and effective therapeutic approaches. Here we used a dosage of 0.4% (which corresponds to 100mg/Kg) of TUDCA, supplemented in the food. Based on the body surface area normalization method for interspecies drug translation (42), the human equivalent dosage is 8 mg/Kg, corresponding to approximately 600 mg/day for a standard body weight of 70 Kg. Considering that the recommended dosage of TUDCA in humans (for liver diseases) is 250-750 mg/Kg, the dosage herein used would be considered safe and within the therapeutic range. In this study we have shown that chronic administration of TUDCA, to the CMVMJD135 transgenic mouse model of MJD significantly improved motor function and reduced the glial overactivation, without affecting ataxin-3 aggregation load in the brain of the CMVMJD135 mice. In fact, perturbations of the brain inflammatory response are a crucial component of neurodegenerative diseases (reviewed in (43)). Microgliosis and astrogliosis are present in mouse models of several diseases, such as AD (44), PD (45), ALS (46) and HD (47) and in some cases are a triggering event of the disease (48). Likewise, we and others have shown the presence of gliosis in mouse models of MJD (15, 38, 49), in accordance to observations in post-mortem brains of MJD patients, which also showed an increase in pro and anti-inflammatory cytokines (50). Here we performed a detailed cytokine profile analysis in early and late-stages of the disease, and found a late up-regulation of both anti and pro-inflammatory molecules, as has been observed in HD (48, 51) and MJD patients (50). These findings were distinct from those observed for other neurodegenerative diseases, where inflammation takes place early in the disease course, since this inflammatory profile was only detected at an age when the phenotype of the CMVMJD135 mice was completely installed. Yet, the astrocytic marker GFAP was slightly increased (but not statistically different) at earlier disease stages, suggesting that the inflammatory process is likely initiated before the complete phenotype manifestation. Microglia might have an important role in MJD pathogenesis, a hypothesis which is currently being explored by us in CMVMJD135 mice brain. Interestingly, TUDCA treatment reverted the inflammatory process to basal levels in the brain of CMVMJD135 mice. The effects of TUDCA on glial cells have already been described in AD (26), but its anti-inflammatory properties are still poorly described in neurodegeneration. Recently, a study in a model of acute

neuroinflammation showed the effects of TUDCA on glial cell activation and migration, as well as on the expression of key inflammatory molecules. In that study, acute treatment with TUDCA was able to reduce the reactive gliosis as well as the levels of iNOS, by suppressing the NFkB pro- inflammatory pathway (32). Accordingly, studies by Joo and colleagues have previously shown that a similar bile acid, UDCA, was able to reduce nitrite production induced by β-amyloid deposition and that this effect was dependent on NFkB blockage (52). We have shown that chronic TUDCA was able to normalize the levels of Il1β, Il10 and TNFα in the brain, and to reduce astrogliosis in the substantia nigra at later stages of the disease.

In conclusion, we have shown the efficacy and safety of chronic TUDCA treatment and established that the inflammation modulatory properties of this compound might be beneficial for MJD. The fact that this bile acid is a FDA-approved compound and that was already tested in ALS patients without adverse events makes us suggest that TUDCA is a good candidate to test in MJD patients.

References

1. Maciel P, Gaspar C, DeStefano AL, Silveira I, Coutinho P, Radvany J, et al. Correlation between CAG repeat length and clinical features in Machado-Joseph disease. Am J Hum Genet. 1995;57(1):54-61.

2. Jardim LB, Pereira ML, Silveira I, Ferro A, Sequeiros J, Giugliani R. Neurologic findings in Machado-Joseph disease: relation with disease duration, subtypes, and (CAG)n. Arch Neurol. 2001;58(6):899-904.

3. Rub U, Schols L, Paulson H, Auburger G, Kermer P, Jen JC, et al. Clinical features, neurogenetics and neuropathology of the polyglutamine spinocerebellar ataxias type 1, 2, 3, 6 and 7. Prog Neurobiol. 2013;104:38-66.

4. Rub U, Brunt ER, Deller T. New insights into the pathoanatomy of spinocerebellar ataxia type 3 (Machado-Joseph disease). Curr Opin Neurol. 2008;21(2):111-6.

5. Paulson HL, Das SS, Crino PB, Perez MK, Patel SC, Gotsdiner D, et al. Machado-Joseph disease gene product is a cytoplasmic protein widely expressed in brain. Ann Neurol. 1997;41(4):453-62.

6. Schmidt T, Landwehrmeyer GB, Schmitt I, Trottier Y, Auburger G, Laccone F, et al. An isoform of ataxin-3 accumulates in the nucleus of neuronal cells in affected brain regions of SCA3 patients. Brain Pathol. 1998;8(4):669-79.

7. Seidel K, Meister M, Dugbartey GJ, Zijlstra MP, Vinet J, Brunt ER, et al. Cellular protein quality control and the evolution of aggregates in spinocerebellar ataxia type 3 (SCA3). Neuropathol Appl Neurobiol. 2012;38(6):548-58.

8. Seidel K, den Dunnen WF, Schultz C, Paulson H, Frank S, de Vos RA, et al. Axonal inclusions in spinocerebellar ataxia type 3. Acta Neuropathol. 2010;120(4):449-60.

9. D'Abreu A, Franca MC, Jr., Paulson HL, Lopes-Cendes I. Caring for Machado-Joseph disease: current understanding and how to help patients. Parkinsonism Relat Disord. 2010;16(1):2-7.

10. Chen X, Tang TS, Tu H, Nelson O, Pook M, Hammer R, et al. Deranged calcium signaling and neurodegeneration in spinocerebellar ataxia type 3. J Neurosci. 2008;28(48):12713-24.

11. Menzies FM, Huebener J, Renna M, Bonin M, Riess O, Rubinsztein DC. Autophagy induction reduces mutant ataxin-3 levels and toxicity in a mouse model of spinocerebellar ataxia type 3. Brain. 2010;133(Pt 1):93-104.

12. Chou AH, Chen SY, Yeh TH, Weng YH, Wang HL. HDAC inhibitor sodium butyrate reverses transcriptional downregulation and ameliorates ataxic symptoms in a transgenic mouse model of SCA3. Neurobiol Dis. 2011;41(2):481-8.

13. Wang HL, Hu SH, Chou AH, Wang SS, Weng YH, Yeh TH. H1152 promotes the degradation of polyglutamine-expanded ataxin-3 or ataxin-7 independently of its ROCK-inhibiting effect and ameliorates mutant ataxin-3-induced neurodegeneration in the SCA3 transgenic mouse. Neuropharmacology. 2013;70:1-11.

14. Goncalves N, Simoes AT, Cunha RA, de Almeida LP. Caffeine and adenosine A(2A) receptor inactivation decrease striatal neuropathology in a lentiviral-based model of Machado-Joseph disease. Ann Neurol. 2013;73(5):655-66.

15. Silva-Fernandes A, Duarte-Silva S, Neves-Carvalho A, Amorim M, Soares-Cunha C, Oliveira P, et al. Chronic treatment with 17-DMAG improves balance and coordination in a new mouse model of Machado-Joseph disease. Neurotherapeutics. 2014;11(2):433-49.

16. Duarte-Silva S, Neves-Carvalho A, Soares-Cunha C, Teixeira-Castro A, Oliveira P, Silva-Fernandes A, et al. Lithium chloride therapy fails to improve motor function in a transgenic mouse model of Machado-Joseph disease. Cerebellum. 2014;13(6):713-27.

17. Alves S, Nascimento-Ferreira I, Auregan G, Hassig R, Dufour N, Brouillet E, et al. Allele-specific RNA silencing of mutant ataxin-3 mediates neuroprotection in a rat model of Machado-Joseph disease. PLoS One. 2008;3(10):e3341.

18. Nascimento-Ferreira I, Santos-Ferreira T, Sousa-Ferreira L, Auregan G, Onofre I, Alves S, et al. Overexpression of the autophagic beclin-1 protein clears mutant ataxin-3 and alleviates Machado-Joseph disease. Brain. 2011;134(Pt 5):1400-15.

19. Nobrega C, Nascimento-Ferreira I, Onofre I, Albuquerque D, Hirai H, Deglon N, et al. Silencing mutant ataxin-3 rescues motor deficits and neuropathology in Machado-Joseph disease transgenic mice. PLoS One. 2013;8(1):e52396.

20. Costa MD, Luna-Cancalon K, Fischer S, Ashraf NS, Ouyang M, Dharia RM, et al. Toward RNAi Therapy for the Polyglutamine Disease Machado-Joseph Disease. Molecular Therapy. 2013;21(10):1898-908.

21. Rodriguez-Lebron E, Costa MD, Luna-Cancalon K, Peron TM, Fischer S, Boudreau RL, et al. Silencing Mutant ATXN3 Expression Resolves Molecular Phenotypes in SCA3 Transgenic Mice. Molecular Therapy. 2013;21(10):1909-18.

22. Vang S, Longley K, Steer CJ, Low WC. The Unexpected Uses of Urso- and Tauroursodeoxycholic Acid in the Treatment of Non-liver Diseases. Glob Adv Health Med. 2014;3(3):58-69.

23. Hylemon PB, Zhou H, Pandak WM, Ren S, Gil G, Dent P. Bile acids as regulatory molecules. J Lipid Res. 2009;50(8):1509-20.

24. Elia AE, Lalli S, Monsurro MR, Sagnelli A, Taiello AC, Reggiori B, et al. Tauroursodeoxycholic acid in the treatment of patients with amyotrophic lateral sclerosis. Eur J Neurol. 2015.

25. Macedo B, Batista AR, Ferreira N, Almeida MR, Saraiva MJ. Anti-apoptotic treatment reduces transthyretin deposition in a transgenic mouse model of Familial Amyloidotic Polyneuropathy. Biochim Biophys Acta. 2008;1782(9):517-22.

26. Nunes AF, Amaral JD, Lo AC, Fonseca MB, Viana RJ, Callaerts-Vegh Z, et al. TUDCA, a bile acid, attenuates amyloid precursor protein processing and amyloid-beta deposition in APP/PS1 mice. Mol Neurobiol. 2012;45(3):440-54.

27. Lo AC, Callaerts-Vegh Z, Nunes AF, Rodrigues CM, D'Hooge R. Tauroursodeoxycholic acid (TUDCA) supplementation prevents cognitive impairment and amyloid deposition in APP/PS1 mice. Neurobiol Dis. 2013;50:21-9.

28. Ramalho RM, Nunes AF, Dias RB, Amaral JD, Lo AC, D'Hooge R, et al. Tauroursodeoxycholic acid suppresses amyloid beta-induced synaptic toxicity in vitro and in APP/PS1 mice. Neurobiol Aging. 2013;34(2):551-61.

29. Keene CD, Rodrigues CM, Eich T, Chhabra MS, Steer CJ, Low WC. Tauroursodeoxycholic acid, a bile acid, is neuroprotective in a transgenic animal model of Huntington's disease. Proc Natl Acad Sci U S A. 2002;99(16):10671-6.

30. Castro-Caldas M, Carvalho AN, Rodrigues E, Henderson CJ, Wolf CR, Rodrigues CM, et al. Tauroursodeoxycholic acid prevents MPTP-induced dopaminergic cell death in a mouse model of Parkinson's disease. Mol Neurobiol. 2012;46(2):475-86.

31. Rodrigues CM, Fan G, Ma X, Kren BT, Steer CJ. A novel role for ursodeoxycholic acid in inhibiting apoptosis by modulating mitochondrial membrane perturbation. J Clin Invest. 1998;101(12):2790-9.

32. Yanguas-Casas N, Barreda-Manso MA, Nieto-Sampedro M, Romero-Ramirez L. Tauroursodeoxycholic acid reduces glial cell activation in an animal model of acute neuroinflammation. J Neuroinflammation. 2014;11:50.

33. Silva-Fernandes A, Costa Mdo C, Duarte-Silva S, Oliveira P, Botelho CM, Martins L, et al. Motor uncoordination and neuropathology in a transgenic mouse model of Machado-Joseph disease lacking intranuclear inclusions and ataxin-3 cleavage products. Neurobiol Dis. 2010;40(1):163-76.

34. Nicklas W, Baneux P, Boot R, Decelle T, Deeny AA, Fumanelli M, et al. Recommendations for the health monitoring of rodent and rabbit colonies in breeding and experimental units. Lab Anim. 2002;36(1):20-42.

35. Silva-Fernandes A, Duarte-Silva S, Neves-Carvalho A, Amorim M, Soares-Cunha C, Oliveira P, et al. Chronic Treatment with 17-DMAG Improves Balance and Coordination in A New Mouse Model of Machado-Joseph Disease. Neurotherapeutics. 2014.

36. Carter RJ, Lione LA, Humby T, Mangiarini L, Mahal A, Bates GP, et al. Characterization of progressive motor deficits in mice transgenic for the human Huntington's disease mutation. J Neurosci. 1999;19(8):3248-57.

37. Silva-Fernandes A, Oliveira P, Sousa N, Maciel P. Motor and Behavioural Abnormalities Associated with Persistent Spontaneous Epilepsy in the fvb/n Mouse Strain. Scand J Lab Anim Sci. 2010;37(3).

38. Cemal CK, Carroll CJ, Lawrence L, Lowrie MB, Ruddle P, Al-Mahdawi S, et al. YAC transgenic mice carrying pathological alleles of the MJD1 locus exhibit a mild and slowly progressive cerebellar deficit. Hum Mol Genet. 2002;11(9):1075-94.

39. Chou AH, Yeh TH, Ouyang P, Chen YL, Chen SY, Wang HL. Polyglutamine-expanded ataxin-3 causes cerebellar dysfunction of SCA3 transgenic mice by inducing transcriptional dysregulation. Neurobiol Dis. 2008;31(1):89-101.

40. Teixeira-Castro A, Jalles A, Esteves S, Kang S, da Silva Santos L, Silva-Fernandes A, et al. Serotonergic signalling suppresses ataxin 3 aggregation and neurotoxicity in animal models of Machado-Joseph disease. Brain. 2015.

41. Bichelmeier U, Schmidt T, Hubener J, Boy J, Ruttiger L, Habig K, et al. Nuclear localization of ataxin-3 is required for the manifestation of symptoms in SCA3: in vivo evidence. J Neurosci. 2007;27(28):7418-28.

42. Reagan-Shaw S, Nihal M, Ahmad N. Dose translation from animal to human studies revisited. FASEB J. 2008;22(3):659-61.

43. Heneka MT, Kummer MP, Latz E. Innate immune activation in neurodegenerative disease. Nat Rev Immunol. 2014;14(7):463-77.

44. Yoshiyama Y, Higuchi M, Zhang B, Huang SM, Iwata N, Saido TC, et al. Synapse loss and microglial activation precede tangles in a P301S tauopathy mouse model. Neuron. 2007;53(3):337-51.

45. St Martin JL, Klucken J, Outeiro TF, Nguyen P, Keller-McGandy C, Cantuti-Castelvetri I, et al. Dopaminergic neuron loss and up-regulation of chaperone protein mRNA induced by targeted over-expression of alpha-synuclein in mouse substantia nigra. J Neurochem. 2007;100(6):1449-57.

46. Frakes AE, Ferraiuolo L, Haidet-Phillips AM, Schmelzer L, Braun L, Miranda CJ, et al. Microglia induce motor neuron death via the classical NF-kappaB pathway in amyotrophic lateral sclerosis. Neuron. 2014;81(5):1009-23.

47. Mangiarini L, Sathasivam K, Seller M, Cozens B, Harper A, Hetherington C, et al. Exon 1 of the HD gene with an expanded CAG repeat is sufficient to cause a progressive neurological phenotype in transgenic mice. Cell. 1996;87(3):493-506.

48. Bjorkqvist M, Wild EJ, Thiele J, Silvestroni A, Andre R, Lahiri N, et al. A novel pathogenic pathway of immune activation detectable before clinical onset in Huntington's disease. J Exp Med. 2008;205(8):1869-77.

49. Switonski PM, Szlachcic WJ, Krzyzosiak WJ, Figiel M. A new humanized ataxin-3 knock-in mouse model combines the genetic features, pathogenesis of neurons and glia and late disease onset of SCA3/MJD. Neurobiol Dis. 2015;73:174-88.

50. Evert BO, Vogt IR, Kindermann C, Ozimek L, de Vos RA, Brunt ER, et al. Inflammatory genes are upregulated in expanded ataxin-3-expressing cell lines and spinocerebellar ataxia type 3 brains. J Neurosci. 2001;21(15):5389-96.

51. Silvestroni A, Faull RL, Strand AD, Moller T. Distinct neuroinflammatory profile in post-mortem human Huntington's disease. Neuroreport. 2009;20(12):1098-103.

52. Joo SS, Won TJ, Lee DI. Potential role of ursodeoxycholic acid in suppression of nuclear factor kappa B in microglial cell line (BV-2). Arch Pharm Res. 2004;27(9):954-60.

Supplementary figures

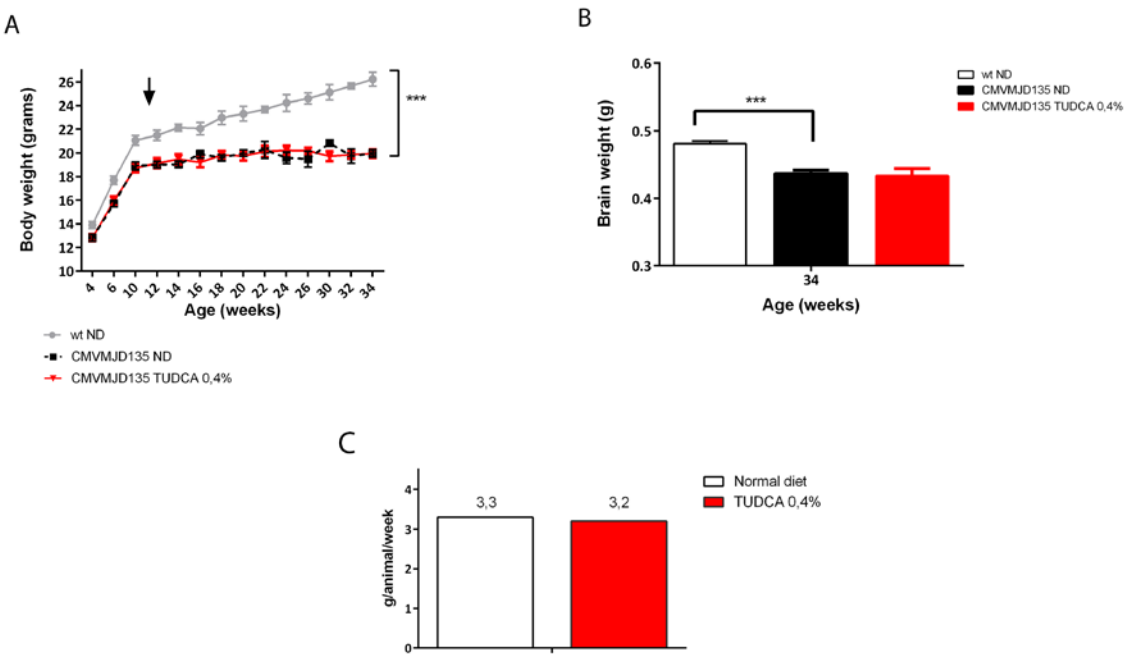

S1. TUDCA had no effect on body and brain weight of CMVMJD135 mice. (A) The body weight gain loss started at 10 weeks of age (black arrow) and **(B)** a 10% reduction of the total brain weight was observed for the CMVMJD135 mice at 34 weeks of age. TUDCA had no impact on both body and brain weight throughout the study. **(C)** The mean food consumption per day/per mouse was around 3 grams and no differences were obtained between diets. *** represent the p<0.001.

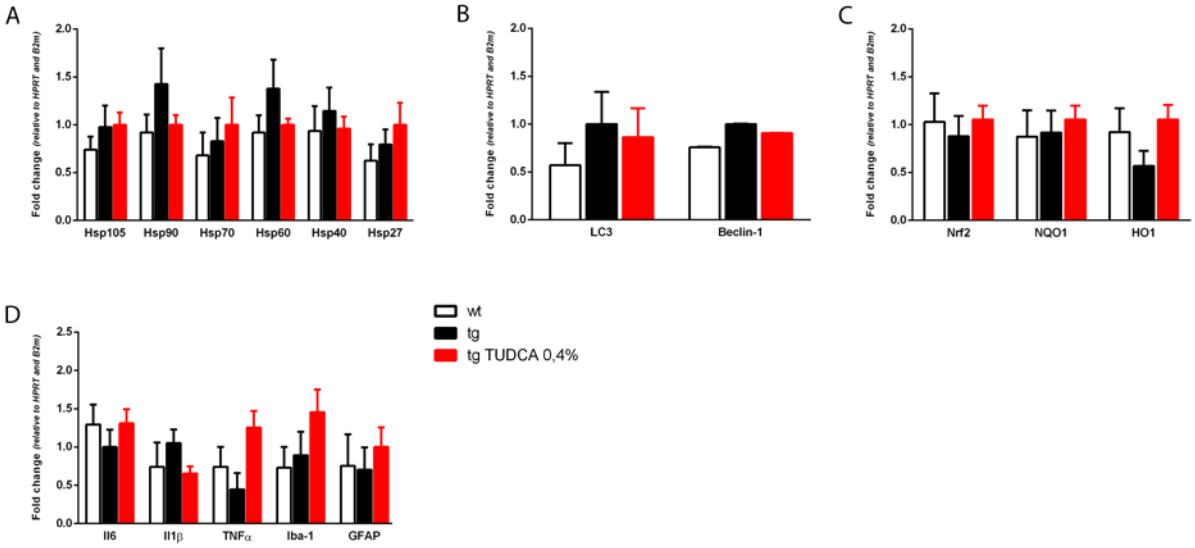

S2. Effect of a shorter TUDCA treatment on mRNA expression of different proteostasis and inflammation-related genes. The expression levels of genes related to proteostasis such as **(A)** molecular chaperones, **(B)** autophagy, **(C)** anti-oxidative response and **(D)** inflammation were analyzed in the brainstem of 23 weeks-old wt and CMVMJD135 mice under normal and TUDCA diets. n=5-6 per group and two technical replicates were performed. Fold change (ΔΔCT method) is represented using B2m and HPRT as housekeepings genes (Student's t test). *, **, represent the p< 0.05; 0.01, respectively.

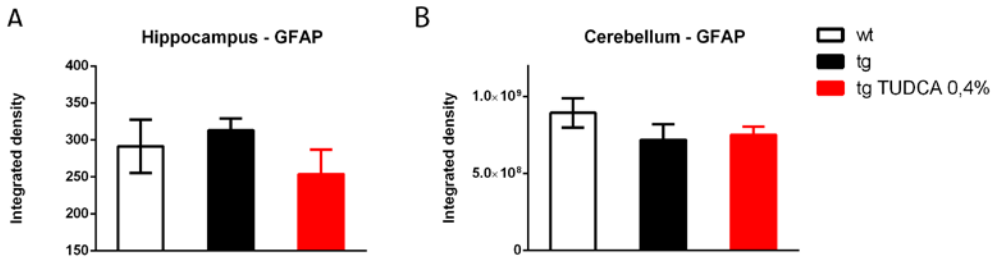

S3. Astrogliosis assessment in the hippocampus and in the cerebellum of the CMVMJD135 mice. No differences between groups were observed in the **(A)** hippocampus and in the **(B)** cerebellum of 34 weeks of age animals when the GFAP astrocyte marker was measured by immunohistochemical procedures. (n=4 per group, 4 slides per animals were analyzed). The staining intensity was measured using the Fiji software (Image J).

Table S1. Summary of comparisons between wt under standard diet and TUDCA supplemented food in the different phenotypic analyses. The values correspond to the p value for each time-point analyzed in the different behavioral tests. No differences were found between treated and untreated wt animals, except at one single time-point (26 weeks of age) for the number of squares travelled in the arena (labeled in yellow), which was 10% higher in treated animals.

			Age (weeks)													
			4	6	10	12	14	16	18	20	22	24	26	30	32	34
Body weight		p value (wt vs wt TUDCA 0.4%)	0.52	0.62	0.68	0.93	0.81	0.33	0.37	0.91	0.86	0.9	0.97	0.43	0.88	0.97
Behavioral test	Beam square 12mm		0.78		0.75		0.27	0.72	0.14	0.1	0.15	0.56	0.9	0.4		
	Beam circle 17mm		0.22		0.52		0.91	0.22	0.21	0.29	0.11	0.06	0.49			
	Motor swimming				0.68		0.94	0.36	0.056	0.51	0.57	0.16	0.3	0.3	0.45	0.12
	Foot dragging								1	1	1	1	1	1	1	1
	Quality of movement								1	1	1	1	0.48	1	1	1
	Hanging wire			0.38	0.3	0.86	0.18	0.33	0.1	0.33		0.33		0.58	0.5	0.52
	Hindlimb tonus			0.21		0.24		0.5		1		1		1		0.11
	Strength to grab			0.56		0.5		1		1		1		1		0.24
	Number of rears				0.83		0.5		0.17		0.87					0.65
	Number of squares in the arena								0.82	0.46	0.78	0.23	0.03	0.1	0.12	0.1
	Tremors				1		1		0.098		0.09		1			0.65
	Limb clasping								1	1	1	1	0.48	1	1	1

Chapter 6

Creatine-supplemented diet delays disease onset and improves the overall phenotype of the CMVMJD135 mouse model of MJD

Creatine-supplemented diet delays disease onset and improves the overall phenotype of the CMVMJD135 mouse model of MJD

Sara Duarte-Silva, Andreia Neves-Carvalho, Joana Silva, Anabela Silva-Fernandes and Patrícia Maciel

1) Life and Health Sciences Research Institute (ICVS), School of Health Sciences, University of Minho, Braga, Portugal;
2) ICVS/3B's - PT Government Associate Laboratory, Braga/Guimarães, Portugal;

* Corresponding author: Patrícia Maciel, PhD. Life and Health Sciences Research Institute (ICVS), School of Health Sciences, ICVS/3B's – PT Government Associate Laboratory, University of Minho, Campus Gualtar, 4710-057 Braga, Portugal. Telephone: 351-253-604824, Fax: 351-253-604820. E-mail: pmaciel@ecsaude.uminho.pt

Abstract

Machado-Joseph disease (MJD) is an autosomal dominant neurodegenerative disorder caused by the expansion of a polyglutamine tract (polyQ) in the C-terminus of the *ATXN3* gene product, ataxin-3. Mitochondrial dysfunction and consequent ATP depletion has been implicated in several neurodegenerative diseases. Thus, buffering intracellular energy levels could be neuroprotective. Creatine kinase and its substrates (creatine and phosphocreatine) are known as cellular energy buffers. Creatine administration increases brain concentrations of phosphocreatine and an inactivation of the mitochondrial permeability pore, which exerts protective effects in the brain. In this study we performed two pre-clinical trials – *PCT1 and PCT2* - using the CMVMJD135 mouse model of MJD (groups of animals with a 133 and 139 CAG repeat mean respectively), to which creatine 2% supplemented food was provided either for 19 (*PCT1*) or 29 (*PCT2*) weeks. Control animals were given the standard diet. The treatment started at the age of 5 weeks, one week before the previously observed onset of symptoms and a battery of motor and neurological behavioral tests was applied bi-weekly.

Oral administration of creatine in the diet led to an overall improvement in the motor phenotype of CMVMJD135 mice on both trials. Interestingly, in *PCT1,* with shorter creatine treatment duration but with less disease severity, the muscular strength deficits of the CMVMJD135 were improved, while in *PCT2*, corresponding to a longer treatment but a high severity disease condition those improvements were not so evident. Creatine-treated animals did, however, show improvement in both trials in motor coordination, limb strength and gait quality, as well as in other neurological parameters such as tremors and clasping. Creatine chronic treatment delayed the onset of several symptoms and, in some cases, completely abolished the appearance of the phenotype until the end of the trial.

The present findings support creatine supplementation as a useful strategy to slow the progression of MJD.

Introduction

Machado-Joseph disease (MJD) is the most common autosomal dominant ataxia worldwide, being caused by a mutation leading to the production of the protein ataxin-3 (ATXN3) with an expanded polyglutamine (polyQ) stretch (1). The symptoms of MJD are extensively heterogeneous varying from ataxia, ophthalmoplegia, diplopia, and dysarthria to peripheral neuropathy, dystonia and/or spasticity (2, 3). Apart from its specificities, MJD shares pathogenesis mechanisms with other PolyQ diseases, Parkinson's disease (PD), Amyotrophic Lateral Sclerosis (ALS) and Alzheimer's disease (AD), ultimately culminating in neuronal death.

One such mechanism is impaired energy metabolism associated with mitochondrial dysfunction. In polyQ diseases, particularly in Huntington's disease (HD), mitochondrial and energetic deficits are well described. Reduced concentrations of creatine and phosphocreatine have been observed in the basal ganglia of HD patients (4); there are also descriptions of a decrease in mitochondrial electron transport enzymes, such as cytochrome C oxydase I, in HD postmortem tissue (5, 6). Recently, a study using a transgenic mouse model of MJD revealed a decreased mtDNA copy number in affected brain regions that was aggravated with age and also the accumulation of mtDNA 3867bp deletions, particularly in the initial stages of the disease (7). This is agreement with findings in MJD patients' samples and in cells expressing mutant ataxin-3, which also showed decreased mtDNA copy number and an accumulation of mtDNA deletions (8). Considering these facts, therapeutic strategies that buffer cellular energy levels emerge as a possibility to prevent or improve the neurodegenerative process.

Creatine is a natural substance, exogenously consumed in the diet and endogenously synthesized by humans (and rodents) mainly in the kidney, pancreas and liver, using the amino acids arginine, glycine and methionine, before entering the bloodstream (9, 10). L-arginine:glycine amidinotransferase (transamidinase) catalyzes the production of guanidinoacetate, that in turn is methylated by S-adenosyl-methionine (catalyzed by GAMT) to produce creatine (11). Nearly 95% of the creatine pool is found in the skeletal muscle and the remaining 5% is found in the brain, liver, testes and kidneys (12). Within the cell, this molecule exists both as free creatine and phosphocreatine (PCr). In tissues such as brain and muscle, PCr functions as an energy buffer during periods of high energy demand (13). The first indication of the importance of creatine in neuronal functioning arose from the knowledge that patients with deficiency in creatine biosynthesis (e.g. GAMT deficiency) develop extrapyramidal movement disorders, seizures and developmental delay (14, 15). Importantly, in two cases, creatine supplementation was able to reverse the neurological impairments (16, 17).

Creatine is considered a key component in maintaining cellular energy homeostasis, and its administration has been reported in a wide number of experimental models of neurodegenerative diseases (18-23). An early study using the MPTP-induced neurodegeneration model of PD showed significant neuroprotection when the mouse food was supplemented with creatine 1% (18). After this initial work using mice, several clinical trials were performed in PD patients, although with very limited results (24, 25). In ALS models, creatine was shown to protect neurons against oxidative damage and improve motor impairments (19). Clinical trials in ALS patients, however, also revealed little improvements (26, 27). Despite these disappointing results, a long-term creatine supplementation was completed in ALS patients (phase II), but without known results so far (ClinicalTrials.gov Identifier: NCT00005766). Creatine supplementation showed to be protective to rat hippocampal neurons in the presence of Aβ toxic species but no clinical trials were conducted to date using creatine in AD patients. Mitochondria dysfunction and bioenergetic deficits are well documented for HD (reviewed in (28-30) and creatine exogenous supplementation was shown to improve motor function, to reduce protein aggregates and increase survival rate or life-span of transgenic mouse models (20, 21, 31). Creatine supplementation to HD patients was shown to be safe and to reduce the levels of 8OH2'dG (DNA damage marker) (32). Accordingly, another phase II clinical trial in HD showed that a high dose (uo to 30 mg per day) of creatine was safe and well tolerated. A phase III clinical trial of creatine usage in HD has terminated this year (with 650 subjects enrolled) but the results are not yet known (ClinicalTrials.gov Identifier: NCT00712426). Since creatine is an endogenous compound and is present in the daily diet, it is not surprising that the side effects caused by creatine supplementation are very few, both for healthy persons and patients (33-35).

All these studies prompted us to test the efficacy of creatine in a transgenic mouse model of Machado-Joseph disease – CMVMJD135 - previously described by us (36), and shown to be a valuable model to perform pre-clinical trials (36, 37). We carried out a chronic treatment of 19 weeks using creatine 2% supplementation in the food of the animals. Creatine supplementation improved and delayed the motor symptoms and the overall phenotype of the CMVMJD135 mice. These results encouraged us to perform a second preclinical trial using creatine 2% supplementation for 29 weeks in a more severe disease condition. In this case, creatine treatment was also able to improve the overall phenotype of the CMVMJD135 animals, albeit to a lesser extent on what concerns muscular deficits. Nevertheless, both trials showed creatine to be efficacious in improving CMVMJD135 mice phenotype, making creatine an appealing compound for MJD treatment.

Material and methods

Ethics statement. All procedures were conducted in accordance with European regulations (European Union Directive 2010/63/EU). Animal facilities and the people directly involved in animal experiments (S.D.S, A.N.C) were certified by the Portuguese regulatory entity — Direcção Geral de Alimentação e Veterinária.

All of the protocols performed were approved by the Animal Ethics Committee of the Life and Health Sciences Research Institute, University of Minho.

Animals. Female CMVMJD135 (background C57BL/6) mice were used in the study. Transgenic and non-transgenic drug- and placebo- treated animals were alternately assigned and housed at weaning in groups of 5 animals in filter-topped polysulfone cages 267 × 207 × 140 mm (370 cm^2 floor area) (Tecniplast, Buguggiate, Italy), with corncob bedding (Scobis Due, Mucedola SRL, Settimo Milanese, Italy) in a conventional animal facility. The progeny produced by mating MJD transgenic with wild-type animals was genotyped at weaning by PCR, as previously described (38). All animals were maintained under standard laboratory conditions: an artificial 12 h light/dark cycle (lights on from 8:00 to 20:00 h), with an ambient temperature of 21±1°C and a relative humidity of 50–60%; the mice were given a standard diet (4RF25 during the gestation and postnatal periods, and 4RF21 after weaning, Mucedola SRL, Settimo Milanese, Italy) and water *ad libitum*. Health monitoring was performed according to FELASA guidelines (39), confirming the Specified Pathogens status of sentinel animals maintained in the same animal room. Humane endpoints for experiment were defined (20% reduction of the body weight, inability to reach food and water, presence of wounds in the body, dehydration), but not needed in practice as the study period was conceived to include ages at which animals do not reach these endpoints. The animals were sacrificed by different methods according to the final purpose: either by decapitation or exsanguination perfusion with saline or PFA 4%; in this case, the animals were deeply anesthetized with a mixture of ketamine hydrochloride (150 mg/kg) plus medetomidine (0.3 mg/kg).

Mouse genotyping. The progeny produced by mating hemizygous MJD transgenics with wild-type animals was genotyped at weaning by PCR, as previously described (38).

Creatine treatment

PCT1 – Preclinical Trial 1. CMVMJD135 and wt female mice were distributed and housed in groups of 5 animals per cage. Creatine was supplemented in the standard diet at 2% (4RF21, Mucedola SRL, purchased at Ultragene, Portugal), as previously described to be the more efficacious dose in a preclinical trial with HD mice (31). At 5 weeks of age the animals were sequentially assigned by cage into four groups of 10-12 animals each: CMVMJD135 and wt under normal diet and CMVMJD135 and wt under diet supplemented with creatine 2%. The treatment had the duration of 19 weeks, until the animals reached 24 weeks of age. Creatine 2% treatment was started at 5 weeks of age due to the previous knowledge that the phenotype in this model starts at 6 weeks of age (36). The mean CAG repeat size (±SD) for all mice used was 133 ± 1 repeat units. The timeline of experiments performed in this trial is represented in Supplementary Fig1A.

PCT2 – Preclinical Trial 2. CMVMJD135 and wt female mice were distributed and housed in groups of 5 animals per cage. Creatine was supplemented in the standard diet at 2% (4RF21, Mucedola SRL, purchased at Ultragene, Portugal) as previously described to be the more efficacious dose (31). At 5 weeks of age the animals were sequentially assigned by cage into four groups of 15 animals each: CMVMJD135 and wt under normal diet and CMVMJD135 and wt under diet supplemented with creatine 2%. The treatment had the duration of 29 weeks, until the animals reached 34 weeks of age. This was chosen based on the fact that CMVMJD135 mice under standard diet were still able to reach the food in the cage and perform most of the behavioral tests used in the study; from our knowledge of the model, after this period of time these animals may no longer be able to reach the food alone and perform some of the behavioral tests. The mean CAG repeat size (±SD) for all mice used was 139 ± 4 repeat units. The timeline of experiments performed in this trial is represented in Fig 2A.

Body weight. All mice were weighted from 4 weeks of age until the end of each trial (*PCT1*: 24 and *PCT2*: 34 weeks of age) every two weeks.

Phenotypic analysis

Beam walk balance test. This test assesses balance but is also sensitive to fine motor coordination. The test was performed as previously described (40). The animals were trained during 3 days in the square beam (12 mm). In the fourth day, they were tested in the training beam and also in one round beam (17 mm). If the animal fell or turned around in the beam, this was considered one

failed trial. Each animal had the opportunity to fail 2 times in each beam. The time the animal took to cross the beam was counted, and time was discounted if the animal stopped in the beam.

Motor swimming test. To analyse voluntary locomotion, the mice were trained for 2 consecutive days (3 trials each animal) to traverse a clear perspex water tank to a safe platform at the end. The perspex tank was 100 cm long and the platform at the end was made from black perspex. The latency to cross the water tank was measured from a distance of 60 cm (the tank was labeled with a blue line to mark the initiation). The water temperature was monitored and set at 23 °C using a thermostat (40). The mice were tested for 3 consecutive days (2 trials per animal) and the latency to traverse the tank registered by the experimenter.

SHIRPA protocol. We established a protocol for phenotypic assessment based on the primary screen of the SHIRPA protocol, which mimics the diagnostic process of general neurological and psychiatric examination in humans (41). Each mouse was placed in a viewing jar (15 cm diameter) for 5 minutes, transferred to a 15-labeled-squares arena (55×33×18 cm), and then a series of anatomical and behavioral features were registered. The full details of the SHIRPA protocol are available at the site: http://empress.har.mrc.ac.uk/browser/?sop_id=10_002_0. In addition, we included the footprint pattern test (see below) to assess gait as described in (40). The protocol was adjusted in order to minimize animal handling and to generate uniformity in waiting times between the tests (42).

Footprint pattern. The footprint test was used to evaluate the gait of the animals. To obtain footprints, the hind- and forepaws of the mice were coated with black and red non-toxic paints, respectively. A clean rectangular paper sheet was placed on the floor of the runway for each run. The animals were then allowed to walk along a 100-cm-long×4.2 cm width×10 cm height corridor in the direction of an enclosed black box. An inclined corridor was used instead of a horizontal, since mice have the tendency to run upwards to escape. Each animal was allowed to achieve one valid trial per age. To evaluate the severity of foot dragging through age the foot printing pattern of CMVMJD135 and wt controls was classified at each time point considering six consecutive steps (0=absent/mild, up to three steps; 1=mild, more than three steps out of six; 2=severe, all steps out of six). The stride length was measured manually as the distance between two pawprints. Three values were measured, for six consecutive steps, and the mean of the three values was used.

Hanging wire grip test. The mice were placed on the top of a metallic grid and inverted 180° towards the surface of the bench. The latency to fall from the grid was registered by the experimenter. The maximum time of the test was 120 seconds.

Molecular analysis

Western-blot. Brain tissue was homogenized in cold 0.1 M Tris-HCl, pH 7.5, 0.1 M EDTA, and a mixture of protease inhibitors (Complete; Roche, Swiss) and was sonicated for 10 seconds. Protein concentration was determined using the Bradford assay (Biorad). Samples were heated for 5 minutes at 100°C, and microfuged for 10 seconds before loading. For each sample, 15 micrograms of total protein were loaded into SDS-Page gels and then transferred to nitrocellulose membranes (Biorad). After incubation with the primary antibodies: rabbit anti-ataxin-3 (1:10.000), mouse p62 (1:1000, Abnova), rabbit LC3 (1:1000, Novus Biologicals), rabbit anti-GFAP (1:500, Dako), mouse anti-α-tubulin (1:200, DSHB) and mouse anti-β-actin (1:200, DSHB), the secondary antibodies were incubated at the following dilutions: anti-rabbit (1:10.000, Biorad) and anti-mouse (1:10.000, Biorad) . Antibody affinity was detected by chemiluminescence (Clarity Western ECL, Biorad). Band quantification was performed using the Image Lab software according to the manufacturer's instructions.

qRTPCR. Total RNA was isolated from CMVMJD135 mouse tissues using TRIZOL (Invitrogen, Calrsbad, CA, USA) according to the manufacturer's protocol. First-strand cDNA, synthesized using oligo-dT (Biorad), was amplified by quantitative reverse-transcriptase PCR (qRT-PCR) according to the guidelines (Biorad). Human and mouse ataxin-3 primers were used for transgene expression quantification (43). The primers used were based on literature (36) or designed using PRIMER-BLAST (http://www.ncbi.nlm.nih.gov/tools/primer-blast/), on the basis of the respective GenBank sequences. All accession numbers and primer sequences are available on request. The reference gene for hypoxanthine guanine phosphoribosyl transferase (Hprt) (accession number from GenBank: NM_013556) was used as an internal standard for the normalization of the expression of selected transcripts. qRT-PCR was performed on a CFX 96TM real time system instrument (Bio-Rad Laboratories, Hercules, CA, USA), with the SoFast Eva Green RT-PCR reagent kit (Bio-Rad Laboratories, Hercules, CA, USA) according to the manufacturer's instructions, using equal amounts of RNA from each sample. Product fluorescence was detected at the end of the elongation cycle. All melting curves exhibited a single sharp peak at the expected temperature.

Neuropathology and immunohistochemistry. Transgenic and wt littermate mice were deeply anesthetized and transcardially perfused with PBS followed by 4% paraformaldehyde (PFA) in PBS. Brains were post fixed overnight in fixative solution and embedded in paraffin. Slides with 4-µm-thick paraffin sections were stained with cresyl violet or processed for immunohistochemistry with rabbit anti-ataxin-3 (1:1000, Millipore), rabbit GFAP (1:500, DAKO Corporation) and rabbit anti-calbindin D-

28K (1:1000, Millipore). Ataxin-3 positive inclusions in the pontine nuclei of 24 or 34 weeks old animals (*PCT1* and *PCT2*, respectively) and calbindin positive cells in the Purkinje cell layer of the cerebellum of 34 weeks old animals (*PCT2*) either under standard or creatine supplemented diets were quantified and normalized for total area using the Fiji software (Image J).

Statistical analysis. The experimental unit used in this study was a single animal. Power analysis was used to determine the sample size as previously described (44). The estimates of required number of CMVMJD135 animals for specific behavioral tests and time-points of analysis are described in (37). Continuous variables with normal distributions (K-S test $p>0.05$) were analyzed with the Student t-test or two-way ANOVA (Factors: genotype and treatment). Behavioral data were subjected to the non-parametric Mann-Whitney U-test when variables were non-continuous or when a continuous variable did not present a normal distribution (Kolmogorov-Smirnov test $p<0.05$). Categorical variables in the SHIRPA protocol were analyzed by contingency tables (Fisher's exact test). All statistical analyses were performed using SPSS 22.0 (SPSS Inc., Chicago, IL). A critical value for significance of $p< 0.05$ was used throughout the study.

Results

PCT1

Treatment with creatine for 19 weeks improves body weight and muscular strength deficits of the CMVMJD135 mice

The amount of food intake per mouse was found to be around 3 g per day, with no significant difference between treated and untreated mice (Suppl. Fig 1B). Creatine treatment for 19 weeks rescued the decreased body weight of CMVMJD135 mice in the last time point of analysis (at 24 weeks of age) (Fig 1A). Loss of muscular strength is the first disease symptom observed in these mice (Chapter 2), which showed to be very difficult to improve with all the compounds tested in this model so far (Chapters 2 to 5). Yet, in this pre-clinical trial creatine 2% avoided the loss of muscular strength during disease progression until the end of the trial, at 24 weeks of age (Fig 1B).

Chronic treatment with creatine improved motor and gait deficits of the CMVMJD135 mice

The beam walk test was performed at two time-points (18 and 24 weeks of age). In this test we evaluate balance and fine coordination of the animals. In the square beam (Fig 1C), the phenotype is generally detectable at 18 weeks of age and progresses during age. Creatine 2% treated mice clearly showed an improvement of the coordination deficits. Also, in the circle beam the phenotype was observed at 24 weeks of age and creatine 2% treatment significantly improved the phenotype to wild-type animals' performance (Fig 1D). Motor coordination was also evaluated in the motor swimming test, this phenotype of the CMVMJD135 mice being evident at 22 weeks of age. In accordance with the previous results observed in the beam walk test, creatine 2% treatment significantly improved this motor deficit in both time points analyzed (Fig 1E). Also, the foot dragging phenotype was improved by creatine 2% treatment since 18 to 24 weeks of age (Fig 1F).

Creatine 2% reduces the ataxin-3 positive nuclear aggregates in key-disease brain regions

We quantified the number of ATXN3 positive nuclear inclusions in the brainstem of CMVMJD135 animals under standard and creatine diets. Creatine 2% treatment was able to significantly decrease the aggregate load in the pontine nuclei and LRt of CMVMJD135 animals (Fig 1G and H respectively).

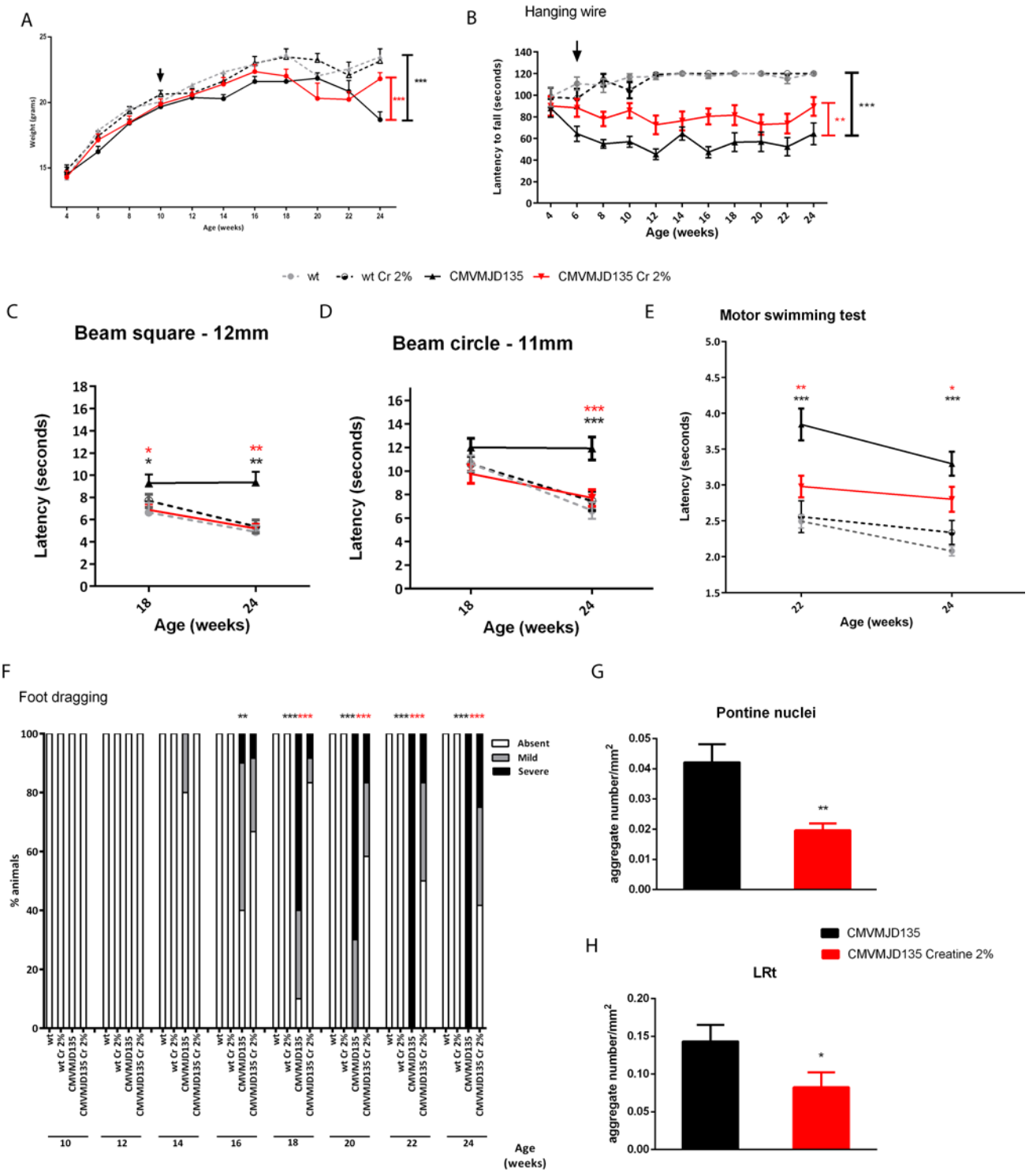

Figure 1. Effect of creatine treatment during 19 weeks on CMVMJD135 mice – *PCT1* (A) The body weight gain loss of the CMVMJD135 mice started at 10 weeks of age (arrow) and Creatine 2% improved body weight gain loss at 24 weeks of age (Repeated measures ANOVA) **(B)** The hanging wire test was performed to evaluate limb strength, and the phenotype onset occurred at 6 weeks of age. Creatine 2% improved this phenotype since the onset of the phenotype until the end of this study (Repeated measures ANOVA was used considering genotype and treatment factors). CMVMJD135-treated mice have a better performance on the beam walk test both in

the **(C)** square and in the **(D)** round beams. In the motor swimming test **(E)** this improvement is also observed in both time-points tested **(F)** the foot dragging phenotype starts being detectable at 16 weeks of age and progresses as animal's age; creatine supplementation improved this phenotype since 18 weeks of age until the end of this pre-clinical study. n=10 for each group used. Symbols represent mean ± SD of the different groups.*, **, *** represent the p< 0.05, 0.01 and 0.001 respectively. The nuclear inclusions positive for ATXN3 are reduced in the CMVMJD135 treated with Creatine 2% in the **(G)** pontine nuclei and **(H)** in the LRt. n=4 for each group (4 slides per animal). Symbols represent mean ± SD of the different groups.*, **, represent the p< 0.05 and 0.01 respectively.

PCT2

Effect of creatine supplementation on body and brain weight of the CMVMJD135 animals

All the animals were tested before any treatments were initiated, at 4 weeks of age. The body weight (Fig 2C), motor coordination (Fig 4A) and muscular strength (Fig 5A) were not different between groups at this age. At 5 weeks of age, creatine 2% supplemented diet started being given to wild-type (wt) and CMVMJD135 animals, while the vehicle groups (wt and CMVMJD135) remained under standard diet. Creatine chronic treatment was kept until the animals reached 34 weeks of age. The amount of food intake per mouse was found to be around 3 g per day, with no significant difference between treated and untreated mice (Fig 2B). Creatine treatment had no impact on body weight gain (Fig 2C). Interestingly, creatine was able to slightly ameliorate the loss in total brain weight of the transgenic animals at 34 weeks of age (Fig 2D).

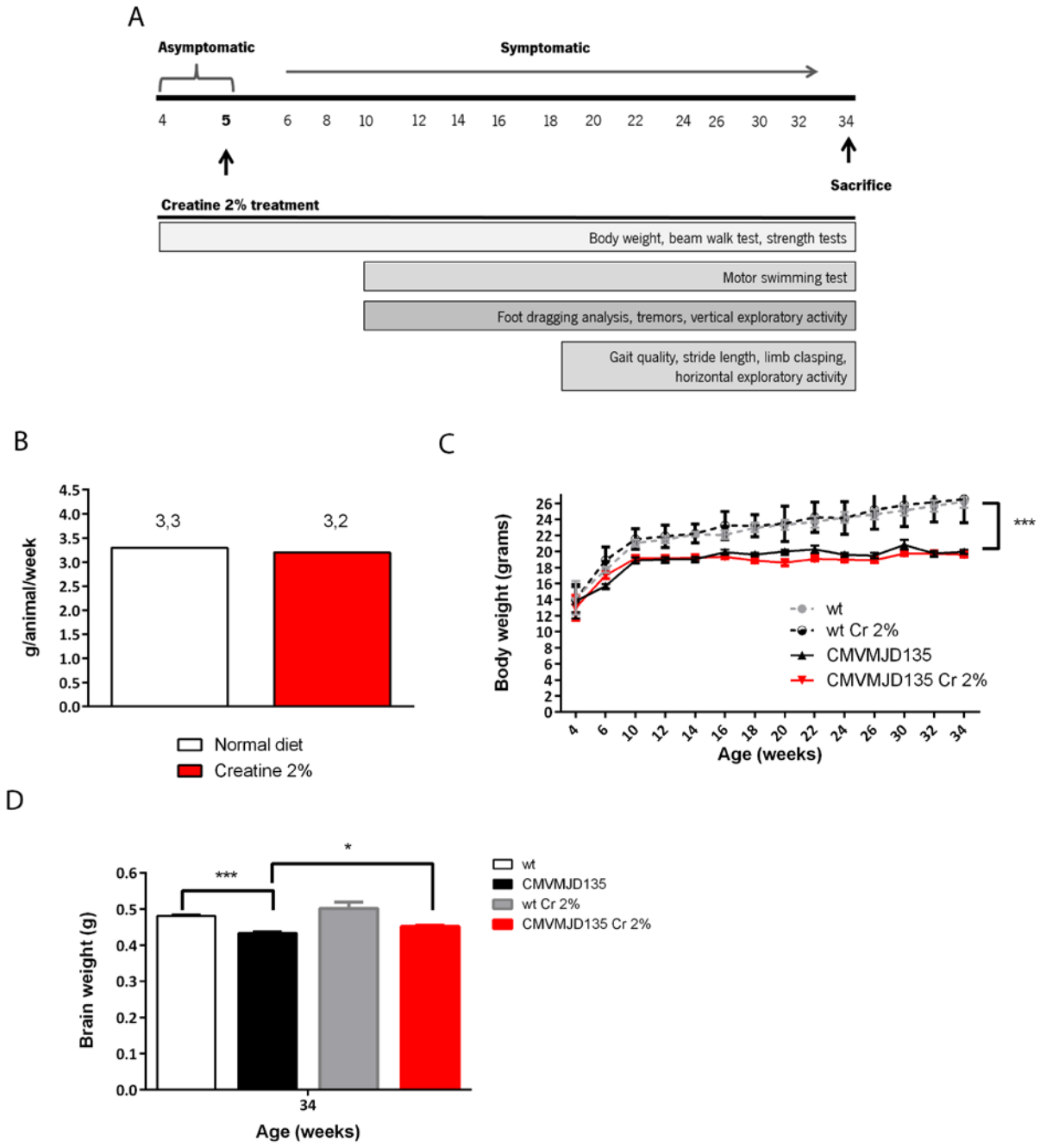

Figure 2. Creatine treatment effects on body and brain weight of CMVMJD135 mice (A) Schematic timeline for the behavioral analysis of creatine 2% pre-clinical trial **(B)** The mean food consumption per day/per mouse was around 3 grams and no differences were obtained between diets (Student's t test). **(C)** The body weight gain loss started at 10 weeks of age and creatine 2% had no impact (Repeated measures ANOVA)**(D)** A 10% reduction of the total brain weight was observed for the CMVMJD135 mice at 34 weeks of age. In creatine-treated animals the brain weight loss was only 6% (Student's t test). *, *** represent the $p<0.05$ and 0.001 respectively.

Creatine supplementation treatment delayed onset and improved symptoms related to muscular strength

The CMVMJD135 mice treated with creatine showed improved forelimb strength and hindlimb muscular tonus (Fig 3A and B, respectively) until the end of the pre-clinical trial, at 34 weeks of age. Furthermore, the onset of these deficits was delayed by 8 weeks (labeled with green #). Yet, the overall muscular strength measured by the hanging wire test showed only a transient amelioration of the phenotype at 12 weeks of age, which was no longer observed as disease progressed (Fig 3C). The muscular strength deficits seem to correlate directly with the CAG repeat length, since in the *PCT1* that we performed, this symptom was significantly ameliorated for a longer period of time, and the effect of creatine was sustained until the end of the trial (Fig 1B).

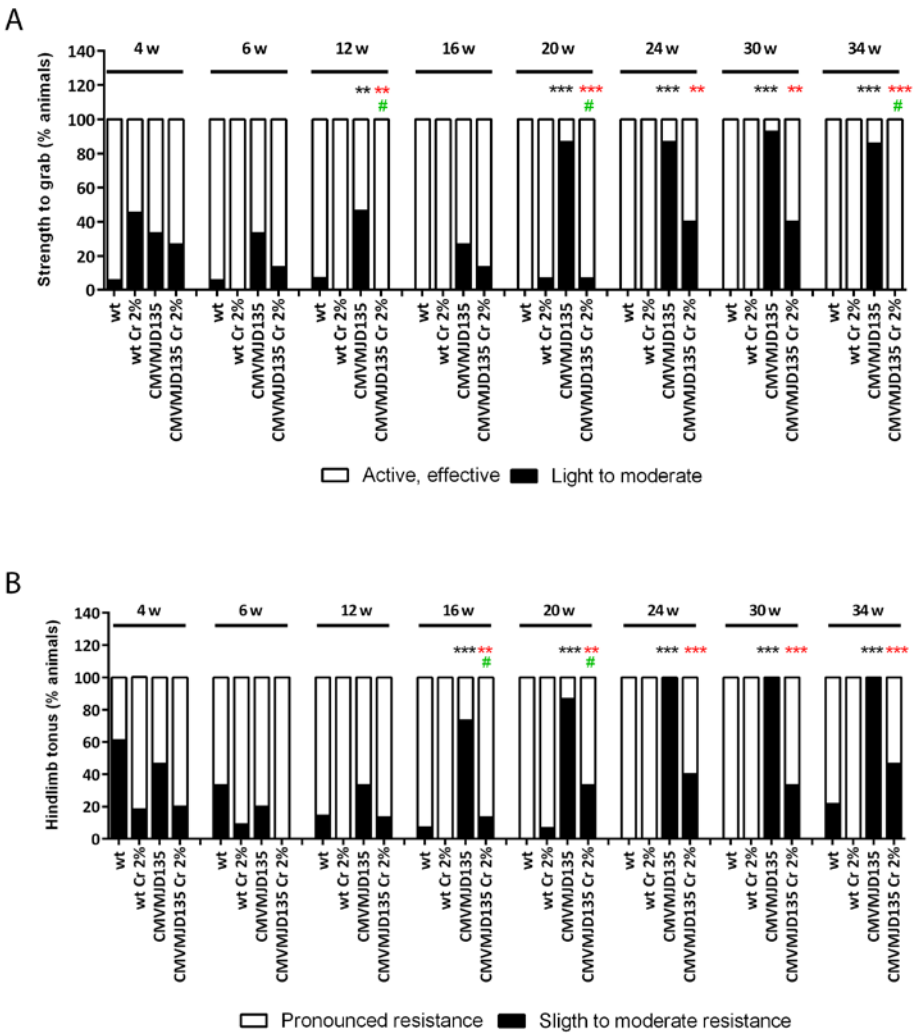

Figure 3 continues next page.

Figure 3 (continued)

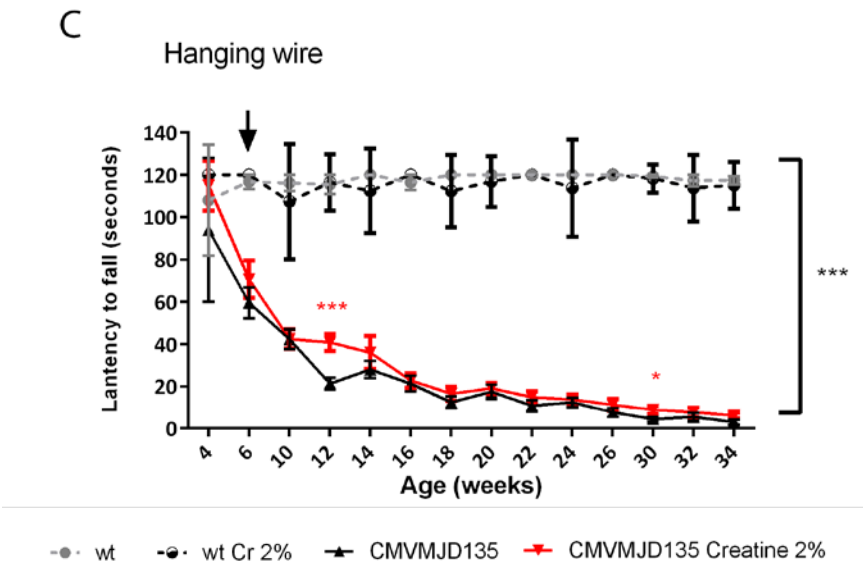

Figure 3. Muscular strength deficits improved by creatine. (A) The animal's strength to grab a grid evaluates the forelimb strength. CMVMJD135 mice started to lose forelimb strength at 12 weeks of age and creatine 2% treatment delayed disease onset by 8 weeks and improved this loss of strength until the end of the study (Fisher's exact test). **(B)** The hindlimb tonus was evaluated and creatine 2% treatment delayed the onset of the phenotype 4 weeks; this improvement was maintained until the end of the trial (Fisher's exact test) **(C)** The hanging wire test was performed to evaluate limb strength and the phenotype onset occurs at 6 weeks of age. Creatine 2% started at 5 weeks had no major impact on this test, except for very transient improvements (Repeated measures ANOVA was used considering genotype and treatment factors). n=15-17 for each group used. Symbols represent mean ± SD of the different groups. **, *** represent the $p< 0.01$ and 0.001 respectively.

Motor coordination was ameliorated by creatine supplementation

To assess motor coordination the beam walk and the motor swimming tests were performed. The onset of the phenotype was observed at 14 and 10 weeks of age, respectively, in this group of CMVMJD135 mice. In the training square beam (12mm), it was possible to observe an improvement by creatine 2% after a long period of treatment, at 26 and 30 weeks of age (Fig 4A). Nevertheless, creatine-treated animals seemed to be improving in this test as animals' age. We were not able to pursue this test to prove this amelioration given that the untreated CMVMJD135 mice were no longer able to traverse the beam. When difficulty was added by using a smaller and round beam (11mm), CMVMJD135 mice under a standard diet were only able to perform the task until 20 weeks of age (Fig 4B). In agreement with the previous result, creatine-treated animals showed an improved phenotype late in life, at 20 weeks of age (Fig 4B). Regarding the motor swimming test, the phenotype onset was

observed at 10 weeks of age (Fig 4C). Creatine treatment improved the coordination deficits since the onset of the phenotype until the end of this pre-clinical trial (34 weeks of age), this improvement being highly significant. Not unexpectedly, wt animals under Creatine 2% diet also performed better at some time-points (14, 16, 18, 20 and 34 weeks of age) when compared with wt animals under standard diet (Fig 4C, green *). The same result was obtained in the *PCT1* for the time-points analyzed (22 and 24 weeks of age) (Fig 1E).

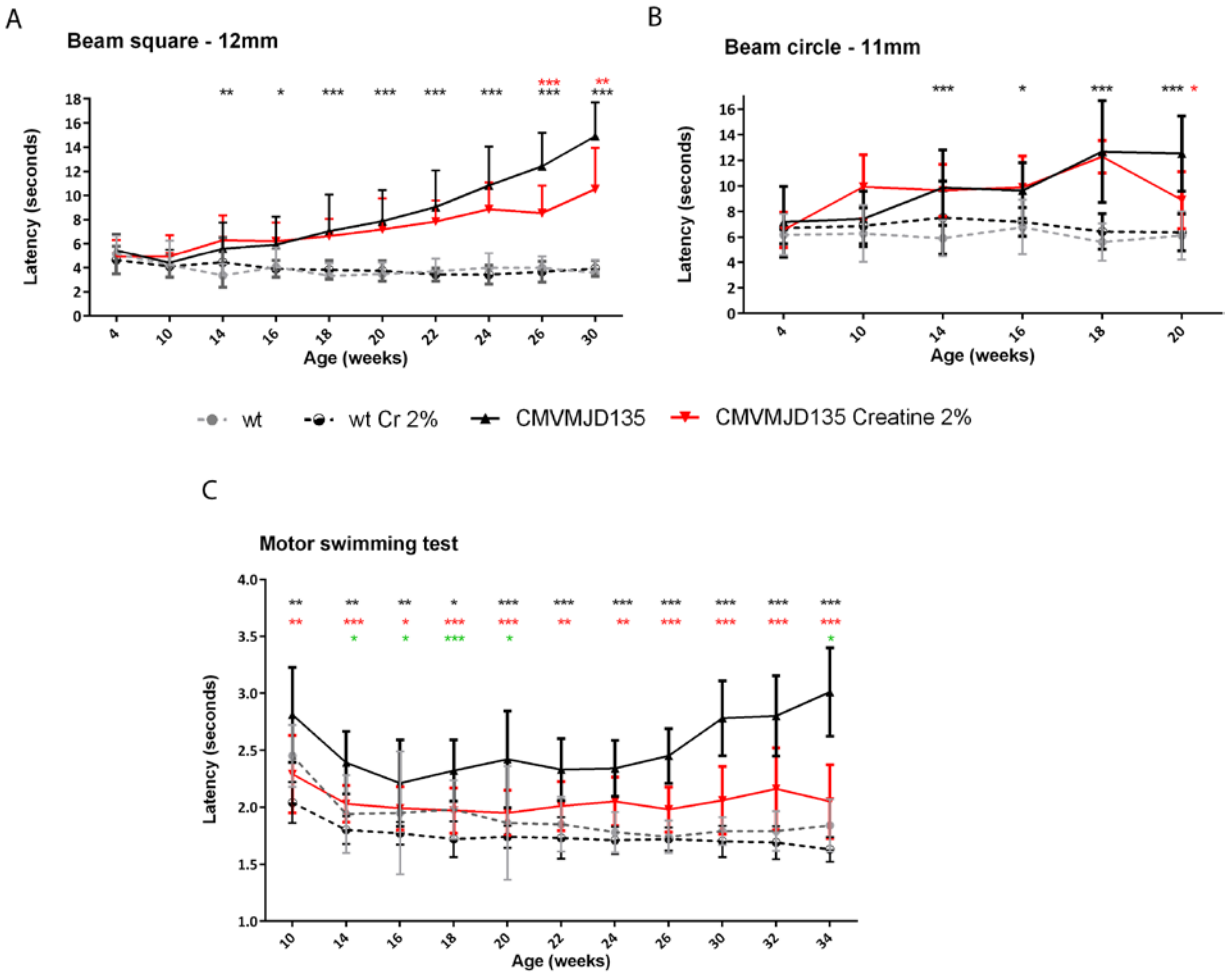

Figure 4. Creatine treatment improved motor uncoordination observed in the CMVMJD135 animals. CMVMJD135-treated mice show a better performance on the beam walk test both in the **(A)** square and in the **(B)** round beams. In the motor swimming test **(C)** this improvement is even more pronounced during disease progression until the end of the trial at 34 weeks of age. Wild-type mice under creatine 2% diet also improved their performance in this test when comparing to wild-type mice under standard diet (green asterisks). n=15-17 for each group used. Symbols represent mean ± SD of the different groups. *, **, *** represent the p< 0.05; 0.01 and 0.001 respectively. Repeated measures ANOVA was used considering genotype and treatment factors.

Creatine chronic treatment improved the quality of movement of the CMVMJD135 mice

Gait quality was qualitatively assessed by observing the animals freely moving in an open arena. The quality of the movement of this group of CMVMJD135 animals became abnormal at 18 weeks of age. Creatine treatment was able to improve and delay this symptom until 34 weeks of age (Fig 5A). Unexpectedly, other parameters used to measure the gait quality of the animals, such as foot dragging and stride length, were not improved by creatine treatment (Fig 5B and C respectively) in this group.

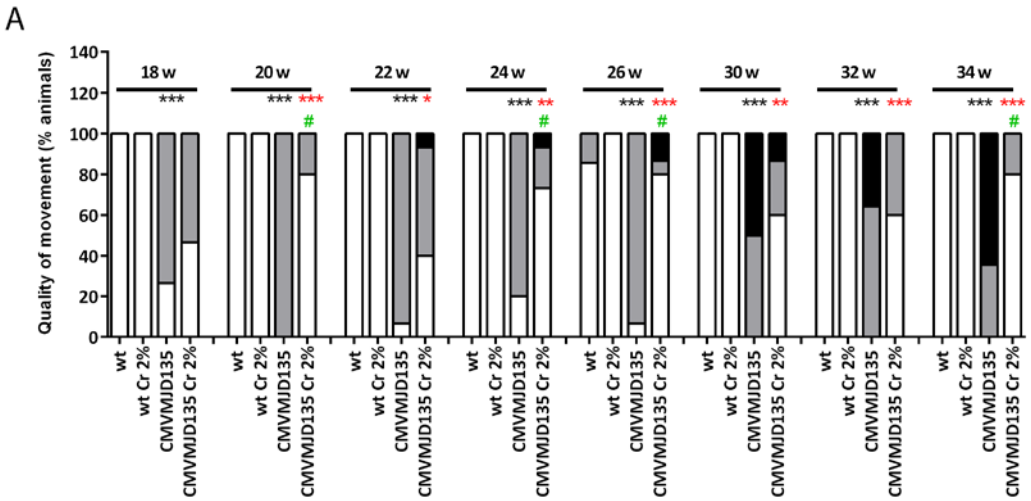

Figure 5 continues next page.

Figure 5 (continued)

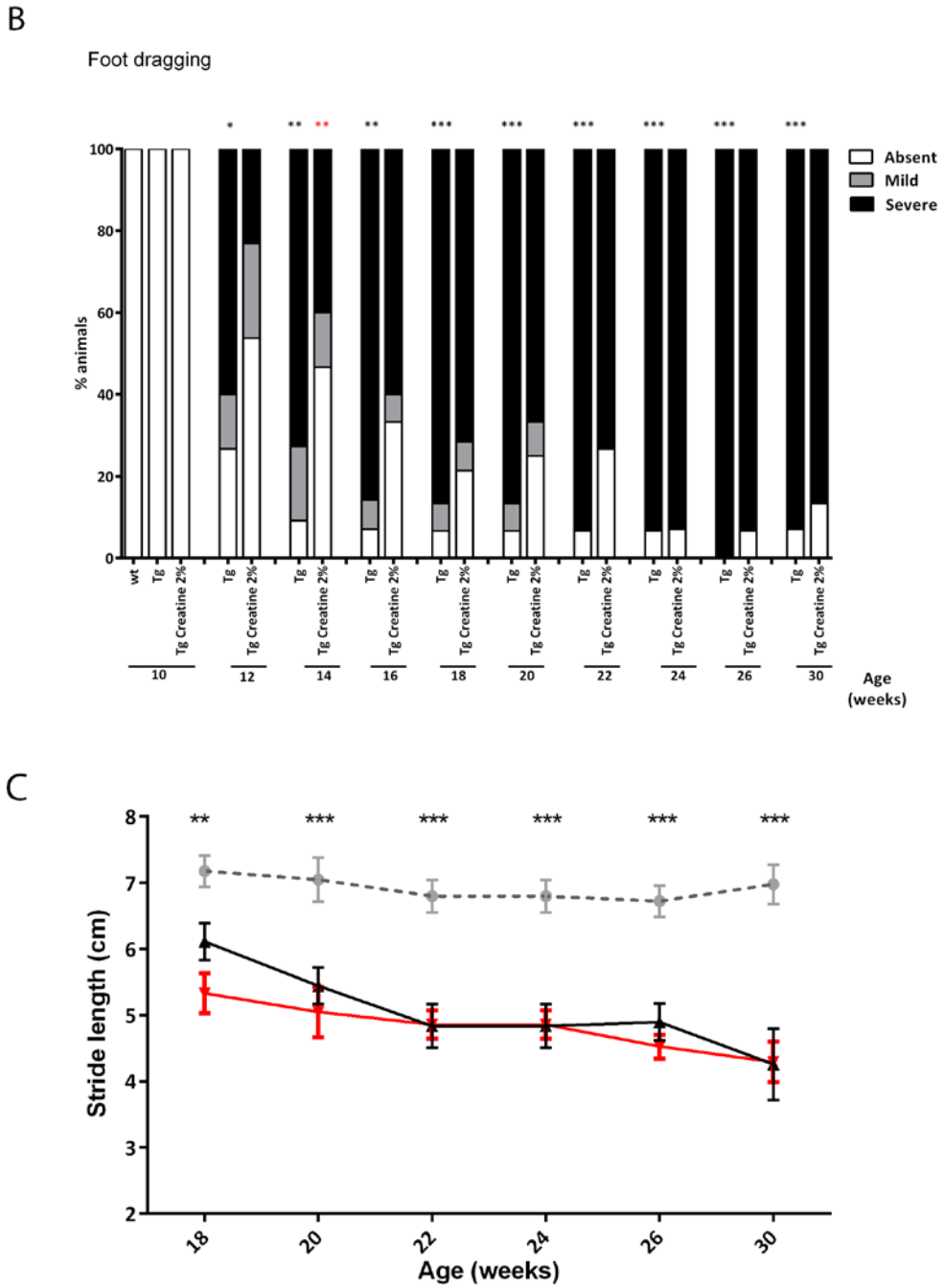

Figure 5. Creatine food supplementation had mild effects on gait quality. (A) Gait quality was evaluated in an open arena being the onset of abnormal gait observed at 18 weeks. Creatine 2% improved this phenotype parameter until 34 weeks of age (Fisher's exact test). **(B)** Foot dragging was analyzed since 10 to 30 weeks of age. CMVMJD135 drag their feet since 12 weeks of age and creatine 2% had no major impact on this parameter (Mann-Whitney U test). **(C)** The stride length was measured and creatine 2% showed no impact on the decreased step length observed in the CMVMJD135 animals (Repeated measures ANOVA was used considering genotype and treatment factors.). n=15-17 for each group used. Symbols represent mean ± SD of the different groups. *, **, *** represent the p< 0.05; 0.01 and 0.001 respectively.

Creatine had mild effects on spontaneous exploratory activity but significant impact on tremors and limb clasping

Spontaneous exploratory activity was measured by counting the number of squares that animals travelled in an arena when there were freely moving. Also, the number of vertical movements (rears) was counted while animals explored a cylinder viewing jar. This group of CMVMJD135 mice travelled significantly less in the arena at 18 weeks of age (Fig 6A) and later. Creatine improved this phenotype very limitedly and only after a long period of treatment, by the age of 34 weeks. In the case of vertical movements, this group of CMVMJD135 mice started to explore significantly less at the age of 22 weeks, and after 29 weeks of creatine 2% treatment transgenic mice performed better and the phenotype is no longer observed (green # at 34 weeks of age) (Fig 6B). Of notice, at the last time-point of analysis (34 weeks of age) untreated CMVMJD135 mice did not perform any vertical movement during the 5 minutes of the test, whereas treated animals showed some (albeit low) exploratory behavior.

Limb clasping is another phenotypic characteristic of the CMVMJD135 mouse model, with onset at 18 weeks of age in this group. Remarkably, creatine treatment delayed the appearance of this symptom by 8 weeks and was able to improve it until the end of the pre-clinical trial (Fig 6C). The effect of creatine treatment was even more pronounced concerning tremors. Creatine completely abolished the onset of this symptom, treated CMVMJD135 animals being comparable to wt mice (Fig 6D).

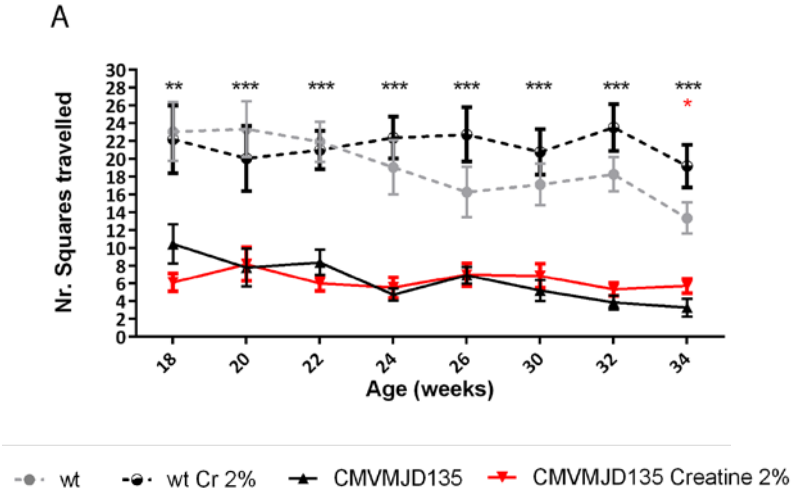

Figure 6 continues next page

Figure 6 (continued)

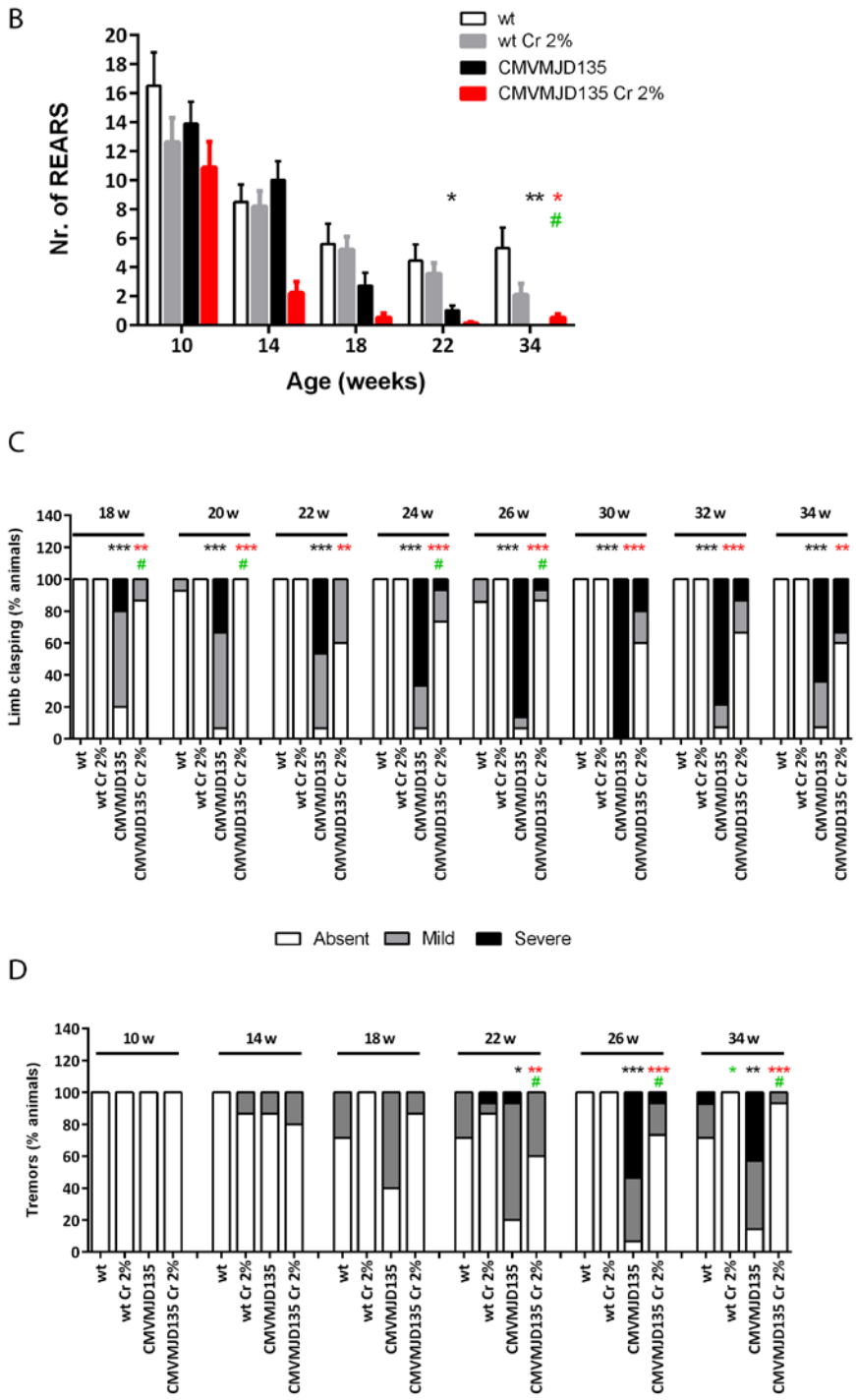

Figure 6. Creatine slightly improves exploratory activity very limitedly and late in life but strongly impacts on tremors and abnormal neurological reflexes. Spontaneous activity was measured by the number of **(A)** squares travelled in an open arena for 1 minute (Repeated measures ANOVA) and **(B)** by the number of vertical movements (rears) (Mann-Whitney U test); these parameters were improved by creatine 2% after a long period of treatment. The limb clasping **(C)** and tremors **(D)** observed in the CMVMJD135 mice were significantly improved by chronic treatment; the phenotype onset was delayed by 8 weeks on the limb clasping and completely abolished in the tremors (Fisher's exact test), n=15-17 for each group used. Symbols represent mean ± SD of the different groups. *, **, *** represent the p< 0.05; 0.01 and 0.001 respectively.

Effect of creatine supplementation on mutant ataxin-3 aggregation

We quantified the number of ATXN3 positive nuclear inclusions in the brainstem of CMVMJD135 animals under standard and creatine diets. As seen in *PCT1*, creatine 2% treatment was able to significantly decrease the aggregate load in the pontine nuclei of CMVMJD135 animals (Fig 7A). Additionally, we found no differences in the levels of mutant ataxin-3 mRNA or total protein levels upon treatment (Fig 7B and C, respectively). Creatine does not seem to be inducing the degradation of mutant ATXN3, namely through autophagy, since LC3 and p62 (autophagy markers) were not altered upon treatment (Fig 7D and E, respectively).

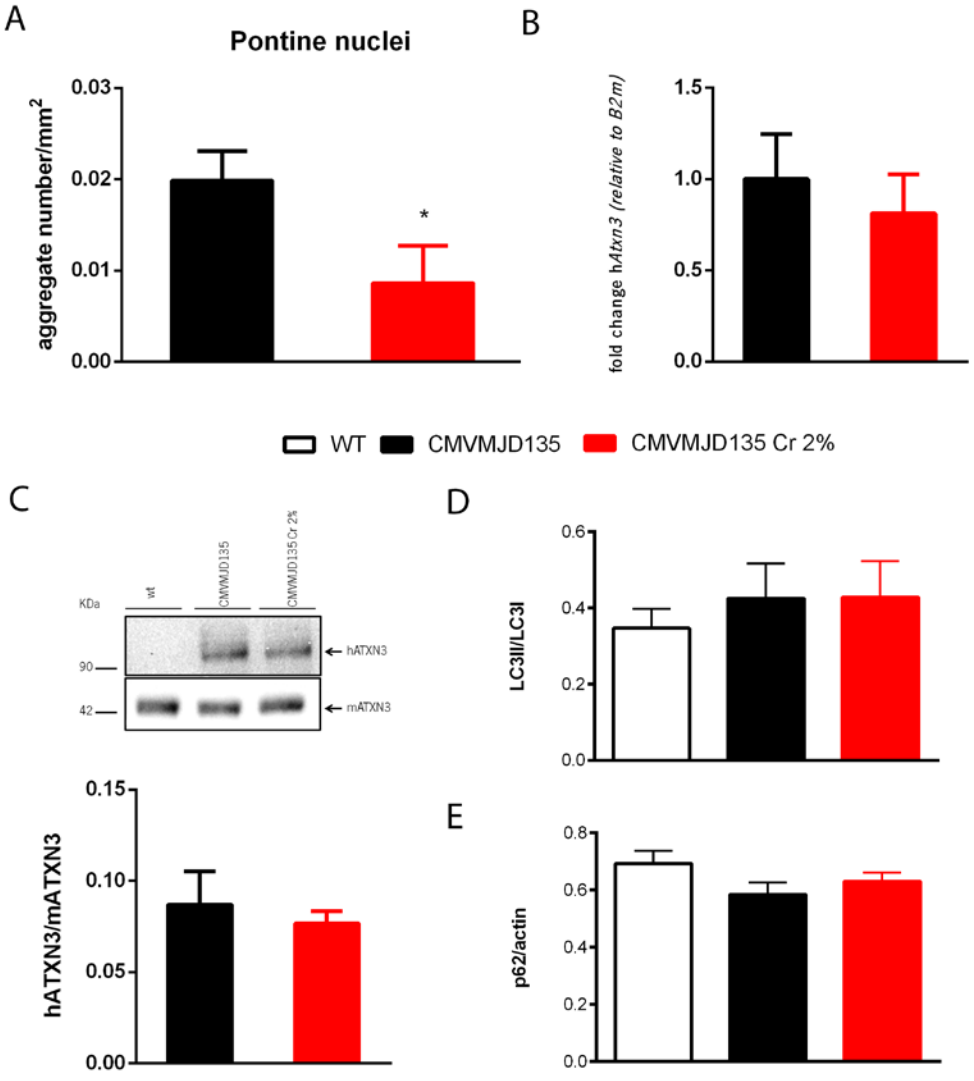

Figure 7. Ataxin-3 positive nuclear inclusions in CMVMJD135 mice brainstem are reduced upon creatine treatment. (A) Neuronal inclusions were counted in the pontine nuclei of 34-week-old animals under normal diet or TUDCA supplementation (n=3 for each condition). Four slides of each animal were used for the analysis (student's t test) **(B)** qRT-PCR analysis of human ATXN3 mRNA expression levels (n=5 and two technical replicates were performed) showed no differences by creatine 2% treatment. Fold change (ΔΔCT method) is represented using B2m as housekeeping gene (student's t test) **(C)** Anti-ataxin-3 western-blot of 34-week-old CMVMJD135

mice (n=4 for each condition; at least 3 technical replicates were performed) in the whole brainstem showed that creatine 2% had no effect on the protein levels of total mutant ataxin-3 (hATXN3). Endogenous ataxin-3 protein (mATXN3) was used as loading control (student's t test). hATXN3 has a molecular weight of approximately 90 kDa and mATXN3 42 kDa. **(D)** Anti-LC3 western-blot of 34-week-old CMVMJD135 mice (n=4 for each condition; at least 3 technical replicates were performed) in the whole brainstem. LC3II was normalized to LC3I. **(E)** Anti-p62 western-blot of 34-week-old CMVMJD135 mice (n=4 for each condition; at least 3 technical replicates were performed) in the whole brainstem. p62 was normalized to β-actin. Values are presented as mean ± SEM; *p<0.05.

Creatine treatment increases the Calbindin D28-K staining the Purkinje cell layer of the cerebellum and decreases astroglisosis in the brainstem of the CMVMJD135 mice

Previously we have shown a mild decrease in calbindin D28-K staining in the Purkinje cell layer of the cerebellum in the CMVMJD135 mice (45) and (Chapter 5). In this study we found that creatine treatment increased the calbindin D28-K staining in the Purkinje cell layer of the cerebellum (p=0.009) (Fig. 8A and B) at 34 weeks of age (*PCT2*), suggesting preservation of these neurons, as shown previously for a SCA1 mouse model (46). Also, we have previously shown that astrogliosis occurs in the brain of CMVMJD135 mice (45) (Chapters 2 and 5) which was normalized by creatine chronic treatment in the brainstem of the CMVMJD135 mice (Fig 9).

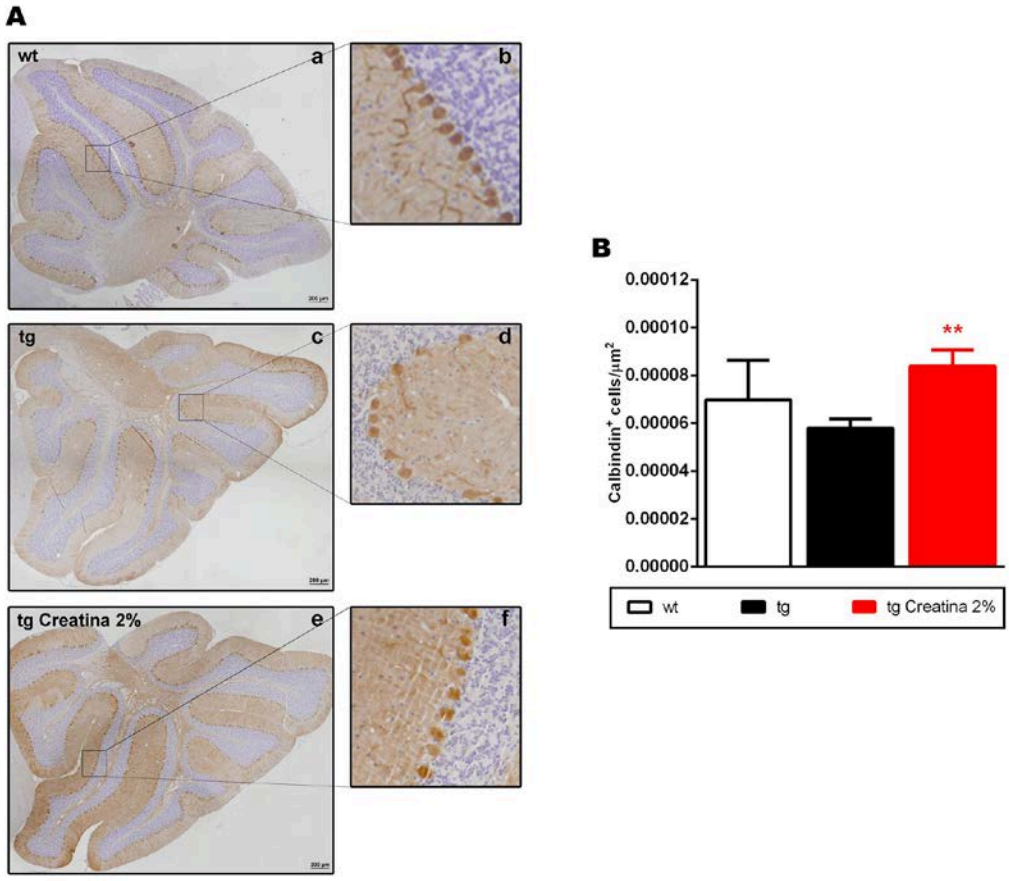

Figure 8. Creatine treatment increases the calbindin D28-K staining the Purkinje cell layer of the cerebellum of the CMVMJD135 mice. (A) representative images of calbindin D28-K staining in wild-type (a-b), CMVMJD135 (c-d) and CMVMJD135-

treated animals (e-f) (n=4 per group, 4 slides per animals were analyzed) and **(B)** quantitative analysis of calbindin D28-K staining. **p<0.01. The calbindin D28-K positive cells were counted using the Fiji software (Image J). Scale bar 200µm.

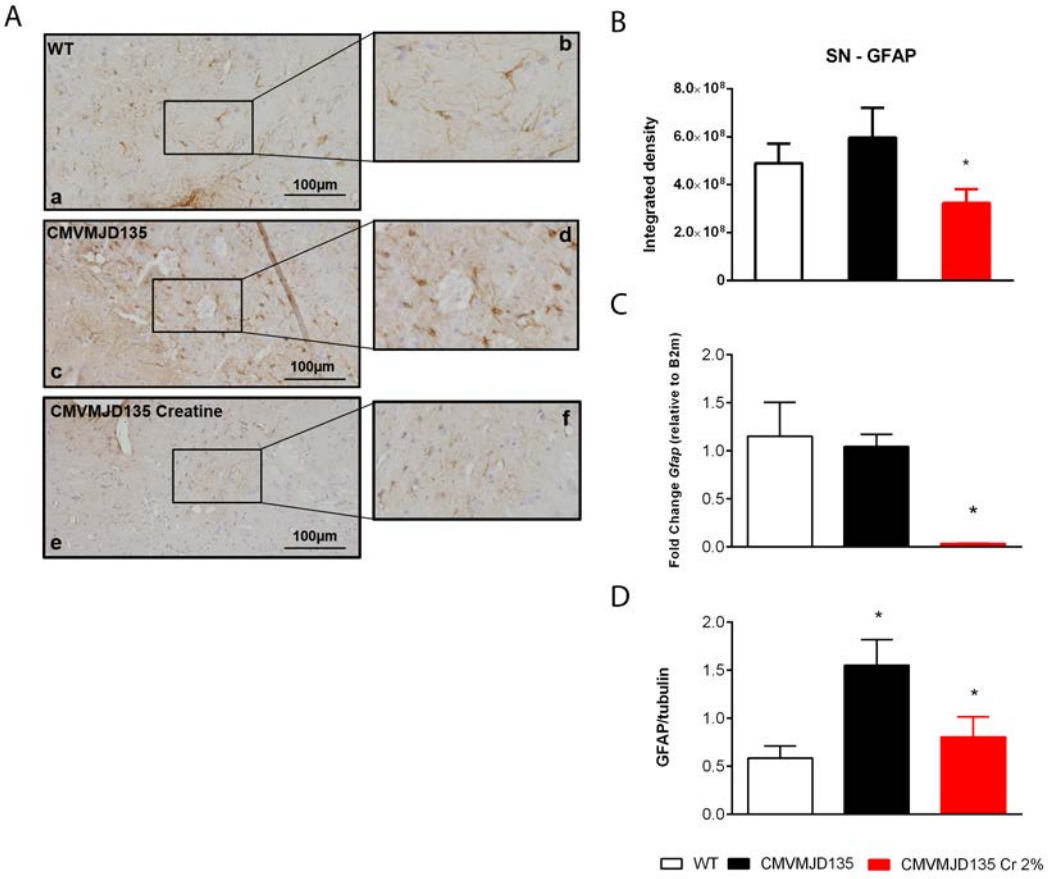

Figure 9. Creatine decreases astrogliosis in the brainstem of the CMVMJD135 mice. Creatine was able to reduce the GFAP staining in the substantia nigra of the CMVMJD135 mice (n=4 per group, 4 slides per animals were analyzed). **(A)** Representative images of GFAP immunohistochemistry analysis in the substantia nigra at 34 weeks of age of: (a-b) wild-type, (c-d) CMVMJD135 and (e-f) CMVMJD135 treated mice. **(B)** The GFAP staining intensity was measured using the Fiji software (Image J). **(C)** qRT-PCR analysis of *Gfap* mRNA expression levels (n=5 and two technical replicates were performed) showed to be reduced by creatine 2% treatment in the brainstem of CMVMJD135 animals. Fold change (ΔΔCT method) is represented using B2m as housekeeping gene (Student's t test). **(D)** Anti-GFAP western-blot of 34-week-old CMVMJD135 mice (n=4 for each condition; at least 3 technical replicates were performed) in the whole brainstem showed that creatine 2% normalized the GFAP protein levels. α-tubulin was used as loading control (Student's t test). Values are presented as mean ± SEM; *p<0.05.

Discussion

Bioenergetic dysfunction and mitochondrial deficits contribute to the pathogenesis of several neurodegenerative diseases either directly and/or indirectly (47-49). Considering this, treatments aimed at improving this cellular energy deficits or improving mitochondrial function may prove to be useful in MJD patients. The neuroprotective role of Creatine in other neuromuscular and neurodegenerative diseases is well documented (18, 19, 23, 46, 50-55).

Here we have shown that creatine 2% food supplementation (500 mg/Kg) during a shorter (19 weeks) or longer period of time (29 weeks) was safe, well tolerated and had a significant impact on CMVMJD135 behavior. The dosage herein used was previously describe to be the most effective in mice (31), corresponding to a consumption of 3 g per day in humans, which is below the dosages tested so far in human neurodegenerative diseases (27, 32). Creatine treatment was able to delay symptom onset as assessed by several behavior parameters such as muscular strength, gait, limb clasping and tremors, the latter symptom being completely abolished. Furthermore, in the first preclinical trial, in which the mean CAG repeat length was lower (133 ± 1 *vs* 139 ± 4, p=0.007) and disease severity less, other phenotypic aspects of the CMVMJD135 mice were also ameliorated, such as gait and body weight.

Creatine supplementation effects on muscle strength and growth are largely documented in a larger number of sports (56, 57). Muscular strength loss is the first disease sign in the CMVMJD135 animals (by 6 weeks of age), and it progresses very fast and severely. In the first preclinical trial performed, creatine supplementation had a significant impact on muscular strength deficits, the treated-CMVMJD135 mice always being better when compared to untreated animals. Yet, creatine treatment in the *PCT2* showed a very limited effect on this test, seen only at 12 weeks of age. Previous pre-clinical trials performed in the CMVMJD135 model, such as 17-DMAG (36) or lithium chloride (37), showed no effect at all on this test, which is very difficult to revert due to the early onset and severity of the phenotype. An earlier treatment would probably be needed to rescue this aspect of the phenotype. Nevertheless, creatine treatment in this study showed a strong impact on other muscular strength parameters, such as hindlimb tonus and forelimb strength even in *PCT2*. The motor performance of CMVMJD135 animals was significantly improved by creatine treatment in both the beam walk and motor swimming tests. Accordingly, in HD mouse models the motor performance on the rotarod was ameliorated by creatine 2% treatment (21, 31). Nevertheless, studies showed no effect of Creatine 2% on motor performance in SCA1 and ALS mouse models (46, 58). Not unexpectedly, our results showed that creatine 2% supplementation also had an impact on the motor performance of wt mice, namely in

the motor swimming test, showing that the effects of creatine are not limited to the disease state. Creatine supplementation was shown to have beneficial effects on healthy people (59), and in conjugation with exercise was shown to improve muscle performance in elderly men and women (60, 61). Accordingly, 1% creatine supplementation increased the lifespan of aged wild-type C57Bl/6J mice and improved the performance in several neurobehavioral tests. This suggests that creatine has a positive impact on health and longevity of wt mice and may justify our results (62).

Furthermore, creatine-fed CMVMJD135 mice showed a mild improvement on gait quality. Yet, it was not possible to observe an improvement in the length of the mouse stride length, a parameter which is consistently diminished in CMVMJD135 mice after a certain age. The lack of efficacy of creatine treatment on gait was also shown in a SCA1 mouse model, where creatine-fed mice did not show improve gait width despite the preservation of Purkinje cells in the cerebellum (46). Nevertheless, in the case of our study the CAG repeat tract length seems to impact the likelihood of improvement of gait abnormalities, since in the first preclinical that we have performed, the foot dragging phenotype of the CMVMJD135 animals was significantly improved throughout the trial, while in *PCT2* a very limited improvement was only observed at 14 weeks of age. Consistently, the appearance of this symptom in the *PCT1* was observed at 16 weeks of age, while in *PCT2* it appeared earlier (12 weeks of age), which may explain our results.

Interestingly, in both trials creatine-treated animals did show a significant improvement in limb clasping, an abnormal reflex that is observed in several brain and spinal cord pathologies, when lesions are present in the cerebellum, basal ganglia and neocortex (63) and which appears later that strength and gait alterations in CMVMJD135 mice.

Although tremors are a rare event in MJD (64), they are quite evident in the CMVMJD135 mice; interestingly, they were completely abolished by creatine 2% treatment, as this symptom remains absent in treated animals until the end of this pre-clinical trial.

In accordance to previous reports in an HD mouse model (21, 31), creatine 2% treatment showed to have a protective effect on gross brain atrophy, given by the total brain weight measured in the endpoint of this pre-clinical trial at 34 weeks of age. CMVMJD135 animals under standard diet at this time-point showed 10% reduction on brain weight, while creatine-treated mice showed 6% of reduction when compared to wt mice at the same age. Nevertheless, a more detailed stereological analysis of the brain addressing neuronal loss in specific brain and spinal cord regions needs to be performed to complement this result.

Creatine 2% treatment has previously been shown to be able to reduce both striatal and pancreatic huntingtin-positive nuclear aggregates (31). Accordingly, we found a reduction on aggregate load in the pontine nuclei of creatine-fed mice at 34 (*PCRT2*) and at 24 weeks of age (*PCRT1*), although no differences were found on total mutant ataxin-3 protein and mRNA levels. Recently, it was demonstrated that β-GPA, a creatine analogue, was able to extend the lifespan of Drosophila melanogaster and to increase Atg8 levels suggesting that this lifespan extension might take place via the activation of AMPK-Atg1-autophagy signaling pathway (65). It is possible that, similar to its analogue, creatine might be able to induce autophagy and therefore reduce the levels of ataxin-3-positive aggregates, a hypothesis that requires further testing. Although the mechanism by which creatine decreases the aggregate load was not addressed in the present study and is also not described in other studies (20, 31), our results suggest that it does not act by increasing mutant ATXN3 degradation, namely through autophagy (data not shown). Alternatively, the energy-dependent protein folding/refolding systems challenged by mutant ATXN3 may become more effective in the presence of creatine supplementation, thus leading to increased solubility of the mutant protein.

An interesting study by Yang and collaborators demonstrated the neuroprotective effects of creatine 2% and Coenzyme 10 (CoQ10) 1% in animals models of PD and HD, and showed the additive effects of both compounds when administered together (66). It would be interesting to test the combination of creatine 2%/CoQ10 1% in CMVMJD135 animals, as this combination might potentiate the effects observed for creatine alone and could eventually further improve the motor benefits that were so evident in this pre-clinical trial.

In summary, the present findings support creatine treatment as a novel therapeutic strategy to delay disease progression and improve symptoms in MJD.

References

1. Maciel P, Gaspar C, DeStefano AL, Silveira I, Coutinho P, Radvany J, et al. Correlation between CAG repeat length and clinical features in Machado-Joseph disease. Am J Hum Genet. 1995;57(1):54-61.

2. Jardim LB, Pereira ML, Silveira I, Ferro A, Sequeiros J, Giugliani R. Neurologic findings in Machado-Joseph disease: relation with disease duration, subtypes, and (CAG)n. Arch Neurol. 2001;58(6):899-904.

3. Linnemann C, Tezenas du Montcel S, Rakowicz M, Schmitz-Hubsch T, Szymanski S, Berciano J, et al. Peripheral Neuropathy in Spinocerebellar Ataxia Type 1, 2, 3, and 6. Cerebellum. 2015.

4. Koroshetz WJ, Jenkins BG, Rosen BR, Beal MF. Energy metabolism defects in Huntington's disease and effects of coenzyme Q10. Ann Neurol. 1997;41(2):160-5.

5. Brouillet E, Hantraye P, Ferrante RJ, Dolan R, Leroy-Willig A, Kowall NW, et al. Chronic mitochondrial energy impairment produces selective striatal degeneration and abnormal choreiform movements in primates. Proc Natl Acad Sci U S A. 1995;92(15):7105-9.

6. Gourfinkel-An I, Vila M, Faucheux B, Duyckaerts C, Viallet F, Hauw JJ, et al. Metabolic changes in the basal ganglia of patients with Huntington's disease: an in situ hybridization study of cytochrome oxidase subunit I mRNA. J Neurochem. 2002;80(3):466-76.

7. N. Kazachkova MR, R. Montiel, T. Cymbron, C. Bettencourt, A. Silva-Fernandes, S. Silva, P. Maciel & M. Lima. Patterns of mitochondrial DNA damage in blood and brain tissues of a transgenic mouse model of Machado–Joseph disease. Neurodegenerative Diseases. 2012.

8. Yu YC, Kuo CL, Cheng WL, Liu CS, Hsieh M. Decreased antioxidant enzyme activity and increased mitochondrial DNA damage in cellular models of Machado-Joseph disease. J Neurosci Res. 2009;87(8):1884-91.

9. Tarnopolsky MA, Beal MF. Potential for creatine and other therapies targeting cellular energy dysfunction in neurological disorders. Ann Neurol. 2001;49(5):561-74.

10. Juhn MS, Tarnopolsky M. Oral creatine supplementation and athletic performance: a critical review. Clin J Sport Med. 1998;8(4):286-97.

11. Guthmiller P, Van Pilsum JF, Boen JR, McGuire DM. Cloning and sequencing of rat kidney L-arginine:glycine amidinotransferase. Studies on the mechanism of regulation by growth hormone and creatine. J Biol Chem. 1994;269(26):17556-60.

12. Walker JB. Creatine: biosynthesis, regulation, and function. Adv Enzymol Relat Areas Mol Biol. 1979;50:177-242.

13. Bogdanis GC, Nevill ME, Boobis LH, Lakomy HK. Contribution of phosphocreatine and aerobic metabolism to energy supply during repeated sprint exercise. J Appl Physiol (1985). 1996;80(3):876-84.

14. Stockler S, Marescau B, De Deyn PP, Trijbels JM, Hanefeld F. Guanidino compounds in guanidinoacetate methyltransferase deficiency, a new inborn error of creatine synthesis. Metabolism. 1997;46(10):1189-93.

15. van der Knaap MS, Verhoeven NM, Maaswinkel-Mooij P, Pouwels PJ, Onkenhout W, Peeters EA, et al. Mental retardation and behavioral problems as presenting signs of a creatine synthesis defect. Ann Neurol. 2000;47(4):540-3.

16. Leuzzi V, Bianchi MC, Tosetti M, Carducci C, Cerquiglini CA, Cioni G, et al. Brain creatine depletion: guanidinoacetate methyltransferase deficiency (improving with creatine supplementation). Neurology. 2000;55(9):1407-9.

17. Stockler S, Hanefeld F, Frahm J. Creatine replacement therapy in guanidinoacetate methyltransferase deficiency, a novel inborn error of metabolism. Lancet. 1996;348(9030):789-90.

18. Matthews RT, Ferrante RJ, Klivenyi P, Yang L, Klein AM, Mueller G, et al. Creatine and cyclocreatine attenuate MPTP neurotoxicity. Exp Neurol. 1999;157(1):142-9.

19. Klivenyi P, Ferrante RJ, Matthews RT, Bogdanov MB, Klein AM, Andreassen OA, et al. Neuroprotective effects of creatine in a transgenic animal model of amyotrophic lateral sclerosis. Nat Med. 1999;5(3):347-50.

20. Dedeoglu A, Kubilus JK, Yang L, Ferrante KL, Hersch SM, Beal MF, et al. Creatine therapy provides neuroprotection after onset of clinical symptoms in Huntington's disease transgenic mice. J Neurochem. 2003;85(6):1359-67.

21. Andreassen OA, Dedeoglu A, Ferrante RJ, Jenkins BG, Ferrante KL, Thomas M, et al. Creatine increase survival and delays motor symptoms in a transgenic animal model of Huntington's disease. Neurobiol Dis. 2001;8(3):479-91.

22. Andreassen OA, Jenkins BG, Dedeoglu A, Ferrante KL, Bogdanov MB, Kaddurah-Daouk R, et al. Increases in cortical glutamate concentrations in transgenic amyotrophic lateral sclerosis mice are attenuated by creatine supplementation. J Neurochem. 2001;77(2):383-90.

23. Brewer GJ, Wallimann TW. Protective effect of the energy precursor creatine against toxicity of glutamate and beta-amyloid in rat hippocampal neurons. J Neurochem. 2000;74(5):1968-78.

24. Hass CJ, Collins MA, Juncos JL. Resistance training with creatine monohydrate improves upper-body strength in patients with Parkinson disease: a randomized trial. Neurorehabil Neural Repair. 2007;21(2):107-15.

25. Investigators NN-P. A randomized, double-blind, futility clinical trial of creatine and minocycline in early Parkinson disease. Neurology. 2006;66(5):664-71.

26. Groeneveld GJ, Veldink JH, van der Tweel I, Kalmijn S, Beijer C, de Visser M, et al. A randomized sequential trial of creatine in amyotrophic lateral sclerosis. Ann Neurol. 2003;53(4):437-45.

27. Shefner JM, Cudkowicz ME, Schoenfeld D, Conrad T, Taft J, Chilton M, et al. A clinical trial of creatine in ALS. Neurology. 2004;63(9):1656-61.

28. Naia L, Ribeiro MJ, Rego AC. Mitochondrial and metabolic-based protective strategies in Huntington's disease: the case of creatine and coenzyme Q. Rev Neurosci. 2012;23(1):13-28.

29. Grunewald T, Beal MF. Bioenergetics in Huntington's disease. Ann N Y Acad Sci. 1999;893:203-13.

30. Browne SE, Ferrante RJ, Beal MF. Oxidative stress in Huntington's disease. Brain Pathol. 1999;9(1):147-63.

31. Ferrante RJ, Andreassen OA, Jenkins BG, Dedeoglu A, Kuemmerle S, Kubilus JK, et al. Neuroprotective effects of creatine in a transgenic mouse model of Huntington's disease. J Neurosci. 2000;20(12):4389-97.

32. Hersch SM, Gevorkian S, Marder K, Moskowitz C, Feigin A, Cox M, et al. Creatine in Huntington disease is safe, tolerable, bioavailable in brain and reduces serum 8OH2'dG. Neurology. 2006;66(2):250-2.

33. Juhn MS, Tarnopolsky M. Potential side effects of oral creatine supplementation: a critical review. Clin J Sport Med. 1998;8(4):298-304.

34. Kim HJ, Kim CK, Carpentier A, Poortmans JR. Studies on the safety of creatine supplementation. Amino Acids. 2011;40(5):1409-18.

35. Mihic S, MacDonald JR, McKenzie S, Tarnopolsky MA. Acute creatine loading increases fat-free mass, but does not affect blood pressure, plasma creatinine, or CK activity in men and women. Med Sci Sports Exerc. 2000;32(2):291-6.

36. Silva-Fernandes A, Duarte-Silva S, Neves-Carvalho A, Amorim M, Soares-Cunha C, Oliveira P, et al. Chronic treatment with 17-DMAG improves balance and coordination in a new mouse model of Machado-Joseph disease. Neurotherapeutics. 2014;11(2):433-49.

37. Duarte-Silva S, Neves-Carvalho A, Soares-Cunha C, Teixeira-Castro A, Oliveira P, Silva-Fernandes A, et al. Lithium chloride therapy fails to improve motor function in a transgenic mouse model of Machado-Joseph disease. Cerebellum. 2014;13(6):713-27.

38. Silva-Fernandes A, Costa Mdo C, Duarte-Silva S, Oliveira P, Botelho CM, Martins L, et al. Motor uncoordination and neuropathology in a transgenic mouse model of Machado-Joseph disease lacking intranuclear inclusions and ataxin-3 cleavage products. Neurobiol Dis. 2010;40(1):163-76.

39. Nicklas W, Baneux P, Boot R, Decelle T, Deeny AA, Fumanelli M, et al. Recommendations for the health monitoring of rodent and rabbit colonies in breeding and experimental units. Lab Anim. 2002;36(1):20-42.

40. Carter RJ, Lione LA, Humby T, Mangiarini L, Mahal A, Bates GP, et al. Characterization of progressive motor deficits in mice transgenic for the human Huntington's disease mutation. J Neurosci. 1999;19(8):3248-57.

41. Rogers DC, Fisher EM, Brown SD, Peters J, Hunter AJ, Martin JE. Behavioral and functional analysis of mouse phenotype: SHIRPA, a proposed protocol for comprehensive phenotype assessment. Mamm Genome. 1997;8(10):711-3.

42. Rafael JA, Nitta Y, Peters J, Davies KE. Testing of SHIRPA, a mouse phenotypic assessment protocol, on Dmd(mdx) and Dmd(mdx3cv) dystrophin-deficient mice. Mamm Genome. 2000;11(9):725-8.

43. Silva-Fernandes A, Oliveira P, Sousa N, Maciel P. Motor and Behavioural Abnormalities Associated with Persistent Spontaneous Epilepsy in the fvb/n Mouse Strain. Scand J Lab Anim Sci. 2010;37(3).

44. Silva-Fernandes A, Duarte-Silva S, Neves-Carvalho A, Amorim M, Soares-Cunha C, Oliveira P, et al. Chronic Treatment with 17-DMAG Improves Balance and Coordination in A New Mouse Model of Machado-Joseph Disease. Neurotherapeutics. 2014.

45. Teixeira-Castro A, Jalles A, Esteves S, Kang S, da Silva Santos L, Silva-Fernandes A, et al. Serotonergic signalling suppresses ataxin 3 aggregation and neurotoxicity in animal models of Machado-Joseph disease. Brain. 2015.

46. Kaemmerer WF, Rodrigues CM, Steer CJ, Low WC. Creatine-supplemented diet extends Purkinje cell survival in spinocerebellar ataxia type 1 transgenic mice but does not prevent the ataxic phenotype. Neuroscience. 2001;103(3):713-24.

47. Salminen A, Haapasalo A, Kauppinen A, Kaarniranta K, Soininen H, Hiltunen M. Impaired mitochondrial energy metabolism in Alzheimer's disease: Impact on pathogenesis via disturbed epigenetic regulation of chromatin landscape. Prog Neurobiol. 2015.

48. Zaltieri M, Longhena F, Pizzi M, Missale C, Spano P, Bellucci A. Mitochondrial Dysfunction and alpha-Synuclein Synaptic Pathology in Parkinson's Disease: Who's on First? Parkinsons Dis. 2015;2015:108029.

49. Ayala-Pena S. Role of oxidative DNA damage in mitochondrial dysfunction and Huntington's disease pathogenesis. Free Radic Biol Med. 2013;62:102-10.

50. Matthews RT, Yang L, Jenkins BG, Ferrante RJ, Rosen BR, Kaddurah-Daouk R, et al. Neuroprotective effects of creatine and cyclocreatine in animal models of Huntington's disease. J Neurosci. 1998;18(1):156-63.

51. Andres RH, Ducray AD, Perez-Bouza A, Schlattner U, Huber AW, Krebs SH, et al. Creatine supplementation improves dopaminergic cell survival and protects against MPP+ toxicity in an organotypic tissue culture system. Cell Transplant. 2005;14(8):537-50.

52. Valastro B, Dekundy A, Danysz W, Quack G. Oral creatine supplementation attenuates L-DOPA-induced dyskinesia in 6-hydroxydopamine-lesioned rats. Behav Brain Res. 2009;197(1):90-6.

53. Ryu H, Rosas HD, Hersch SM, Ferrante RJ. The therapeutic role of creatine in Huntington's disease. Pharmacol Ther. 2005;108(2):193-207.

54. Smith RN, Agharkar AS, Gonzales EB. A review of creatine supplementation in age-related diseases: more than a supplement for athletes. F1000Res. 2014;3:222.

55. Lin YS, Cheng TH, Chang CP, Chen HM, Chern Y. Enhancement of brain-type creatine kinase activity ameliorates neuronal deficits in Huntington's disease. Biochim Biophys Acta. 2013;1832(6):742-53.

56. Buford TW, Kreider RB, Stout JR, Greenwood M, Campbell B, Spano M, et al. International Society of Sports Nutrition position stand: creatine supplementation and exercise. J Int Soc Sports Nutr. 2007;4:6.

57. Wallimann T, Tokarska-Schlattner M, Schlattner U. The creatine kinase system and pleiotropic effects of creatine. Amino Acids. 2011;40(5):1271-96.

58. Derave W, Van Den Bosch L, Lemmens G, Eijnde BO, Robberecht W, Hespel P. Skeletal muscle properties in a transgenic mouse model for amyotrophic lateral sclerosis: effects of creatine treatment. Neurobiol Dis. 2003;13(3):264-72.

59. Gualano B, Novaes RB, Artioli GG, Freire TO, Coelho DF, Scagliusi FB, et al. Effects of creatine supplementation on glucose tolerance and insulin sensitivity in sedentary healthy males undergoing aerobic training. Amino Acids. 2008;34(2):245-50.

60. Gotshalk LA, Volek JS, Staron RS, Denegar CR, Hagerman FC, Kraemer WJ. Creatine supplementation improves muscular performance in older men. Med Sci Sports Exerc. 2002;34(3):537-43.

61. Gotshalk LA, Kraemer WJ, Mendonca MA, Vingren JL, Kenny AM, Spiering BA, et al. Creatine supplementation improves muscular performance in older women. Eur J Appl Physiol. 2008;102(2):223-31.

62. Bender A, Beckers J, Schneider I, Holter SM, Haack T, Ruthsatz T, et al. Creatine improves health and survival of mice. Neurobiol Aging. 2008;29(9):1404-11.

63. Lalonde R, Strazielle C. Brain regions and genes affecting limb-clasping responses. Brain Res Rev. 2011;67(1-2):252-9.

64. Bettencourt C, Santos C, Coutinho P, Rizzu P, Vasconcelos J, Kay T, et al. Parkinsonian phenotype in Machado-Joseph disease (MJD/SCA3): a two-case report. BMC Neurol. 2011;11:131.

65. Yang S, Long LH, Li D, Zhang JK, Jin S, Wang F, et al. beta-Guanidinopropionic acid extends the lifespan of Drosophila melanogaster via an AMP-activated protein kinase-dependent increase in autophagy. Aging Cell. 2015.

66. Yang L, Calingasan NY, Wille EJ, Cormier K, Smith K, Ferrante RJ, et al. Combination therapy with coenzyme Q10 and creatine produces additive neuroprotective effects in models of Parkinson's and Huntington's diseases. J Neurochem. 2009;109(5):1427-39.

Supplementary figure

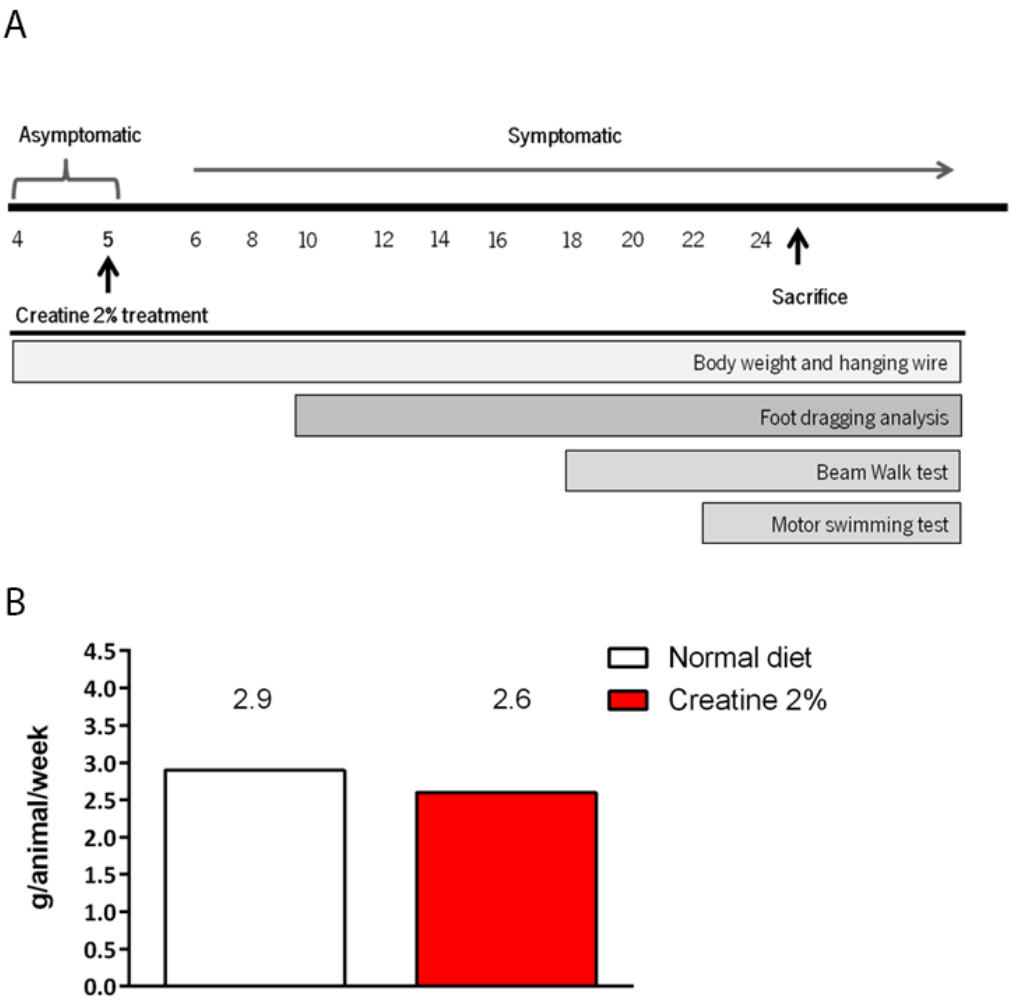

Supp. Fig 1. (A) Schematic timeline for the behavioral analysis of creatine 2% pre-clinical trial **(B)** The mean food consumption per day/per mouse was around 3 grams and no differences were obtained between diets (Student's t test).

Chapter 7

General Discussion and Future Perspectives

7. General Discussion and Future Perspectives

7.1 MJD mouse models for pre-clinical trials: the CMVMJD135 mouse line

Machado-Joseph disease is a severe and clinically heterogeneous disease for which there is no effective therapy.

Mouse models of human diseases are created both to understand the pathogenesis of the disorders and to find successful therapies for them. The MJD mouse models generated so far are of extreme importance because they allow an increase in the knowledge of MJD pathogenesis and potential therapeutic targets. Ideally, mouse models should recapitulate the human phenotype and neuropathology to a full extent. However, this rarely occurs and scientists try their best to generate the closest model to the human condition. Almost all MJD transgenic models follow the *construct validity* criterium to validate an animal model as they are based on expression of a mutant version of the ATXN3 gene bearing an expanded polyQ tract (1). Yet, not all recapitulate the *face validity* criterium. Face validity comprises the disease phenotype, including physical symptoms, neuropathologic and neurochemical aspects, and also accounts for the temporal progression of the disease. The CMVMJD135 mouse model (Chapter 2, 3, 4, 5, and 6) used in this thesis work mimics the human disorder quite closely at the phenotypic level (Table 1). The disease symptoms of this model appear gradually in life and progress as the mice age. Motor and gait deficits, loss of muscular strength and other neurological symptoms such as abnormal reflexes and tremors are present (Fig 1).

This model also present intranuclear inclusions, as well as neuropathologic affection in key disease regions resembling the human disease such as (i) cellular loss in the pontine and dentate nuclei, in substantia nigra and spinal cord (ii) a reduction of calbindin positive Purkinje cells (Chapter 5) as well as a reduced thickness of the molecular layer of the cerebellum, (iii) reduced cholinergic neurons in the facial nuclei and spinal cord, (iv) a reduction of TH positive neurons and astrogliosis in the substantia nigra (Chapter 2, 5 and 6), (v) gross brain atrophy (late in life) and (vi) and alterations in the brain cytokine profile (Chapter 5), as was described for MJD patients (2-5) (Fig 1). Although the onset of the symptoms occurs very early in this model (at 6 weeks of age), the disease progresses slowly over time and the animals do not die prematurely, living as long as the wild type mice under the standard conditions of care in our animal facility (including making food and water available to animals that are unable to reach them).

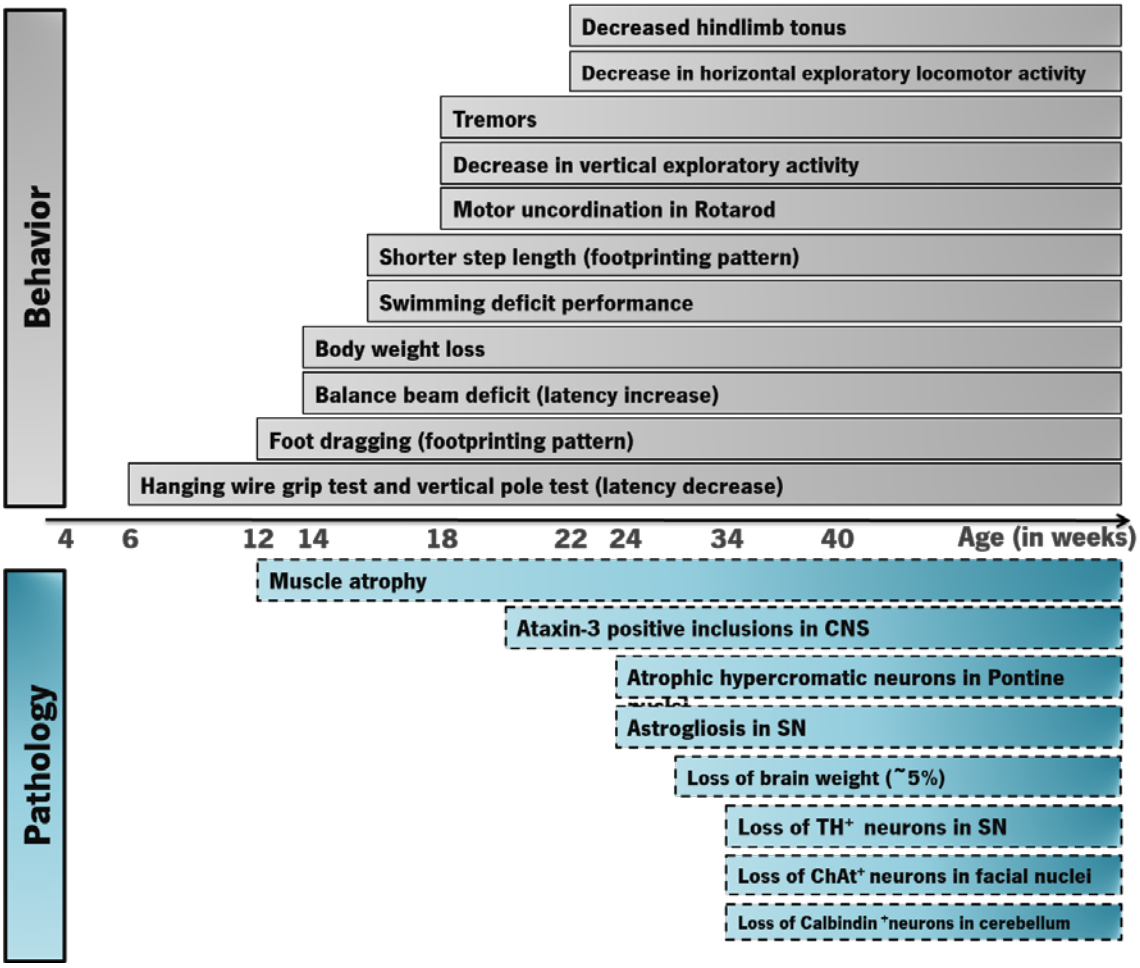

Figure 1. Summary of the progression of behavioral and pathological findings in the CMVMJD135 mice. Ages at onset of symptoms are an estimate from the earlier studies of this model, described in Chapters 2-6. The dashed lines indicate unknown age of onset of the pathologic findings, as further mapping of the appearance of pathological features is ongoing. Ages presented are an estimate from the studies of this model in chapters 2-6 and (6).

Table 1. Phenotypic and pathologic aspects of the CMVMJD135 mouse model and MJD patients. List of symptoms and pathologic aspects of MJD found in the CMVMJD135 mice and human patients. CNS – central nervous system; PN – pontine nuclei; SN – substantia nigra; 7N – facial nuclei; TH – tyrosin hydroxilase; VN – vestibular nuclei.

Face validity					
Symptoms			Pathologic aspects		
CMVMJD135 mouse model		**Human MJD patients**	**CMVMJD135 mouse model**		**Human MJD patients**
Muscular strength deficits Gait abnormalities Balance and motor problems Body weight loss Tremors Decreased exploratory activity Loss of limb tonus		Muscle atrophy Gait ataxia Motor uncoordination Weight loss Intention and resting tremor Cramps Spasticity Dystonia Peripheral neuropathy Dysfagy Ophthalmoplegia Hyporeflexia Hyperreflexia Bulging eyes Restless legs syndrome Bradykinesia Dysarthria Diplopia	Muscle atrophy Ataxin-3 inclusions in the CNS Atrophic hypercromatic neurons in the PN Astrogliosis in the SN Loss of TH^+ neurons in the SN Loss of $Chat^+$ neurons in the 7N Loss of $Calbindin^+$ neurons in the Cerebellum Loss of brain weight Decreasead thickness of the molecular layer of the Cerebellum Altered cytokine profile		Muscle atrophy Ataxin-3 inclusions in the CNS Atrophy in total brainstem, including midbrain, pons and medulla, total cerebellum, cerebellar hemispheres and cerebellar vermis, putamen and caudate nucleus Neuronal loss and gliosis in the SN, PN and VN, as well as in cranial nerves, Clarke's columns and anterior horns of the spinal cord Loss of brain weight Microgliosis in the PN Altered cytokine profile

During disease progression, MJD patients have concomitant complications such as respiratory infections or bronchopneunomia, mostly due to the bed ridden status and/or dysphagia problems, that ultimately constitutes one of the most frequent causes of death in MJD (7, 8). In mice respiratory problems were not observed, most likely due to the horizontal and downward aspect of mice's upper respiratory and gastrointestinal tract, which becomes less favorable to the occurrence of aspirations pneumonia or other respiratory pathology. Together, all the phenotypic and neuropathologic readouts, makes the CMVMJD135 an excellent model to perform pre-clinical trials and to study the mechanism(s) underlying MJD pathogenesis, which are comprised in the two main goals of animal models development according to Chadman and collaborators: (*i) testing hypotheses about the mechanisms underlying the disease, and (ii) translational evaluation of pharmacological, behavioral, and other treatments for the disease* (1). Regarding the last criterium for validating animal models, *Predictive validity* exists when the response of the model to known treatments is similar to that in the human disease; i.e., if a treatment is known to be effective in humans it should also be in the animal models for that specific disease. In the particular case of MJD, no standard treatment exists for comparison. Importantly, no pre-clinical trials were used to test the potential efficacy of the few specific drugs that have been taken to the actual clinical trials performed so far in humans (Chapter 1, table 6). Some studies performed in animal models have shown some promising results, as is the case for autophagy inducers or HDCA inhibitors (9, 10), among others. Yet, none of these approaches have been tested in MJD patients to date. Nevertheless, we have performed one pre-clinical trial using lithium chloride (Chapter 3) that showed to have no overall impact in the CMVMJD135 phenotype, a result that was in accordance with the clinical trial performed simultaneously in MJD patients (11) that also showed no efficacy concerning its defined primary outcome.

7.2 Are we performing good pre-clinical trials? Problems and recommendations

The spreading of knowledge in Science is of extreme importance since it drives scientific progress. A major problem regarding pre-clinical trials, and knowing that new discoveries hinge on previous observations, consists on the lack of or insufficient reporting of the study design, experiment conduction and analysis. This issues leads to the inability to replicate the majority of findings between different labs or even by the original authors of the work (12, 13), the estimates for irreproducible studies being 70-90% (13). Reproducibility does not mean that the studies should be replicated in perfect detail, but should corroborate the major findings of the original study. A major issue contributing to irreproducibility is that the majority of experiments are performed in a non-blinded fashion, driving to

observer bias (14, 15). Rigorous methodologies (blinding, repeating experiments, use of validated reagents, use of the correct controls) should be performed since the initial step of the experiment, and pilot studies should be performed as rigorously as the study itself, since this will avoid unnecessary costs for the investigators and also for pharmaceutical companies that might be interested in testing the investigators findings (16). In order to improve animal studies and consequently the translation with success to the clinics, researchers have argued for a focus on hypothesis-based research, a rigorous study plan, training and more adequate statistics (17, 18). Also, pharmacokinetic studies are of extreme importance before any evaluation of potential effect (19). Besides the most common recommendations, including blinding, randomization and power analysis, other issues should be taken in consideration such the correct use of controls, dose-response determination, replication in different models and independent replication. Considering this, the US National Institute of Neurological Disorders and Stroke (NINDS) developed several recommendations for improving the reporting and design of the pre-clinical trials. In this meeting, the committee board found several issues regarding transparency of reporting: (1) poor experimental design, (2) lack of information on research parameters when reporting the results using animal model and suggested that a effort should be done by the funding agencies and journal editorial boards to allow and demand more detailed methodologies in the manuscripts and research grant applications (20). Animal experiments often fail to be reproduced when tested in humans (21, 22). Landis et al listed some parameters that should be followed to obtain a rigorous study design (20) (Box 1).

BOX 1 - Standards for rigorous study design

(i) Randomization

Animals should be randomly assigned to the experimental groups and the collected data should be processed randomly or blocked in a proper manner.

(ii) Blinding

The experimenters should consider three different situations. *Allocation concealment*, where the researcher should be blind of the group to which a given animal will be allocated; *Blinded conduct,* states that investigators and animal caretakers involved in the study should be blinded to de allocation sequence and finally *Blinded assessment of the outcome*, where the researcher performing the experiments and analyzing the data should be blinded to the treatments.

(iii) Sample-size estimation

Statistical method used to determine sample size should be reported; statistic methods should be reported.

(iv) Data handling

The endpoint of the pre-clinical trial should be defined in advance according to the study purpose. Any data removed before analysis should be reported. The readouts should be defined and potential replicate issues need to be considered during study design.

After the publication of these suggestions to improve reporting transparency and study design in 2012, the National Institute of Health (NIH) proposed additional recommendations based on the previous study described above (20). The later recommendations are more directed to the journals boards where the Information for Authors should be reformulated, including a statistical analysis checklist and no limit space or generous limits for the methods section (including online versions). Furthermore, (and some journals already adopted this), community-based standards should be used, such as nomenclature standards and reporting standards for animal studies (e.g. ARRIVE guidelines (23)). NIH also strongly encourages the scientific community to share information as much as possible. This might be achieved by deposition of the data in public repositories, sharing software's and describe as much as possible the biological material (animal model, cell lines) and the reagents (antibodies characteristics, primers, among others).

Chance and bias are two aspects that should be taken in consideration when performing pre-clinical trials. Several studies in neurodegenerative diseases have demonstrated the lack of efficacy of the compounds tested in mouse models when translated to humans. On these reviews, recommendations are suggested for each specific disease (24-27). In the case of MJD, the pre-clinical and clinical trials are not as explored as for other polyglutamine diseases. As discussed in Chapter 1, very few clinical trials were conducted for MJD, most of them being case reports (Chapter 1, table 6). Double-blinded clinical trials were performed, but the sample size of those trials was very small and the duration often short (Table 5, Chapter 1). Also for pre-clinical trials, very few compounds were tested to date in MJD mouse models (Table 4, Chapter 1) and most often the same compound was not tested in different mouse models of the disorder.

In the present work, five hypothesis-based compounds were tested in the CMVMJD135 mouse model, one of which was tested in two independent replicates (Chapter 6). The pre-clinical trials performed here were initiated before publication of the recommendations mentioned previously in this section (Box 1), however they were conducted having in consideration the points **(iii)** and **(iv)**. Also, the statistical analysis was carried out rigorously and considering all the multiple evaluations performed in the tests. Regarding points **(i)** and **(ii)**, logistic issues did not allow us to perform the studies using randomization or blinding (the experimenter was only blind to the genotype of the animals). At this moment and for the future, with the gathering of more human resources, pre-clinical trials in the CMVMJD135 mice will be performed randomly and in a blinded manner to avoid bias. Although, during the CMVMJD135 mice phenotype characterization, we had performed the behavior tests both in male and females and the symptoms progression is similar between genders (Chapter 2) , the compounds

presented in this work, should also be tested in both genders; we have used males in Chapters 2, 3 and 4, and females in Chapters 5 and 6. These compounds were tested in an early symptomatic stage (one week before the disease onset) in order to study if the disease progression could be delayed. This approach could be beneficial to those patients who are diagnosed molecularly before the symptoms' appearance due to the availability of a genetic test specific for MJD. Nevertheless, some MJD patients are only diagnosed after disease onset, and in that way, it would be important to test these compounds post-symptomatically, to validate them further before human trials.

In all pre-clinical studies presented here, four groups of animals were used. Wild-type littermates were in all cases also assigned to treatment groups, which allowed us to study possible effects of the compounds in wild-type animals. Indeed, confirming the relevance of including such control groups, the combination of lithium chloride and CCI-779 showed to be detrimental to wild-type mice (Chapter 3), while Creatine improved the performance of wild-type animals suggesting some lack of specificity of its action, which does not diminish the relevance of the findings (Chapter 6).

Furthermore, the study design was slightly different between the different studies. In each pre-clinical trial we learned more about the CMVMJD135 mouse model (both at phenotypic and neuropathologic levels), which allowed us to improve and re-design the study in the following trials. The first trials (Chapter 2, 3 and 4) allowed us to understand that the duration of the trial should be increased, and that was applied in the following studies (chapter 5 and 6). Nevertheless, we could only increase the treatment duration until after a certain age, after which CMVMJD135 mice are not able to adequately reach food and water by themselves and/or to perform many of the tasks.

Also, it was possible to verify a direct and positive correlation between genotype/phenotype, meaning that higher CAG repeat length leads to a more severe phenotype; this correlation forced us to control the CAG repeat length of each individual in each trial in order to obtain homogeneous groups in the preclinical studies. We also shortened the interval of the phenotype evaluation, testing the animals every two weeks; this allowed a better phenotype discrimination of the possible effects of the compound under test, however it also resulted in a training effect that modified the phenotype.

Five of the compounds (except TUDCA) were tested previously in our lab in another animal model, a *C. elegans* model of MJD (28) as recommended by FELASA (to test first in alternative models) (29), showing beneficial effects. Yet, it is of great importance to test those that had positive effects in mice (17-DMAG – Chapter 2; TUDCA – Chapter 5 and Creatine – Chapter 6) in other mouse models of MJD, to further demonstrate their efficacy. In addition, it is also important to replicate these pre-clinical trials in the CMVMJD135 model itself and in different genders. We have replicated the Creatine study,

mainly because the results obtained in the first trial (*PCT1* – Chapter 6) prompted us to perform an improved trial using a more extensive and optimized study design (*PCT2* - Chapter 6), and even though the second group of transgenic animals had a higher mean repeat length, the results between both independent studies were consistent, further strengthening the findings.

What have we learned about MJD pathogenesis and therapeutic targets with pre-clinical trials?

7.3 Hsp90 inhibitors and autophagy inducers in MJD

Hsp90 inhibitors are known to possess the unique pharmacological effect of inducing a stress response, and, in addition to their use as anticancer agents, have also been developed as pharmacological HSP inducers for application in protein folding disorders (30, 31). We tested the efficacy of 17-DMAG, an Hsp90 inhibitor, in improving the behavioral deficits of the CMVMJD135 mice. Several studies demonstrated the positive effects of 17-AAG and its analogues (including 17-DMAG, which is less toxic) in models of polyQ diseases (32-35). Accordingly, in our study (Chapter 2) behavioral deficits were transiently improved by 17-DMAG administration and neuropathologic findings were ameliorated. Surprisingly, 17-DMAG did not induce the HSR in the brain of CMVMJD135 animals as we were expecting. However, the protein levels of mutant ataxin-3 as well as the aggregate load were diminished after 17-DMAG treatment, suggesting that other mechanism (s) would be occurring in the cells. Indeed, we found that 17-DMAG was inducing autophagy and therefore probably the degradation of mutant ataxin-3 through this mechanism (not excluding others, as the UPS). Other studies have also shown that 17-DMAG is able to induce autophagy (36, 37), and other mechanism(s) of action of 17-DMAG rather than inducing the HSR were proposed for SBMA (35). We evaluated the autophagy process in the brain of the CMVMJD135 animals by using autophagy markers according to the guidelines for autophagy evaluation (38) and found no significant differences in several autophagy markers (Chapter 3 and Chapter 5), suggesting that autophagy is not overactived or blocked in this model. Nevertheless, autophagy induction seems to be a promising target to modulate in polyQ diseases and there is an extensive body of literature demonstrating its beneficial effects (9, 39-50). Thus, and considering the benefic effects of 17-DMAG, we tested other autophagy inducers: lithium chloride and CCI-779. The potential beneficial effects of pharmacological autophagy induction was previously suggested in studies using CCI-779 or beclin-1 overexpression in rodent models of MJD (9,

51). Unexpectedly, the use of lithium chloride (Chapter 3) had no overall effect on the behavioral deficits of CMVMJD135 mice, in spite of activating autophagy as expected. Accordingly, a human clinical trial using lithium carbonate was performed in the same year demonstrating that albeit well tolerated, lithium had no major impact on disease progression in MJD patients (11). In another attempt to increase autophagy, we also tested a combination of two autophagy inducers that act independent or dependently of mTOR, lithium and CCI-779, respectively (Chapter 4). This combinatory approach was previously tested in a HD fly model with promising results (43). Also, this combination was tested in our *C.elegans* MJD model and shown to be non-toxic and to improve the locomotor deficit observed in the AT3q130 worms. In the CMVMJD135 mice, however, this combinatory therapy showed no beneficial effects and even demonstrated to be deleterious to both transgenic and wild-type mice perturbating neurological function and general health, at doses that shown to be safe in mice when administered alone (Chapter 3 and (9)). These discrepant results suggest that the same compounds can have different outcomes in different animal models, which reinforces the importance of testing the same compound in different models. Pre-clinical trials with compounds that revealed to be ineffective in the disease models are often more difficult to publish and, therefore, often remain not known by the scientific community. This may lead to a bias and to the continuously re-testing of these compounds that might not offer success in humans. The editorial decisions might, thus have implications in the decision of performing (or not) clinical trials in humans. Here, and for this reason, we made a point of reporting negative results with lithium chloride and lithium chloride in combination with temsirolimus.

7.4 Supplementation with endogenously produced neuroprotective compounds in MJD

TUDCA and creatine are two compounds produced endogenously by the human body (52-54) and commonly used as diet supplements. These two diet supplements are considered safe, even at high concentrations and used in a chronic basis (55-57). Furthermore, they are able to cross the blood brain barrier and exert neuroprotection (58-61). In our study, both TUDCA and creatine showed an overall improving of the CMVMJD135 mice phenotype (Chapter 5 and 6).

TUDCA was extensively studied in models of different neurodegenerative diseases and in all cases the results have been very promising (62-67); furthermore, this compound was already shown to have promising effects in ALS patients (56) without major adverse events.

TUDCA is considered a pleiotropic signaling molecule, which might be of extreme relevance in disorders that are complex and multi-factorial. Classically, TUDCA act as an anti-apoptotic agent at the

mitochondrial level, physically binding to the Bax protein, inhibiting its translocation from the cytosol do the mitochondria (68, 69). However, TUDCA targets several other cellular pathways, having anti-oxidant (65-67), mitochondria-protective (68) and anti-inflammatory properties (62, 63, 70). In chapter 5, we show that TUDCA acted in CMVMJD135 mice most likely through its anti-inflammatory properties by reducing astrogliosis and normalizing the cytokine profile in the brain. However, we also tested other target cellular pathways, such as the HSR, (which we have shown not to be altered in the basal situation in CMVMJD135 mice - chapter 2). Indeed, we found no differences in the HSR in the CMVMJD135 model at late stages (34 weeks of age), but we cannot exclude that this is not happening earlier in life, as was shown for HD (71) or in specific cellular subtypes. Furthermore, we have shown that mutant ataxin-3 and aggregate load in the brain of the CMVMJD135 mice were reduced upon autophagy induction by 17-DMAG (Chapter 2), reinforcing the importance of autophagy in this type of disease, as suggested by others (9, 44, 49). TUDCA is also known as an autophagy inducer (72), but in our study we did not observe autophagy induction upon treatment with this compound, nor a reduction in the aggregate load in the brain of CMVMJD135 mice. Nevertheless, TUDCA showed to be neuroprotective in CMVMJD135 mice. As previously shown by us (6), a loss of Calbindin staining of the Purkinje cell layer of the cerebellum occurs in CMVMJD135 animals, which was significantly improved by TUDCA chronic treatment.

Creatine, an important molecule in the body and especially in the skeletal muscle (54), improved both coordination deficits but only partially rescued the muscular strength deficits of the CMVMJD135 mice, suggesting an effect at the level of neurons. Furthermore, and in agreement with what was observed in Chapter 2 for 17-DMAG, creatine diminished the ataxin-3 positive aggregates in the brainstem. So far, we do not known the molecular mechanism (s) underlying these effects of creatine in CMVMJD135 mice. In further studies we plan to address the metabolic profile in the muscle and brain of these mice, as well as other possible neuroprotective mechanism of creatine, which may be of relevance to different diseases for which this compound exerted neuroprotection (73-75).

7.5 Relevance of the novel findings and main conclusions of the work

In this work we have characterized and validated a new MJD mouse model that constitutes a powerful framework for pre-clinical studies. The CMVMJD135 mice carry several measurable readouts at the phenotypic and neuropathologic levels, recapitulating several key pathological hallmarks of MJD and displaying an early-onset, and readily quantifiable motor phenotype. Because the CMVMJD135

mirrors several aspects of the human disorder, it may represent the best available mouse model for future preclinical trials.

We also conducted five hypothesis-based preclinical trials with candidate therapeutic compounds for MJD (Fig 2). The main advantage of hypothesis-based pre-clinical trials relies on the previous known target of each compound, making it a more goal-directed study, together with the possibility of understanding the drug effect at the behavior and molecular levels and therefore contributing to the continuous exploration of pathogenic mechanism(s).

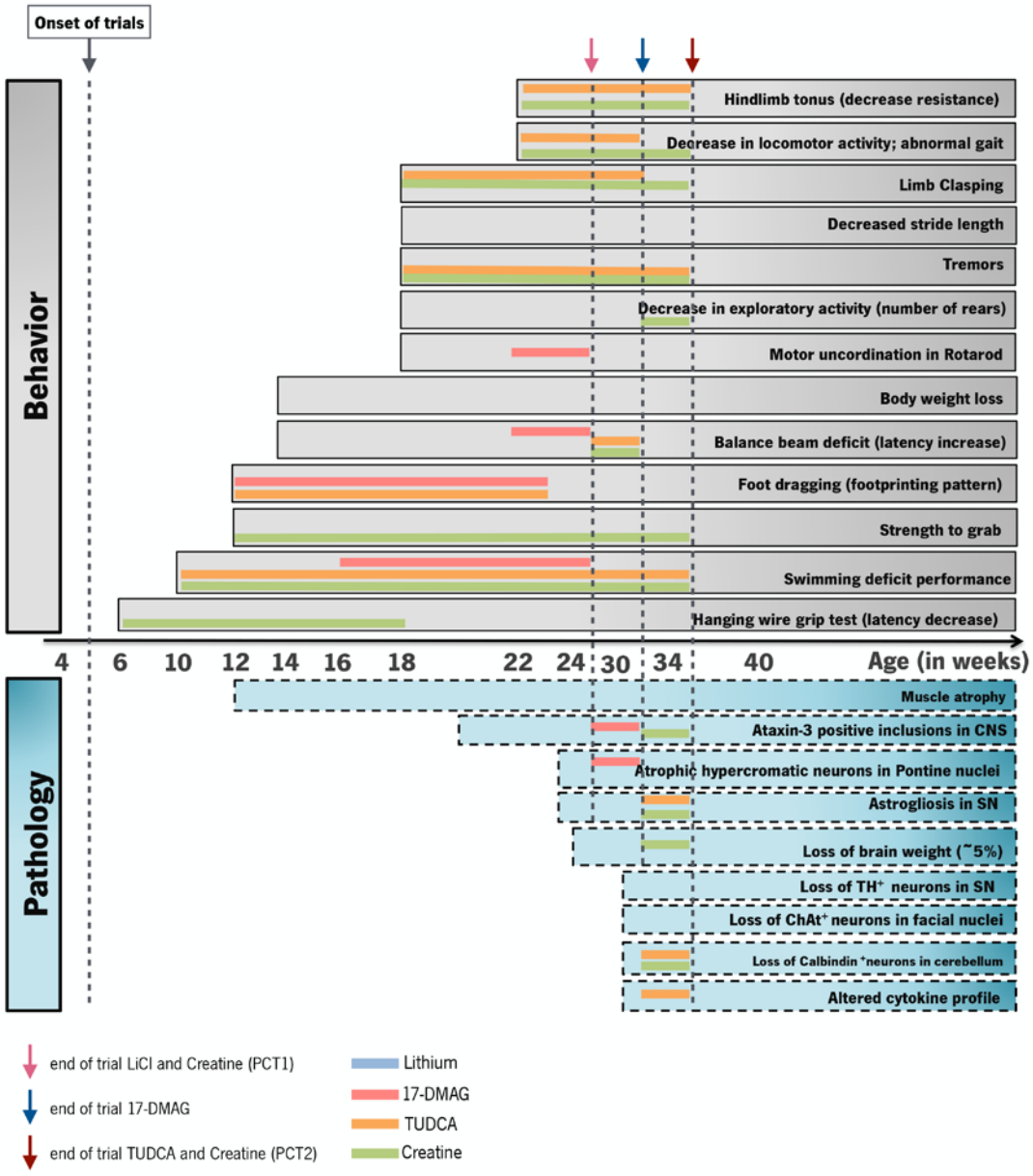

Figure 2. Summary of the beneficial effect of the different compounds tested on CMVMJD135 phenotype and neuropathology. The color lines represent the duration of the improvement for each preclinical trial.

Although the major goal of this thesis was to test proteostasis network-related targets and compounds, the experiments may conduct us to other possibilities, as for instance neuroinflammation (the effect of the compounds tested in this work, in several proteostasis-related branches and inflammation, are summarized in Fig 3). From the five compounds tested here, TUDCA and creatine showed the most significant impact at the behavioral level. The percentage of effect on the motor swimming test for TUDCA was 57.25%, for creatine 85.39% and for 17-DMAG 45.26%. We were not able to calculate the percentage of effect of lithium since in this trial we did not perform motor swimming test. Interestingly, the effect of Citalopram (a molecule found by unbiased screening in *C. elegans* and shown to be highly effective in the CMVMJD135 mouse (6) was similar to that observed for creatine, i.e., 82.51%. Indeed, when we compare the performance of the CMVMJD135 mice on the motor swimming test in all ages tested (10 to 34 weeks of age, tested every two weeks) we do not observe differences between the treatments (TUDCA versus creatine, p=0.557, repeated measures). Nevertheless, taking into account a more refined analysis, using the first five points of analysis (10 to 20 weeks of age) we can conclude that CMVMJD135 mice under creatine supplementation performed better in the motor swimming test when compared to the CMVMJD135 mice under TUDCA supplementation (TUDCA versus creatine, p=0.010, repeated measures), suggesting that creatine had a greater positive effect during the first 10 weeks and after this time-point (20 weeks of age), TUDCA and creatine have the same effect on this test. These results reinforce the value of these compounds as promising ones to be further tested in human clinical trials, particularly given their safety profile. Furthermore, these compounds are FDA-approved and were already tested for toxicity in several diseases as well as in healthy persons. Both compounds are considered to be pleiotropic molecules acting at several cellular targets which might explain, to some extent, their positive impact at the behavior level. Another interesting approach may comprise the combination one of these compounds with others tested in our lab, or with each other, possibly leading to synergistic effects, an approach that needs to be adequately tested at the pre-clinical and clinical levels. Furthermore, the non-positive results obtained in pre-clinical trials are equally important for the MJD therapy field, since they bring significant improvements in the knowledge of the molecular mechanism (s) that are (or not) underlying neuropathology in CMVMJD135 mice, and help to guide the future preclinical and clinical trials, in MJD and also in other polyQ diseases towards more relevant targets.

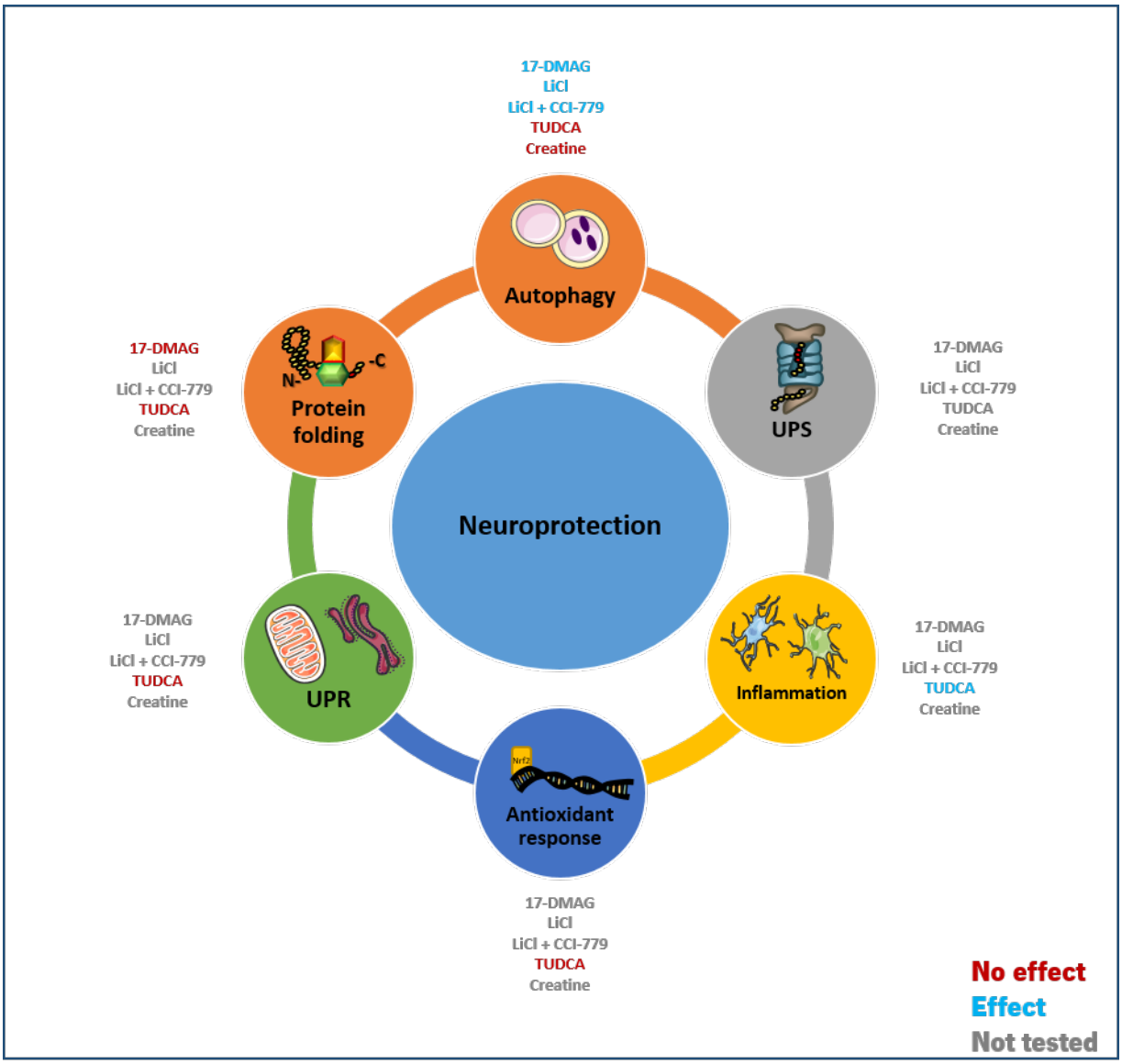

Figure 3. Schematic representation of proteostasis-related signaling pathways and inflammation, and the impact of each compound tested in this work on those branches.

References

1. Chadman KK, Yang M, Crawley JN. Criteria for validating mouse models of psychiatric diseases. Am J Med Genet B Neuropsychiatr Genet. 2009;150B(1):1-11.

2. Paulson HL, Das SS, Crino PB, Perez MK, Patel SC, Gotsdiner D, et al. Machado-Joseph disease gene product is a cytoplasmic protein widely expressed in brain. Ann Neurol. 1997;41(4):453-62.

3. Seidel K, Meister M, Dugbartey GJ, Zijlstra MP, Vinet J, Brunt ER, et al. Cellular protein quality control and the evolution of aggregates in spinocerebellar ataxia type 3 (SCA3). Neuropathol Appl Neurobiol. 2012;38(6):548-58.

4. Rub U, Brunt ER, Deller T. New insights into the pathoanatomy of spinocerebellar ataxia type 3 (Machado-Joseph disease). Curr Opin Neurol. 2008;21(2):111-6.

5. Evert BO, Vogt IR, Kindermann C, Ozimek L, de Vos RA, Brunt ER, et al. Inflammatory genes are upregulated in expanded ataxin-3-expressing cell lines and spinocerebellar ataxia type 3 brains. J Neurosci. 2001;21(15):5389-96.

6. Teixeira-Castro A, Jalles A, Esteves S, Kang S, da Silva Santos L, Silva-Fernandes A, et al. Serotonergic signalling suppresses ataxin 3 aggregation and neurotoxicity in animal models of Machado-Joseph disease. Brain. 2015.

7. Friedman JH. Azorean (Machado-Joseph) disease. R I Med J. 1988;71(4):149-53.

8. Lima L, Coutinho P. Clinical criteria for diagnosis of Machado-Joseph disease: report of a non-Azorena Portuguese family. Neurology. 1980;30(3):319-22.

9. Menzies FM, Huebener J, Renna M, Bonin M, Riess O, Rubinsztein DC. Autophagy induction reduces mutant ataxin-3 levels and toxicity in a mouse model of spinocerebellar ataxia type 3. Brain. 2010;133(Pt 1):93-104.

10. Chou AH, Chen SY, Yeh TH, Weng YH, Wang HL. HDAC inhibitor sodium butyrate reverses transcriptional downregulation and ameliorates ataxic symptoms in a transgenic mouse model of SCA3. Neurobiol Dis. 2011;41(2):481-8.

11. Saute JA, de Castilhos RM, Monte TL, Schumacher-Schuh AF, Donis KC, D'Avila R, et al. A randomized, phase 2 clinical trial of lithium carbonate in Machado-Joseph disease. Mov Disord. 2014;29(4):568-73.

12. Prinz F, Schlange T, Asadullah K. Believe it or not: how much can we rely on published data on potential drug targets? Nat Rev Drug Discov. 2011;10(9):712.

13. Peers IS, Ceuppens PR, Harbron C. In search of preclinical robustness. Nat Rev Drug Discov. 2012;11(10):733-4.

14. Begley CG. Six red flags for suspect work. Nature. 2013;497(7450):433-4.

15. Rosenthal R, Lawson R. A Longitudinal Study of the Effects of Experimenter Bias on the Operant Learning of Laboratory Rats. J Psychiatr Res. 1964;2:61-72.

16. Begley CG, Ioannidis JP. Reproducibility in science: improving the standard for basic and preclinical research. Circ Res. 2015;116(1):116-26.

17. Winquist RJ, Mullane K, Williams M. The fall and rise of pharmacology–(re-)defining the discipline? Biochem Pharmacol. 2014;87(1):4-24.

18. Marino MJ. The use and misuse of statistical methodologies in pharmacology research. Biochem Pharmacol. 2014;87(1):78-92.

19. McGonigle P, Ruggeri B. Animal models of human disease: challenges in enabling translation. Biochem Pharmacol. 2014;87(1):162-71.

20. Landis SC, Amara SG, Asadullah K, Austin CP, Blumenstein R, Bradley EW, et al. A call for transparent reporting to optimize the predictive value of preclinical research. Nature. 2012;490(7419):187-91.

21. Pound P, Ebrahim S, Sandercock P, Bracken MB, Roberts I, Reviewing Animal Trials Systematically G. Where is the evidence that animal research benefits humans? BMJ. 2004;328(7438):514-7.

22. Kaste M. Use of animal models has not contributed to development of acute stroke therapies: pro. Stroke. 2005;36(10):2323-4.

23. Kilkenny C, Browne W, Cuthill IC, Emerson M, Altman DG, Group NCRRGW. Animal research: reporting in vivo experiments: the ARRIVE guidelines. Br J Pharmacol. 2010;160(7):1577-9.

24. Ludolph AC, Bendotti C, Blaugrund E, Chio A, Greensmith L, Loeffler JP, et al. Guidelines for preclinical animal research in ALS/MND: A consensus meeting. Amyotroph Lateral Scler. 2010;11(1-2):38-45.

25. Shineman DW, Basi GS, Bizon JL, Colton CA, Greenberg BD, Hollister BA, et al. Accelerating drug discovery for Alzheimer's disease: best practices for preclinical animal studies. Alzheimers Res Ther. 2011;3(5):28.

26. Kwak SP, Wang JKT, Howland DS. Target Validation for Huntington's Disease. In: Lo DC, Hughes RE, editors. Neurobiology of Huntington's Disease: Applications to Drug Discovery. Frontiers in Neuroscience. Boca Raton (FL)2011.

27. Katz DM, Berger-Sweeney JE, Eubanks JH, Justice MJ, Neul JL, Pozzo-Miller L, et al. Preclinical research in Rett syndrome: setting the foundation for translational success. Dis Model Mech. 2012;5(6):733-45.

28. Teixeira-Castro A, Ailion M, Jalles A, Brignull HR, Vilaca JL, Dias N, et al. Neuron-specific proteotoxicity of mutant ataxin-3 in C. elegans: rescue by the DAF-16 and HSF-1 pathways. Hum Mol Genet. 2011;20(15):2996-3009.

29. Guillen J. FELASA guidelines and recommendations. J Am Assoc Lab Anim Sci. 2012;51(3):311-21.

30. Whitesell L, Bagatell R, Falsey R. The stress response: implications for the clinical development of hsp90 inhibitors. Curr Cancer Drug Targets. 2003;3(5):349-58.

31. Bagatell R, Paine-Murrieta GD, Taylor CW, Pulcini EJ, Akinaga S, Benjamin IJ, et al. Induction of a heat shock factor 1-dependent stress response alters the cytotoxic activity of hsp90-binding agents. Clin Cancer Res. 2000;6(8):3312-8.

32. Fujikake N, Nagai Y, Popiel HA, Okamoto Y, Yamaguchi M, Toda T. Heat shock transcription factor 1-activating compounds suppress polyglutamine-induced neurodegeneration through induction of multiple molecular chaperones. J Biol Chem. 2008;283(38):26188-97.

33. Tokui K, Adachi H, Waza M, Katsuno M, Minamiyama M, Doi H, et al. 17-DMAG ameliorates polyglutamine-mediated motor neuron degeneration through well-preserved proteasome function in an SBMA model mouse. Hum Mol Genet. 2009;18(5):898-910.

34. Waza M, Adachi H, Katsuno M, Minamiyama M, Sang C, Tanaka F, et al. 17-AAG, an Hsp90 inhibitor, ameliorates polyglutamine-mediated motor neuron degeneration. Nat Med. 2005;11(10):1088-95.

35. Thomas M, Harrell JM, Morishima Y, Peng HM, Pratt WB, Lieberman AP. Pharmacologic and genetic inhibition of hsp90-dependent trafficking reduces aggregation and promotes degradation of the expanded glutamine androgen receptor without stress protein induction. Hum Mol Genet. 2006;15(11):1876-83.

36. Palacios C, Martin-Perez R, Lopez-Perez AI, Pandiella A, Lopez-Rivas A. Autophagy inhibition sensitizes multiple myeloma cells to 17-dimethylaminoethylamino-17-demethoxygeldanamycin-induced apoptosis. Leuk Res. 2010;34(11):1533-8.

37. Rusmini P, Simonini F, Crippa V, Bolzoni E, Onesto E, Cagnin M, et al. 17-AAG increases autophagic removal of mutant androgen receptor in spinal and bulbar muscular atrophy. Neurobiol Dis. 2011;41(1):83-95.

38. Klionsky DJ, Abdalla FC, Abeliovich H, Abraham RT, Acevedo-Arozena A, Adeli K, et al. Guidelines for the use and interpretation of assays for monitoring autophagy. Autophagy. 2012;8(4):445-544.

39. del Cano-Espinel M, Acebes JR, Sanchez D, Ganfornina MD. Lazarillo-related Lipocalins confer long-term protection against type I Spinocerebellar Ataxia degeneration contributing to optimize selective autophagy. Mol Neurodegener. 2015;10:11.

40. Menzies FM, Garcia-Arencibia M, Imarisio S, O'Sullivan NC, Ricketts T, Kent BA, et al. Calpain inhibition mediates autophagy-dependent protection against polyglutamine toxicity. Cell Death Differ. 2015;22(3):433-44.

41. Tsunemi T, Ashe TD, Morrison BE, Soriano KR, Au J, Roque RA, et al. PGC-1alpha rescues Huntington's disease proteotoxicity by preventing oxidative stress and promoting TFEB function. Sci Transl Med. 2012;4(142):142ra97.

42. Roscic A, Baldo B, Crochemore C, Marcellin D, Paganetti P. Induction of autophagy with catalytic mTOR inhibitors reduces huntingtin aggregates in a neuronal cell model. J Neurochem. 2011;119(2):398-407.

43. Sarkar S, Krishna G, Imarisio S, Saiki S, O'Kane CJ, Rubinsztein DC. A rational mechanism for combination treatment of Huntington's disease using lithium and rapamycin. Hum Mol Genet. 2008;17(2):170-8.

44. Williams A, Jahreiss L, Sarkar S, Saiki S, Menzies FM, Ravikumar B, et al. Aggregate-prone proteins are cleared from the cytosol by autophagy: therapeutic implications. Curr Top Dev Biol. 2006;76:89-101.

45. Ravikumar B, Duden R, Rubinsztein DC. Aggregate-prone proteins with polyglutamine and polyalanine expansions are degraded by autophagy. Hum Mol Genet. 2002;11(9):1107-17.

46. Ravikumar B, Vacher C, Berger Z, Davies JE, Luo S, Oroz LG, et al. Inhibition of mTOR induces autophagy and reduces toxicity of polyglutamine expansions in fly and mouse models of Huntington disease. Nat Genet. 2004;36(6):585-95.

47. Xilouri M, Stefanis L. Chaperone mediated autophagy to the rescue: A new-fangled target for the treatment of neurodegenerative diseases. Mol Cell Neurosci. 2015;66(Pt A):29-36.

48. Frake RA, Ricketts T, Menzies FM, Rubinsztein DC. Autophagy and neurodegeneration. J Clin Invest. 2015;125(1):65-74.

49. Harris H, Rubinsztein DC. Control of autophagy as a therapy for neurodegenerative disease. Nat Rev Neurol. 2012;8(2):108-17.

50. Cortes CJ, La Spada AR. Autophagy in polyglutamine disease: Imposing order on disorder or contributing to the chaos? Mol Cell Neurosci. 2015;66(Pt A):53-61.

51. Nascimento-Ferreira I, Santos-Ferreira T, Sousa-Ferreira L, Auregan G, Onofre I, Alves S, et al. Overexpression of the autophagic beclin-1 protein clears mutant ataxin-3 and alleviates Machado-Joseph disease. Brain. 2011;134(Pt 5):1400-15.

52. Norlin M, Wikvall K. Enzymes in the conversion of cholesterol into bile acids. Curr Mol Med. 2007;7(2):199-218.

53. Tarnopolsky MA, Beal MF. Potential for creatine and other therapies targeting cellular energy dysfunction in neurological disorders. Ann Neurol. 2001;49(5):561-74.

54. Walker JB. Creatine: biosynthesis, regulation, and function. Adv Enzymol Relat Areas Mol Biol. 1979;50:177-242.

55. Kim HJ, Kim CK, Carpentier A, Poortmans JR. Studies on the safety of creatine supplementation. Amino Acids. 2011;40(5):1409-18.

56. Elia AE, Lalli S, Monsurro MR, Sagnelli A, Taiello AC, Reggiori B, et al. Tauroursodeoxycholic acid in the treatment of patients with amyotrophic lateral sclerosis. Eur J Neurol. 2015.

57. Pan XL, Zhao L, Li L, Li AH, Ye J, Yang L, et al. Efficacy and safety of tauroursodeoxycholic acid in the treatment of liver cirrhosis: a double-blind randomized controlled trial. J Huazhong Univ Sci Technolog Med Sci. 2013;33(2):189-94.

58. Quinn M, McMillin M, Galindo C, Frampton G, Pae HY, DeMorrow S. Bile acids permeabilize the blood brain barrier after bile duct ligation in rats via Rac1-dependent mechanisms. Dig Liver Dis. 2014;46(6):527-34.

59. Smith RN, Agharkar AS, Gonzales EB. A review of creatine supplementation in age-related diseases: more than a supplement for athletes. F1000Res. 2014;3:222.

60. Andres RH, Ducray AD, Schlattner U, Wallimann T, Widmer HR. Functions and effects of creatine in the central nervous system. Brain Res Bull. 2008;76(4):329-43.

61. Cortez L, Sim V. The therapeutic potential of chemical chaperones in protein folding diseases. Prion. 2014;8(2).

62. Yanguas-Casas N, Barreda-Manso MA, Nieto-Sampedro M, Romero-Ramirez L. Tauroursodeoxycholic acid reduces glial cell activation in an animal model of acute neuroinflammation. J Neuroinflammation. 2014;11:50.

63. Ramalho RM, Nunes AF, Dias RB, Amaral JD, Lo AC, D'Hooge R, et al. Tauroursodeoxycholic acid suppresses amyloid beta-induced synaptic toxicity in vitro and in APP/PS1 mice. Neurobiol Aging. 2013;34(2):551-61.

64. Lo AC, Callaerts-Vegh Z, Nunes AF, Rodrigues CM, D'Hooge R. Tauroursodeoxycholic acid (TUDCA) supplementation prevents cognitive impairment and amyloid deposition in APP/PS1 mice. Neurobiol Dis. 2013;50:21-9.

65. Keene CD, Rodrigues CM, Eich T, Chhabra MS, Steer CJ, Low WC. Tauroursodeoxycholic acid, a bile acid, is neuroprotective in a transgenic animal model of Huntington's disease. Proc Natl Acad Sci U S A. 2002;99(16):10671-6.

66. Castro-Caldas M, Carvalho AN, Rodrigues E, Henderson CJ, Wolf CR, Rodrigues CM, et al. Tauroursodeoxycholic acid prevents MPTP-induced dopaminergic cell death in a mouse model of Parkinson's disease. Mol Neurobiol. 2012;46(2):475-86.

67. Macedo B, Batista AR, Ferreira N, Almeida MR, Saraiva MJ. Anti-apoptotic treatment reduces transthyretin deposition in a transgenic mouse model of Familial Amyloidotic Polyneuropathy. Biochim Biophys Acta. 2008;1782(9):517-22.

68. Rodrigues CM, Fan G, Ma X, Kren BT, Steer CJ. A novel role for ursodeoxycholic acid in inhibiting apoptosis by modulating mitochondrial membrane perturbation. J Clin Invest. 1998;101(12):2790-9.

69. Rodrigues CM, Ma X, Linehan-Stieers C, Fan G, Kren BT, Steer CJ. Ursodeoxycholic acid prevents cytochrome c release in apoptosis by inhibiting mitochondrial membrane depolarization and channel formation. Cell Death Differ. 1999;6(9):842-54.

70. Nunes AF, Amaral JD, Lo AC, Fonseca MB, Viana RJ, Callaerts-Vegh Z, et al. TUDCA, a bile acid, attenuates amyloid precursor protein processing and amyloid-beta deposition in APP/PS1 mice. Mol Neurobiol. 2012;45(3):440-54.

71. Labbadia J, Cunliffe H, Weiss A, Katsyuba E, Sathasivam K, Seredenina T, et al. Altered chromatin architecture underlies progressive impairment of the heat shock response in mouse models of Huntington disease. J Clin Invest. 2011;121(8):3306-19.

72. Shen S, Zhang Y, Zhang R, Tu X, Gong X. Ursolic acid induces autophagy in U87MG cells via ROS-dependent endoplasmic reticulum stress. Chem Biol Interact. 2014;218:28-41.

73. Andres RH, Ducray AD, Perez-Bouza A, Schlattner U, Huber AW, Krebs SH, et al. Creatine supplementation improves dopaminergic cell survival and protects against MPP+ toxicity in an organotypic tissue culture system. Cell Transplant. 2005;14(8):537-50.

74. Matthews RT, Yang L, Jenkins BG, Ferrante RJ, Rosen BR, Kaddurah-Daouk R, et al. Neuroprotective effects of creatine and cyclocreatine in animal models of Huntington's disease. J Neurosci. 1998;18(1):156-63.

75. Kaemmerer WF, Rodrigues CM, Steer CJ, Low WC. Creatine-supplemented diet extends Purkinje cell survival in spinocerebellar ataxia type 1 transgenic mice but does not prevent the ataxic phenotype. Neuroscience. 2001;103(3):713-24.

Appendices

Appendix 1

List of primers used in this thesis work.

Primer ID	Forward	Reverse
Hsp105	TCTATTCTGACCCTCAAGGAGTTCC	TGTTCCAGCTTCACTGTTGTCTTGC
Hsp90	CACCCTGCTCTGTACTACTACTCGG	GCCAATGCCTGTGTCCACCAAAGTC
Hsp70	ATCAGTGGGCTGTACCAGGG	TTGACAGTAATCGGTGCCCAA
Hsp60	CTCGGGCCTATGCCAAAGAT	TTCTTCCCTTTGGCCCCATT
Hsp40	CGCTACCACCCGGACAAG	GGTACCATTAGCACCACCACT
Hsp27	TCACGGCTACTATGTTCGGC	CAGAAACGCCTGGAACTTGC
GRP75	AAGAGAGAGACAGGGGTTGATT	CCAGAAGCATCCATGGTAAGG
HO-1	CAGAAGAGGCTAAGACCGCC	GCAGTATCTTGCACCAGGCTA
NQO1	ACGGTCCTTTCCAGAATAAGAAGA	ACCTGGAAGCCACAGAAACG
BDNF	GACAAGGCAACTTGGCCTAC	TTCGATGACGTGCTCAAAAG
LC3	TTCTTCCTCCTGGTGAATGG	GTGGGTGCCTACGTTCTCAT
Beclin-1	CTTACCACAGCCCAGGCGAAA	GCCAGAGCATGGAGCAGCAA
TNFa	GCCACCACGCTCTTCTGTCT	TGAGGGTCTGGGCCATAGAAC
Il1b	ACCTTCCAGGATGAGGACATGA	AACGTCACACACCAGCAGGTTA
Il6	ACACATGTTCTCTGG GAAATCGT	AAGTGCATCATCGTTGTTCATACA
Il10	AGGACTTTAAGGGTTACTTGGGTT	GCTCCACTGCCTTGCTCTTATT
iNOS	CTCGGAGGTTCACCTCACTGT	GCTGGAAGCCACTGACACTT
Iba-1	GAAGCGAATGCTGGAGAAAC	CTCATACATCAGAATCATTCTC
GFAP	GGCGAAGAAAACCGCATCAC	CCCGCATCTCCACAGTCTTT
LCN2	CCAGTTCGCCATGGTATTTT	GGTGGGGACAGAGAAGATGA
XBP7	CAGCACTCAGACTATGTGCA	
XBP10		GTCCATGGGAAGATGTTCTGG
XBP11	CTGAGTCCGAATCAGGTGCAG	
IMPA-1	CAGGGACAGCAAGGATGAACAT	TTGGGATTGTGTACAGCTGTGTGG
B2m	CCTTCAGCAAGGACTGGTCT	TCTCGATCCCAGTAGACGGT
HPRT	GCTGGTGAAAAGGACCTCT	CACAGGACTAGAACACCTGC